EFFECT OF REACTOR IRRADIATION
ON SANTOWAX OM AND WR

Department of Nuclear Engineering

Massachusetts Institute of Technology

Cambridge, Massachusetts 02139

LEGAL NOTICE

EFFECT OF REACTOR IRRADIATION
ON SANTOWAX OM AND WR

by

E. A. Mason

M. L. Lee

S. T. Brewer

W. N. Bley

DEPARTMENT OF NUCLEAR ENGINEERING

MASSACHUSETTS INSTITUTE OF TECHNOLOGY

CAMBRIDGE, MASSACHUSETTS   02139

(

ACKNOWLEDGEMENT

PREVIOUS RELATED REPORTS

	MITNE-4	(SRO-85)	MITNE-41
(IDO 11,101)	MITNE-7	(SRO-87)	MITNE-48
(IDO 11,102)	MITNE-9	(MIT-334-11)	MITNE-55
(IDO 11,103)	MITNE-12	(MIT-334-12)	MITNE-59
(IDO 11,104)	MITNE-21	(MIT-334-23)	MITNE-63
(IDO 11,105)	MITNE-22	(MIT-334-33)	MITNE-66
(IDO 11,106)	MITNE-29	(MIT-334-34)	MITNE-68
(IDO 11,107)	MITNE-39	(MIT-334-48)	MITNE-75
		(MIT-334-70)	MITNE-78

ABSTRACT

Irradiations of the terphenyl mixtures, Santowax OM and WR, were made in the M.I.T. In-pile Loop Facility at temperatures ranging from 300°C (572°F) to 427°C (800°F). These potential coolants for nuclear reactors were irradiated while flowing through a stainless steel in-pile loop installed in a special fuel element in central position (Fuel Position 1) of the MITR. Steady-state operating conditions were maintained by continually removing coolant samples from the loop and feeding processed coolant to the loop. The coolant samples were processed using a High Boiler (HB) distillation procedure to remove HB. The distilled terphenyls and Low and Intermediate Boilers (LIB) were returned to the loop along with fresh makeup.

The dose rates to the terphenyl coolant due to fast neutrons and gamma-rays were measured using adiabatic calorimeters. Resonance and threshold foils were used as a check on the calorimetric measurements of the fast neutron fraction of the total dose rate. This fraction was 0.36 for the Santowax OM irradiations and 0.38 for the Santowax WR irradiations. The MITR was operated at 5 MW thermal power except for three of the Santowax OM irradiations when the power was 2 MW. The average dose rate to the total coolant was 0.057 and 0.067 watts/gram at 5 MW (0.023 watts/gram at 2 MW) and the in-core dose rate to the coolant was 1.2 and 1.3 watts/gram at 5 MW (0.47 watts/gram at 2 MW).

Three steady-state low temperature (300°C) irradiations of Santowax OM were made at different terphenyl concentrations to determine the apparent reaction order for radiolysis and the rate constants for degradation by radiolysis. The results indicated an apparent reaction order of radiolysis of 1.7 ± 0.1, which is the same value reported by M.I.T. earlier for meta-rich terphenyls. The fast neutron effect ratio, G_N/G_γ, of 3.3 was estimated for the total terphenyl in Santowax OM. Using these values to allow for the effects of coolant composition and fast neutron fraction, the radiolytic rate constants were found to be in good agreement with the results of low temperature irradiations of Santowax OM made at various fast neutron fractions by the other laboratories.

Of the nine high temperature (above 350°C) irradiations, three were made at 2 MW reactor thermal power with Santowax OM, three at 5 MW with santowax OM, and three at 5 MW with Santowax WR. The results of these high temperature irradiations were correlated using a degradation model which assumes that the rate of total degradation represents the linear sum of radiolysis and radiopyrolysis (i.e., pyrolysis of irradiated coolant). No significant differences were found in the first-order radiopyrolysis rates for Santowax OM and WR. No significant difference was observed in the rate of radiopyrolysis for Santowax OM due to a change in the dose rate. Combining the recent results with results of earlier irradiations at M.I.T., the best estimate of the first-order radiopyrolysis rate constants for irradiated Santowax OM and WR is

$$k_{P,omp,1}(T) = \exp(a - \Delta E_P/RT)$$

where

$$a = 34 \pm 7, \quad \Delta E_P = 54 \pm 9 \text{kcal/mole}$$

Six autoclave pyrolysis experiments were made, three with unirradiated Santowax WR and three with irradiated Santowax WR. Thermal decomposition rates of the unirradiated coolant are significantly lower than those of the irradiated coolant. The latter are not significantly different from those determined during steady-state in-pile irradiation.

Procedures for estimating coolant makeup rates in organic-cooled reactors are presented and discussed.

Physical property measurements included density, viscosity and number average molecular weight. Heat transfer measurements made on Santowax WR showed that the experimental data can be correlated within 10% bv the generally applicable McAdam's equation of

$$Nu = 0.023 \, Re^{0.8} Pr^{0.4}.$$

TABLE OF CONTENTS

CHAPTER 4

LOW TEMPERATURE TERPHENYL DEGRADATION

CHAPTER 5

HIGH TEMPERATURE TERPHENYL DEGRADATION

APPENDIX A1

CALORIMETRY AND FOIL DOSIMETRY

APPENDIX A2

CIRCULATING COOLANT MASS AND
TEMPERATURE PROFILES AROUND LOOP

APPENDIX A3

CALCULATION OF DEGRADATION RESULTS AND STATISTICS

APPENDIX A4

DEGRADATION RATE CALCULATIONS FOR
M.I.T. AUTOCLAVE PYROLYSIS EXPERIMENTS

APPENDIX A5

OPERATIONAL PROCEDURES FOR THE
CONTINUOUS SAMPLING AND MAKEUP SYSTEM

APPENDIX A6

CALCULATION OF RADIOLYSIS AND RADIOPYROLYSIS
RATE CONSTANTS FROM DATA OF M.I.T. AND OTHER LABORATORIES

LIST OF FIGURES

LIST OF TABLES

CHAPTER 1

SUMMARY

1.1 Introduction

This study of the effect of reactor irradiation on
Santowax OM and WR is a continuing effort of the Organic
Coolant Project at M.I.T. to provide information concerning
the performance of organic coolants in nuclear reactors.
These mixed terphenyl coolants have been circulated through
an in-pile loop in the M.I.T. Reactor under conditions of
temperature, pressure, dose, and coolant composition simil-
ar to those of an organic-cooled reactor in order to deter-
mine the effects of fast neutron and gamma ray radiolysis
and of pyrolysis on the rate and nature of coolant degrada-
tion. Such information is required in the design and opti-
mization of organic-cooled reactors as a basis for (1) the
selection of the type of organic coolants, (2) the selec-
tion of coolant operating conditions and coolant composition,
(3) the thermal and hydraulic design of the reactor system,
and (4) the prediction of long term operating characteris-
tics of the coolant system.

Most concepts for organic-cooled reactors have been
based on the use of various mixtures of isomers of terphenyl,
due to their combination of good stability (to radiation
and heat) and low vapor pressure (1.1). Table 1.1 shows
typical compositions and melting points of some of the
common terphenyl mixtures considered to be most suitable
as reactor coolants.   The principal mode of degradation
of the (unirradiated) coolants listed in Table 1.1 is that
of polymerization of the terphenyls to higher molecular
weight products, referred to as High Boilers (HB). A small

Table 1.1

Typical Compositions and Melting Points of Common Organic Coolants

	Santowax[b] OM	Santowax[b] OMP	Santowax[b] WR	OM-2[c]	HB-40
Biphenyl, w/o	3	2	<2	<1	0
O-terphenyl, w/o	65	10	15-20	20	18
M-terphenyl, w/o	30	60	75	76	<0.5
P-terphenyl, w/o	2	28	5	4	<0.5
Hydro-terphenyls, w/o	0	0	0	0	82
High Boiler (HB), w/o	0	0	0	0	0
Melting Point[a] (unirradiated material), $^\circ$F	178	350	185	185	Liquid at normal room temperatures

[a] Final liquidus point

[b] Santowax is a trade-mark of the Monsanto Chemical Company

[c] Produced by Progil of France

-1.2-

fraction of the terphenyls is also converted into hydrocarbon
gases and compounds of low and intermediate molecular weight.
The totality of reaction products is referred to as Degrada-
tion Products (DP). The presence of Degradation Products
alters not only the physical and heat transfer properties
of the coolant but also its response to radiation and heat.

Earlier(1961-1966) in-pile loop irradiations (1.2,1.3,
1.4,1.5) conducted by the M.I.T. Organic Coolant Project have
studied the behavior of the commercially available terphenyl
mixtures Santowax OMP and Santowax WR, both of which are
rich in meta terphenyl (see Table 1.1). The results of the
M.I.T. irradiations were correlated by means of rate constants
for the degradation of terphenyls by radiolysis and radio-
pyrolysis (pyrolysis of irradiated coolant). Rate constants
were obtained for the degradation of the individual isomers
in the coolant mixture as well as for the disappearance of
total terphenyl. Based on these studies, it was concluded
that the total degradation of meta-rich terphenyl coolants
under reactor irradiation (fast neutrons and gamma rays)
can be estimated by linearly adding the effects of degrada-
tion by radiation and heat.

However, the results of Canadian irradiations (1.6,
1.7, 1.14) of encapsulated samples of pure ortho and pure
meta terphenyls, reported in 1965 and 1966, indicated that
the radiolytic degradation of ortho terphenyl increased con-
siderably more rapidly with increasing temperature than for
the case of pure meta terphenyl. Furthermore, these rates
of degradation obtained from the radiolysis of pure ortho
terphenyl were considerably greater than the rates of degrada-
tion due to both radiolysis and radiopyrolysis of either
ortho or meta terphenyl observed in the irradiations of
meta-rich coolants by M.I.T. (1.4). The rates of degrada-
tion of pure meta terphenyl obtained during the AECL ex-

periments (1.14) were, however, in close agreement with the
results obtained by M.I.T. for meta terphenyl in mixed ter-
phenyls (1.4). These comparisons suggested that terphenyl
isomers (particularly ortho terphenyl) might behave different-
ly when irradiated alone and in mixed isomer form.

In 1966, the Heavy Water Organic Cooled Reactor (HWOCR)
program of the United States Atomic Energy Commission was
considering both ortho-rich Santowax OM and meta-rich Santo-
wax WR as reactor coolants. To provide additional informa-
tion required in order to make a coolant selection, a series
of nine irradiations of Santowax OM was begun employing
steady-state conditions in the M.I.T. Organic Loop. Three
irradiations on Santowax WR were also included to provide
additional information on meta-rich coolants for comparison.
The following information was sought:

(1)   the effects of radiolysis and pyrolysis on the
       degradation rates of the total terphenyl mixture,
(2)   the relative rates of degradation of both ortho
       and meta terphenyls in the ortho-rich coolant,
(3)   the effect of dose rate on terphenyl degradation
       in the range of dose rates likely to be experienced
       in organic-cooled reactors,
(4)   the relative distribution of the degradation pro-
       ducts (DP), the Low and Intermediate Boilers (LIB)
       and the High Boilers (HB) and,
(5)   the steady-state physical and heat transfer pro-
       perties of the irradiated coolant mixture.

During the period from July 1, 1966 to July 30, 1967,
a series of nine constant temperature irradiations (Runs 19A-
25) of ortho-rich Santowax OM were conducted in the M.I.T.
in-pile loop over a range of temperatures from 300°C to
427°C and a range of terphenyl concentrations from 63% to

86% of the total coolant. Two different dose rates were employed (corresponding to nominal reactor thermal power levels of 2 and 5 MW); in both cases the fractions of the total (gamma and fast neutron) dose rates due to fast neutron attenuations was 0.36. From these irradiations, the terphenyl degradation rates, both radiolytic and radiopyrolytic, were determined. From August 1, 1967 to March 10, 1968, meta-rich Santowax WR was irradiated at 5 MW of reactor power under conditions duplicating as nearly as possible three of the high temperature irradiations of Santowax OM. The results of these duplicated runs permitted direct comparison of the ortho-rich coolant with the meta-rich coolant with respect to the degradation rates of the total coolant, the relative degradation rates of ortho and meta terphenyls and the effects of radiolysis and radiopyrolysis.

Furthermore, pyrolysis experiments in an out-of-pile autoclave were also conducted during the period from January 8, 1968 to April 3, 1968, to measure the rates of thermal decomposition of irradiated and unirradiated Santowax WR.

In addition to determining degradation rates, measurements were also made of the physical properties of Santowax OM (such as density, viscosity and number average molecular weight) as well as of heat transfer characteristics.

1.2 In-pile Loop Irradiation - Equipment and Procedure

1.2.1 Loop Equipment

A detailed description of the M.I.T. organic coolant loop has been given by Morgan and Mason (1.2). Modifications of the loop equipment up to June 30, 1966 have been described by other M.I.T. reports (1.3, 1.4, 1.5). Further modifications made since then are described in Chapter

2 of this report.

Nine irradiations (Runs 19A-25) of Santowax OM were con-
ducted using In-pile Section No. 4; three irradiations (Runs
26-28) of Santowax WR utilized In-pile Section No. 5. Dia-
grams showing the design of these two in-pile sections are
presented in Figures 1.1 and 1.2; the portions in the re-
actor core were identical and had a volume of 280 cc. Fig-
ure 1.3 shows the orientation of an in-pile section in a
fuel element; all twelve irradiations reported in detail
here (Runs 19A-28) were irradiated in the central fuel posi-
tion (No. 1) of the M.I.T. Reactor. A schematic flow dia-
gram of the entire M.I.T. Organic Loop System (as utilized
for Runs 19A-28) is presented in Figure 1.4. A summary of
the important operating conditions for the twelve irradia-
tions carried out between November 1, 1966 and February 26,
1968, is presented in Table 1.2.

1.2.2 Loop Operations

At the beginning of each irradiation run, the coolant
composition was adjusted to the desired total terphenyl
concentration and temperature during a period of unsteady
state. The rates of fresh coolant addition and irradiated
coolant removal for processing were adjusted until the de-
sired steady composition was observed for a period of about
one week. This marked the beginning of the steady-state
irradiation run during which irradiated coolant was removed
(either continuously or in small intermittent batches)
for processing, and replaced by makeup coolant. The irradi-
ated coolant was processed using a High Boiler distillation
procedure to remove high molecular weight degradation pro-
ducts. The temperature of the distillation pot was ad-
justed so that the terphenyls were distilled over leaving

IN PILE SECTION NO. 4

IN PILE SECTION NO. 5

High Density Concrete

Spiral Offset

Bend Offset

Lead

$35\frac{3}{16}"$

$34\frac{3}{8}"$

$109\frac{1}{4}"$

$8\frac{3}{8}"$

$35\frac{3}{16}"$

$109\frac{1}{4}"$

3/8"OD x 0.028" Wall
Monitor Tube

1.25"OD x 0.035" Wall
Aluminum Thimble

$1\frac{1}{16}"$ OD x 0.035 Wall
Irradiation Capsule

5/8"OD x 0.010" Wall
Baffle Tube (inlet)

3/8"OD x 0.028" Wall
Monitor Tube

Reactor
Core
24"

₵ Fuel

$13\frac{1}{16}"$

Reactor
Core
24"

Fuel ₵

$13\frac{11}{32}"$
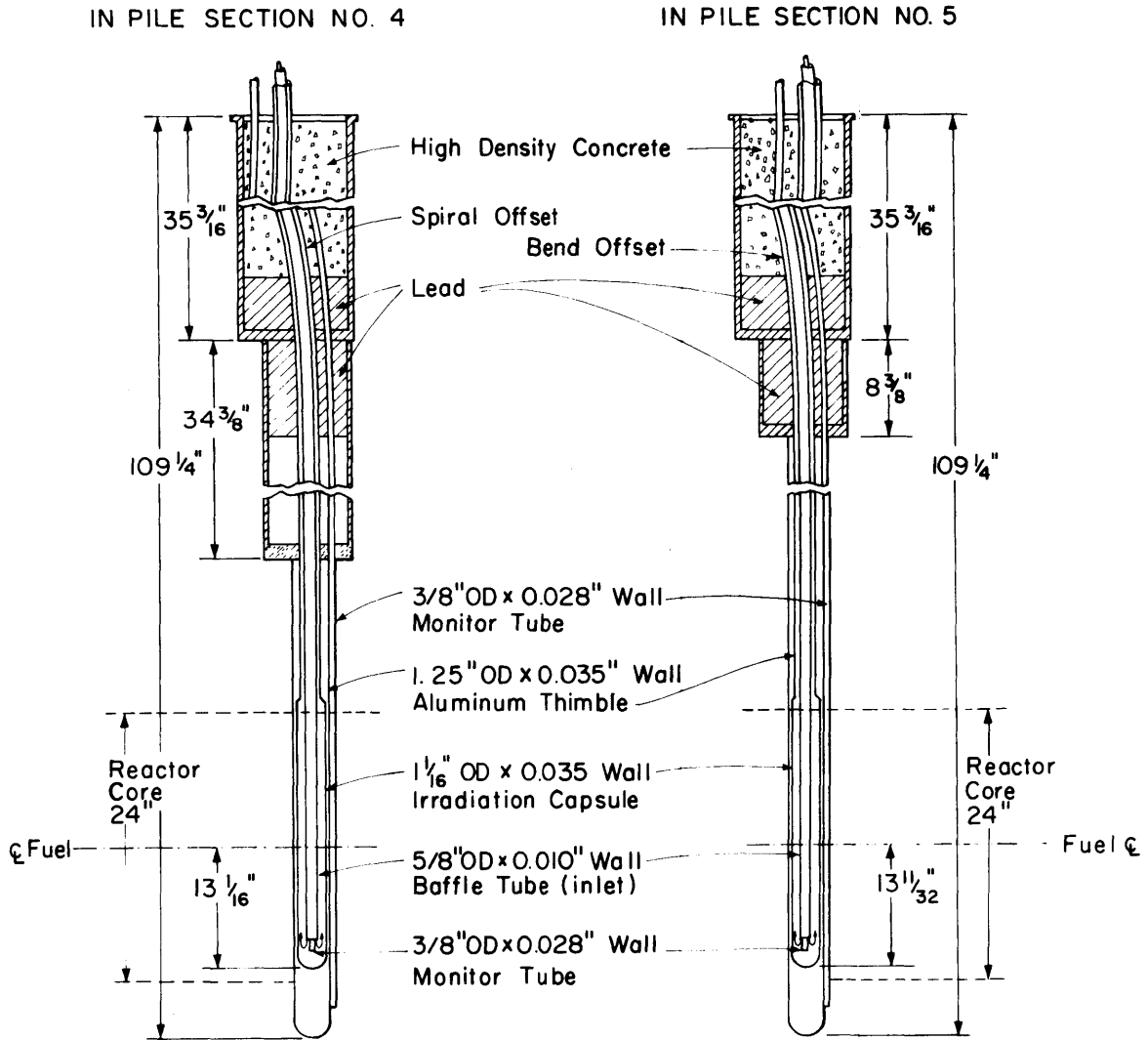
FIGURE 1.1 SIMPLIFIED DRAWING OF IN-PILE SECTION NO. 4 AND NO. 5

Core
Axial
Centerline

I 1/16" OD × 0.035" Wall
304 Stainless Steel
Irradiation Capsule
(Outlet)

5/8 "OD × 0.010" Wall
321 Stainless Steel
Baffle Tube (Inlet)

Direction of
Coolant Flow

3/8 "OD × 0.028" Wall
316 Stainless Steel
Monitor Tube

I 1/4 "OD × 0.035" Wall
6061 Aluminum Thimble

Fuel Element
Assembly Nozzle

13 11/32" In-pile Section No. 5

13 1/16" In-pile Section No. 4

1/2"

1/2"

Note : Aluminum –
monitor tube and
leak detector tube
not shown.

2 1/2"

FIGURE I.2   SIMPLIFIED ELEVATION CUT-AWAY VIEW OF LOWER
END OF IRRADIATION CAPSULE OF IN-PILE SECTIONS
No. 4 and No. 5 INSTALLED IN MITR FUEL ELEMENT
ASSEMBLY

1/8" OD 0.015" Wall Aluminum Leak Detector Tube

3/8" 0.028" Wall Aluminum Monitor Tube

1 1/16" OD × 0.035" Wall 304 Stainless Steel Irradiation Capsule (Outlet)

1/2" Wide Hold Down Straps

Fuel Plates (outside plates contain no fuel)

5/8" OD × 0.010" Wall 321 Stainless Steel Baffle Tube (Inlet)

3"

3/8" OD × 0.028" Wall 316 Stainless Steel Monitor Tube

3"

1.25" OD × 0.035" Wall 6061 Aluminum Thimble

-1.6-

FIGURE 1.3 DRAWING OF FUEL ELEMENT CROSS SECTION WITH POSITION OF IN-PILE SECTION SHOWN

LEGEND

⋈ NEEDLE VALVE

DIAPHRAGM,OPERATED VALVE

Ⓟ PRESSURE GAGE

φ RUPTURE DISK

N CHECK VALVE

GG GAGE GLASS

PR PRESSURE REGULATOR
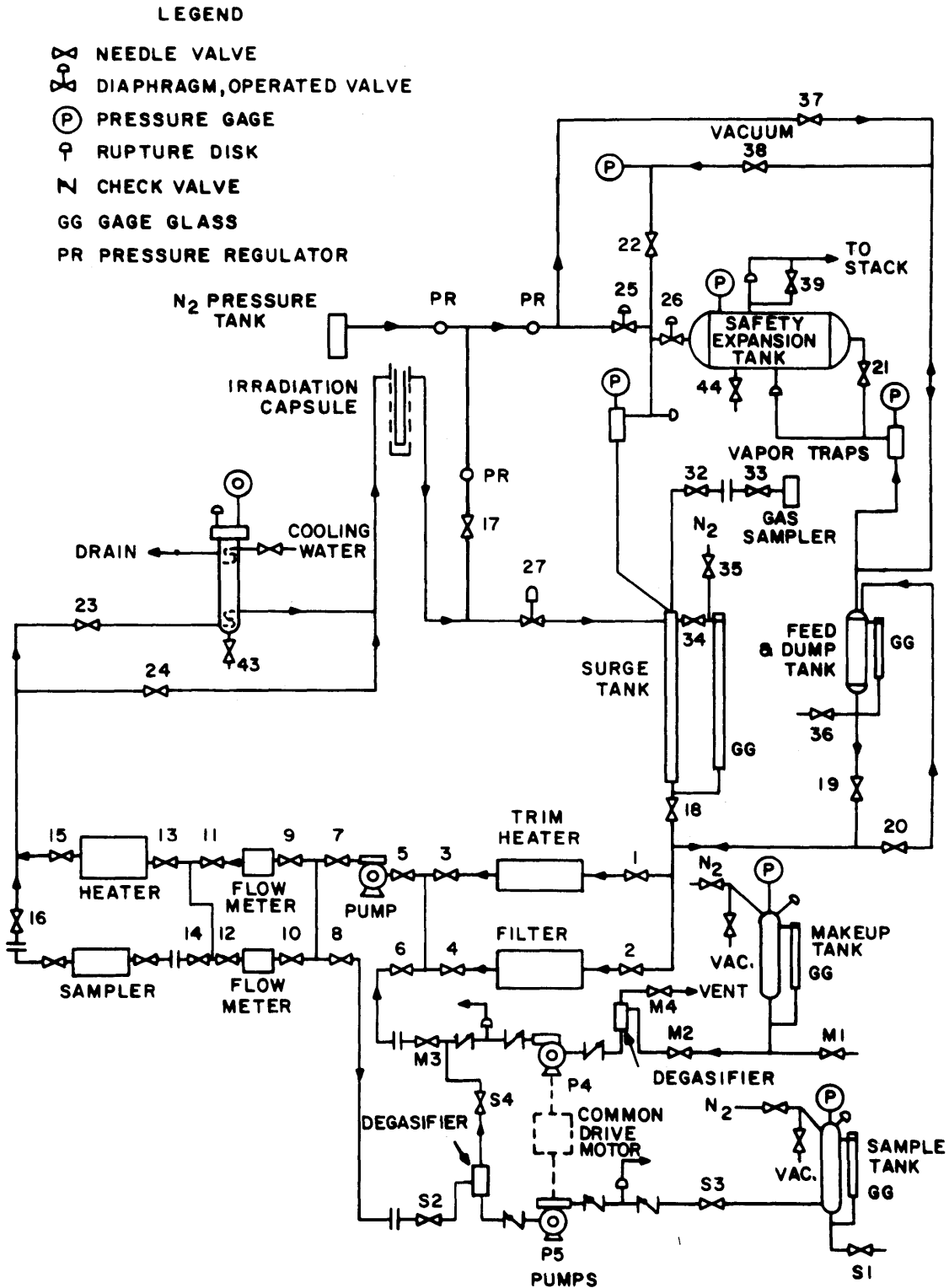
FIGURE 1.4 SCHEMATIC FLOW DIAGRAM OF MIT ORGANIC LOOP WITH
SAMPLING AND MAKEUP SYSTEM I

Table 1.2

Summary of Irradiation Schedule

November 1966 - February 1968

Total Terphenyl Concentration C_{omp}(w/o)	Capsule Irradiation Temperature			
	572°F 300°C	700°F 371°C	750°F 399°C	800°F 427°C
86	Run 19A-OM 5MW, f_N = 0.36			
78-82	Run 20B-OM 5MW, f_N = 0.36	Run 23-OM 2MW, f_N = 0.36 Run 23A-OM 5MW, f_N = 0.36 Run 26-WR 5MW, f_N = 0.38	Run 21-OM 2MW, f_N = 0.36 Run 24-OM 5MW, f_N = 0.36 Run 27-WR 5MW, f_N = 0.38	
76-78				Run 22-OM 2MW, f_N = 0.36 Run 25-OM 5MW, f_N = 0.36 Run 28-WR 5MW, f_N = 0.38
63	Run 19A-OM 5MW, f_N = 0.36			

MW = reactor thermal power, MW   OM = Santowax OM

f_N = fraction of total dose due to fast neutron attenuation   WR = Santowax WR

only a trace (<0.2%) of para terphenyl in the distilled
bottom. The distillate was then mixed with an amount of
fresh unirradiated coolant equal to the amount of High Boiler
removed from distillation. The mixture formed the makeup
coolant which was returned to the loop to replace the irradi-
ated coolant removed for processing. Samples of the irradi-
ated and makeup coolant were retained for analysis.

1.2.3 Measurement and Calculation of Dose Rates

In order to relate changes in coolant composition and
properties to the radiation dose, measurements of the dose
rates were made along the axis of fuel element No. 1 immedi-
ately before installation of the in-pile section and
immediately after its withdrawal. The small changes in dose
rates occurring during an irradiation due to fuel burnup
were monitored by means of neutron detectors placed in the
two monitor tubes which formed part of the in-pile sections.

The dose rates to terphenyl in the in-pile section
due to fast neutrons and gamma radiation were measured
using adiabatic calorimeters at various positions along
the irradiation capsule. These dose rates (watts/grams)
are directly related to the reactor power level by an in-
pile dose rate factor, F^{SW} (watt-cc/MW-gram). The latter
was determined by an axial integration of the dose rates
measured along the irradiation capsule. Measurements of
the neutron spectrum by means of resonance and threshold foils
were also made along the axial position of the in-pile irradi-
ation capsule to determine the neutron spectrum. The re-
sults of these measurements were used in evaluating the
calorimeter measurements; the rate of energy deposition from
fast neutrons in terphenyl due to elastic scattering was also cal-

culated from the neutron spectrum as a check on the calorimeter measurements.

Table 1.3 summarizes the results of dose rate measurements in Fuel Position 1 for In-pile Sections No. 4 and No. 5. The differences in F^{SW} between pre-irradiation and post-irradiation are due to fuel burnup in the central fuel assembly which contains the in-pile irradiation capsule.

1.3 Coolant Degradation - Theory

1.3.1 Kinetics

Two major effects are responsible for the degradation of terphenyl coolants in nuclear reactors, namely radiolysis and pyrolysis (heat). Radiolysis is degradation due to nuclear radiation such as fast neutrons and gamma radiation. Pyrolysis occurs only at higher temperatures (>350°C) where thermal decomposition of the terphenyl becomes progressively more important with increasing temperature. However, it has been found (1.4, 1.5, 1.9, 1.10) that the rate of thermal decomposition is greater for irradiated coolants than for unirradiated coolants. Therefore, to differentiate, thermal decomposition of unirradiated coolant is designated pyrolysis while thermal decomposition of irradiated coolant is designated radiopyrolysis.

The terphenyl balance on any coolant system can be expressed as shown in the following figure and Equation (1.1):

w_i, C_{omp} →

M_C = total coolant mass

C_{omp} = total terphenyl (omp) concentration

$\bar{r}$ = average dose rate

→ W_{omp} (terphenyl degraded)

→ w_o, C_{omp}

Inlet (feed)   Outlet (bleed)

Coolant System
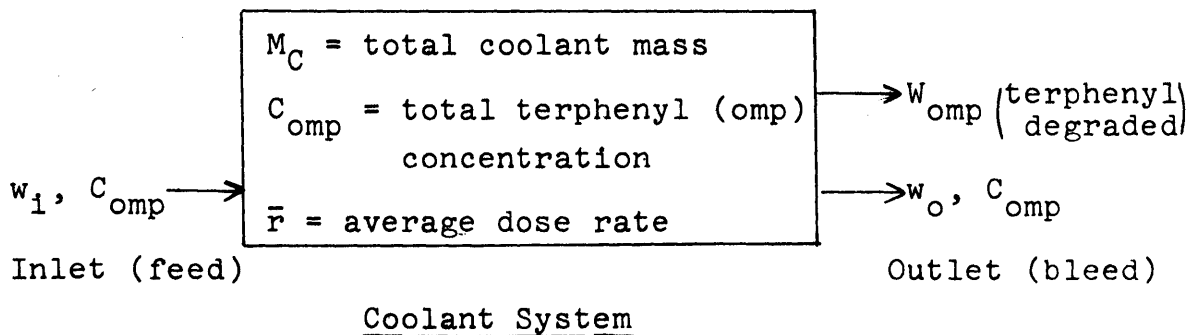
Table 1.3

Summary of Dose Rate Measurements in
Fuel Position 1 of MITR

	In-pile Section No. 4[a]		In-pile Section No. 5[a]	
	Pre-irradiation	Post-irradiation	Pre-irradiation	Post-irradiation
Total in-pile dose rate factor F_T^{SW}, watt-cc/MW-gm	81.6 ± 2.0	69.6 ± 1.4	89.1 ± 1.0	80.5 ± 1.6
Gamma-ray in-pile dose rate factor F_T^{SW}, watt-cc/MW-gm	51.4 ± 1.4	44.5 ± 1.0	55.6 ± 0.8	49.7 ± 1.0
Fast neutron in-pile dose rate factor F_T^{SW}, watt-cc/MW-gm	30.2 ± 1.4	25.1 ± 1.2	33.5 ± 0.8	30.8 ± 1.2
Fast neutron fraction, f_N	0.37	0.36	0.38	0.38
Average Dose rate to coolant,[d] $\bar{r}$, watts/gram	0.026[b] or 0.066[c]	0.023[b] or 0.057[c]	0.073[c]	0.065[c]
Maximum dose rate to coolant, watts/gram	0.68[b] or 1.71[c]	0.56[b] or 1.41[c]	1.80[c]	1.60[c]
Total energy deposition[d] rate, watts	130[b] or 320[c]	110[b] or 270[c]	350[c]	310[c]

[a] Error limits are 2σ

[b] At reactor power of 1.94 MW

[c] At reactor power of 4.88 MW

[d] Results based on 6000 cc total coolant volume in the loop at 0.8 gm/cc

$$W_{omp} = w_i C_{omp} - w_o C_{omp} - \frac{d(M_C C_{omp})}{dt}$$

$$= w_i C_{omp} - w_o C_{omp} - M_C \frac{dC_{omp}}{dt} - C_{omp} \frac{dM_C}{dt} \qquad (1.1)$$

where

w_i = inlet coolant feed rate, gms/hr

w_o = outlet coolant bleed rate, gms/hr

C^f_{omp} = total terphenyl concentration in the feed, weight fraction

C_{omp} = total terphenyl concentration in the coolant, weight fraction

W_{omp} = time rate of total terphenyl degradation rate gms/hr

An empirical model describing the degradation rate of terphenyl has been developed at M.I.T. in which it is assumed that the rate of degradation depends only on the concentration of the terphenyls and that radiolysis and radiopyrolysis are independent and linearly additive. The degradation rate equation expressing this model is shown as Equation (1.2) (see Appendix A3.1 for details).

$$W_{omp} = k_{R,omp,n} C^n_{omp} M_C \frac{d\tau}{dt} + k_{P,omp,m} C_{omp} M_C \qquad (1.2)$$

or in terms of a G value (which represents the energy rate of degradation),

$$\frac{W_{omp}}{\bar{r} M_C} = \frac{G(-omp)}{11.65} \qquad \text{(gms/watt-hr)} \qquad (1.3)$$

where

G(-omp) = molecules of terphenyl degraded/100 ev

11.65 = conversion factor, (molecules)(watt-hr)/ (gram)(100 ev)

$\bar{r}$ = $d\tau/dt$ = average specific dose rate in M_C, watts/gm

τ = specific dose, watt-hr/gm

M_C = coolant mass in the system, grams

$\bar{r}M_C$ = average rate of energy deposition in the total coolant, watts

$k_{R,omp,n}$ = radiolysis rate constant for total ter-phenyl with apparent radiolysis kinetics order n, $(watt\text{-}hr/gram)^{-1}$

$k_{P,omp,m}$ = radiopyrolysis rate constant for total terphenyl with apparent radiopyrolysis kinetics order m, $(hr)^{-1}$

Combining Equations (1.1), (1.2) and (1.3)

$$\frac{w_i}{\bar{r}M_C}\left[C_{omp}^f - C_{omp}\right] - \frac{dC_{omp}}{d\tau} = k_{R,omp,n}C_{omp}^n + \frac{k_{P,omp,m}}{\bar{r}}C_{omp}^m$$

$$= \frac{G(-omp)}{11.65} \qquad (1.4)$$

For <u>steady-state</u> runs, $dC_{omp}/d\tau$ is zero. For the individual terphenyl isomers (ortho, meta and para terphenyls), Equation (1.4) is modified to describe the disappearance rate as

$$\frac{w_i}{M_C\bar{r}}\left[C_i^f - C_i\right] - \frac{dC_i}{d\tau} = k_{R,i,a+b}C_i^a C_{omp}^b$$

$$+ k_{P,i,c+d}C_i^c C_{omp}^d = \frac{G(-i)}{11.65}$$

$$(1.5)$$

where

C_i^f = concentration of ith terphenyl isomer in the feed, weight fraction

c_i = concentration of ith terphenyl isomer in the coolant system, weight fraction

$k_{R,i,a+b}$ = radiolysis rate constant for i^{th} isomer with apparent reaction order a+b (watt-hr/gram)$^{-1}$

$k_{P,i,c+d}$ = radiopyrolysis rate constant for i^{th} isomer with apparent reaction order c+d (hr)$^{-1}$

Both Equations (1.4) and (1.5) had been used extensively and successfully in describing the degradation rate of meta-rich terphenyl coolant such as Santowax WR and OM-2 (1.4, 1.5). One of the primary objectives of this report will be to test the adequacy of this empirical model in describing the degradation rate of ortho-rich terphenyl coolant such as Santowax OM.

1.3.2 Method of Calculating Degradation Rates for Steady-State Irradiation

The G values for the disappearance of total terphenyl, terphenyl isomers, or for the formation of high boiler (HB) during a period of steady-state irradiation in the organic coolant loop are obtained using Equation (1.6)

$$G(-i) = \frac{11.65W_i}{F^{SW}\rho[MWH]} \quad \frac{\text{molecules of } i^{th} \text{ isomer degraded (or formed)}}{100 \text{ ev absorbed in total coolant}}$$

$$(1.6)$$

and

$$G^*(-i) = \frac{G(-i)}{C_i}$$

$$= \frac{\text{molecules of } i^{th} \text{ terphenyl isomer degraded (or formed)}}{100 \text{ ev absorbed in the } i^{th} \text{ isomer}}$$

$$(1.7)$$

where

$G(-i)$ = G value for the disappearance of total terphenyl, terphenyl isomer, or for the formation of HB

W_i = total mass of terphenyl or terphenyl isomer degraded or HB formed, gms

F^{SW} = total in-pile dose rate factor, watt-cc/MW-gm

ρ = density of coolant at irradiation temperature, gms/cc

$[MWH]$ = length of steady-state irradiation, reactor megawatt-hours

C_i = average concentration of total terphenyl or terphenyl isomer, or HB, weight fraction

In Equation (1.6), the mass of terphenyl degraded or HB produced, W_i, is determined by making a terphenyl balance around the system using Equation (1.1). The flow rates of coolant makeup, w_i, and coolant removed for processing, w_o were measured by carefully weighing all coolant added to, or removed from, the loop over the measured time of the radiation run. The concentration of terphenyl in the coolant was analyzed by vapor phase chromatography from which the weight fractions of the ortho, meta and para terphenyls (hence the total terphenyl)were determined. The High Boiler concentration of the coolant was determined by the distillation processing of coolant in batches of about 3000 grams. By definition, the concentration of the Degradation Products (DP) is (100 - w/o of total terphenyl). The difference between DP and HB concentrations is referred to as the concentration of the Low and Intermediate Boilers (LIB). The circulating mass of coolant, M_C, was measured using a tritium dilution technique (tritiated terphenyl was added to the coolant system and samples of coolant analyzed for tritium content).

To calculate G values from Equation (1.6) the length of steady-state irradiation is expressed in terms of MWH of reactor operation. The megawatts (MW) reactor power was calculated from the measured known flow rate of the reactor coolant (heavy water) and temperature rise of the heavy water through the core of M.I.T. Reactor (MITR).

The density, ρ, of samples of irradiated coolant was determined at several different temperatures using glass pycnometers immersed in a fused-salt bath. The temperature of coolant in the irradiation zone (and other parts of the system) was measured by means of immersion thermocouples.

1.3.3 Low Temperature Irradiation - Radiolytic Degradation

At irradiation temperature below about $350°C$, the radio-pyrolysis effect on the terphenyl coolant is negligible as compared with the radiolysis effect. Degradation of terphenyl can be considered as due to radiation alone. With $k_p \sim 0$, Equations (1.2) and (1.3) can be written as

$$G_R(-omp) = 11.65 \, k_{R,omp,n} c_{omp}^n \qquad (1.8)$$

where

$G_R(-omp)$ is the G value for the degradiation of total terphenyls due to radiolysis.

Both $G_R(-omp)$ and $k_{R,omp,n}$ are treated as temperature and fast neutron fraction dependent. The degradation of organic coolants in nuclear reactors is caused primarily by fast neutrons and gamma radiation. We assume that the G value due to radiolysis may be written as the sum of the G values due to neutrons and gamma radiation each weighted respectively by the faction of its dose rate contribution, f_N and f_γ,

$$G_R = G_N f_N + G_\gamma f_\gamma \qquad (1.9)$$

and

$$f_N + f_\gamma = 1 \tag{1.10}$$

Combining Equations (1.8), (1.9) and (1.10),

$$\frac{G_R(-omp)}{11.65} = k_{R,omp,n} C_{omp}^n$$

$$= \frac{G_\gamma^o}{11.65}\left[\left[\frac{G_N}{G_\gamma} - 1\right]f_N + 1\right] C_{omp}^n \tag{1.11}$$

where

$$G_\gamma^o = \frac{G_\gamma}{C_{omp}^n}$$ is the initial degradation rate due to gamma radiation

G_N/G_γ is called the fast neutron effect ratio

Equation (1.8) was used to determine the radiolytic reaction order, n and the radiolytic reaction rate constant, $k_{R,omp,n}$. Equation (1.11) was used to correlate terphenyl irradiation results of M.I.T. and those of other laboratories.

1.3.4 High Temperature Irradiation - Radiopyrolytic Degradation

The thermal decomposition of terphenyl coolant becomes progressively more important at temperatures above $350^\circ C$ ($662^\circ F$). For temperatures above $750^\circ F$, the degradation rate due to radiopyrolysis becomes the predominant component of the total degradation rate in the case of organic-coolant reactors where the mass of the coolant holdup at high temperatures is generally quite large.

Any attempt to separate the total rate of degradation observed under irradiation at high temperature into these two components involves assumptions regarding the effect of temperature on each process and regarding the effect of each

process on the other . In the model employed here, it
has been assumed that the effects of the two processes add
independently and that the temperature dependence of radioly-
sis over the entire range of interest can be obtained by
extrapolating from the dependence at low temperatures (where
radiopyrolysis effects are negligible). The empirical Equation
(1.4) is used to calculate the radiopyrolytic reaction rate
by subtracting the radiolytic degradation rate from the
total rate measured. Rearranging Equation (1.4), we have

$$k_{P,omp,m} = \left[\frac{G(-omp)}{11.65 C_{omp}^m} - k_{R,omp,n} C^{n-m} \right] \bar{r} \qquad (1.12)$$

Since $k_{R,omp,n}$ determined in low temperature irradiations is
a function of temperature, an Arrhenius relation is used to
estimate the magnitude of $k_{R,omp,n}$ at higher temperature. The
activation energy of radiolysis is generally small. 1 kcal/
mole appears to be the best choice based on results from other
laboratories.

1.4 Terphenyl Coolant Degradation - Results

    1.4.1 Low Temperature Irradiation of Santowax OM

       The operating conditions for the low temperature (300°C
or 572°F) irradiations of Santowax OM are summarized in Table
1.4 along with the degradation rate G values obtained.

       The values of G_R from Table 1.4 are plotted versus C_{omp}
using logarithmic coordinates in Figure 1.5. Early results
for Santowax WR and OM-2 from an earlier report (1.5) are
also included. For the three cases where three data points
are available, a straight line correlation results; straight
lines are therefore drawn through the two data points
available for each of the other two cases.

       From Equation (1.11), the kinetic order of radiolysis,
n, is seen to be the slope of the linear correlation of log G

Table 1.4

Operating Conditions and Results
of Santowax OM Irradiations at M.I.T.
300°C(572°F)

Run No.	Average Dose Rate (w/g)	Reactor Power (MW)	Concentration, w/o					$G_R(-omp)$[b]	$G_R(HB)$	$G^*(-omp)$[b]
			o	m	p	omp	HB			
19A	0.060	5	41.5	20.1	1.5	63.1	26.4	0.178 ±0.012	0.160 ±0.014	0.282 ±0.038
20A	0.065	5	57.7	26.6	1.8	86.1	6.1	0.307 ±0.024	0.232 ±0.016	0.357 ±0.028
20B	0.061	5	53.1	25.6	1.8	80.5	8.5	0.270 ±0.020	0.205 ±0.018	0.336 ±0.025

[a] Fast Neutron Fraction, $f_N = 0.36$, in Fuel Position 1

[b] Error limits are 2σ

Symbol		Lab.	Run no.	f_N	n
II	▽	Euratom	Cl-42-320	0.28	1.6
IV	□	Euratom	C3-40-320	0.126	1.8
III	◇	Euratom	C6-41-320	0.20	1.3
V	▲	MIT	14,16,17	0.07	1.7
I	●	MIT	19A,20A,20B	0.36	1.7

Error Limits are 2σ

G(-omp), Molecules / 100 ev

TERPHENYL CONCENTRATION, C_{omp}, weight fraction
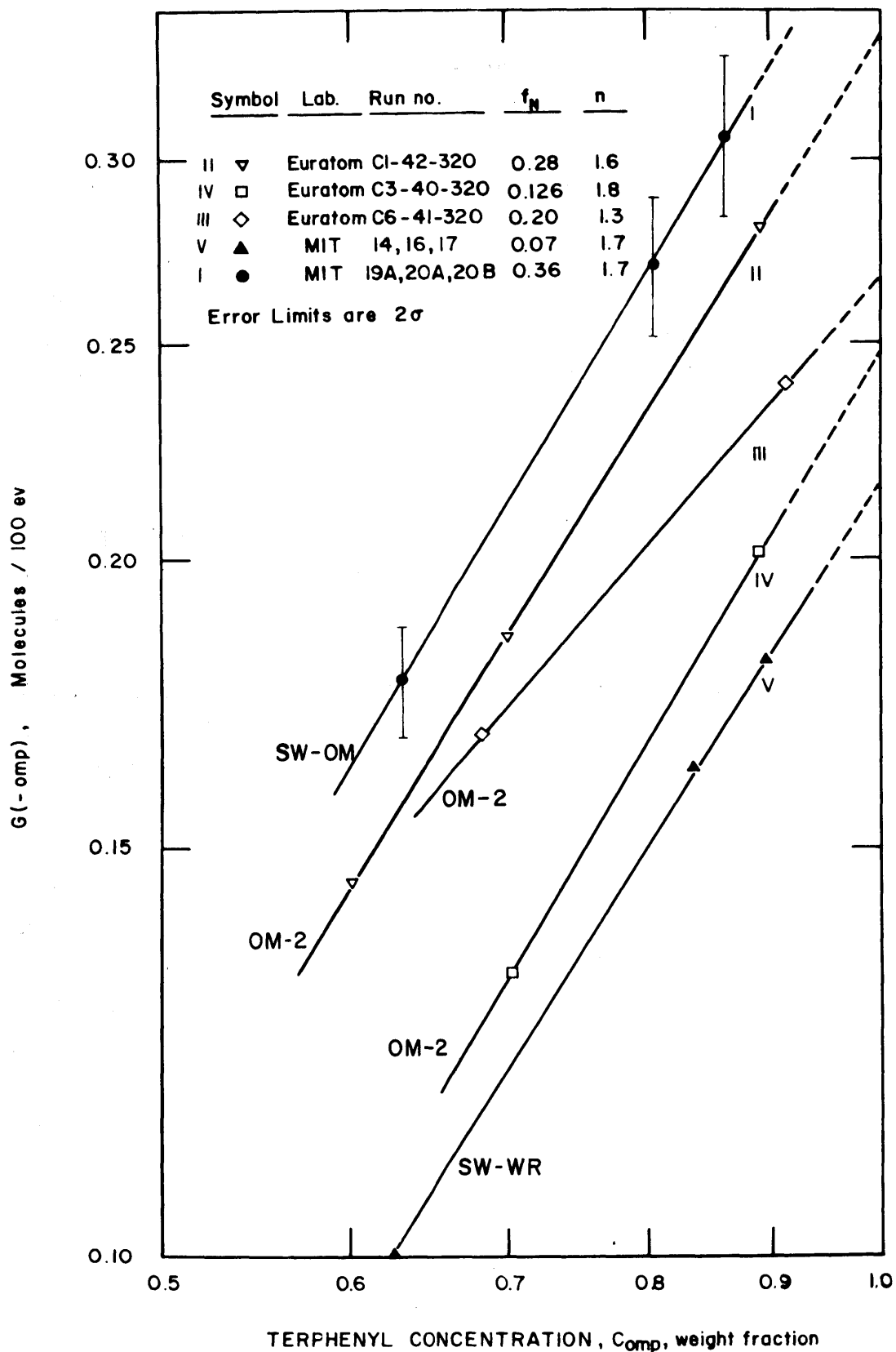
FIGURE 1.5   CORRELATION OF EURATOM AND M.I.T. STEADY-STATE IRRADIATIONS AT LOW TEMPERATURE

versus log C_{omp}. Curve I represents a least-square fit of
the three experimental data points of Santowax OM. The
value of n is 1.7 $\pm$ 0.1(2σ) which is the same value as re-
ported earlier for meta-rich OM-2 and Santowax WR.

The relative stabilities of ortho and meta terphenyls
in Santowax OM in these low temperature irradiations are
presented in Table 1.5. Within the accuracy of the experi-
ments, no significant difference in the stability of ortho
and meta terphenyls is found for these radiations, carried
out at a fast neutron dose fraction, f = 0.36. The same
has been reported earlier by Mason and Timmins (1.5) on
Santowax WR. The relative stabilities of the individual
terphenyl isomers also do not change significantly with
variation in the isomer concentration or the total terphenyl
concentration. This result implies that the constants a and
b of Equation (1.5) are approximately a = 1 and b = 0.7 (for
n = 1.7).

Equation (1.11) indicates that the values of the radiol-
ysis rate constants, k_R, depend on the magnitude of f_N, accord-
ing to the model employed here. This is the reason for the
spread between the lines shown in Figure 1.5. However, all
irradiations of Santowax OM at M.I.T. were made at a fixed
fast neutron dose fraction f_N = 0.36. As a result, the values
of the two quantities, G_N/G_γ and G_γ^O, which indicate the rela-
tive degradation effects of fast neutrons and gamma rays,
could not be obtained from Santowax OM. Mason and Timmins
(1.5) have reported the following values of G_N/G_γ and G_γ^O which
were based on correlation of low temperature irradiations
of meta-rich terphenyls at various values of f_N by M.I.T. and
Euratom.

Table 1.5

Relative Stabilities of Ortho- and Meta-Terphenyl

Isomers in Santowax OM Irradiated at 300°C [a]

Run No.	Relative Degradation Rates $G^*_R(-1)/G^*_R(omp)$ [b]	
	Ortho	Meta
19A	1.04 ± 0.05	0.95 ± 0.05
20B	1.08 ± 0.06	0.87 ± 0.05
20A	1.01 ± 0.06	0.99 ± 0.06

[a] Steady-state irradiation at Fuel Position 1 ($f_N = 0.36$); 5 MW, nominal reactor power

[b] Error limits are 2σ

Table 1.6

Relative Effects of Fast Neutrons and Gamma-Rays
on Irradiations of Meta-Rich Terphenyls (1.5)

		Total Terphenyl	Ortho Terphenyl	Meta Terphenyl
G_N/G_γ	$(320°)$	3.9	2.7	4.5
G_γ^O	$(320°)$	0.19	0.25	0.18

To obtain an estimate of G_N/G_γ and G_γ^O for total ter-
phenyl in irradiated Santowax OM the values presented in
Table 1.6 for the isomers were weighted by the relative
amounts of the isomers present (in the M.I.T. irradiations
of Santowax OM, o:m weight ratio was about 2:1). The
resulting values for Santowax OM were

$$G_N/G_\gamma(320°C) = 3.3$$
$$G_\gamma^O (320°C) = 0.22$$

Substitution of these values, and the corresponding val-
ues for meta-rich terphenyls, into Equation (1.11) gives

Meta-rich terphenyl

$$k_{R,omp,1.7}(320°C) = 1.6 \times 10^{-2}\left[2.9f_N + 1\right] \frac{watt-hr}{gm}^{-1}$$

(1.13)

Santowax OM

$$k_{R,omp,1.7}(320°C) = 1.9 \times 10^{-2}\left[2.3f_N + 1\right] \frac{watt-hr}{gm}^{-1}$$

(1.14)

Radiolysis rate constants of Santowax OM predicted from
Equation (1.14) agree quite well with values obtained at a
number of different fast neutron fractions; see Table 1.7.

Table 1.7

Summary of Low Temperature Irradiations of
Santowax OM[a]

Reference	Dose Rate watts/gm	f_N	$k_{R,omp,1,7}(320°)$, $(wh/g)^{-1}$ [b]	
			Experimental	Calculated[b]
AECL (1.8)	73	0	0.019	0.019
AECL (1.15)	0.33	0.3	0.028	0.032
AECL (1.6)	0.1	0.51	0.046-0.059	0.041
AI (1.16)	1.2	0.28	0.028[c]	0.031
AECL (1.17)	0.1-0.15	0.55-0.62	0.037[d]	0.043-0.046
M.I.T. Runs 19A, 20A and 20B	0.06	0.36	0.035	0.035

[a]All results normalized to 320°C using ΔE_R = 1 kcal/mole and n = 1.7 except
as noted

[b]Based on Equation (1.14)

[c]Based on initial decomposition rate

[d]Based on second-order kinetics

1.4.2 Autoclave Pyrolysis Experiments

The rates of thermal decomposition of unirradiated and previously irradiated Santowax WR were measured using an out-of-pile autoclave apparatus. The purpose was to confirm the pyrolysis rate constants of several earlier runs completed at M.I.T. (1.5) which, though checking quite well with those of AECL results (1.8), differed appreciably from Euratom measurements (1.9, 1.10).

Table 1.8 summarizes the results of six pyrolysis experiments, three of which were made with unirradiated Santowax WR and the rest with irradiated Santowax WR.

Figure 1.6 shows the first-order pyrolysis rate constant from the autoclave pyrolysis experiments in an Arrhenius plot. In addition the AECL values and the Euratom values for fresh (unirradiated) meta terphenyl and meta-rich terphenyl mixtures are included for comparison. The present results obtained with fresh Santowax WR check very well with the AECL values as well as with results from previous autoclave experiments at M.I.T. (1.5). The Euratom measurements are lower by a factor of about three.

1.4.3 High Temperature Irradiation of Santowax OM and Santowax WR

Table 1.9 summarizes the results of the high temperature ($371°C$ - $427°C$) irradiations of Santowax OM and Santowax WR for the period covered by this report. Figure 1.7 is an Arrhenius plot of the radiopyrolysis rate constants (for first-order kinetics) obtained from the results of the high temperature irradiations using Equation (1.12) (with n = 1.7; m = 1); these results are shown as closed data points. Curve IV is a least-square fit of the M.I.T. radiopyrolysis data from Runs 21 through 28.

Table 1.8

Summary of M.I.T. Autoclave
Pyrolysis Results of Santowax WR

Run No.	Coolant	Temperature ^oF	^oC	Concentration. w/o OMP	DP	First Order[a] Rate Constant $k_{P,omp,1}$ $(hr)^{-1}$
1F	fresh SW-WR	796	425	91-70	9-30	$1.68 \pm 0.11 \times 10^{-3}$
2F	fresh SW-WR	832	445	91-57	9-43	$5.27 \pm 0.11 \times 10^{-3}$
3F	fresh SW-WR	769	409	91-69	9-31	$5.07 \pm 0.13 \times 10^{-4}$
4F	irradiated SW-WR	772	411	80-56	20-44	$1.21 \pm 0.03 \times 10^{-3}$
5F	irradiated SW-WR	828	442	79-40	21-60	$7.97 \pm 0.08 \times 10^{-3}$
6F	irradiated SW-WR	798	426	80-49	20-51	$3.00 \pm 0.05 \times 10^{-3}$

[a]Error limits are 2σ
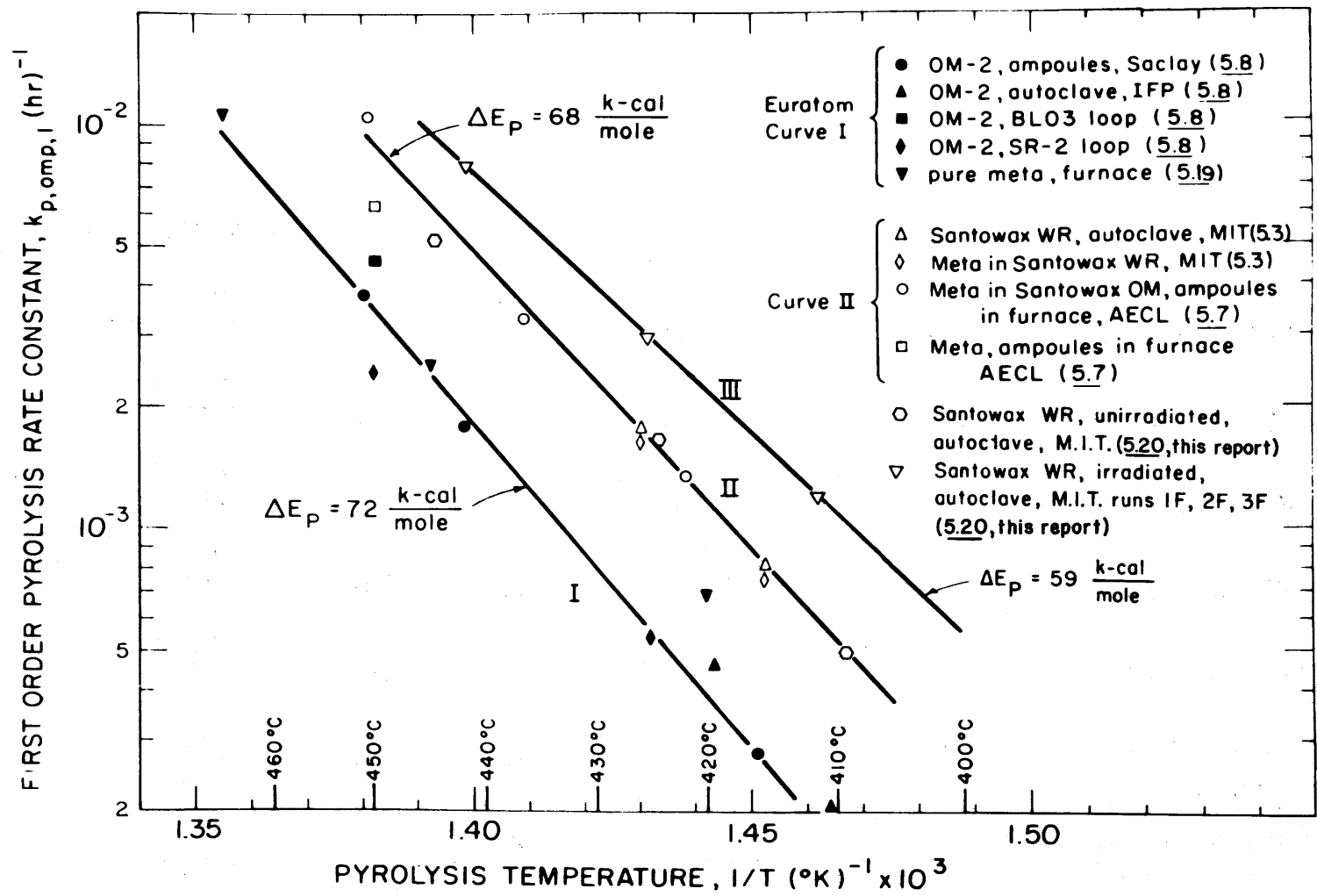
FIGURE 1.6 PYROLYSIS AND RADIOPYROLYSIS RATES OF META TERPHENYL AND META - RICH TERPHENYL MIXTURES

Table 1.9

Results of Santowax OM and WR Irradiations
at High Temperatures in the M.I.T. Loop in Fuel Position 1

March 9, 1967 - February 16, 1968

Run No.	Coolant	Temperature, °F Irradiation Capsule	Loop Effective	Average Dose Rate (watt/gm)	Concentration w/o OMP	DP	HB	Degradation Rates[a] G(-omp)	G*(-omp)	G(-HB)	f_N
21	SW-OM[b]	750	734	0.024	78.0	22.0	9.0	0.48 ±0.05	0.61 ±0.06	0.41 ±0.03	0.36
22	SW-OM	800	781	0.023	78.5	21.5	8.9	1.15 ±0.09	1.47 ±0.11	0.67 ±0.08	0.36
23	SW-OM	700	684	0.022	80.6	19.4	7.7	0.36 ±0.05	0.44 ±0.06	0.35 ±0.08	0.36
23A	SW-OM	700	685	0.057	81.8	18.2	6.5	0.33 ±0.03	0.40 ±0.04	0.30 ±0.02	0.36
24	SW-OM	750	730	0.057	80.6	19.4	7.1	0.38 ±0.03	0.47 ±0.04	0.35 ±0.02	0.36
25	SW-OM	800	781	0.056	76.0	24.0	7.7	0.68 ±0.05	0.89 ±0.06	0.55 ±0.03	0.36
26	SW-WR	700	685	0.068	82.5	17.5	9.1	0.33 ±0.02	0.40 ±0.03	0.29 ±0.02	0.38
27	SW-WR	750	739	0.065	79.3	20.7	8.2	0.39 ±0.03	0.49 ±0.04	0.32 ±0.02	0.38
28	SW-WR	800	790	0.065	76.3	23.7	10.6	0.64 ±0.04	0.83 ±0.05	0.58 ±0.04	0.38

[a] Error limits are 2σ

[b] SW = Santowax
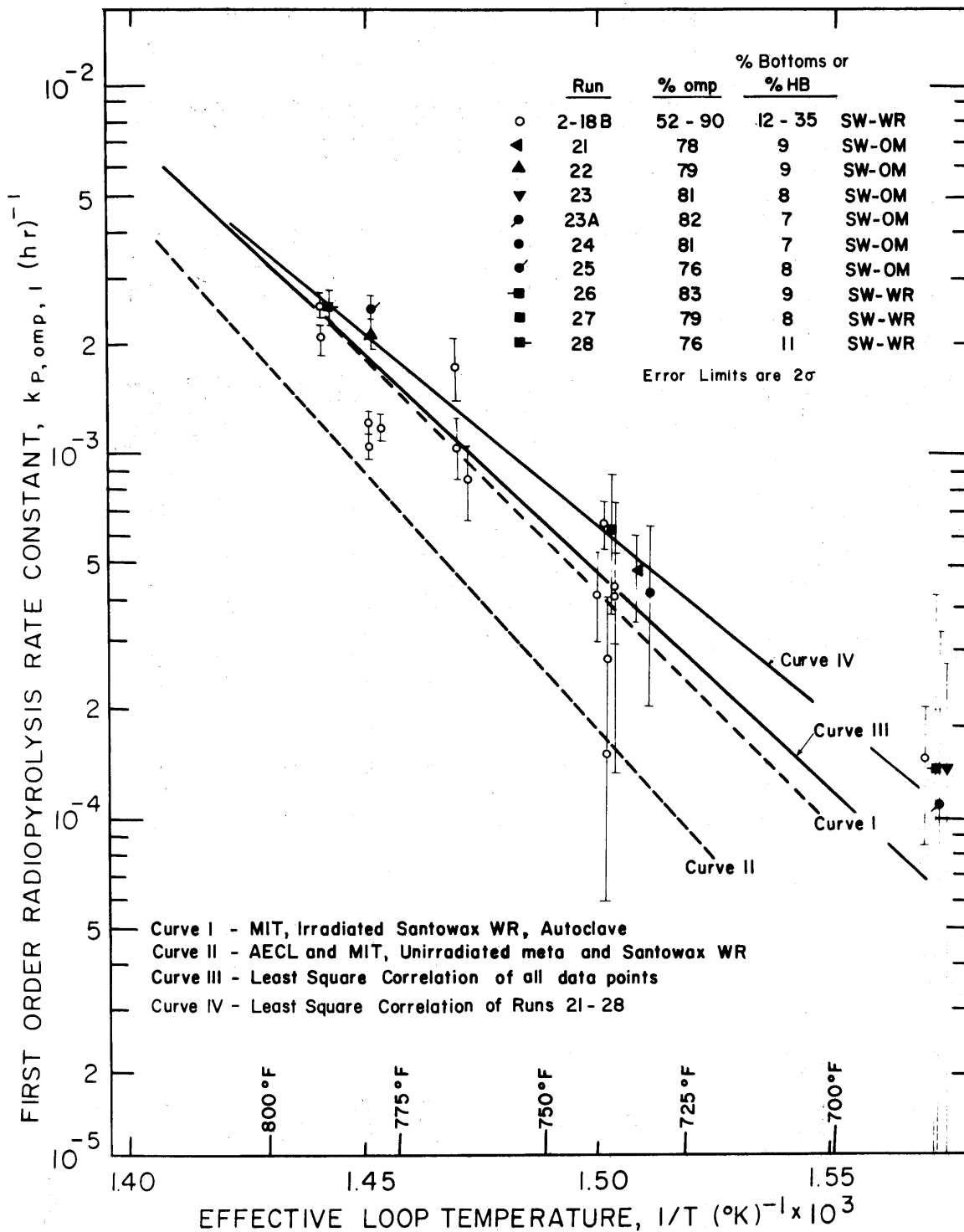
FIGURE 1.7 CORRELATION OF FIRST ORDER RADIOPYROLYSIS
RATE CONSTANTS — MIT RUNS

The activation energy for radiopyrolysis indicated by this line is $\Delta E_{P,1}$ = 48 $\pm$ 7 (2σ) kcal/mole. Also included in this figure are open data points representing all the previous M.I.T. high temperature irradiations of Santowax OMP and WR plus three other curves as follows:

Curve I   Radiopyrolysis rate constants from M.I.T. post-irradiaion pyrolysis of irradiated Santowax WR (from Curve III Figure 1.6), $\Delta E_{P,1}$ = 59 $\pm$ 2 (2σ) kcal/mole

Curve II   Pyrolysis rate constants of unirradiated meta terphenyl and Santowax WR (from Curve II Figure 1.6), $\Delta E_{P,1}$ = 68 $\pm$ 4 (2σ) kcal/ mole

Curve III   Radiopyrolysis rate constants - least-square fit of all M.I.T. data points for Santowax OM and WR, $\Delta E_{P,1}$ = 54 $\pm$ 9 (2σ) kcal/mole.

Except for the three open data points at an effective loop temperature of 1.45 x 10^{-3} ($^\circ$K)$^{-1}$ which represent irradiations made at a fast neutron dose fraction, f_N = 0.07, the irradiations were made with f_N between 0.36 and 0.40.

For the irradiation conditions employed, the following conclusions can be drawn:

(1)   There is no significant difference in the radio-pyrolysis rates for Santowax OM and Santowax WR (Curve IV correlates the nine recent irradiations of these two coolants)

(2)   There is no significant difference in radiopyrolysis rates of Santowax OM with a change in dose rate of irradiation by a factor of about 2.5 (compare Runs 21,22, 23 with 23A, 24, 25).

(3)   Thermal decomposition (radiopyrolysis) rates of irradiated coolant are significantly higher than those of the unirradiated coolant.

(4) Within the statistical limits of measurements, radiopyrolysis rates measured by post-irradiation autoclave pyrolysis experiments agree with those determined by steady-state in-pile irradiation.

(5) Comparison of the results of Runs 26, 27 and 28 and earlier M.I.T. irradiations of Santowax WR does not reveal a significant correlation between radiopyrolysis and coolant composition.

The standard errors on the radiopyrolysis rate constants, k_p, for the M.I.T. in-pile irradiation are about $\pm$ 90% at 370°C, $\pm$ 25% at 400°C and $\pm$ 10% at 430°C. The large uncertainty limits at lower temperatures are due to the extremely small effect of radiopyrolysis in the presence of the predominating effect of radiolysis.

Based on the results of the M.I.T. high temperature irradiations, the best estimate of first-order radiopyrolysis rate constants for irradiated Santowax OM or WR is

$$k_{P,omp,1}(T) = \exp(a - \Delta E_p/RT) \quad (hr)^{-1} \qquad (1.15)$$

where

$$a = 34 \pm 7 \ (2\sigma)$$
$$\Delta E_p = 54 \pm 9 \ (2\sigma), \ kcal/mole$$
T is the temperature, $^\circ$K
R is the gas constant, 1.987×10^{-3} kcal/mole-$^\circ$K

Capsule irradiations of pure ortho terphenyl and pure meta terphenyl by AECL (1.14) at dose rates from 0.1 to 5 watts/gram have indicated that at high temperatures ($>350^\circ$C), the radiolytic decomposition rate of these pure isomers is (1) dose-rate dependent, (2) significantly higher for pure ortho terphenyl than that for pure meta terphenyl and (3) independent of the type of radiation (e.g., fast neutron and

gamma radiations). Comparisons of these experimental results
with the results of high temperature irradiations of Santowax
OM by AECL (1.6, 1.15) at dose rates of 0.1 and 0.3 watts/gram
and with the results of the present series of steady-state
irradiations of Santowax OM at M.I.T. at in-pile dose rates of
0.5 and 1.3 watts/gram (average dose rates to total coolant of
0.02 and 0.06 watts/gram) lead to the following conclusions:

(1) The high temperature radiation stability of ortho
     terphenyl in mixed terphenyl coolants is greater
     than for the pure ortho isomer.

(2) The dose rate effects indicated by the pure iso-
     mers (especially ortho terphenyl) do not have a
     significant effect on the degradation of Santo-
     wax OM in the temperature range of 600°F and 800°F
     (300°C and 425°C), which is of interest for
     organic-cooled nuclear reactors.

(3) An activation energy of radiolysis, ΔE_R, of 1
     kcal/mole is reasonable for use in predicting the
     total rate of degradation (radiolysis and radio-
     pyrolysis) for Santowax OM at temperatures up to
     about 800°F.

The above conclusions are also applicable to meta-rich
terphenyl as indicated by Mason and Timmins (1.5).

Further, comparison between Santowax OM (ortho-rich)
and Santowax WR (meta-rich) both irradiated at approximately
the same conditions shows that the stabilities of the ortho
and meta terphenyl isomers in an ortho-rich mixture of ter-
phenyl are about equal to those in a meta-rich mixture of
terphenyl. The greater degradation rate reported for pure
ortho terphenyl (1.14) suggests that the presence of other
terphenyl isomers retards the radiolytic degradation rate of
ortho terphenyl as compared to the radiolytic degrada-

tion rate in pure ortho terphenyl.

1.5 Physical Properties and Heat Transfer

Densities of samples taken during steady-state irradiations of Santowax OM were measured by means of calibrated pycnometers over the temperature range from 400°F to 800°F. The pyconometers were pressurized with nitrogen and immersed in a high temperature fused-salt bath. Viscosities of the same samples were measured by means of semi-micro capillary viscometers of the Oswald type. Table (1.10) summarizes the results of these measurements.

Table 1.10

Summary Of Density And Viscosity
Measurements of Santowax OM

%HB	400°F		600°F		800°F	
	$\rho(\frac{gms}{cc})$	$\mu(cp)$	$\rho(\frac{gms}{cc})$	$\mu(cp)$	$\rho(\frac{gms}{cc})$	$\mu(cp)$
0	0.951	0.79	0.855	0.32	0.759	0.18
10	0.965	0.93	0.871	0.41	0.778	0.24
20	0.979	1.15	0.888	0.48	0.797	0.28
30	0.993	1.40	0.904	0.58	0.815	0.34

The values shown in Table 1.10 represent smoothed values obtained from measurements of coolant samples taken during Runs 19A through Run 25 of the steady-state irradiation of Santowax OM. These values are in good agreement with measurements of density and viscosities of Santowax OM as reported by other laboratories (1.11, 1.12).

For each sample measured, the density was found to be linearly dependent on temperature. Among samples of various

High Boiler (HB) concentration, the density increases with increasing HB concentration. Based on the M.I.T. density measurements, an empirical correlation of the effect of both temperature and HB concentration on the density of Santowax OM is given as follows:

$$\rho = 1.143 + 0.91 \times 10^{-3}[HB]$$
$$-\left[4.8 \times 10^{-4} - 1.2 \times 10^{-6}[HB]\right][T]$$

$$(1.16)$$

where

ρ is the sample density, gm/cc

HB   is the High Boiler concentration, w/o

T   is the sample temperature, $^{\circ}F$

This correlation correlates the densities of all the irradiated Santowax OM samples measured at M.I.T. within 1%.

Both the viscosity and density of Santowax OM were found to be slightly lower (about 5%) than those of Santowax WR (1.5).

The viscosities of all irradiated samples were found to follow the relation

$$\mu = \mu_{o} \exp\left(-\Delta E/RT\right) \qquad\qquad (1.17)$$

where

μ is the sample viscosity, centipoise

μ_o is a constant for given sample

ΔE is an "activation energy," kcal/mole

The activation energy, ΔE, for Santowax OM ranges from 4.2 to 4.6 kcal/mole and that for Santowax WR ranges from 4.3 to 4.8 kcal/mole (1.5). The difference in ΔE, ρ, and μ between Santowax OM and Santowax WR may be related to the

ratio of LIB/HB. At the same temperature and same ter-
phenyl concentration during the irradiation, the LIB/HB
ratio of Santowax OM has been found to be higher than that
of Santowax WR. The viscosity was found to increase with
increasing HB concentration. However, at the same HB
concentration, the viscosity of either Santowax OM or
Santowax WR is smaller for samples irradiated at higher
temperatures (>350°C). Again, this may be due to LIB/HB a
ratio, which increases with increasing temperature of irradi-
ation.

The number average molecular weight (MW_N) of irradiated
Santowax OM was found to increase from about 230 ± 5% at
7% HB to about 270 ± 5% at 26% HB. These values are about
5-10% lower than the corresponding values for Santowax
WR (1.5). The number average molecular weight of the
High Boiler fraction of the coolant was found to depend on
the irradiation temperature. It varied between 510 to 570
for low temperature irradiations (<350°C) and was about
470 for high temperature irradiations (>350°C). These
values are about 5-10% smaller than the corresponding values
for Santowax WR. Thermal cracking of the heavy molecules
at higher temperatures (>350°C) of irradiation may be the
reason for the lower MW_N in the HB fraction, and the larger
ratio of LIB/HB in Santowax OM may account for the smaller
value of MW_N compared to that of Santowax WR.

Heat transfer measurements were made by means of a
tubular test heater installed in the out-of-pile section
of the loop. Two test heaters (TH7 and TH8) of similar
design (stainless steel tubing, 1/4-inch OD x 0.020-inch
wall) were used. They were heated by electric current and
could produce up to 400,000 Btu/ft^2-hr heat flux from the
wall to the coolant. The heat transfer coefficients of the
coolant were based on the equation

$$U = \frac{Q/A}{T_{w,i} - T_B} \quad Btu/hr\text{-}ft^2\text{-}°F \qquad (1.18)$$

where

Q/A is the heat flux into the coolant, $Btu/hr\text{-}ft^2$

$T_{w,i}$ is the average inside wall surface temperature, $°F$

T_B is the average bulk temperature of coolant, $°F$.

Test Heater TH7 was used during the irradiation of Santowax OM. Heat transfer measurements made in April, 1967 showed a decrease of heat transfer coefficient to about 70% of that calculated using McAdam's correlation (1.13). A scaling heat transfer coefficient of about 2600 $Btu/hr\text{-}ft^2\text{-}°F$ was indicated. Previous heat transfer measurements made up to April, 1966 on this same test heater had shown no evidence of fouling (1.5). No heat transfer measurements were made during the one year period from April, 1966 to April, 1967 due to modification of the loop irradiation facility. The most likely cause of scale formation on the test heat wall is the introduction of impurities to the loop system during this period when modifications of the system were being performed.

TH7 was replaced by TH8 during the remaining Santowax WR irradiations. Extensive heat transfer measurements were made over a temperature range from $630°F$ to $800°F$, High Boiler concentrations from 8% to 20.5%, Reynolds Numbers from 3×10^4 to 1.3×10^5 and Prandtl Numbers from 5.2 to 8.2. The heat transfer data can be correlated to within $\pm$ 10% by the forced convection equation of McAdam's as expressed by Equation (1.19)

$$Nu = 0.023 \ Re^{0.8} Pr^{0.4} \qquad (1.19)$$

Figure 1.8 shows the experimental data and correlation using Equation (1.19). The dashed lines indicate the 10% deviation
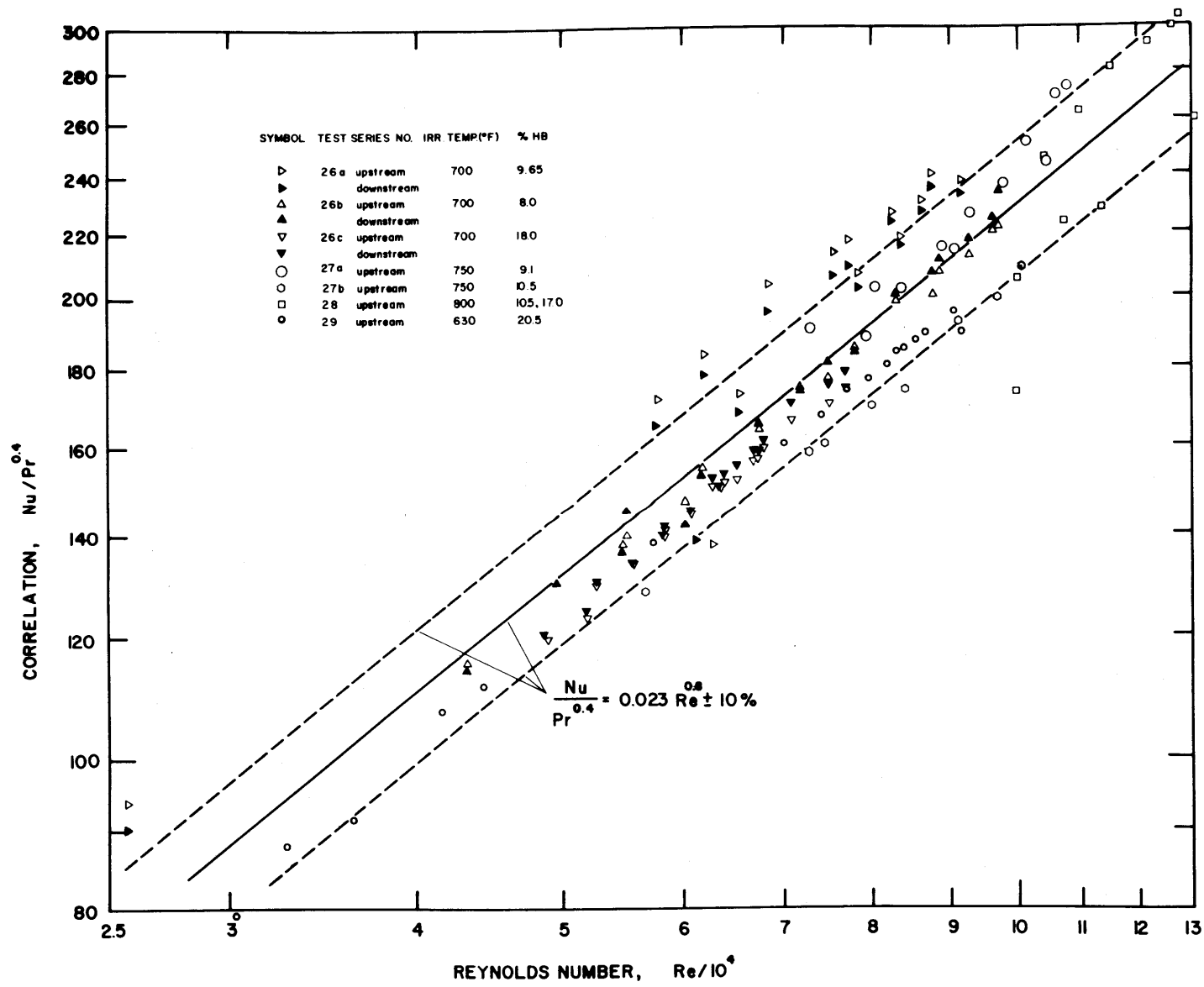
FIGURE 1.8 CORRELATION OF FORCED CONVECTION HEAT TRANSFER DATA

limits.

1.6 Application to Organic Cooled Nuclear Reactors

The information concerning the rates of degradation due to radiolysis and radiopyrolysis can be used to predict the rates of coolant degradation, and required makeup, in nuclear reactors. If the coolant reprocessing system of an organic-cooled reactor is operated using High Boiler distillation, the ultimate formation rate (and therefore removal rate) of HB will be equal to the terphenyl degradation rate - any low and intermediate boilers (LIB) will remain in the system (until converted either back to terphenyl or to HB).

The total terphenyl makeup rate for an organic-cooled reactor in steady-state can be calculated from the following relationships

$$W_{omp} = W_R + W_P \tag{1.20}$$

$$W_R = \frac{G_R(-omp)}{11.65} \, \overline{r}M_C = k_{R,omp,1.7}C_{omp}^{1.7} \, \overline{r}M_C \tag{1.21}$$

$$W_P(N) = \frac{M_N C_{omp}}{T_2 - T_1} \int_{T_1}^{T_2} k_{P,omp,1}(T) \, dT \tag{1.22}$$

where

W_{omp} is the time rate of total terphenyl degradation, gms/hr

W_R is the time rate of radiolytic degradation, gms/hr

W_P is the time rate of radiopyrolytic degradation, gms/hr

$W_P(N)$ is the time rate of radiopyrolytic degradation in the Nth zone of the reactor coolant system, gms/hr

$\bar{r}M_C$	is the rate of radiation energy deposition in the coolant, watts
C_{omp}	is the total terphenyl concentration of the coolant, weight fraction
M_C	is the coolant mass contained in the reactor coolant system, grams
M_N	is the mass of coolant in a zone, N, of the coolant system having an inlet coolant temperature T_1 and an outlet temperature T_2
ΔT_j	is a small increment of temperature with average temperature T_j, $^\circ K$
$k_{R,omp,1}(T_j)$	is the radiopyrolysis rate constant for irradiated coolant evaluated at temperature T_j, $(hr)^{-1}$
$k_{R,omp,1.7}$	is the radiolysis rate constant evaluated at the mean temperature of the coolant in the reactor core, $(watt-hr/gm)^{-1}$

As an example, a design of a heavy water moderated, organic-cooled nuclear reactor designed to produce 750 MWe (1.18) will be used. A simplified flow diagram of the coolant system is presented in Figure 1.9; coolant temperature in the various parts of the system are shown. The results of calculations of the coolant makeup rate for reactor outlet temperatures of 750°F and 800°F for coolant with a total terphenyl concentration of 90% are presented in Table 1.11. At a reactor outlet temperature of 750°F, radiolysis accounts for about 2/3 of the total degradation, while for 800°F radiolysis accounts for only about 1/4. Radiopyrolysis in the outlet header is the predominate source of coolant degradation at 800°F.
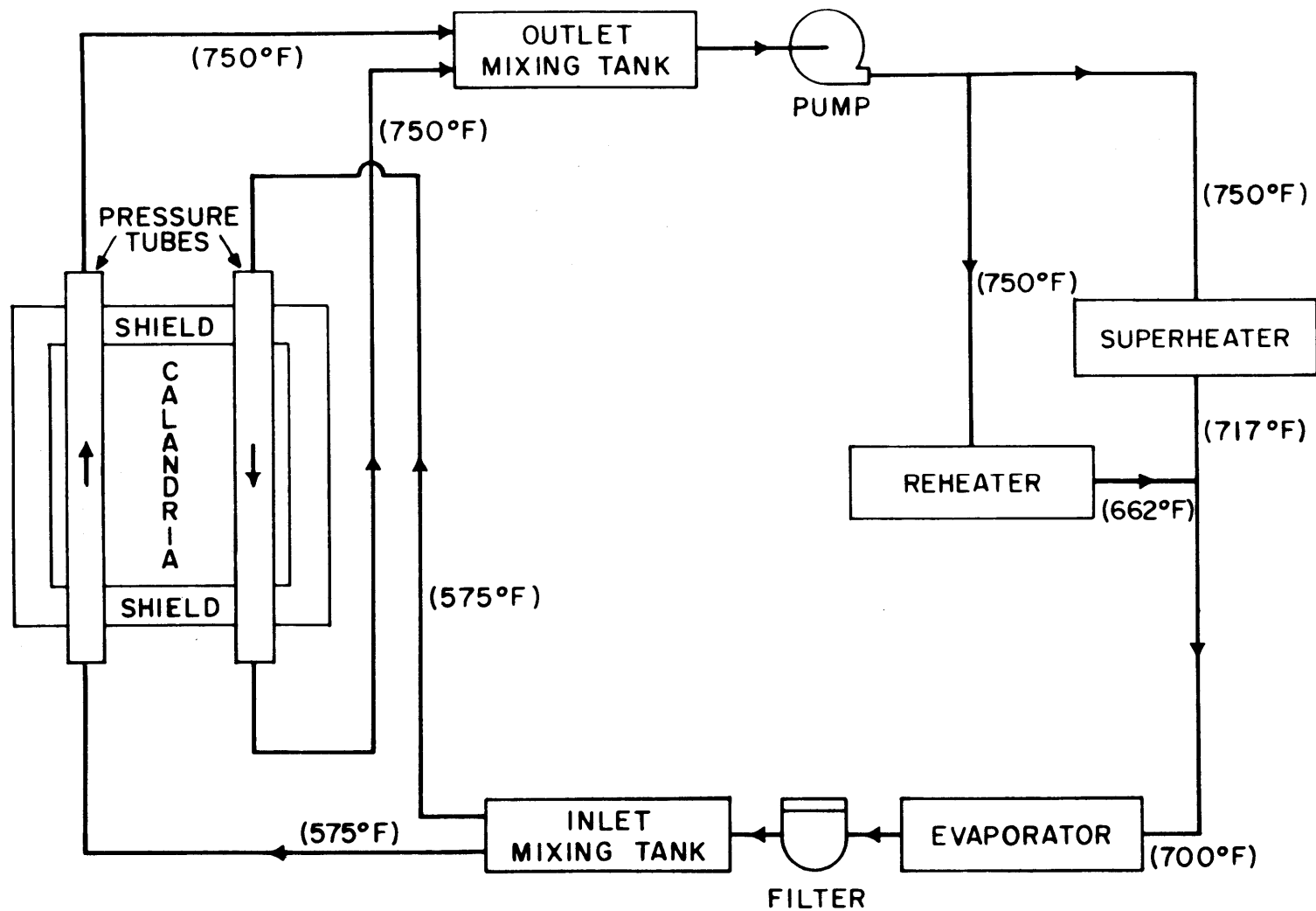
FIGURE 1.9 SIMPLIFIED ORGANIC COOLANT FLOW DIAGRAM – 750 MWE HWOCR

Table 1.11

Calculated Coolant Makeup Rates for 750 MWe HWOCR Demonstration Plant

$$(C_{omp} = 0.90)$$

Zone	Description	Coolant Mass (lbs)	750°F Core Outlet Coolant temperature		800°F Core Outlet Coolant Temperature	
			Temp. (°F)	Total Terphenyl Degradation Rate (lbs/hr)	Temp. (°F)	Total Terphenyl Degradation Rate (lbs/hr)
Radiopyrolysis						
I	Cold leg, inlet header	536,000	575	–	625	4
II	Decay heat loop	43,000	650	1	700	6
III	Reactor core	64,000	575-750	6	625-800	33
IV	Outlet header, hot leg	690,000	750	517	800	2648
V	Superheater	73,000	750-717	38	800-767	189
VI	Evaporator	49,000	700-574	1	750-624	8
VII	Reheater	52,000	750-662	14	800-712	75
	Sub-total (radiopyrolysis)			577		2963
Radiolysis	(radiolysis)			902		930
	Total Makeup Rate			1479		3893
	Coolant Makeup Cost (mills/kwhe) ($0.12/lb coolant cost)			0.27		0.62

Figure 1.10 shows the effect of terphenyl content in the coolant for two reactor outlet temperatures, 750°F and 800°F. Degradation rises rapidly with increasing terphenyl content. However, the coolant viscosity increases as terphenyl content decreases (due to increased HB content). Optimization between the effects of coolant composition on makeup expense versus expenses related to pumping and heat transfer is required to arrive at an economic design.
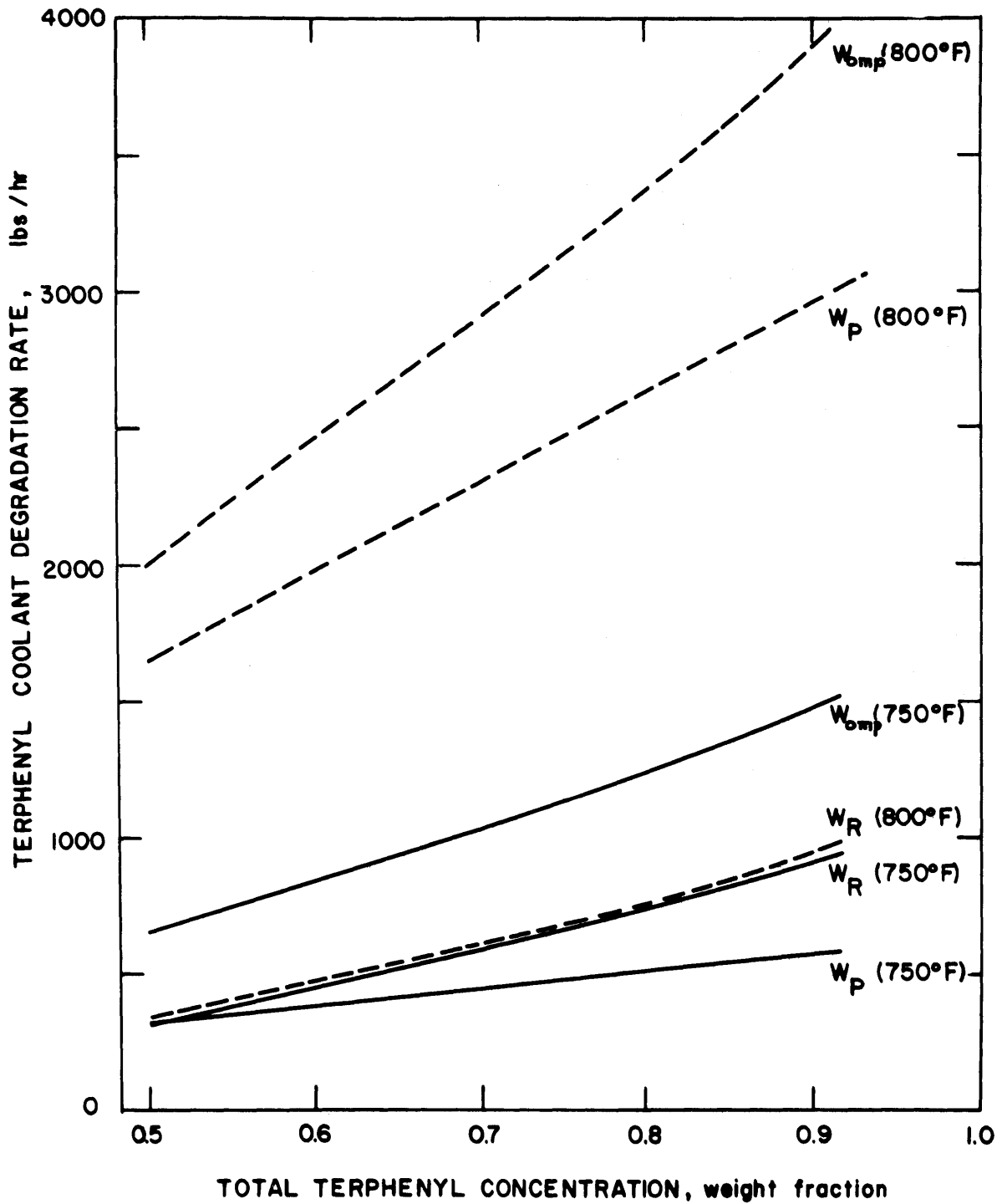
FIGURE 1.10   EFFECT OF COOLANT COMPOSITION AND CORE OUTLET
TEMPERATURE ON TERPHENYL DEGRADATION RATE FOR
ORGANIC-COOLED REACTOR - DEMONSTRATION PLANT

CHAPTER 2

EQUIPMENT AND OPERATION

2.1 Loop Equipment

2.1.1 Introduction

Loop Equipment refers to the equipment enclosing the circulating volume (e.g. in-pile section and irradiation capsule, test heater, trim heater, flow meters, pumps, cooler, and Surge Tank) and supporting instrumentation and control equipment (e.g. temperature recorders, temperature controller, flow rate instrumentation, alarm circuitry, etc.). Most of this equipment has been described in previous M.I.T. reports (2.1, 2.2, 2.3, 2.4), and some is discussed in other chapters of this report. Section 2.1.2 is a directory for finding loop equipment descriptions in this and previous reports.

2.1.2 Summary of References for Descriptions of Loop Equipment

Equipment Name	Period of Use	Reference
Surge Tank	Oct. 1958 – March 1968	(2.1)
Trim Heater	Oct. 1958 – March 1968	(2.1)
Filter	Oct. 1958 – March 1968	(2.1)
Circulating Pumps		
No. 1	Oct. 1958 – March 1968	(2.1)
No. 2	Oct. 1958 – Oct. 1966	(2.1)

2.1.2 Summary of References for Descriptions of Loop Equipment, continued

Equipment Name	Period of Use	Reference
Test Heater		
1 - 7	Oct. 1958 - March 1968	(2.1, 2.2, 2.3, 2.5)
8	July 1967 - March 1968	Present Report, See (2.6) and 3.6.2
Cooler		
1	Oct. 1958 - March 1968	(2.1)
2	Oct. 1958 - Oct. 1966	(2.1)
In-pile Assembly		
1 - 3	Oct. 1958 - June 1967	(2.1, 2.2, 2.4)
4		Present Report See 2.1.3
5		Present Report See 2.1.3

2.1.3 In-pile Sections and Irradiation Capsules

Morgan and Mason (2.1) have given a complete description of the M.I.T. In-pile Loop Facility. Further modifications of the facility up to June, 1966, have been reported in M.I.T. reports (2.2, 2.3, 2.4).

For the period covered in this report, two in-pile sections, No. 4 and No. 5 were used. They were similar in design except for details of the shield plug construction. Figure 2.1 shows the simplified diagram of the assembly of the two in-pile sections. The two in-pile sections were made to fit down the axis of central fuel element (Fuel Position 1) of the MITR, as shown in Figure 2.2. The portions in the

IN PILE SECTION NO. 4   IN PILE SECTION NO. 5

High Density Concrete

Spiral Offset

Bend Offset

Lead

$35\frac{3}{16}$"

$34\frac{3}{8}$"

$8\frac{3}{8}$"

$109\frac{1}{4}$"

3/8"OD x 0.028" Wall Monitor Tube

1.25" OD x 0.035" Wall Aluminum Thimble

$1\frac{1}{16}$" OD x 0.035 Wall Irradiation Capsule

5/8"OD x 0.010" Wall Baffle Tube (inlet)

3/8"OD x 0.028" Wall Monitor Tube

Reactor Core 24"

¢ Fuel

$13\frac{1}{16}$"

Reactor Core 24"

Fuel ¢

$13\frac{11}{32}$"
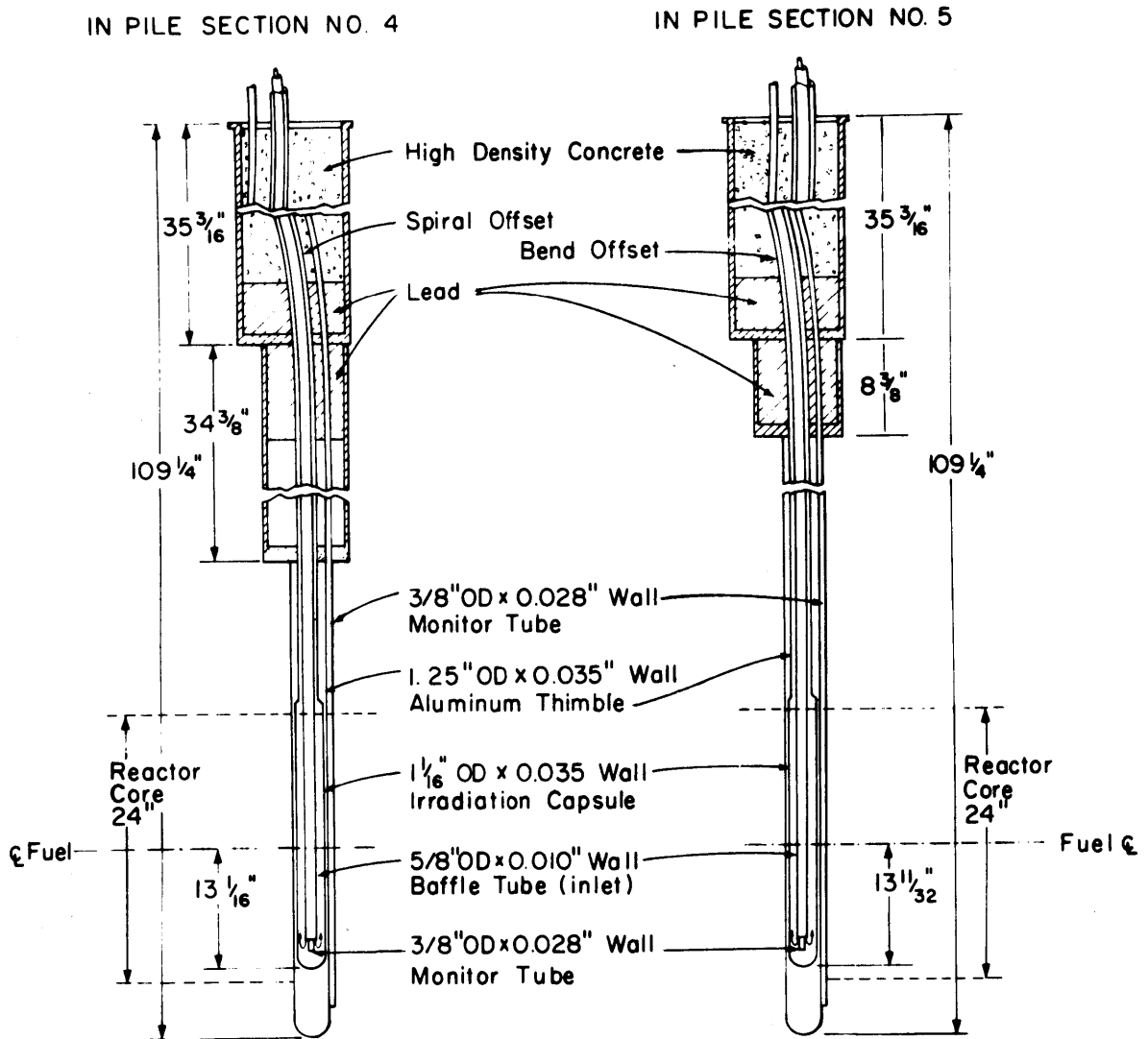
FIGURE 2.1 SIMPLIFIED DRAWING OF IN-PILE SECTION NO. 4 AND NO. 5

1/8" OD 0.015" Wall
Aluminum Leak
Detector Tube

3/8" 0.028" Wall
Aluminum Monitor Tube

1 1/16" OD x 0.035" Wall
304 Stainless Steel
Irradiation Capsule (Outlet)

1/2" Wide
Hold Down Straps

Fuel Plates
(outside plates
contain no fuel)

5/8" OD x 0.010" Wall
321 Stainless Steel
Baffle Tube (Inlet)

3"

3"

3/8" OD x 0.028" Wall
316 Stainless Steel
Monitor Tube

1.25" OD x 0.035" Wall
6061 Aluminum Thimble
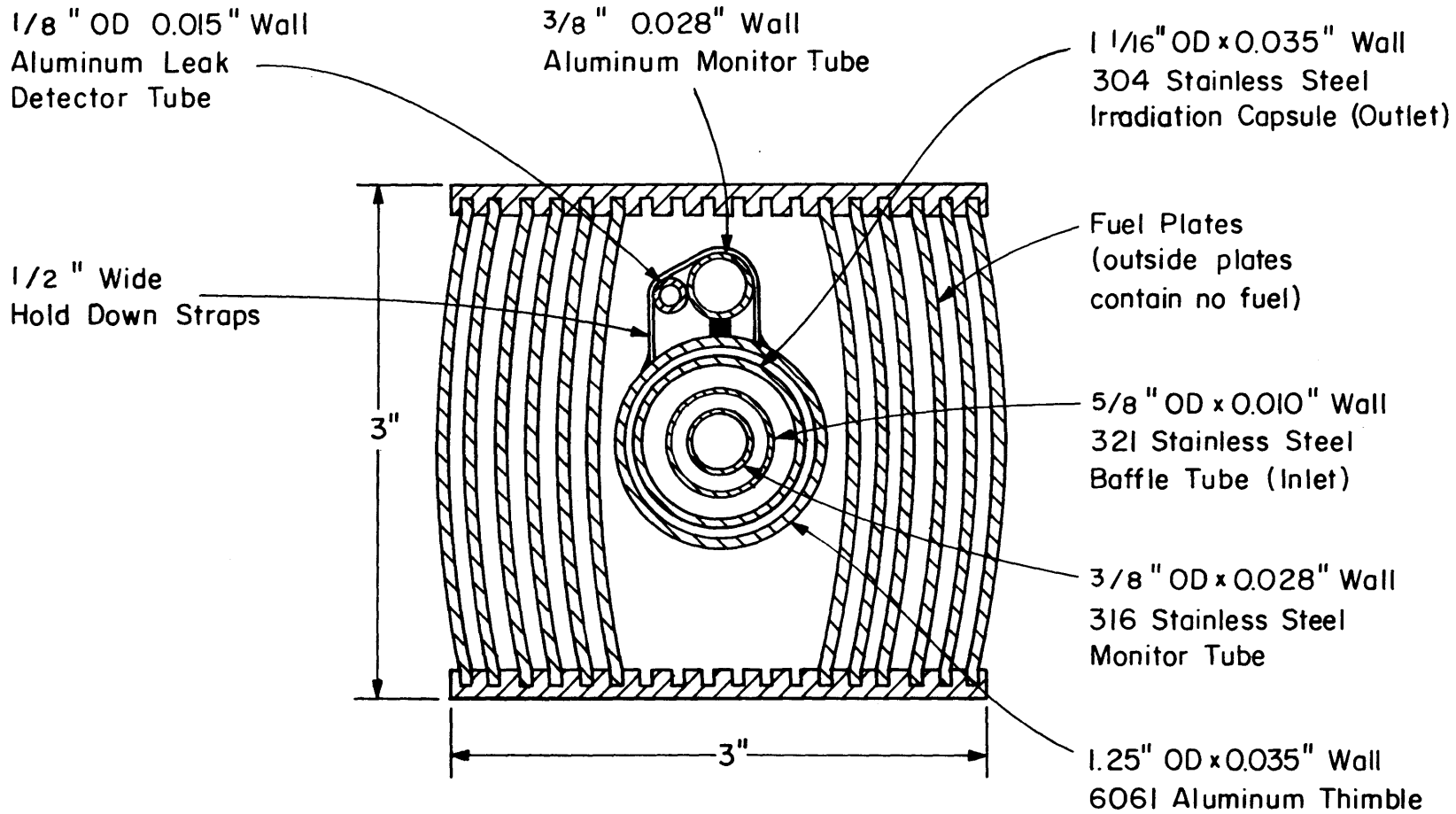
FIGURE 2.2 DRAWING OF FUEL ELEMENT CROSS SECTION WITH
POSITION OF IN-PILE SECTION SHOWN

-2.4-

irradiation field consisted of a 1 1/4 inch-OD x 0.035 inch-wall of 6061 aluminum thimble containing a stainless steel irradiation capsule (1 1/16 inch-OD x 0.035 inch-wall). The aluminum thimble was used to separate the reactor coolant (D_2O) from contact with the hot irradiation capsule. The irradiation capsule assembly, as shown in Figure 2.3, had two annular stainless tubes; a 5/8 inch-OD x 0.010 inch-wall 321 stainless steel baffle tube and a 3/8 inch-OD x 0.028 inch-wall central monitor tube. All these dimensions were identical to the in-pile Section No. 3 as described in an earlier M.I.T. report (2.4), except that the irradiation capsule of In-pile Section No. 3 was installed inside a cadmium-lined sample assembly whereas those in In-pile Sections No. 4 and No. 5 were installed in a partial-plate fuel element as described in M.I.T. reports (2.2, 2.3) and shown in Figure 2.3. The aluminum monitor tube located adjacent to the capsule had a dimension of 3/8 inch-OD x 0.028 inch-wall which was slightly larger than that of In-pile Section No. 3 (5/16 inch-OD x 0.035 inch-wall).

The inlet to the capsule for the organic coolant flowed between the central tube and the baffle tube and the outlet between the 1-1/16 inch-OD capsule wall. From the bottom of the capsule to 26.75 inches above, the volume per unit length of the capsule was calculated to be 10.57 cc/inch. From 26.75 inches up, the corresponding value was reduced to 5.85 cc/inch due to a reduction of the outer 1 1/16 inch-OD stainless steel capsule to 7/8 inch-OD x 0.035 inch-wall stainless steel tube. Beyond 25 inches above the core center-line, the dose to the organic coolant could be considered as negligible. The total active volume of coolant in the in-pile irradiation zone of both In-pile Sections No. 4 and No. 5 was 280 cc. Table 2.1 shows the design and operating speficication of the M.I.T. In-pile Loop for both In-pile Sections No. 4 and No. 5.

Core
Axial
Centerline

1 1/16" OD × 0.035" Wall
304 Stainless Steel
Irradiation Capsule
(Outlet)

5/8" OD × 0.010" Wall
321 Stainless Steel
Baffle Tube (Inlet)

Direction of
Coolant Flow

3/8" OD × 0.028" Wall
316 Stainless Steel
Monitor Tube

1 1/4" OD × 0.035" Wall
6061 Aluminum Thimble

Fuel Element
Assembly Nozzle

13 11/32" In-pile Section No. 5

13 1/16" In-pile Section No. 4

1/2"

1/2"

Note: Aluminum-
monitor tube and
leak detector tube
not shown.

2 1/2"

FIGURE 2.3 SIMPLIFIED ELEVATION CUT-AWAY VIEW OF LOWER
END OF IRRADIATION CAPSULE OF IN-PILE SECTIONS
No. 4 and No. 5 INSTALLED IN MITR FUEL ELEMENT
ASSEMBLY

Table 2.1

Design and Operating Specifications of the

M.I.T. In-Pile Loop

	In-Pile Section	
	No. 4	No. 5
Bulk Temperature	to 800° F	to 800° F
Loop Pressure	to 600 psig	to 600 psig
Material of Construction	Types 304 and 316 Stainless Steel	Types 304 and 316 Stainless Steel
Volume of In-Core Capsule	280 cc	280 cc
Circulating Volume (0" Level in Surge Tank)	5300 cc	5100 cc
In-Pile to Out-of-Pile Volume Ratio	0.05	0.05
Maximum Circulating Flow Rate	2.3 gallons/min.	2.3 gallons/min.
Maximum Test Heater Heat Flux	400,000 Btu/ft^2-hr	400,000 Btu/ft^2-hr
Test Heater Wall Temperature	to 1000° F	to 1000° F
Velocity in Test Heater	to 23 ft/sec	to 23 ft/sec
Specific Dose Rate to Terphenyl Coolant at Axial Center of Reactor in Fuel Position 1	0.32 watts/gm/MW of reactor power	0.35 watts/gm/MW of reactor power
Average Dose Rate to all Circulating Terphenyl Coolant in Fuel Position 1	0.023 watts/gm[a] 0.057 watts/gm[b]	0.067 watts/gm[b]
Total Energy Deposition Rate from Neutrons and Gamma Interactions	115 watts[a] 285 watts[b]	335 watts[b]
Fast Neutron Fraction of Total Dose Rate	0.36	0.38

[a] At Reactor Power Level of 1.94 MW

[b] At Reactor Power Level of 4.85 MW

2.2 Processing Equipment

2.2.1 Definition

Process systems, as defined here, are those systems used to remove organic coolant from the circulating volume, reprocess it, and feed the reprocessed organic to the circulating volume in order to maintain the circulating volume composition at steady-state against degradation. As shown in the following, this includes (a) a device for feeding and bleeding the circulating volume and (b) reprocessing apparatus, in this case a vacuum still, though other processes such as hydrocracking could be tested.

```
┌──────────────┐      ┌──────────────┐      ┌──────────────────┐
│     Loop     │─────→│  Feed and    │─────→│  Reprocessing    │
│  circulating │      │    Bleed     │      │   Apparatus      │
│    volume    │←─────│   Device     │←─────│ (Distillation)   │
└──────────────┘      └──────────────┘      └──────────────────┘
```
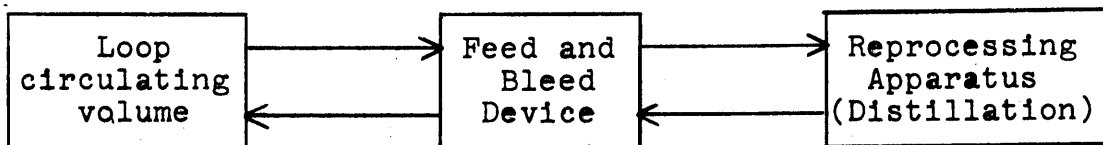
Flow Diagram of Processing System

Two feed and bleed devices have been used at this project: (1) Single Capsule System, described in Section 2.2.2, used for Run 19A currently reported and all previous degradation runs reported by M.I.T., limited to low degradation rate runs; and (2) The Continuous Sampling and Makeup Systems (S & M I, II) described in Section 2.2.3, used for degradation rate runs (reactor power 5 MW, coolant temperature, 800°F).

The reprocessing method used was high boiler (HB) distillation, The capacity of the apparatus was increased during the period of this report to make possible 5000 gm batch distillations in conjunction with the S & M system processing for high degradation rate runs.

2.2.2 Single Capsule Processing System

In Run 19A (currently reported) and all previous degradation runs (2.1, 2.2, 2.3), feeding and bleeding was accomplished by single capsule method. The capsules had capacities

ranging from 20 to 300 gms.

A capsule processing cycle is described below. The capsule was filled first with processed coolant, and then connected to the sampling position between valves 14 and 16 (refer to Figure 2.4). After the capsule had been warmed with heating tape, the valves connecting the capsule to the loop were opened and the capsule became an integral part of the circulating coolant in the loop. Subsequently the valves were closed off and cooled to freeze the coolant at the valves with dry ice. The capsule was then removed and the coolant in the capsule was emptied out to the distillation flask, flushed and recharged with processed coolant. This cycle was repeated throughout the run. The cycling time and the size of the capsule controlled the coolant concentration. The procedures involved in the cycle were quite tedious and time consuming (about three hours turn-around time). Following the increase in reactor power in November of 1965 from 2 MW to 5 MW, it was evident that the capsule operation would no longer be adequate.

2.2.3 Continuous Sampling and Makeup Systems - (S & M I and S & M II)

The processing rate in the single capsule method was limited by requirements of good mixing and by the maximum tolerable perturbation of loop composition accompanying an instantaneous batch dilution. For degradation runs at high temperature and reactor power of 5 MW, the single capsule method was not adequate.

The S & M systems were designed to make these high degradation rate runs possible. Figure 2.4 shows S & M I, connected to the loop (circulating volume) at values 8 and 6, and Figure 2.5 shows S & M II, connected to the loop at valves 16 and 14. Though differing in some details, both systems have the following essential features:

(1) two positive displacement pumps (one each for sampling and makeup) driven by a common motor;

(2) a timer mechanism actuating the motor for some
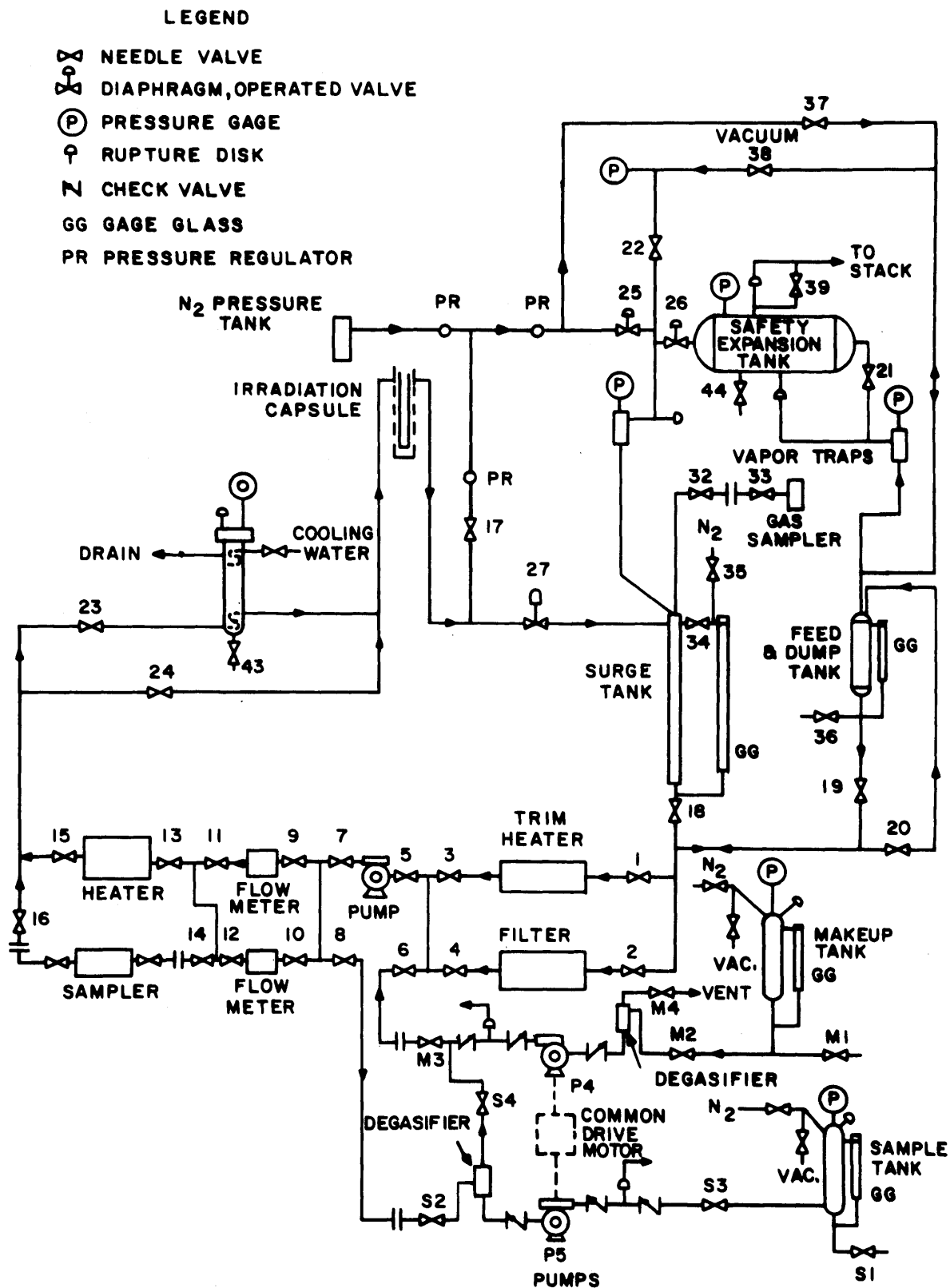
FIGURE 2.4 SCHEMATIC FLOW DIAGRAM OF MIT ORGANIC LOOP WITH
SAMPLING AND MAKEUP SYSTEM I
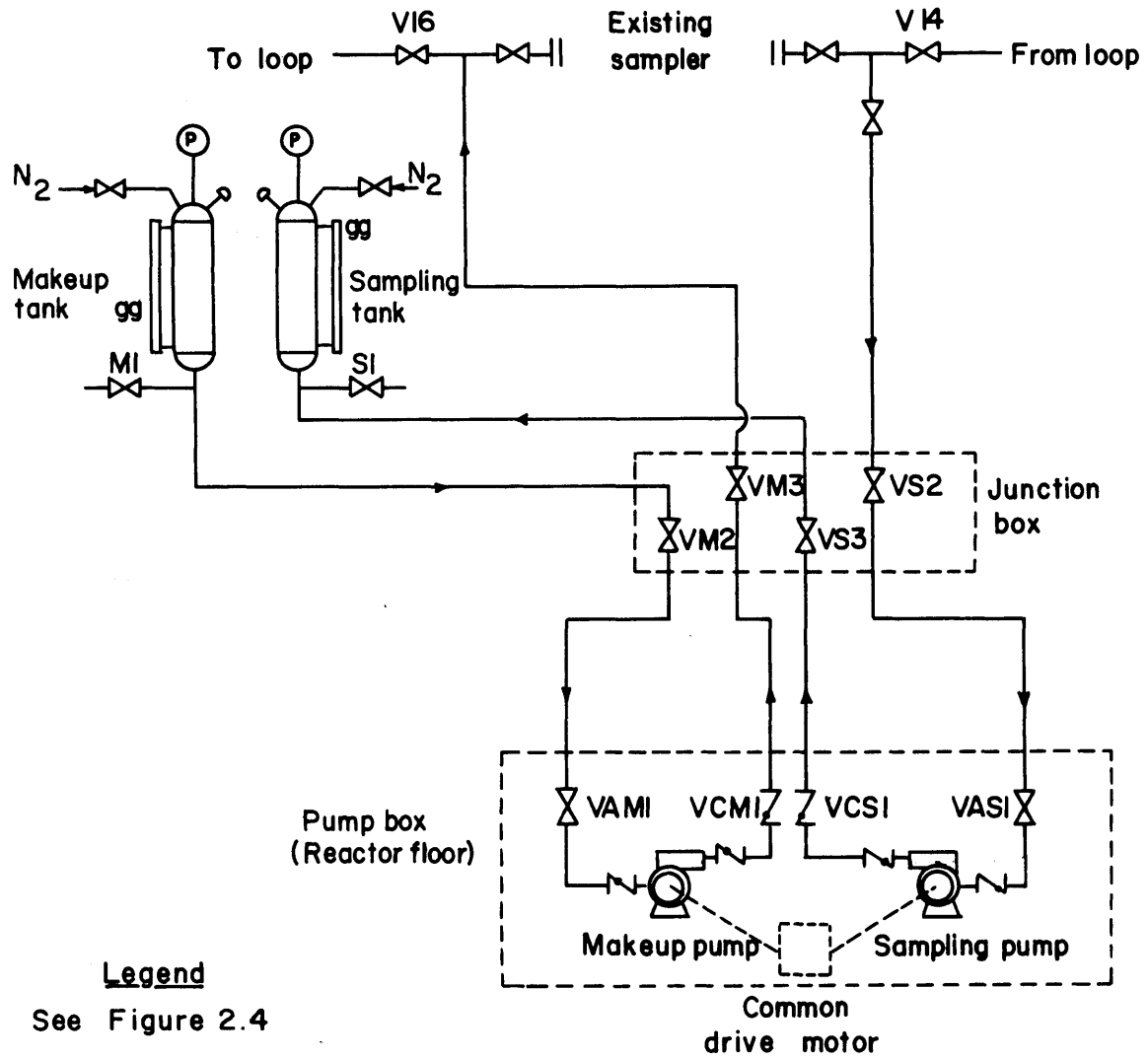
FIGURE 2.5   SCHEMATIC FLOW DIAGRAM OF SAMPLING AND MAKEUP
SYSTEM II, MIT ORGANIC COOLANT LOOP.

preset percentage of a time period;

(3) individually adjustable stroke for each pump's plunger;

(4) a "Sample Tank" of approximately 5000 cc to receive organic coolant from the loop;

(5) a "Make-up Tank" of approximately 5000 cc capacity containing reprocessed organic coolant;

(6) a portable "Transfer Tank", not shown in Figures 2.4 and 2.5, to transfer coolant from the Sampling Tank to distillation apparatus and from the distillation apparatus to the Makeup Tank under nitrogen blanket (see Appendix A5 for operation procedures of these transfers).

S & M I was used for degradation Runs 20A to 25, but was supplanted by S & M II for the remaining Runs (26 to 28) because it was thought that pump performance could be improved by increasing the net positive static suction head. S & M I pumps were mounted on an elevation approximately the same as the bottom of the Sampling and Makeup Tanks, while S & M II pumps were installed on the reactor building floor, approximately 12 feet below the bottom of the Sampling and Makeup Tanks.

Neither S & M system operated satisfactorily. It was necessary to correct for pump mismatch (or failure) by so-called F' and K' (manually operated) transfers (see Appendix A5 for operating procedures). These were manual transfers (without use of pumps) of organic coolant into and out of the circulating volume, via the S & M system plumbing. For the last two runs (27 and 28), in fact, the pumps were abandoned altogether and processing was accomplished entirely by F' and K' transfers.

Table 2.2 lists specifications, manufacturers, etc. for S & M system equipment.

Table 2.2

Equipment Specifications for Sampling and Makeup System

	S & M I	S & M II
Pump		
(1) Manufacturer	American Meter Controls 100 Series, Model No. 110362 Motor Driven Proportioning Pumps	Same as S & M I
(2) Maximum Capacity	0.32 gallon/hour	Same as S & M I
Sampling and Makeup Tanks		
(1) Capacity and Material	6000 cc Stainless Steel	Same as S & M I
(2) Calibration	230 cc/in	Same as S & M I
(3) Pressure Relief Device	Rupture Disc, Stainless Steel, rated 860 psig at 72° F, 550 psig at 800° F	Same as S & M I
(4) Gage Glass	0-25 inches graduated to 1/8 inch, 330 cc holdup below 0" level	Same as S & M I
Transfer Tank		
(1) Capacity and Material	$\sim$6000 cc Stainless Steel	Same as S & M I
Piping		
(1) Material	Stainless Steel	Same as S & M I
(2) Size	1/8 to 3/8 inch O.D.	1/4 to 3/8 O.D.
Valves		
(1) Material	Stainless Steel	Same as S & M I
(2) Manufacturer and Type	(a) Hoke Inc. 440 Series Bellows Seal Valve (b) Autoclave Engineers, Inc., Speed Valve	Same as S & M I
Degasifier		
(1) Material	Stainless Steel	None
(2) Capacity	200 cc	

2.3 Loop Operation

2.3.1 General

Except for the period between February 27, 1967 through June 4, 1967 when the M.I.T. reactor operating power was lowered to 2 MW level, the nominal power level was 5 MW throughout the period covered by this report. The reactor was operated approximately 100 hours each week from Monday morning to Friday afternoon. The organic loop operation had to match closely the schedule of the reactor operation at full power. The loop temperature reached the desired irradiation temperature each Monday at about the same time the reactor power reached the operating full power level, and the loop temperature was lowered to about 400° F over the weekend as soon as the reactor was shut down on Friday.

All the irradiation runs during the period from November 1, 1966 to February 16, 1968 were made at Fuel Position 1, located at the center of the M.I.T. reactor core. No attempt was made to carry out transient operation. The high degradation rate at Fuel Position 1 with reactor operated at 5 MW would shorten the transient period such that only limited number of coolant sampling could be carried out during this period. As a result, the statistical error would be so large that the results of measurement of the degradation rate would be of little significance.

Prior to the steady-state operation, a dilution of the loop coolant was generally required with fresh (unirradiated) terphenyl to bring the terphenyl concentration to within $\pm$ 3% of the desired steady-state level. The processing system was adjusted by means of the pump stroke and a mechanical timer which turned the pump motor on and off at preset values. The coolant then underwent a transient period to allow the terphenyl and the high boiler concentrations to approach the desired steady-state values. As soon as the concentrations had leveled off, the processing rate was fixed and the steady-state condition was established. During the steady-state period, the concentrations were found to be constant within $\pm$2%.

2.3.2 High Boiler (HB) Distillation

The high boiler (HB) distillation was similar in principle to that reported by Sawyer and Mason (2.2) except that the volume of coolant to be distilled per batch was increased to approximately 3000 grams. The apparatus was set up to distill up to 5000 grams per batch at a pressure of 10 mm Hg of nitrogen. The coolant to be distilled was transferred from the Transfer Tank under nitrogen blanket into a cylindrical round bottom Pyrex flask of 5000 cc capacity. The flask was heated in a cylindrical electric heater of 1 KW. The distillate was collected in a 5000 cc round flask which was connected to the vacuum system and the nitrogen system of the distillation unit through a cold trap cooled with liquid nitrogen. For each steady-state run, the cutoff temperatures of the distillation bottom and of the vapor were determined by vapor phase chromotography of the distillation bottom for both para and meta terphenyl contents. The cut-off temperatures were adjusted so that less than 0.2 w/o of the para terphenyl remained in the still bottom after the distillation was completed. This corresponded to cut-off temperatures of approximately 260° C in the vapor entering the condensing arm and 320° C in the distillate bottom for the Santowax OM runs (Runs 19A to 25) and 290° C and 400° C for the Santowax WR runs (Runs 26 to 28) for a coolant batch of around 3000 grams. Total time of distillation was approximately 90 minutes for 3000 grams coolant.

2.3.3 Chronology of Organic Loop Operations - July 1, 1966 to March 31, 1968

A summary of the loop operations is shown in Table 2.3.
A brief description of the loop operations and calorimetry and dosimetry measurements is given in Appendix A8 for the period of July 1, 1966 to March 31, 1968.

Table 2.3

Summary of Loop Operation During Period

of July 1, 1966 to March 7, 1968

Date	Operation	Reactor Power(MW)	Reactor
8/17/66	Calorimetry Series XXII		Stainless Steel Thimble, Fuel Position #1
9/1/67-1/3/67	Installation & Testing of S & M I		
10/8/66	Calorimetry Series XXIII		Stainless Steel Thimble, Fuel Position #1
10/29/66	In-pile Section No. 4 Installed		Fuel Position #1
11/1/66-12/8/66	Run 19	5	Approach to Steady-State, 572° F, Santowax OM
12/9/66-12/30/66	Run 19A	5	Steady-State, 572° F, Santowax OM. C_{omp} = 63%
12/15/66	Foil Dosimetry No. 43C		Aluminum Monitoring Tube, Fuel Position #1
1/3/67	S & M I in operation		
1/3/67-1/10/67	Run 20	5	Approach to Steady-State, 572o F, Santowax OM
1/10/67-1/24/67	Run 20A	5	Steady-State, 572° F, Santowax OM, C_{omp} = 86%
1/24/67-1/30/67	Run 20B	5	Approach to Steady-State, 572o F, Santowax OM
1/30/67-2/21/67	Run 20B	5	Steady-State, 572° F, Santowax OM, C_{omp} = 81%
2/27/67-6/4/67	Reactor Power at 2MW		
3/9/67-3/13/67	Run 21	2	Approach to Steady-State, 750° F, Santowax OM
3/13/67-3/24/67	Run 21	2	Steady-State, 750° F, Santowax OM, C_{omp} = 80%
3/17/67	Foil Dosimetry No. 44C	2	Aluminum Monitoring Tube, Fuel Position #1
4/3/67-4/5/67	Run 22	2	Approach to Steady-State, 800°F, Santowax OM
4/5/67-4/18/67	Run 22	2	Steady-State, 800° F, Santowax OM, C_{omp} = 79%

Table 2.3 (continued)

Date	Operation	Reactor Power(MW)	Remarks
4/25/67 5/15/67	Run 23	2	Approach to Steady-State, 700°F, Santowax OM
5/15/67- 6/4/67	Run 23	2	Steady-State, 700°F, Santowax OM, C_{omp} = 80%
6/4/67	Reactor power at 5MW		
6/4/67- 6/18/67	Run 23A	5	Steady-State, 700°F, Santowax OM, C_{omp} = 82%
6/18/67- 7/7/67	Run 24	5	Steady-State, 750°F, Santowax OM, C_{omp} = 80%
6/21/67	Foil Dosimetry No. 45C		Aluminum Thimble, Fuel Position #13
6/22/67	Calorimetry Series XXIV		Aluminum Thimble, Fuel Position #13
7/12/67- 7/17/67	Run 25	5	Approach to Steady-State 800°F, Santowax OM
7/17/67- 7/28/67	Run 25	5	Steady-State, 800°F, Santowax OM, C_{omp} = 76%
7/28/67	In-pile Section No. 4 Removed		
8/2/67	Foil Dosimetry No. 47		Stainless Steel Thimble, Fuel Position #1
8/3/67- 8/4/67	Calorimetry Series XXV		Stainless Steel Thimble, Fuel Position #1
8/31/67	Foil Dosimetry No. 48		Stainless Steel Thimble, Fuel Position #1
9/7/67- 9/8/67	Calorimetry Series XXVI		Stainless Steel Thimble, Fuel Position #1
10/8/67	In-pile Section No. 5 Installed		Fuel Position #1
11/1/67	Foil Dosimetry No. 49C		Aluminum Monitoring Tube, Fuel Position #1
11/6/67	S & M II in operation		
11/6/67- 11/16/67	Run 26A	5	Approach to Steady-State 700°F, Santowax WR
11/16/67- 12/6/67	Rune 26	5	Steady-State, 700°F, Santowax WR, C_{omp} = 83%

Tables 2.3 (continued)

Date	Operation	Reactor Power(MW)	Remarks
12/18/67-12/27/67	Run 27	5	Approaching to Steady-State, 750°F, Santowax WR
12/27/67 1/15/68	Run 27	5	Steady-State, 750° F Santowax WR, C_{omp} = 80%
1/5/68	Foil Dosimetry No. 50C		Aluminum Monitoring Tube, Fuel Position #1
1/22/68	Run 28	5	Approach to Steady-State, 800°F, Santowax WR
2/6/68-2/16/68	Run 28	5	Steady-State, 800°F, Santowax WR, C_{omp} = 76%
2/16/68-2/22/68	Calorimetry Series XXVII		Aluminum Monitoring Tube, Fuel Position #1
2/22/68-2/23/68	Foil Dosimetry No. 51C		Aluminum Monitoring Tube, Fuel Position #1
2/24/68	In-pile Section No. 5 Removed		
2/28/68	Foil Dosimetry No. 52C		Stainless Steel Thimble, Fuel Position #1
2/26/68	Calorimetry Series XXVIII		Stainless Steel Thimble, Fuel Position #1
3/6/68-3/7/68	Calorimetry Series XXIX, XXX		Stainless Steel Thimble, Fuel Position #1

2.4 Autoclave Pyrolysis Experiment

2.4.1 Introduction

Earlier M.I.T. reports (2.3, 2.4) showed discrepancy between M.I.T. experimental data and Euratom data for the autoclave pyrolysis of unirradiated meta-rich terphenyls (e.g. Santowax WR and OM-2). Although M.I.T. data agreed quite well with those of AECL, they were higher than Euratom data by at least a factor of three. Furthermore, very few autoclave pyrolysis experiments with irradiated coolant had been conducted. Consequently, additional autoclave pyrolysis experiments of meta-rich terphenyls (e.g. Santowax WR) were performed to establish more clearly the pyrolysis rates of unirradiated and irradiated coolants.

2.4.2 Equipment

The autoclave pyrolysis apparatus was built at M.I.T. to measure the pyrolysis rate of the unirradiated terphenyl mixtures and the radiopyrolysis rate of the irradiated terphenyl mixture. Mason, Timmins, et. al. (2.4) have described in details the apparatus and its operation. Therefore only brief description will be given here except where modifications have since been made.

The autoclave reactor vessel was the bolted closure type (Model BC-300, Autoclave Engineers, Erie, Penn.) provided with two openings which permitted charging and sampling of the liquid and gaseous samples. No provision was made for stirring the sample in the autoclave. But mixing, if required, could be achieved by bubbling nitrogen into the vessel through the liquid sampling line. The schematic diagram of the pyrolysis apparatus is shown in Figure 2.6. All parts and fittings of the system were made of stainless steel and leak-checked at 600 psi. The autoclave rested inside a salt bath containing a eutectic mixture of 7% $NaNO_3$, 40% $NaNO_2$ and 53% KNO_3. Five Chromolox heaters (1 KW each) were mounted around the tank containing the salt bath and an additional heater (0.27 KW)
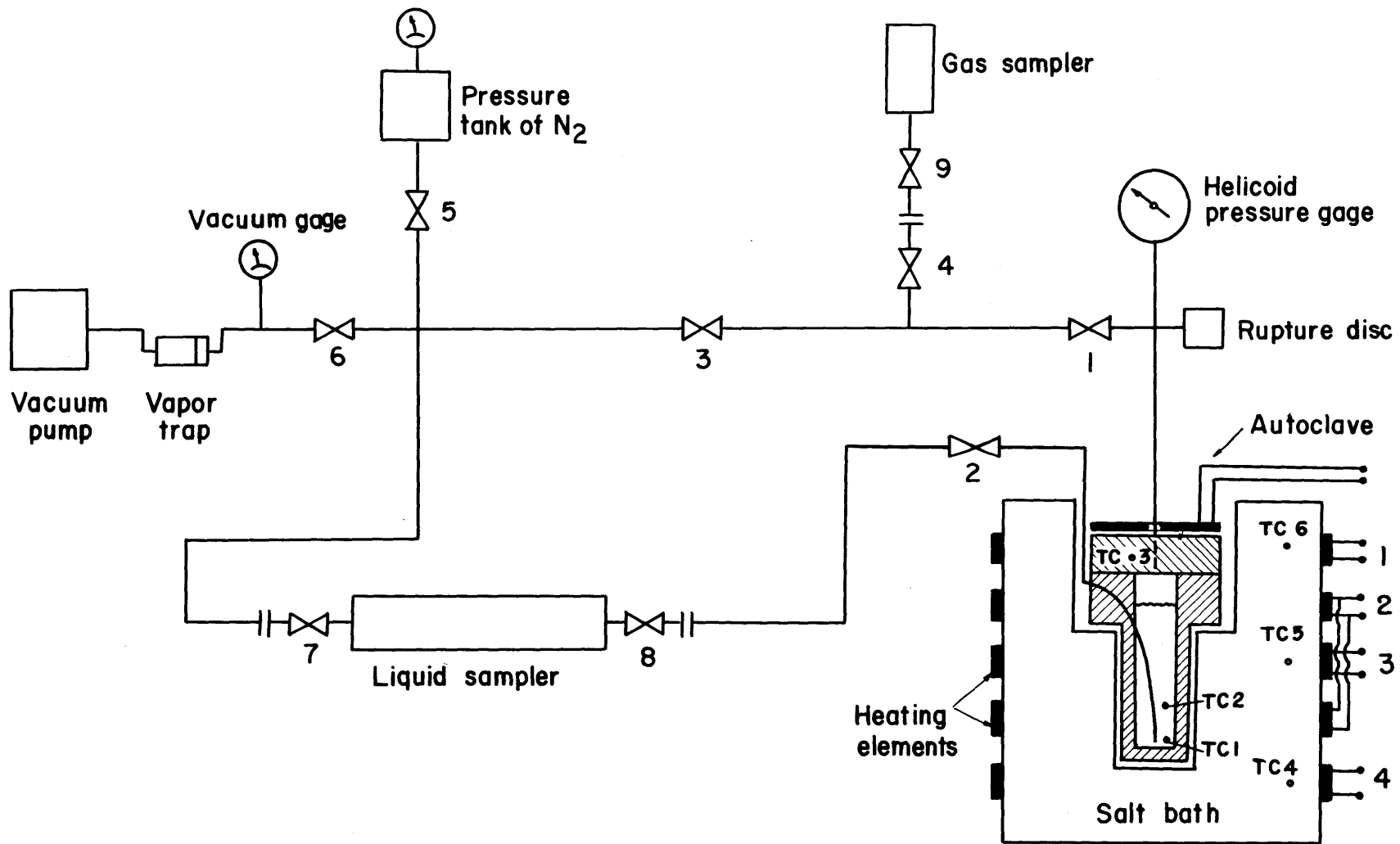
FIGURE 2.6   SCHEMATIC   DIAGRAM   OF   PYROLYSIS   APPARATUS

was placed on top of the autoclave (see Figure 2.6). All these heaters were connected to Variacs in order to have the best uniform temperature in the autoclave.

Temperature was controlled by a Pyr-O-Volt controller (Honeywell Model No. 105R212-PS-26) connected to heater No. 3 and monitored by an Iron-Constantan at position 5 in the salt bath. Temperatures at six different places in the salt bath and the autoclave were recorded by a Bristol's recorder (Model 64A-24P4570-21) which had a range of $500-1000^{\circ}$ F and a sensitivity of 20 microvolt (approximately 1° F).

A temperature safety cut-off was provided by the same recorder which could turn off heater No. 3 by means of a relay. The cut-off temperature was normally set at 20° F above the nominal temperature of the pyrolysis experiment.

2.4.3 Operation

Before charging the autoclave with terphenyl mixture, all parts of the system were evacuated and purged several times with prepurified nitrogen. The organic sample was then charged into the autoclave by means of a charging cylinder connected to valve No. 2. After charging, the system was pressurized with prepurified nitrogen to about 100 psi.

Owing to the holdup in the line from the autoclave to the liquid sampler (approximately 1 cc), two samples of approximately 3 cc each were taken successively and only the second one was representative of the organic liquid in the autoclave.

The liquid samples were analyzed by vapor phase chromatography. At least four analyses were made on two aliquots prepared from each sample.

2.4.4 Chronology of the Autoclave Pyrolysis Experiments

A total of six runs were made using the autoclave pyrolysis apparatus described in the previous section. For all these runs, Santowax WR was used. Three of the runs were made with unirradiated coolant and the rest with irradiated coolant using the coolant samples taken during Run 26 and Run 27.

(See Section 2.3.)

Run 1F began on January 15, 1968 using unirradiated Santo-
wax WR at an average temperature of 796 $\pm$ 3° F. Before charg-
ing the autoclave system, the coolant was degassed by several
thermal cycles under nitrogen pressure of about 2 mm Hg. In
each cycle, the coolant was heated slowly until it was com-
pletely melted and then cooled gradually to room temperature.
This run lasted about 160 hours and the total terphenyl con-
centration was reduced to 70% from an initial value of 91%.
A total of eight samples were taken during the run.

Run 2F was made at an average temperature of 833 $\pm$ 2° F
using the same unirradiated Santowax WR as Run 1F. The run
began on January 24, 1968 and lasted about 85 hours. Eight
samples were taken and the terphenyl concentration was re-
duced from 91% to 57%.

Run 3F was made at an average temperature of 769 $\pm$ 2° F
using the same unirradiated Santowax WR as the two previous
runs. The run lasted 547 hours starting from February 8, 1968.
Twelve samples were taken and the terphenyl concentration
changed from 91% to 69%. Run 3F concluded the series on un-
irradiated Santowax WR.

Run 4F was the first of the three runs made on irradiated
Santowax WR. The coolant used was obtained from coolant sam-
ples of Run 26 and Run 27 which had a terphenyl concentra-
tion of 80% and a high boiler concentration of 9%. No de-
gassing procedure was done on the coolant prior to charging in
order to retain the same quality as that used in the loop.
The run was started on March 7, 1968 and lasted about 303 hours.
The average temperature was 772 $\pm$ 2° F except for four hours
following the first sample where a temperature drop of 10° F
was observed due to a failue of the fuse on the control heater.
No significant change was noted in decomposition rate because
of the relatively lower temperature of the run. The terphenyl
concentration changed from 80% to 56% during this run.

Run 5F was made at an average temperature of 828 $\pm$ 3° F.

It was started on March 26, 1968 and lasted about 83 hours. An increase in temperature of 8° F which lasted five hours occurred between sample 5F-4B and 5F-5A owing to a failure of the fuse on heater No. 4. Again no appreciable change in decomposition rate was noted. During this run, the terphenyl was degraded from an initial concentration of 79% to a final of 40%.

Run 6F began on April 3, 1968 and lasted about 160 hours at an average temperature of $798 \pm 3^\circ$ F. Eight samples were taken during the run and the terphenyl concentration changed from 80% to 49%. This concluded the series on irradiated Santowax WR.

CHAPTER 3

PHYSICAL PROPERTIES AND HEAT TRANSFER

3.1 Introduction

The physical property measurements on irradiated and unirradiated ortho-rich terphenyl at M.I.T. include density, viscosity, number average molecular weight of coolant and highboiler samples. Thermal conductivity, specific heat, vapor pressure or gas solubility measurements have not been made due to lack of equipment and manpower. Melting point of the irradiated coolant has not been measured since all of the coolant removed from the loop was in the form of viscous dark liquid at room temperature.

Heat transfer measurements were made with Santowax OM at bulk temperatures varying from 560° F to 785° F and at flow velocities from 9 ft/sec to 20 ft/sec. Scale buildup on the Test Heater (TH7) was indicated by correlating the results of measurement with Wilson method prior to Run 23. Subsequent heat transfer measurements were made between Run 23 and Run 25 covering a period of about a month at coolant temperatures ranging from 700° F to 790° F. No significant further buildup of scale on Test Heater wall was found.

A new Test Heater (TH8) was installed prior to the irradiation of Santowax WR (Runs 26, 27 and 28). Intensive heat transfer measurements were carried out throughout the period of these runs at bulk temperature varying from 500° F to 800° F and at flow velocities from 8 ft/sec to 21 ft/sec.

Comparison of physical property measurements of Santowax OM at M.I.T. with published data (3.5, 3.7) and comparison of heat transfer measurements of Santowax WR with those reported earlier by M.I.T. (3.9) are presented in this chapter.

3.2 Density

The density measurements of the ortho-rich terphenyl, both irradiated and unirradiated, were made by means of a calibrated pycnometer in which the volume of a known mass of organic coolant was determined by measuring the liquid height in two capillary tubes connected to a small reservoir of organic coolant. The pycnometer was calibrated at different capillary heights by mercury at 25° C with known volume. The volume change of the pycnometer due to thermal expansion at elevated temperatures was calculated and found to be negligible. A detailed description of the equipment and procedure used in density measurement was given by Morgan and Mason (3.1) as well as by Mason, Timmins et. al. (3.2).

A linear least-square fit of the density data for each sample in the form of Equation (3.1) has been made.

$$\rho = a + bT \qquad\qquad (3.1)$$

where

ρ is the sample density, gm/cc

a, b are constants for a given sample

T is the temperature of measurement, °F

The variation of the density of irradiated and unirradiated Santowax OM with temperature and high boiler (HB) concentration is shown in Figure 3.1. Data from Runs 21, 22, 23, (2MW reactor power), all of which fall within the lines bracketing 0 - 10% HB, have not been included. Table 3.1 shows the calculated values of the constants a and b of Equation (3.1) for each run.
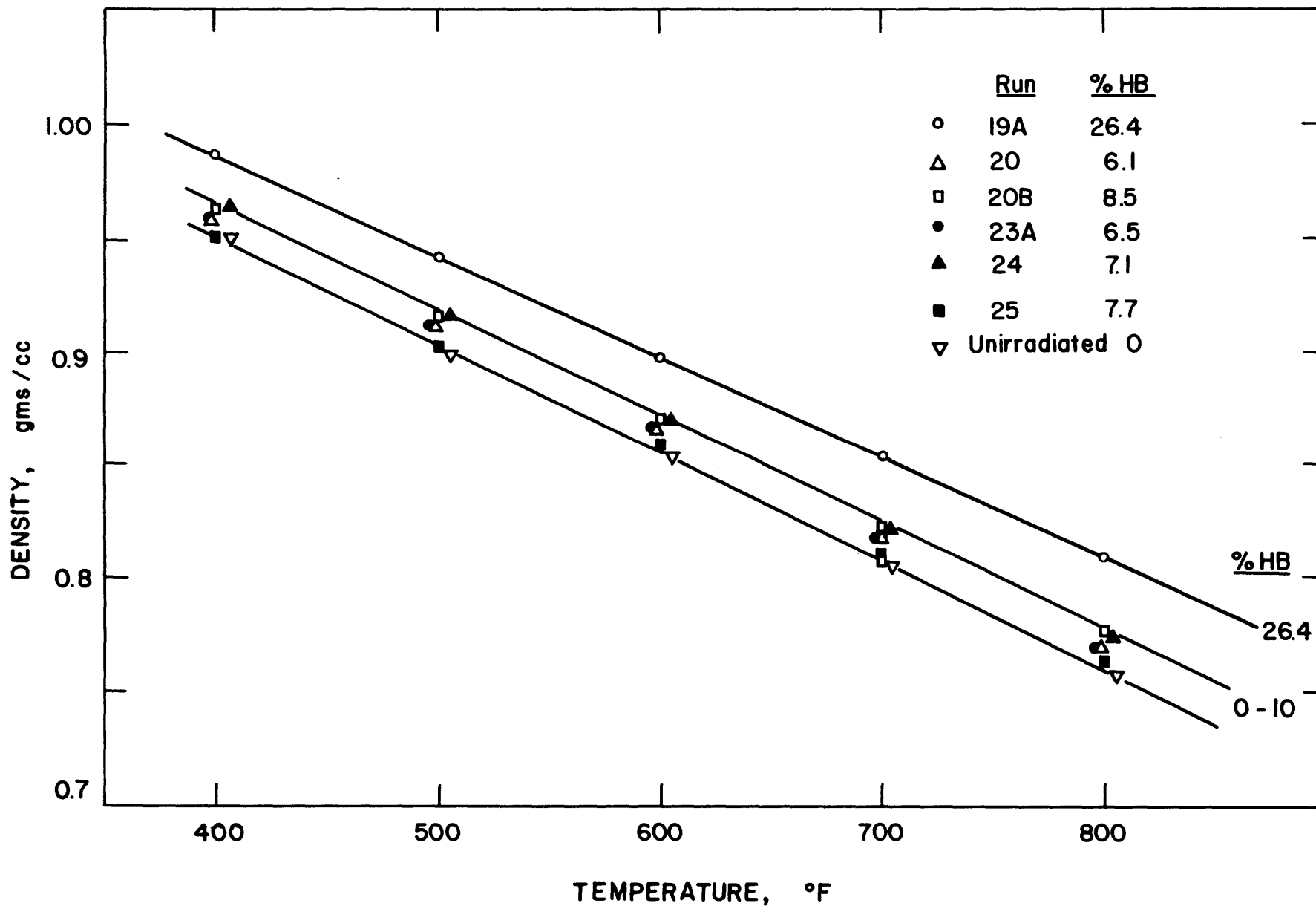
FIGURE 3.1   EFFECT OF TEMPERATURE ON THE DENSITY OF SANTOWAX OM

Table 3.1

Results of Density Measurements on Santowax OM

Run	%HB	$\rho = a + bT$ Equation (3.1)
19A	26.4	$1.164 - 4.41 \times 10^{-4} T$
20A	6.1	$1.146 - 4.69 \times 10^{-4} T$
20B	8.5	$1.150 - 4.67 \times 10^{-4} T$
21	9.0	$1.150 - 4.53 \times 10^{-4} T$
22	8.9	$1.153 - 4.63 \times 10^{-4} T$
23	7.8	$1.145 - 4.68 \times 10^{-4} T$
23A	6.5	$1.149 - 4.75 \times 10^{-4} T$
24	7.1	$1.155 - 4.78 \times 10^{-4} T$
25	7.7	$1.136 - 4.62 \times 10^{-4} T$
unirradiated	0	$1.143 - 4.80 \times 10^{-4} T$

The effect of temperature and HB concentration on the density of Santowax OM is correlated empirically in Equation (3.2)

$$\rho = 1.143 + 0.91 \times 10^{-3}(HB) - [4.8 \times 10^{-4} - 1.2 \times 10^{-6}(HB)](T)$$

$$(3.2)$$

where

    ρ is the sample density, gm/cc

    HB is the percent high boiler, w/o

    T is the sample temperature, ^{O}F

This correlation predicts within 1% of the densities of all the irradiated Santowax OM samples measured at M.I.T.

Table 3.2 compares the density data of Santowax OM as obtained from Equation (3.2) with those reported by Mandel (3.5, 3.10), Atomics International, and by Hatcher and

Table 3.2

Comparison of Densities of Santowax OM

Reported in Literature

% HB	Density, gm/cc								
	400° F			600° F			800° F		
	MIT[a]	AI-CE[b]	MIT[a]	MIT[a]	AI-CE[b]	AECL[c]	MIT[a]	AI-CE[b]	AECL[c]
0	0.951	0.950	0.936	0.855	0.859	0.846	0.759	0.765	0.755
10	0.965	0.963	0.952	0.871	0.873	0.861	0.778	0.779	0.771
20	0.979	0.980	0.967	0.888	0.889	0.877	0.797	0.796	0.786
30	0.993	0.999	0.983	0.904	0.907	0.892	0.815	0.815	0.802

[a] Calculated from Equation(3.2)for Santowax OM

[b] Reported by Mandel (3.5, 3.10), Atomics International-Combustion Engineering, for Santowax OM

[c] Calculated from correlation presented by Hatcher and Tomlinson (3.7), AECL, for Santowax OM

Tomlinson (3.7), AECL. The densities obtained by M.I.T. agree within 1% of those reported by AI-CE. The AECL density values are generally 1% to 1-1/2% lower than the M.I.T. or the AI-CE values.

Empirical correlations of the temperature and HB effect on the density of Santowax WR and Santowax OMP (both rich in meta terphenyl) were reported earlier by Mason and Timmins (3.2) as

$$\rho = 1.153 + 0.43 \times 10^{-3}(HB) - [4.75 \times 10^{-4} - 1.23 \times 10^{-6}(HB)]T$$

$$(3.3)$$

and also by Sawyer and Mason (3.3) as

$$\rho = 1.152 + 0.60 \times 10^{-3}(B) - [4.87 \times 10^{-4} - 1.77 \times 10^{-6}(B)]T$$

$$(3.4)$$

where B is the percent bottoms using the procedure of bottoms distillation which provides a deeper cut (i.e. more high boiling components in the distillate) than a HB distillation.

A comparison of Equations (3.2) and (3.3) shows that the density of Santowax OM is about 1% less than that of Santowax WR and Santowax OMP at low HB concentrations but becomes nearly equal for HB = 30%.

3.3 Viscosity

Semi-micro capillary viscometer of the Oswald type was used for the determination of the kinematic viscosities of samples of both irradiated and unirradiated Santowax OM. Sawyer and Mason (3.3) have described the details of the experimental procedures and setup. Water at 27° C was used as a calibration liquid and the viscometer constant was determined as a function of the liquid volume by means of least-square fitting. Thermal expansion of the viscometer glass at elevated temperatures was calculated and found to be negligible. The viscosity of the samples was calculated from the efflux time through an appropriate equation of calibration.

Nitrogen was used to pressurize both the viscometer and the pycnometer at 70 psi to prevent boiling of the samples

at high temperatures.

Least-square methods were applied to the viscosity data for each sample to obtain the relation

$$\mu = \mu_o \exp[\Delta E/RT] \tag{3.5}$$

where

μ is the viscosity of the sample, centipoise

μ_o is a constant, centipoise

ΔE is an "activation energy", k-cal/g-mole

R is the gas constant, k-cal/g-mole-^{o}K

T is the sample temperature, ^{o}K

Figure 3.2 shows the viscosity of Santowax OM as a function of sample temperature and concentration. At the same temperature, viscosity of the coolant sample increases with increasing HB. The viscosities of Santowax OM are generally 5% to 10% lower than the previously reported values for Santowax WR and OM-2 (3.1, 3.2, 3.4, 3.5, 3.6).

The activation energy for the viscosity, ΔE, of Equation (3.5) is shown in Figure 3.3 for Santowax OM. The values of ΔE for Santowax OM ranging from 4.2 to 4.6 k-cal/mole appear to be 5% to 10% lower than those calculated for Santowax WR (3.4). It also appears that, at approximately the same HB concentration, ΔE decreases with increasing temperature of irradiation. This decrease in ΔE of Santowax OM as compared to that of Santowax WR and OM-2 could be related to the ratio of Low and Intermediate Boilers (LIB) to High Boiler (HB). At same temperature and same terphenyl concentration, the LIB/HB ratio of Santowax OM has been found to be higher than that of Santowax WR (see Appendix A3 and (3.2, 3.3, 3.4)). Note also that the LIB/HB ratio increases with increasing temperature of irradiation for both Santowax OM and Santowax WR.

Figure 3.4 shows the effect of HB concentration on the viscosity at 400° F. The solid line is drawn through the open points obtained from samples irradiated at temperature equal to or less than 700° F. It shows that the viscosity of the coolant increases with increasing HB concentration.
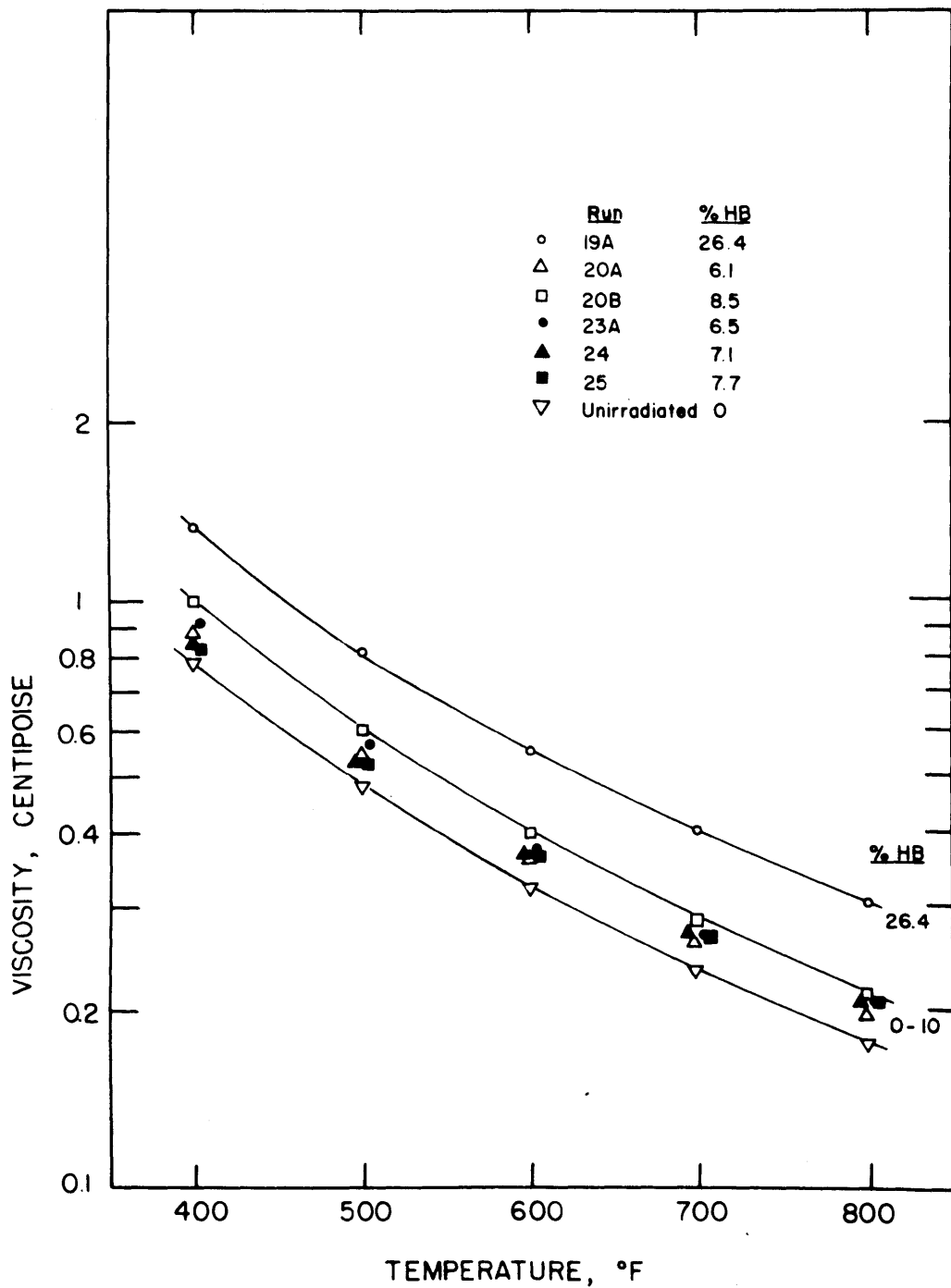
FIGURE 3.2   EFFECT OF TEMPERATURE ON THE VISCOSITY OF SANTOWAX OM
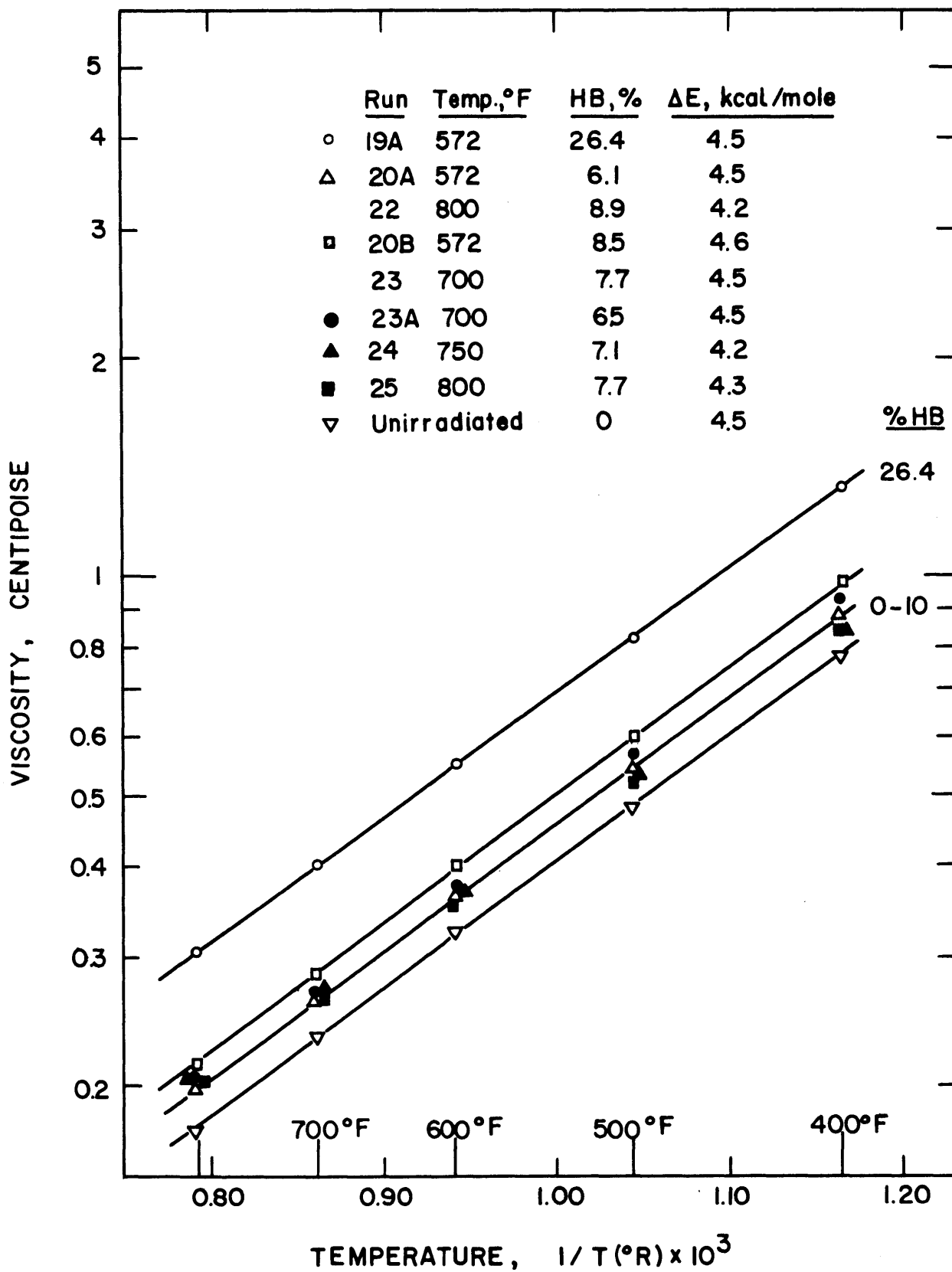
FIGURE 3.3   EFFECT OF HIGH BOILER CONCENTRATION AND TEMPERATURE
ON THE VISCOSITY AND ACTIVATION ENERGY OF SANTOWAX OM

Run	Temp.,°F	HB,%
o 19A	572	26.4
△ 20A	572	6.1
□ 20B	572	8.5
⋊ 23	700	7.7
⋎ 23A	700	6.5
● 22	800	8.9
▲ 24	750	7.1
■ 25	800	7.7
▽ —	Unirradiated 0	
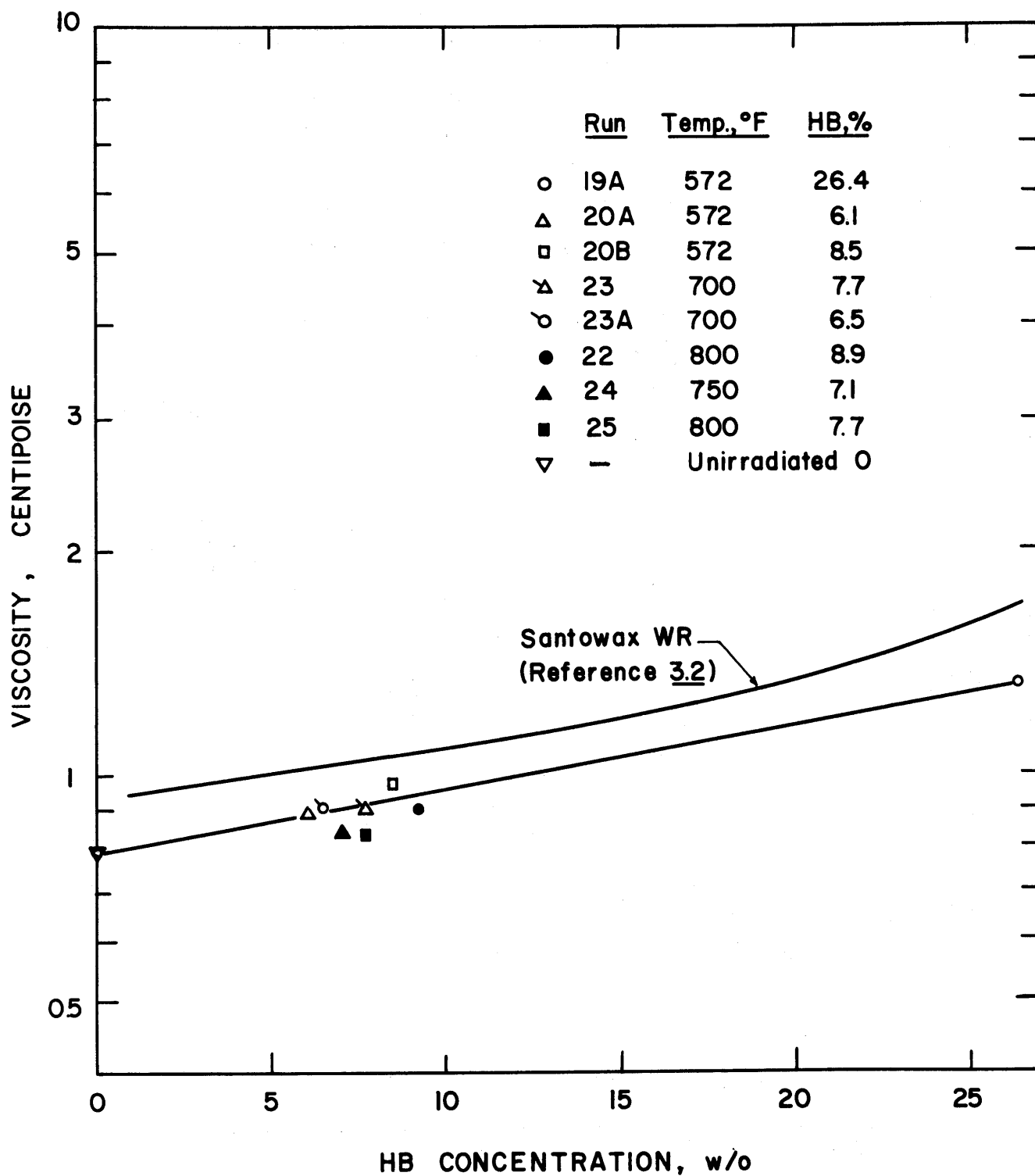
FIGURE 3.4   CORRELATION OF VISCOSITY WITH HIGH BOILER
CONCENTRATION OF SANTOWAX OM

The closed points represent the viscosities, also at 400° F, of the samples irradiated at higher temperatures (>700° F). It appears that the viscosity decreases with increasing irradiation temperature. Earlier M.I.T. report (3.2) on Santowax WR also indicated a decrease of viscosity with increasing irradiation temperature as shown in the same figure.

Table 3.3 compares the viscosity data of Santowax OM as measured by M.I.T. with those reported by Mandel (3.5, 3.10), Atomics International, and by Hatcher and Tomlinson (3.7), AECL. The M.I.T. values tabulated were obtained by interpolations from Figures 3.2 and 3.3. Except for those values at 400° F, the viscosity values agree within 2%. At 400°F, the viscosity data of AECL are 20-30% lower than the AI-CE data and 10-20% lower than the M.I.T. data. The AECL viscosity data are calculated from an empirical correlation which was established primarily for temperatures ranging from 300° C to 400° C.

3.4   Number Average Molecular Weight

A Mechrolab Model 310A osmometer was used for the determinations of the number average molecular weight of the irradiated Santowax OM and the high boiler samples obtained during the steady-state runs.

The measured molecular weight of the coolant samples was used to indicate if a steady-state was reached of the total terphenyl concentration of the coolant during the irradiation. It will also serve to investigate the distribution of the molecular species as a function of irradiation temperature and HB concentration.

The osmometer compares the lowering of the vapor pressure of a pure solvent (e.g. tetrahydrofuran) by a standard (e.g. biphenyl and ortho terphenyl) and by the sample with unknown molecular weight. Bley and Mason (3.8) described in detail the procedure of measurement.

The average number molecular weight (MW_N) is defined as

Table 3.3

Comparison of Viscosities of Santowax OM

Reported in Literatures

% HB	Viscosity, Centipoise								
	400° F			600° F			800° F		
	MIT[a]	AI-CE[b]	AECL[c]	MIT[a]	AI-CE[b]	AECL[c]	MIT[a]	AI-CE[b]	AECL[c]
0	0.79	0.85	0.61	0.32	0.31	0.31	0.18	0.17	0.16
10	0.93	1.04	0.75	0.41	0.39	0.39	0.24	0.23	0.20
20	1.15	1.23	0.92	0.48	0.48	0.48	0.28	0.28	0.24
30	1.40	1.42	1.14	0.58	0.56	0.59	0.32	0.34	0.30

[a] Interpolated from Figures 3.2 and 3.3.

[b] Reported by Mandel (3.5, 3.10), Atomics International-Combustion Engineering, for Santowax OM.

[c] Calculated from correlation presented by Hatcher and Tomlinson (3.7), AECL, for Santowax OM.

$$MW_N = \frac{\sum C_i}{\sum C_i / A_i} \qquad\qquad (3.6)$$

where

C_i is the weight fraction of species i in the mixture

A_i is the molecular weight of species i

The values of MW_N of the total coolant and the HB fraction of the coolant for samples removed during the steady-state irradiations of Santowax OM are tabulated in Table 3.4. In most cases, every other sample removed from the loop during a steady-state run was analyzed for MW_N. Table 3.4 shows that from the samples analyzed for each steady-state run, the MW_N values are constant within the reproducibility of the measurement (± 5%). This indicates that the coolant composition during the irradiations of Santowax OM at M.I.T. were at steady-state.

The relationship between the number average molecular weight and the concentration of degradation products of Santowax OM is shown in Figure 3.5. The average value of the measured MW_N is used for each steady-state run. Both the MW_N of the total coolant and that of the HB fraction are shown. The open points represent those runs with irradiation temperatures less than or equal to 700° F and the closed points are for runs at temperatures over 700° F. For the coolant, the number average molecular weight appears to increase with increasing concentration of the degradation products. On the other hand, the number average molecular weights of the HB fraction appear to form two groups, namely one group as indicated by open points with irradiation temperature of 700° F or less and the other by closed points with irradiation temperatures above 700° F. The MW_N of the open points (low temperature irradiations) are at least 10% higher than those of the high-temperature irradiations. Earlier M.I.T. reports, (3.2, 3.3), and (3.8) found this same behavior with Santowax WR. Thermal cracking at irradiation

Table 3.4

Number Average Molecular Weights of

Steady-State Runs Santowax OM Samples

Sample	Irradiation Temperature $^\circ F$	% HB	MW_N Coolant	MW_N HB
19A-L5*	572	27.2	271	548
19A-L10	572	26.0	272	592
19A-L15	572	26.7	266	586
20A-S5*	572	6.7	235	497
20A-S10	572	5.8	234	516
20B-S4*	572	9.7	235	518
20B-S6	572	8.2	241	530
20B-S8	572	8.3	242	517
21-L1	750		243	
21-L2*	750		239	
21-L3	750		238	
21-L4	750		239	
21-L5	750		238	
21-L6	750		240	
21-L7	750		229	
21-S2*	750	9.0		458
21-S4	750	7.3		443
22-S2*	800	10.4	238	478
22-S4	800	8.4	237	458
23-S2	700	8.6	250	482
23-S4	700	8.5	243	511
23-S6	700	10.6	247	532

Table 3.4 (continued)

Sample	Irradiation Temperature $^{\circ}F$	% HB	MW_N Coolant	HB
23-S8*	700	6.9	249	
23-S9	700	7.3		503
23-S10	700	8.1	247	
23A-S2*	700	7.1	241	497
23A-S3	700	6.1	237	
23A-S4	700	5.8	244	525
23A-S5	700	6.6	226	
24-S1	750		252	552
24-S3*	750	6.8	252	504
24-S5	750	7.7	252	443
24-S8	750	7.0	258	453
25-S2*	800	8.3	247	484
25-S4	800	7.8	241	475
25-S5	800	8.0		462
25-S6	800	7.6	233	
25-S8	800	7.5	253	456
25-S9	800	7.1		447
25-S10		7.6	247	
25-S12	800	7.8	241	447
Unirradiated			256	

*Beginning of Steady-State
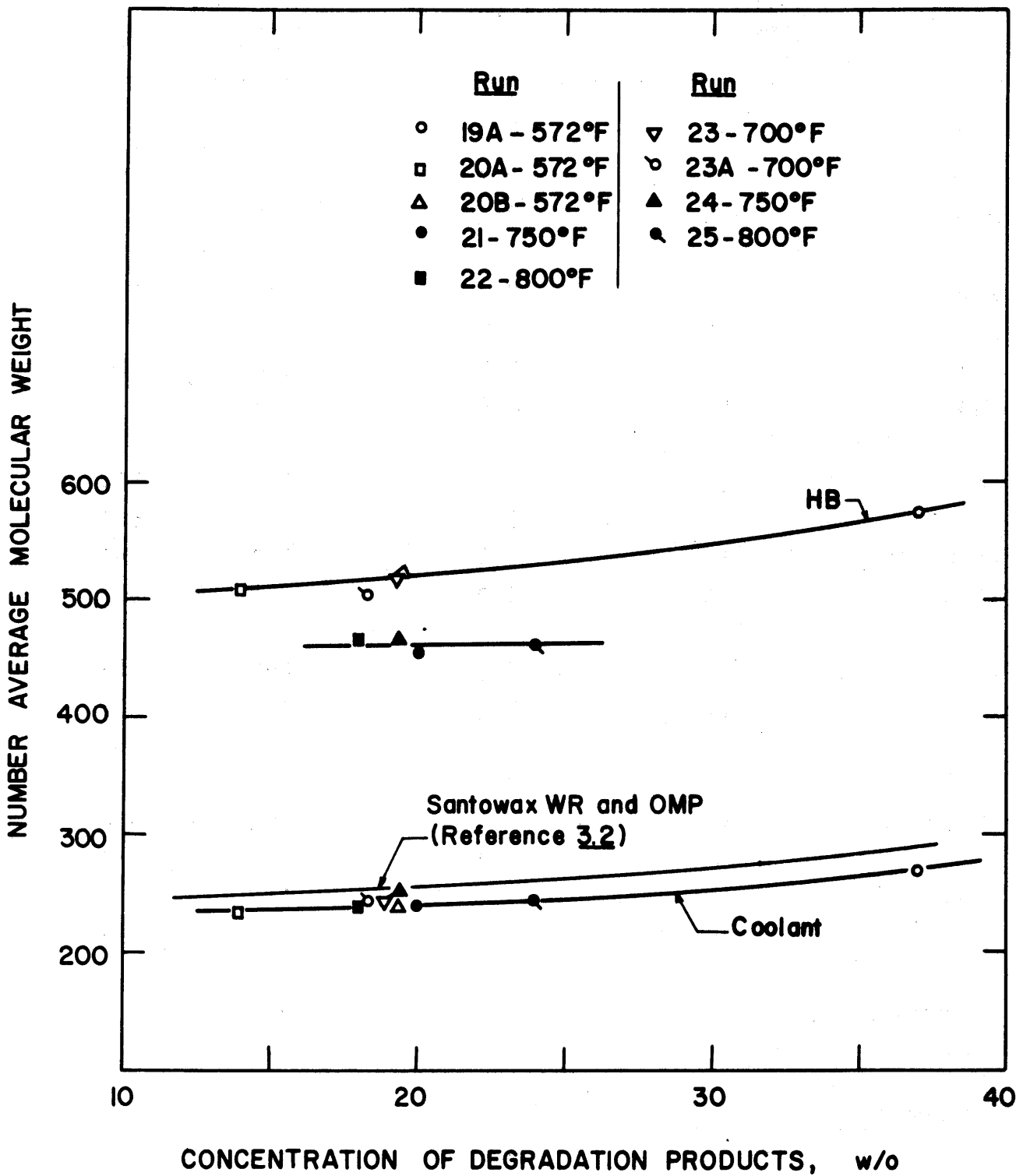
FIGURE 3.5   NUMBER AVERAGE MOLECULAR WEIGHTS OF COOLANT
AND HIGH BOILER FROM SANTOWAX OM IRRADIATIONS

temperatures of above 700° F of the heavy molecules was thought to play the role in lowering the MW_N of the HB fraction. By comparing the results of MW_N of Santowax OM with those of Santowax WR in the above-mentioned earlier M.I.T. reports, the MW_N of Santowax OM is approximately 10% lower on the average than that of Santowax WR at the same DP concentration. The MW_N of Santowax WR and OMP is also shown in Figure 3.5 as reported by Mason and Timmins (3.2).

This again could be related to the larger LIB/HB ratio of Santowax OM as compared to that of Santowax WR at the same temperature and terphenyl concentration (or DP concentration) as mentioned earlier in Section 3.3. No significant difference in the values of MW_N of the HB fraction can be found between Santowax OM and Santowax WR.

3.5 Melting Range

All of the coolant samples removed from the loop during any of the irradiation runs of Santowax OM are viscous dark liquids at room temperature. The HB concentrations of these samples vary from 6% to 27% and the DP concentrations from 18% to 37%. Thus the melting points of these samples have not been determined since they remain as sub-cooled liquids at room temperature. The liquid characteristics of irradiated Santowax OM would be an advantage for use of this coolant in power reactors relative to Santowax WR or Santowax OMP which are solid at room temperature up to about 20% DP concentration.

3.6 Heat Transfer

Earlier M.I.T. reports (3.2, 3.9) have shown that heat transfer data of Santowax WR using Test Heaters TH6 and TH7 at Reynold's Number from 16,000 to 130,000 can be fitted within ± 10% to a Dittus-Boelter type of equation as

$$Nu = 0.023 \ Re_B^{0.8} \ Pr_B^{0.4} \qquad (3.7)$$

where the subscript "B" refers to the bulk properties of the coolant. Hatcher, Finlay and Smee (3.10) reported correlation

of the measured heat transfer coefficient of Santowax OM
(30% HB) by the equation

$$Nu_B = 0.00835 \, Re_B^{0.9} \, Pr_B^{0.4} \qquad (3.8)$$

which is also in close agreement with the earlier M.I.T.
correlations (3.3, 3.9) on Santowax OMP and Santowax WR,
and recent M.I.T. correlation (3.13) on Santowax WR.

3.6.1 Fouling Measurements on Test Heat TH7

3.6.1.1 Introduction - Test heater TH7 was in-
stalled on October 28, 1964 and replaced by TH8 in July 1967.
During the period from April 1, 1966 to April 18, 1967, no
heat transfer run was made because the major work force was
involved in the installations of the In-pile Section No. 4
and the new processing system. The first heat transfer run
(22HT1) was made on April 18, 1967 during the steady-state
irradiation of Santowax (Run 22) at 800° F and 2MW nominal
reactor power. Results of 22HT1 indicated possible fouling
of the Test Heater section TH7. Run 22 was therefore ter-
minated and seven heat transfer runs were made during the
period from April 20, 1967 to June 16, 1967 at a bulk coolant
temperature from 562° F to 700° F to determine whether any
scale had been formed on the interior wall of the Test Heater.
Detailed description and operation of the heat transfer
measurement and the procedures used for reduction of heat
transfer data can be found from earlier M.I.T. reports (3.1,
3.9).

3.6.1.2 Results of Heat Transfer Measurements - TH7
Table 3.5 summarizes the operating conditions and measured
heat transfer coefficients for these runs.

The heat transfer coefficient of the coolant can gener-
ally be expressed by

$$h = \frac{k}{D}Nu = \frac{k}{D} aRe^b Pr^c = A[k(\frac{\rho}{\mu})^b Pr^c]V^b \qquad (3.9)$$

where

Table 3.5

Heat Transfer Data From Test Heater TH7

April 20, 1967 to June 16, 1967

Run No.	Coolant Velocity, V (ft/sec)	Heat Flux Q/A (Btu/hr-ft^2)	$T_{wall} - T_{bulk}$ ($^\circ$F)	Re_B	Pr_B	Heat Transfer Coeff., U_2 (Btu/hr-ft^2-$^\circ$F)	T_{bulk} ($^\circ$F)
23-3	18.8	55,540	61.4	64,290	7.92	905	562
23-5	10.2	52,670	84.6	35,330	7.85	623	566
23-7	8.9	129,900	220.1	30,450	7.92	591	562
23-9	15.4	135,000	170.7	52,770	7.90	791	565
23-11	19.7	114,400	97.4	97,130	5.89	1,174	687
23-13	20.0	120,800	101.3	99,180	5.86	1,193	699
23A-5	18.8	108,800	95.0	92,220	6.04	1,146	688

h is the heat transfer coefficient

a, b and c are constants

A is a constant depending on the geometry of the
coolant flow

The quantity $k(\frac{\rho}{\mu})^b Pr^c$ is a function of the physical proper-
ties of the coolant and the temperature. For same physical
properties and temperature, the heat transfer coefficient
is then proportional to V^b only. However, if there is scale
buildup on the heated wall, the combined or measured heat
transfer, U, is related to the scale heat transfer coeffi-
cient, h_S, by

$$\frac{1}{U} = \frac{1}{h} + \frac{1}{h_S} \tag{3.10}$$

where U, the measured or experimental heat transfer coefficient,
is calcualted by

$$U = \frac{Q/A}{T_{wall} - T_{bulk}} \tag{3.11}$$

Rewriting Equation (3.9) assuming constant physical proper-
ties and temperature,

$$h = V^b/B \tag{3.12}$$

with $1/B = A(\frac{\rho}{\mu})^b Pr^c k$, and substituting Equation (3.12) into
Equation (3.10), we have

$$\frac{1}{U} = \frac{1}{h_S} + \frac{B}{V^b} \tag{3.13}$$

Wilson's method (3.12) consists of plotting the recipro-
cal of the experimental heat transfer coefficient, 1/U,
against $1/V^b$. The intercept of such a plot would therefore
yield the scaling heat transfer coefficient, h_S.

For the seven heat transfer runs made to determine
whether Test Heater TH7 had scale buildup, the first four
runs were made at an average coolant bulk temperature of
564° F, whereas the rest were made at 691° F. The quantity
$k(\frac{\rho}{\mu})^b Pr^c$ was nearly constant (within 0.5%) within each group.

Two values of b were chosen, namely 0.8 and 0.9, correspond-
ing to those of Equations (3.7) and (3.8). Figure 3.6 shows
the Wilson plot for these runs. The values U and V were taken
directly from Table 3.5. The three data points from Runs 23-9,
23-11 and 23A-5 (at average bulk temperature of 691° F) had
nearly the same flow velocity. Therefore no significant con-
clusion can be drawn from them on the Wilson plot. The solid
lines were linear correlation using least-square fit of the
data points at 564° F. Both lines intercept the ordinate at
approximately the same value of 3.9 x 10^{-4} ft^2-hr-°F/Btu.
This indicates a scale heat transfer coefficient, h_S, of 2590
Btu/ft^2-hr-°F.

An alternative method to study scale formation is to com-
pare the experimentally determined heat transfer coefficient,
U, with the value h, calculated from the McAdams equation such
as Equation (3.7) or from empirically correlated equation on
Santowax OM such as Equation (3.8).

Table 3.6 shows the Nusselt numbers and the heat trans-
fer coefficients, h, for these runs using both Equations (3.7)
and (3.8). The ratio h to experimental values of heat trans-
fer coefficients are also tabulated for comparison. This
ratio varies between 1.3 and 1.6 using Equation (3.7) and 1.4
and 1.7 using Equation (3.8).

If it is assumed this lowering of experimental heat trans-
fer coefficient from the coefficient as calculated from
Equation (3.7) or (3.8) is due to a layer of scale, the excess
temperature drop due to scale formation and the scale thick-
ness can be calculated. The temperature drop across the scale
can be expressed as

$$\Delta T_{SC} = \Delta T_{WB}(1 - U/h) \tag{3.14}$$

where

ΔT_{SC} is the temperature drop across the scale

$\Delta T_{WB} = (T_{wall} - T_{bulk})$ is the temperature drop
between the inside wall temperature and the
average bulk temperature of the coolant
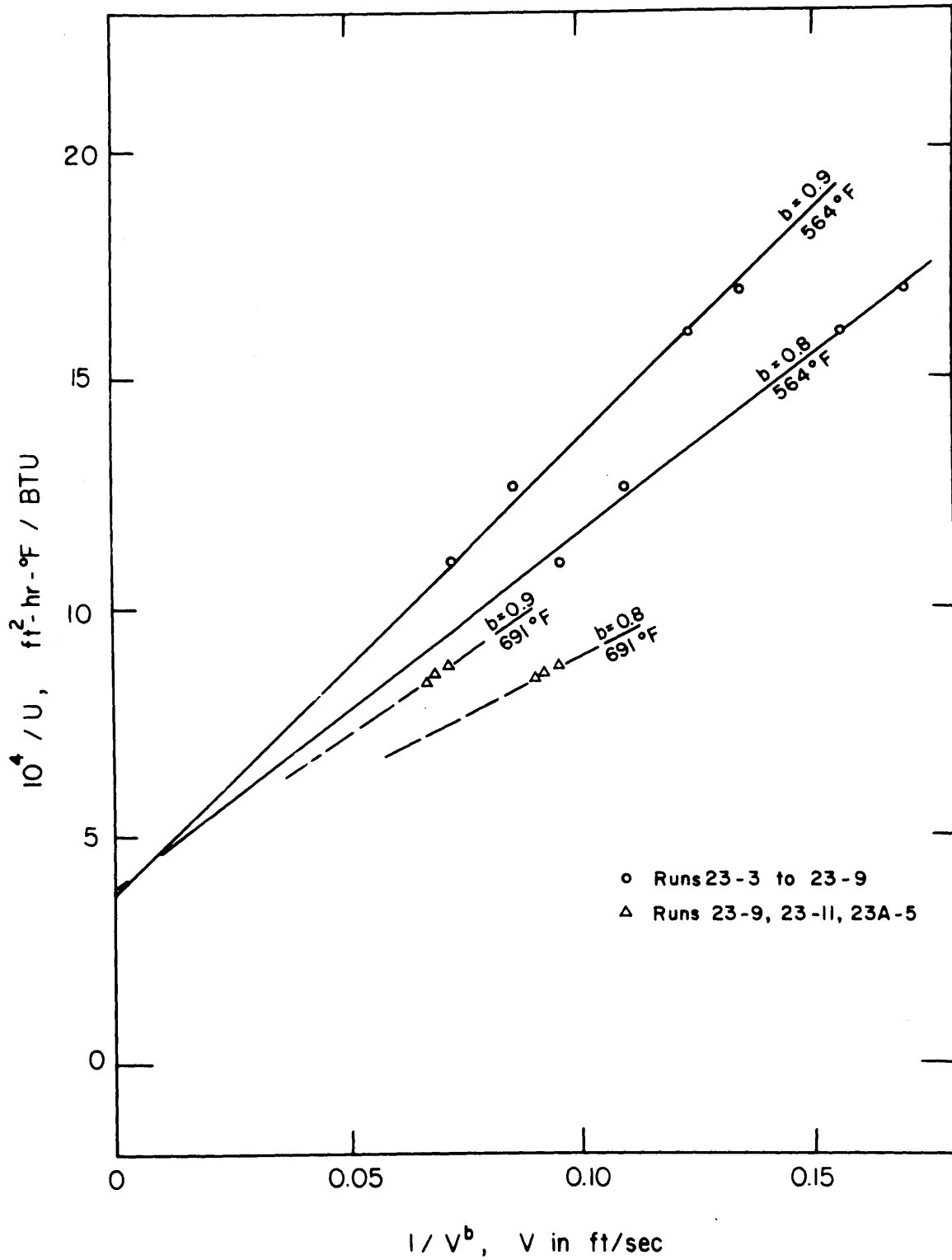
FIGURE 3.6 WILSON PLOT FOR TEST HEATER TH7 (RUNS 23,23A)

Table 3.6

Summary of Heat Transfer Runs

on Test Heater TH7

April 20, 1967 - June 16, 1967

Run No.	Nu_B (a)	(b)	$h, (Btu/ft^2-hr-^\circ F)$ (a)	(b)	U $(Btu/ft^2-hr-^\circ F)$	h/U (a)	(b)	$\Delta T_{SC}(^\circ F)$ (a)	(b)	Δt_{SC}(mils) (a)	(b)
23-3	370	406	1,435	1,574	905	1.58	1.74	23	26	15	17
23-5	228	236	885	915	623	1.42	1.47	25	27	17	19
23-7	203	207	788	803	591	1.33	1.36	55	59	15	16
23-9	315	340	1,222	1,317	791	1.55	1.67	62	67	17	19
23-11	457	523	1,680	1,920	1,174	1.43	1.64	33	42	11	13
23-13	464	532	1,670	1,950	1,192	1.40	1.64	34	43	10	13
23A-5	443	504	1,625	1,855	1,145	1.42	1.62	32	40	11	13

(a) Calculated from Equation (3.7)

(b) Calculated from Equation (3.8)

U   is the experimentally determined heat transfer coefficient

h   is the heat transfer coefficient calculated from Equation (3.7) or (3.8).

The scale thickness can be expressed as

$$\Delta t_{SC} = \frac{k_{SC} \Delta T_{SC}}{Q/A} \; . \qquad (3.15)$$

Where

Δt_{SC} is the scale thickness, feet

k_{SC} is the thermal conductivity of the scale, $Btu/ft\text{-}hr\text{-}^{\circ}F$

Q/A is the heat flux, $Btu/ft^2\text{-}hr\text{-}^{\circ}F$

A value of k_{SC} of 3 $Btu/ft\text{-}hr\text{-}^{\circ}F$ (3.11), similar to that for petroleum coke was assumed. The calculated values of ΔT_{SC} and Δt_{SC} are also tabulated in Table 3.6. An average thickness of 15 mils of scale has been found through calculation.

While the irradiation runs were being continued at 750° F (Run 24) and 800° F (Run 25), heat transfer measurements were continued to monitor further scale buildup. Five such measurements were made each during Run 24 and during Run 25. For these measurements, no flow variation was attempted. The results of these measurements are tabulated in Table 3.7.

Comparing the h/U values of Tables 3.5, 3.6 and 3.7, a small increase of around 7% is noted between Run 23 and Run 25. However in view of the experimental error involved in heat transfer measurement of around 10% (3.9), this increase in h/U is not significant to draw conclusion of further scale buildup since Run 23. It should be noted that the decrease of Pr and the increase of Re between Runs 24 and 25 in Table 3.7 at same coolant velocity were essentially due to lowering of density and viscosity from Run 24 at 750° F to Run 25 at 800° F.

Table 3.7

Summary of Heat Transfer Run

on Test Heater TH7
June 19, 1967 - July 21, 1967

Run No.	Coolant Velocity, V (ft/sec)	Re_B	Pr_B	N_B	Heat Transfer Coefficient $(Btu/ft^2-hr-{}^\circ F)$		h/U	T_{bulk} $({}^\circ F)$
					$h^{(a)}$	U		
24-1	17.9	98,470	5.40	511	1,852	1,040	1.78	733
24-4	18.0	99,370	5.39	515	1,864	1,049	1.77	735
24-5	18.7	105,100	5.30	538	1,943	1,098	1.76	737
24-7	18.8	105,400	5.31	537	1,940	1,142	1.70	733
24-9	20.1	113,300	5.28	575	2,075	1,174	1.78	735
25-1	18.9	117,900	4.87	577	2,050	1,115	1.84	784
25-2	19.0	120,700	4.79	585	2,074	1,112	1.86	785
25-4	19.2	122,100	4.77	590	2,089	1,142	1.83	784
25-7	18.9	117,700	4.89	576	2,049	1,137	1.80	781
25-8	18.9	121,900	4.73	587	2,076	1,147	1.81	785

(a) Calculated from Equation (3.8)

3.6.1.3 <u>Conclusion and Discussion on Heat Transfer</u>
<u>Measurements on TH7</u> - A decrease of measured heat transfer coefficient of Test Heat TH7 to nearly 70% of that calculated using McAdams or Dittus-Boelter types of equation confirms that there was scale formation on the test heater wall. This is substantiated by the results of the Wilson's plot. The scale formation calculated was approximately 15 mils in thickness with a scale heat transfer coefficient of about 2600 $Btu/ft^2-hr-{}^oF$.

Upon disassembling Test Heat TH7, the interior wall showed, by visual examination, a dull but smooth surface after several rinsings of acetone. The wall of a new test heater (e.g. TH8) has a shiny appearance. No chemical or physical measurements were made on the scale due to the lack of facilities to carry out such measurements.

Three types of solid formation on heat transfer surfaces were recognized through the use of organic coolant as reported by Hatch, et al. (<u>3.11</u>), namely

(1) <u>fouling or scale formation</u> on the heat transfer surface at normal operating temperature (below 500°C)

(2) <u>coke-out</u> which is a rapid formation and deposition of degradation products on high temperature surface (above 620°C)

(3) <u>coke formation</u> by radiolysis of stagnant or nearly stagnant coolant resulting in buildup of solid polymerized coolant.

Since the test heater used at M.I.T. Loop is located out-of-pile, coke formation is not possible. The wall temperature of the test heater is constantly monitored at several localities. High temperature alarms were set at 950°F (509°C) and were tested every Monday morning prior to the startup of loop irradiation. Therefore, coke-out type of

scale formation is not likely.

The fouling or scale formation on the heat transfer sur-
face at normal operating temperature is strongly dependent
on impurities in the coolant (3.11). The presence of chlorine
and oxygen in the coolant will promote fouling. Chlorine con-
tamination of the coolant is not likely in the M.I.T. loop.
However the possibility of oxygenation of loop coolant can-
not be ruled out.

A review of loop operation records between April, 1966
and April, 1967, in which period no heat transfer measure-
ment had been made on Test Heater TH7, showed no abnormality
in loop operation. Between this period, several major items
of work had been performed, namely (1) the removal of In-
pile Section No. 3 from Fuel Position 20, (2) the draining
of Santowax WR from the loop at the end of Run 18A, (3) the
installation of In-pile Section No. 4 at Fuel Position 1,
(4) the charging of loop with Santowax OM and (5) the in-
stallation of the Makeup and Sampling System (S & MI). Since
the heat transfer measurement made during irradiation run
in April, 1966 did not indicate any scale formation in TH7
as reported by Mason and Timmins (3.2), the most likely cause
of fouling could be the introduction of impurities to the
loop system (including possible oxygenation of loop coolant)
during the period when one or more of the above-mentioned
major items of work were being performed.

3.6.2   Heat Transfer Measurement on Santowax WR using Test Heater TH8

3.6.2.1   Introduction - Test Heater TH8 as shown
in Figure 3.7 is almost of the same design as Test Heaters
TH7, TH6 and TH5 which were described in earlier M.I.T. re-
ports (3.1, 3.3, 3.9). Detailed description of Test Heat
TH8 has been reported by Spierling (3.13). However TH8
differs from TH7 in some respects as follows.

In TH7, the wall thermocouples were clamped on to a
thin sheet of mica which interposed between the wall and the
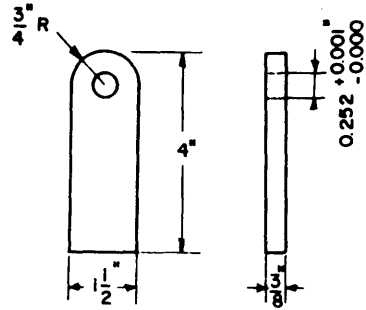
DETAIL I - COPPER ELECTRODE

FLASH CHROME PLATE 0.0002" MINIMUM THICKNESS

(3 REQUIRED)
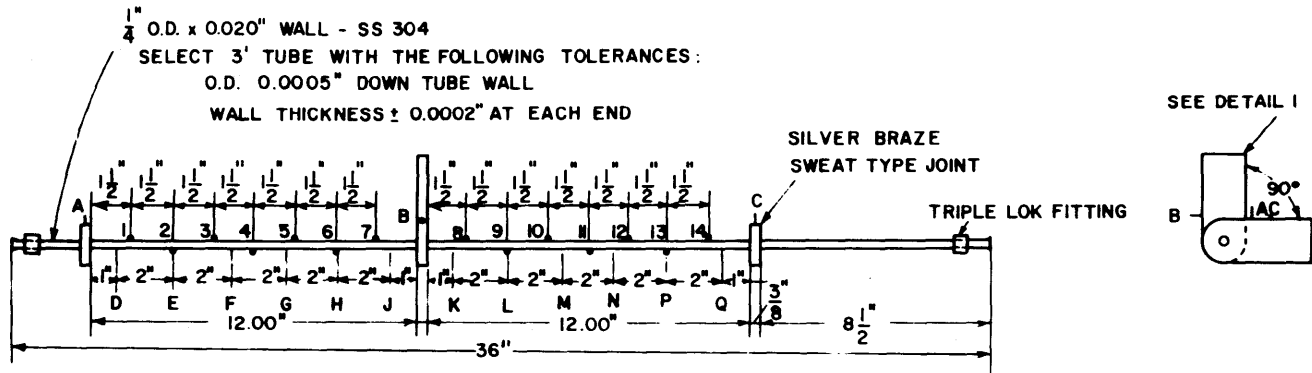
$\frac{1}{4}$" O.D. x 0.020" WALL - SS 304

SELECT 3' TUBE WITH THE FOLLOWING TOLERANCES:

O.D. 0.0005" DOWN TUBE WALL

WALL THICKNESS ± 0.0002" AT EACH END

SILVER BRAZE
SWEAT TYPE JOINT

SEE DETAIL I

TRIPLE LOK FITTING
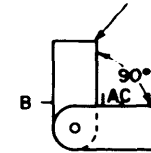
A-C ARE 0.020" SS 304 VOLTAGE TAPS, 5" LONG

1-14 ARE CHROMEL- ALUMEL THERMOCOUPLES

D-Q ARE POINTS AT WHICH THE O.D. IS TO BE MEASURED - 4 PLACES RADIALLY AT EACH POINT

TABULAR LISTING OF ALL MEASUREMENTS TO BE INCLUDED WITH HEATER

ALL THERMOCOUPLES ARE TO BE CALIBRATED VERSUS A NATIONAL BUREAU OF STANDARDS CALIBRATED THERMOCOUPLE

FIGURE 3.7   TEST HEATER 8

thermocouple bead. This arrangement was made so as to eliminate errors in wall temperature measurements that might arise due to electric and magnetic effects and possibly in the small differences as how the individual thermocouples were attached to the wall. An electric oven was built around the insulated test heater to eliminate any difference in temperature between the thermocouple bead and the wall due to mica insulation. However, experience with TH7 showed that it was not easy to fulfill all conditions necessary to make the oven temperature profile similar or nearly equal to the temperature profile of the test heater wall. Furthermore, it was found that the oven had, at several localities, a direct effect on the temperature reading of the wall thermocouple possibly due to proximity of the oven heating wire to the affected thermocouples.

The mica insulation was discontinued in TH8, and emphasis was placed on an optimum procedure of spot welding the thermocouples to the heater wall. Inspection of the workmanship on spot welding the thermocouples showed that the individual weldings were nearly identical. The electric oven around the insulated test heater was also discontinued. Instead, the heat losses from the test heater were carefully measured as a function of test heater wall temperature and the ambient temperature surrounding the test heater. Detailed description of TH8 and the results of experimental measurements of the heat loss from the test heater had recently been reported by Spierling (3.13). It was concluded that the rate of heat lost through conduction and natural convection across the insulation surrounding TH8 with constant heat flux at test heater wall could be expressed by the equation

$$Q_{loss} = 0.045(T_W - T_A)^{1.2} \qquad (3.16)$$

where

Q_{loss} is the rate of heat loss through the insulated test heater, watts.

T_W is the average wall temperature of the test heater, $^{\circ}F$.

T_A is the ambient temperature, $^{\circ}F$.

The rate of total heat produced, Q_{tot}, by the test heater by means of electric heating was known from the voltage measurement and the test heater resistance. The rate of heat, Q, transferred to the coolant flowing through the test heater is therefore equal to $Q_{tot} - Q_{loss}$. The heat transfer coefficient of the coolant can then be expressed as

$$U = \frac{Q_{tot} - Q_{loss}}{A(T_{wi} - T_b)} \qquad (3.17)$$

where

T_{wi} is the average inside wall temperature of the test heater, $^{\circ}F$

T_b is the average bulk temperature of the coolant in the test heater section

A is the heat transfer area

3.6.2.2 - Results of Heat Transfer Measurements - TH8

Irradiation of Santowax OM was completed before TH8 was installed. After TH8 was in operation, only Santowax WR was scheduled for in-pile irradiation. Therefore all of the results of heat transfer measurements with Test Heater TH8 were obtained using Santowax WR as coolant.

A total of 141 heat transfer measurements were made during the steady-state runs 26, 27 and 28 in Fuel Position 1. The test heater consists of the upstream and the downstream sections sharing the common central electrode (see Figure 3.7). Heat transfer measurement can be carried out using either or both section. However, only Test Series 26 used both sections. The rest of the measurements used only the upstream section because one of the wall thermocouples on the downstream section malfunctioned after the completion of Test Series 26. Detailed descriptions of heat transfer measurements and data for TH8 have been reported by Spierling (3.13). Figure 3.8

The chart shows the following legend:

SYMBOL	TEST SERIES NO.		IRR. TEMP.(°F)	% HB
▷	26a	upstream	700	9.65
▶		downstream		
△	26b	upstream	700	8.0
▲		downstream		
▽	26c	upstream	700	18.0
▼		downstream		
○	27a	upstream	750	9.1
○	27b	upstream	750	10.5
□	28	upstream	800	105, 17.0
○	29	upstream	630	20.5

$$\frac{Nu}{Pr^{0.4}} = 0.023\ Re^{0.8} \pm 10\%$$

CORRELATION, $Nu/Pr^{0.4}$

REYNOLDS NUMBER, $Re/10^4$
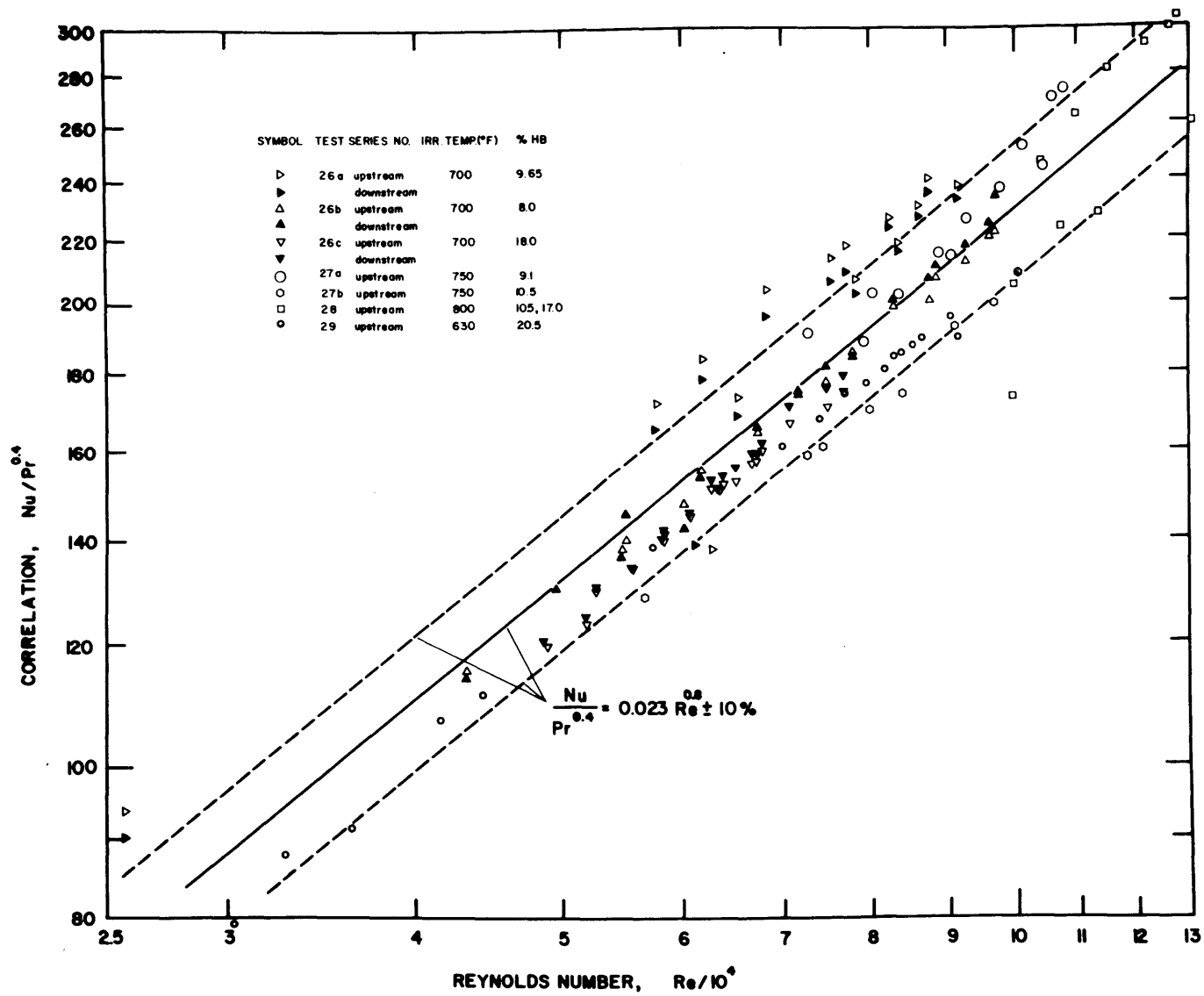
FIGURE 3.8 CORRELATION OF FORCED CONVECTION HEAT TRANSFER DATA

-3.31-

shows all of the heat transfer data from TH8. The well-known McAdams correlation (3.12)

$$Nu = 0.023Re^{0.8}Pr^{0.4} \qquad (3.18)$$

is also shown; the dashed lines represent 10% error limits. It is noted that the majority of the data points fall within the 10% error limits of Equation (3.18).

The computer program MNHTR developed by Sawyer and Mason (3.3) was used to correlate the heat transfer data using both the Dittus-Boelter type of relation

$$Nu = aRe^{b}Pr^{c} \qquad (3.19)$$

and the Sieder-Tate type of relation

$$Nu = aRe^{b}Pr^{c}(\mu/\mu_{w})^{d} \qquad (3.20)$$

The program evaluates the constant a, b, c and d using a least-squares procedure by allowing all these constants to vary or by fixing some of the constants in order to find the best values for the remaining. Results of such correlation are discussed in Section 3.6.2.4.

3.6.2.3 Wilson's Method to Determine Scale Buildup
on Test Heater TH8 - The Wilson method (3.12) similar to that described in Section 3.6.1 is used here to determine scale buildup on Test Heater TH8. Figure 3.8 shows such a plot for Test Series 26a, 26c and 29. The constant b of Equations (3.18), (3.19) and (3.20) is chosen to be 0.8 (i.e., $1/V^{0.8}$ is used as abscissa in Figure 3.9). The data points of each series fit quite well on a straight line. The intercepts of the three lines in Figure 3.9 on the ordinate are nearly zero ($1/U \sim 0$). This indicates that no significant fouling or scale had formed up to the time that Test Series 29 was conducted.

When the test heater is indeed free of scale, the value of $1/h_{s}$ in Equation (3.10) is zero and U = h. Thus a plot
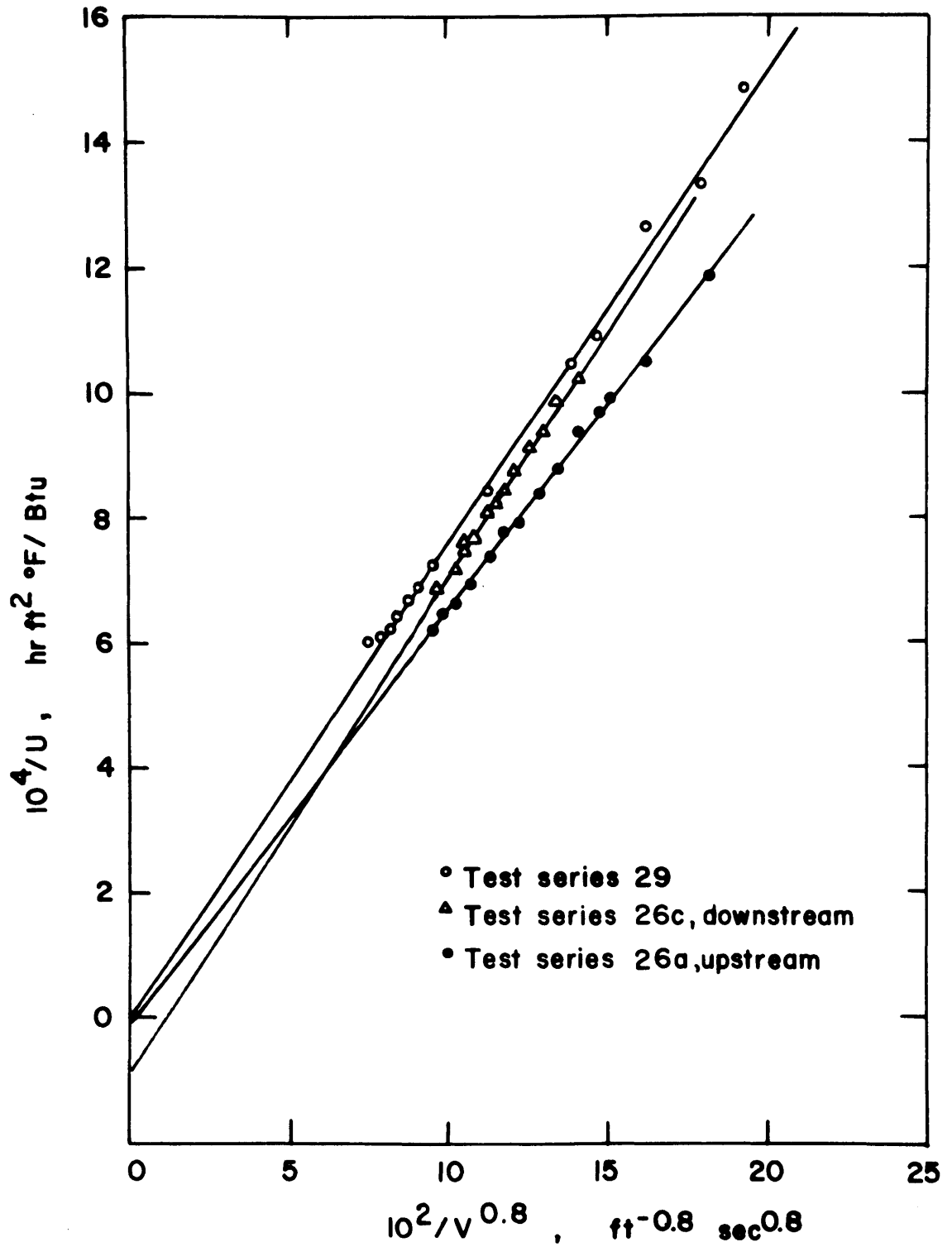
FIGURE 3.9   TYPICAL WILSON PLOTS

of experimental data in the form U versus $1/V^b$ should pass through the origin if b has the proper value. The "best" value of b can thus be obtained by a least-square fit of the data according to Equation (3.13), with $h_S = 0$, for each test series. Table 3.8 shows the results of such calculations.

3.6.2.4 Conclusion and Discussion on the Results of Heat Transfer Measurements on TH8

Figure 3.8 shows that the McAdam's equation

$$Nu = 0.023Re^{0.8}Pr^{0.4} \qquad (3.18)$$

correlates the heat transfer data quite well (within $\pm$ 10%). The same conclusion was reached by Swan and Mason (3.9) based on both heat transfer and pressure drop (friction factor) data.

The computer correlations of the heat transfer data according to Equations (3.19) and (3.20) indicate Reynolds Number exponents, b, from 0.8 to 0.9 and Prandtl Number exponents, c, from 0.33 to 0.40 with nearly the same RMS deviation (6.2% to 7.2%). (See Appendix A7 for details.) The additional term μ/μ_w appearing in the Sieder-Tate relation does not improve the correlation. Through the application of Wilson's method as shown in Figure 3.9 and Table 3.8, the Reynolds Number exponents range from 0.77 to 0.86. When the constants b and c were fixed at 0.8 and 0.4, respectively, the least-square value of the constant a of Equation (3.19) was found to be 0.0223 (very nearly the same as 0.023 in Equation (3.18), and the data had a RMS deviation of 7.1%.

A Reynolds Number exponent of 0.9 has been suggested by several investigators (3.11, 3.14, 3.15). However as pointed out in the preceding paragraph, there does not appear to be any statistically significant basis for choosing b = 0.9 over 0.8 (see Appendix A7). Therefore it is a matter of choice by each individual of the type of heat transfer correlation to be used. From the heat transfer measurements based on this report and earlier M.I.T. reports (3.3, 3.13)

Table 3.8

Intercepts on Wilson Plot and Reynolds
Number Exponents for Heat Transfer Measurements
with Test Heater TH8

Date Group	Nominal Coolant Temperature $^\circ$F	HB w/o	Intercepts for b = 0.8 (Btu/hr ft^2 $^\circ$F)$^{-1}$	Calculated Values of b for 1/U = 0
26a upstream	700	8.0	$- 1.50 \times 10^{-5}$	0.82
26a downstream	700	8.0	$- 6.55 \times 10^{-5}$	0.86
26b upstream	700	9.6	2.83×10^{-5}	0.77
26b downstream	700	9.6	1.34×10^{-5}	0.78
26c upstream	700	18.0	$- 5.80 \times 10^{-5}$	0.86
26c downstream	700	18.0	$- 9.32 \times 10^{-5}$	0.88
27b	750	10.5	$- 4.32 \times 10^{-5}$	0.84
29	630	20.5	2.12×10^{-6}	0.80

and a consideration of the uncertainties in the physical properties of the coolant and in the heat transfer measurements, the heat transfer coefficient of terphenyl coolants can be predicted by the generally applicable McAdam's equation.

CHAPTER 4

LOW TEMPERATURE TERPHENYL DEGRADATION

4.1 Introduction

During the period from November 1, 1966 to July 27, 1967, nine steady-state irradiations were made on the ortho-rich terphenyl, the Santowax OM, in Fuel Position 1 of the M.I.T. reactor at 36% fast neutron fraction, f_N. Table 4.1 shows a summary of the steady-state irradiations made during this period. The three Santowax WR irradiations (Runs, 26, 27 and 28) made during the remaining period covered by this report are also included in this table. The first three Runs (19A, 20A and 20B) were made at 300° C (572° F) with a reactor power of approximately 5 MW. These runs were scheduled for the purpose of investigating the radiolysis effect. Thermal decomposition (pyrolysis effect) is negligible at this low temperature or irradiation. The major objective of these low temperature irradiations of Santowax OM were

(1) to determine the kinetic order of radiolysis
(2) to determine the radiolysis rate constant
(3) to determine the relative radiolytic stability of the individual isomers.

The experimental results are compared with the results of the earlier irradiations of Santowax WR as reported by M.I.T. (4.1, 4.2) in order to investigate any differences in the behavior of the ortho-rich terphenyl and meta-rich terphenyl coolants exposed to the neutron and gamma dose rates of the M.I.T. reactor.

4.2 Low Temperature Degradation - Theory

At low temperatures (<320° C), thermal degradation is negligible as compared to the radiolytic degradation. By

Table 4.1

Summary of Irradiation Conditions and Experimental Results of Steady-State Run at Fuel Position 1

Dec. 19, 1966 to Feb. 16, 1968

Run No.	Irrad. Temp. (Coolant)	Average Dose Rate r (watts/gm)	Concentration - w/o					$G(-1)$ or $G(\rightarrow HB)$ molecules/100ev					$G^*(-1) = G(-1)/C_1$				LIB/HB	f_N
			C_o	C_m	C_p	C_{omp}	HB	$G(-o)$	$G(-m)$	$G(-p)$	$G(-omp)$	$G(HB)$	$G^*(-o)$	$G^*(-m)$	$G^*(-p)$	$G^*(-omp)$		
19A	572°F (SW-OM)	0.060	41.5	20.1	1.5	63.1	26.4	0.122	0.054	0.003	0.178	0.160	0.293	0.266	0.183	0.282	0.40	0.36
20A	572°F (SW-OM)	0.065	57.7	26.6	1.8	86.1	6.1	0.207	0.094	0.005	0.307	0.232	0.359	0.354	0.297	0.357	1.28	0.36
20B	572°F (SW-OM)	0.061	53.1	25.6	1.8	80.5	8.5	0.193	0.074	0.003	0.270	0.205	0.363	0.290	0.180	0.336	1.29	0.36
21	750°F (SW-OM)	0.024	50.6	25.5	1.9	78.0	9.0	0.351	0.124	0.001	0.476	0.405	0.694	0.487	0.046	0.611	1.44	0.36
22	800°F (SW-OM)	0.023	50.3	26.2	2.0	78.5	8.9	0.846	0.287	0.020	1.153	0.674	1.683	1.094	0.990	1.469	1.42	0.36
23	700°F (SW-OM)	0.022	51.4	26.9	2.3	80.6	7.7	0.271	0.083	0.003	0.357	0.348	0.524	0.311	0.149	0.443	1.52	0.36
23A	700°F (SW-OM)	0.057	52.0	27.3	2.5*	81.8	6.5	0.230	0.093	0.003	0.326	0.298	0.440	0.342	0.112	0.398	1.77	0.36
24	750°F (SW-OM)	0.057	50.6	27.5	2.6	80.6	7.1	0.255	0.115	0.005	0.376	0.349	0.508	0.420	0.213	0.468	1.78	0.36
25	800°F (SW-OM)	0.056	46.5	26.8	2.7	76.0	7.7	0.470	0.195	0.013	0.678	0.553	1.013	0.728	0.479	0.893	2.12	0.36
26	700°F (SW-WR)	0.068	14.0	61.9	6.6	82.5	9.1	0.065	0.245	0.018	0.328	0.289	0.463	0.396	0.266	0.397	0.92	0.38
27	750°F (SW-WR)	0.065	12.4	60.4	6.5	79.3	8.2	0.076	0.294	0.020	0.389	0.324	0.608	0.487	0.302	0.491	1.52	0.38
28	800°F (SW-WR)	0.065	11.1	59.2	6.1	76.3	10.6	0.121	0.484	0.031	0.636	0.584	1.094	0.818	0.515	0.834	1.24	0.38

assuming that the rate of degradation of total terphenyl is a function of the terphenyl concentration only, the degradation rate equation can be expressed as (See Appendix A3).

$$\frac{w_1}{\bar{r}M_c}\left[C^f_{omp} - C_{omp}\right] - \frac{dC_{omp}}{d\tau} = k_{R,omp,n}C^n_{omp} = \frac{G_R(-omp)}{11.65} \quad (4.1)$$

where

w_1 = feed rate of organic coolant to the loop, gms/hr

$\bar{r} = \frac{d\tau}{dt}$ = average dose rate to the total coolant, watts/gm

M_c = mass of organic coolant, gm

C^f_{omp} = weight fraction of total terphenyl feeding the loop,

C_{omp} = weight fraction of total terphenyl removed from the loop,

τ = specific dose, watt-hr/gm

$k_{R,omp,n}$ = radiolysis rate constant of total terphenyl for the nth kinetics order of radiolysis, (watt-hr/gm)$^{-1}$

$G_R(-omp)$ = G value of total terphenyl degradation, molecules degraded/100 ev absorbed

11.65 = conversion factor, (molecules)(watt-hr)/(100 ev)(gm)

For steady-state operations with constant concentration (or weight fraction) of the total terphenyl in the coolant, Equation (4.1) becomes

$$\frac{G_R(-omp)}{11.65} = k_{R,omp,n}C^n_{omp} = \frac{w_1}{\bar{r}M_c}\left[C^f_{omp} - C_{omp}\right] \quad (4.2)$$

In reactor irradiation, both neutron and gamma radiations contribute to the degradation of organic coolant. We assume that the G value of radiolytic degradation is the sum of G value

due to neutron radiation (G_N) and the G value due to gamma radiation (G_γ), each of which is weighted by a fraction (f_N or f_γ) corresponding to the dose rate fraction contributed by each type of radiation. The G value of radiolysis of Equation (4.2) can then be expressed as

$$G_R = G_N f_N + G_\gamma f_\gamma \qquad (4.3)$$

Since $f_N + f_\gamma = 1$ in reactor irradiation, Equation (4.3) becomes

$$G_R = G_N f_N + \left[1 - f_N\right] G_\gamma \qquad (4.4)$$

Substituting Equation (4.4) into Equation (4.2),

$$\frac{G_R(-omp)}{11.65} = \frac{G_\gamma^o}{11.65} \left[\left[\frac{G_N}{G_\gamma} - 1\right] f_N + 1 \right] C_{omp}^n = k_{R,omp,n} C_{omp}^n \qquad (4.5)$$

where

G_γ^o is equal to G_γ / C_{omp}^n

G_N/G_γ is called the "fast neutron effect ratio"

In expressing the degradation rates of the individual isomers in a mixture of terphenyl isomers, some modification of Equation (4.1) is necessary. Here we assume that the degradation rate of an individual isomer is a function of not only its concentration but also the concentration of the total terphenyl in the coolant. This assumption postulates that interactions between both like and unlike isomers can occur in a mixture of isomers. Equation (4.1) is modified to express the degradation rate of an individual i^{th} isomer at low irradiation temperature as follows:

$$\frac{G_R(-i)}{11.65} = k_{R,i,a+b} C_i^a C_{omp}^b \qquad (4.6)$$

4.3   Results of Low Temperature Irradiations

As mentioned earlier in Section 4.1, three runs, namely 19A

20A and 20B, have been completed at 300° C (572° F) for the measurement of the apparent reaction order of radiolysis, n, and the radiolytic reaction rate constant, $k_{R,omp,n}$. Table 4.2 presents a summary of results of these runs. Detailed descriptions of these irradiations and the degradation calculations are given in Appendix A3.

4.3.1 Apparent Kinetics Order of Radiolysis

Using the G values obtained from the low temperature runs where the thermal decomposition is negligible, the values of n in Equation (4.2) can be evaluated. Figure 4.1 shows a log-log plot of G against C_{omp}. The three data points representing Runs 19A, 20A and 20B are shown on this figure by closed circles. Figure 4.1 also includes similar data for Santowax WR and OM-2 (Curves II through V) as reported earlier by Mason and Timmins (4.1). The fast neutron fractions, f_N, for each run are also shown in this figure. Equation (4.2) shows the kinetic order of radiolysis, n, is just the slope of the straight lines shown in Figure 4.1. Curve I in Figure 4.1 is obtained by a linear least-square fit of the three experimental points. The slope thus calculated is

$$n = 1.7 \pm 0.1 \ (2\sigma)$$

No significant difference can be found between the radiolytic reaction order of Santowax OM and that of Santowax WR or OM-2, that is, n = 1.7 applies equally well to ortho-rich terphenyl mixture such as Santowax OM and to meta-rich terphenyl mixture such as Santowax WR and OM-2.

Note in Equation (4.5) that the values of the intercepts of Figure 4.1 at C_{omp} = 1 are related to the fast neutron fraction, f_N, i.e., the larger the f_N, the larger the G(-omp). The values of the intercepts are also related to G_γ^o and G_N/G_γ, which will be discussed in the following section.

Table 4.2

Summary of Results of Low Temperature Steady-State Runs[a]

of Santowax OM

Run No.	Coolant Composition, wt%					G(-i), molecules/100ev[b]				
	ortho	meta	para	total omp	HB	G(-o)	G(-m)	G(-p)	G(-omp)	G(-HB)
19A	41.5	20.1	1.53	63.1	26.4	0.122 ±0.008	0.054 ±0.004	0.003 ±0.001	0.178 ±0.011	0.160 ±0.014
20B	53.1	25.6	1.83	80.5	8.48	0.193 ±0.014	0.074 ±0.006	0.003 ±0.001	0.270 ±0.020	0.205 ±0.018
20A	57.7	26.6	1.77	86.1	6.07	0.207 ±0.016	0.094 ±0.008	0.005 ±0.001	0.307 ±0.024	0.232 ±0.016

[a] Irradiation temperature, $300°C(572°F)$; Fuel Position 1 (f_N = 0.36); 5 MW nominal reactor power

[b] Error limits are 2σ
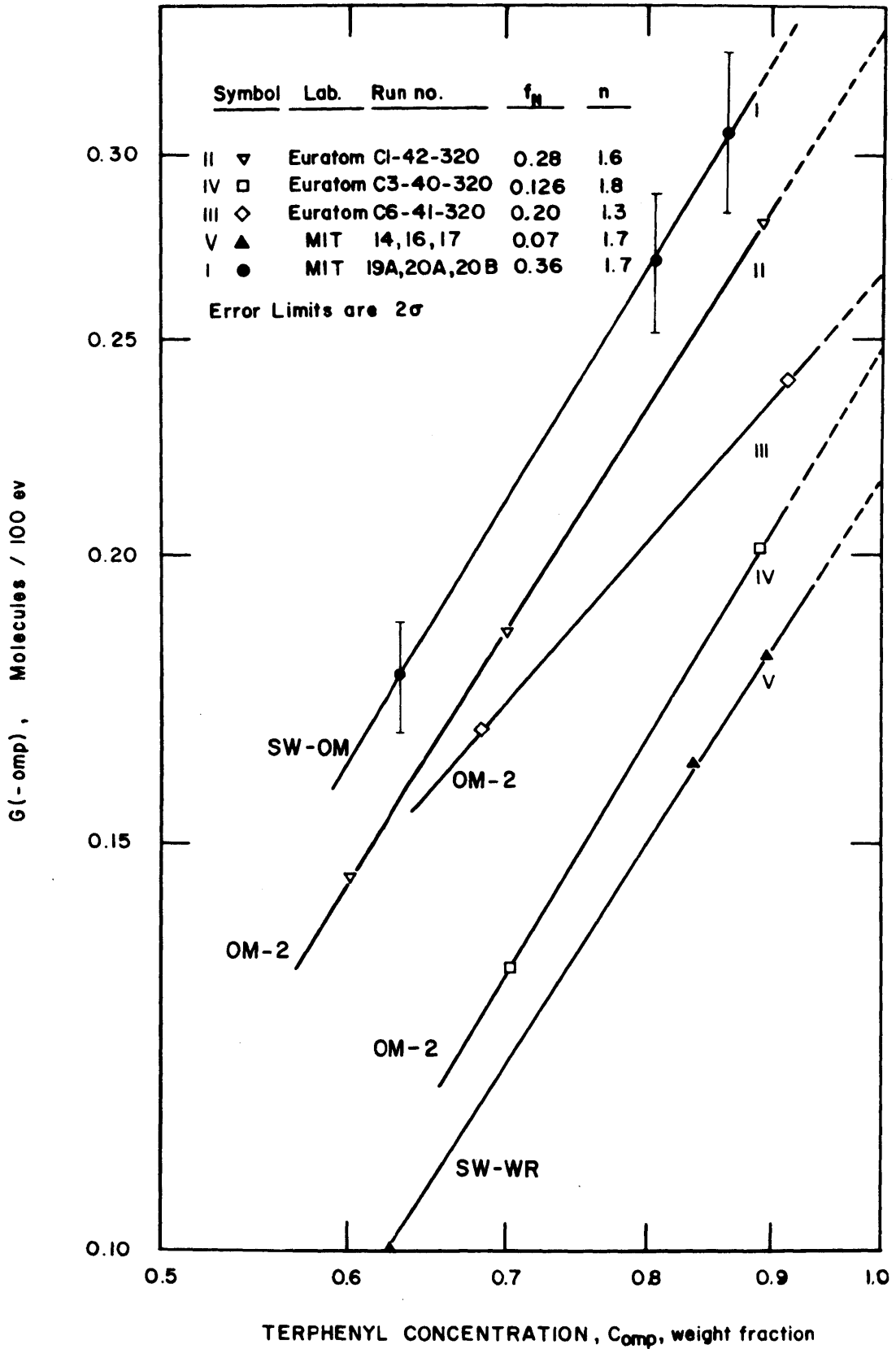
FIGURE 4.1   CORRELATION OF EURATOM AND M.I.T. STEADY-STATE IRRADIATIONS AT LOW TEMPERATURE

4.3.2 Radiolysis Rate Constants and Fast Neutron Effect Ratio

The experimental results given in Table 4.1 and the apparent kinetic order of radiolysis as determined in the last section are now used to determine the radiolysis rate constants, $k_{R,omp,n}$, by means of Equation (4.2) for the three steady-state irradiations of Santowax OM at 300° C. The results are tabulated in Table 4.3.

Table 4.3

Summary of Radiolysis Rate Constants

of Low Temperature Steady-State Irradiations[a]

of Santowax OM

Run No.	C_{omp}	G_R [b]	$k_{R,omp,1.7}$ [b] $(300^{\circ}$ C) $(watt-hr/gm)^{-1}$	$k_{R,omp,1.7}$ [c] $(320^{\circ}$ C) $(watt-hr/gm)^{-1}$
19A	0.631	0.178 ± 0.011	0.0334 ± 0.0020	0.0344 ± 0.0021
20B	0.805	0.270 ± 0.020	0.0335 ± 0.0025	0.0345 ± 0.0026
20A	0.861	0.307 ± 0.024	0.0340 ± 0.0027	0.0350 ± 0.0028

[a] Irradiation temperature, 300° C (572° F); Fuel Position 1, $f_N = 0.36$

[b] Error limits are 2σ

[c] Normalized to 320° C by $\Delta E_R = 1$ kcal/g-mole and n = 1.7

Values of $k_{R,omp,1.7}$ at 320°C are shown in Table 4.3 because they will be compared to the values obtained for meta-rich terphenyls normalized to 320° C as reported by Mason, Timmins,

et al. (4.1).

Mason, Timmins, et al. (4.1) reported radiolysis rate constants of meta-rich terphenyl mixtures of Santowax WR, Santowax OMP and OM-2 irradiated at M.I.T., EURATOM and AECL at different fast neutron fractions. Using Equation (4.5), they correlated the values of $k_{R,omp,1.7}$ (normalized to 320° C and n = 1.7) at various f_N and obtained

$$G_\gamma^o = 0.19 \pm 0.02 \ (2\sigma) \text{ and}$$

$$G_N/G_\gamma = 3.9 \pm 0.4 \ (2\sigma)$$

Rearranging Equation (4.5),

$$k_{R,omp,1.7} = \frac{G_\gamma^o}{11.65}\left[\left[\frac{G_N}{G_\gamma} - 1\right]f_N + 1\right] \qquad (4.5)$$

and substituting the above values of G_γ^o and G_N/G_γ

$$k_{R,omp,1.7}(320^\circ \text{ C}) = 1.61\text{x}10^{-2}\left[2.9f_N + 1\right] \ (\text{wh/g})^{-1}$$
$$(4.7)$$

The radiolysis rate constants of Santowax OM normalized to 320° C and n = 1.7 are shown in the last column of Table 4.3. In normalizing the data from the irradiation temperature of 300° C to 320° C, the temperature effect on the radiolysis rate constant was expressed by the following Arrhenius relation

$$k_{R,omp,n}(T) = k_{R,omp,n}(T_o)\exp\left(\frac{-\Delta E_R}{R}\frac{T_o-T}{T_oT}\right) \qquad (4.8)$$

where

ΔE_R is an activation energy of radiolysis, kcal/g-mole

T and T_o are irradiation temperature, $^\circ$K

R is the gas constant, kcal/g-mole,$^\circ$K

An activation energy of radiolysis of ΔE_R = 1 kcal/g-mole was used. This assumed value of ΔE_R will be discussed in detail in Section 5.3 of Chapter 5. Since the present series of irradiation of Santowax OM were made at one value of

f_N (f_N = 0.36, Fuel Position 1), a determination of G_γ^o and G_N/G_γ is not possible. However, Mason and Timmins (4.1) reported the following G_γ^o and G_N/G_γ values for ortho and meta terphenyls in a mixture of meta-rich terphenyl at 320° C.

Ortho Terphenyl	Meta Terphenyl
G_γ^o = 0.25	G_γ^o = 0.18
G_N/G_γ = 2.7	G_N/G_γ = 4.5

An estimate of G_γ^o and G_N/G_γ values for Santowax OM can be made from these values using the isomer concentration as a weighting factor. For the three steady-state low temperature irradiations of Santowax OM, the ratio of concentration of ortho terphenyl to meta terphenyl is very nearly 2:1 (See Table 4.2). Neglecting the small concentration of para terphenyl in Santowax OM,

$$\frac{G_N}{G_\gamma}(320^oC) = \frac{1}{3}\left[4.5\right] + \frac{2}{3}\left[2.7\right] = 3.3 \qquad (4.9)$$

$$G_\gamma^o(320^oC) = \frac{1}{3}\left[0.18\right] + \frac{2}{3}\left[0.25\right] = 0.23 \qquad (4.10)$$

Substituting these values of G_N/G_γ and G_γ^o into Equation (4.7), we have for Santowax OM at 320° C

$$k_{R,omp,1.7}(320^oC) = 1.97 \times 10^{-2}\left[2.3f_N + 1\right] \ (wh/g)^{-1} \qquad (4.11)$$

Using f_N = 0.36 (Runs 19A, 20A and 20B) in Equation (4.11), the value of $k_{R,omp,1.7}(320^o$ C) = 0.0360 (watt-hr/gm)$^{-1}$. The average experimental value of $k_{R,omp,1.7}(320^o$ C) as shown in Table 4.3 is 0.0346 (watt-hr/gm)$^{-1}$.

Alternatively, we can use G_N/G_γ = 3.3 of Equation (4.9) and the measured value of $k_{R,omp,1.7}(320^o)$ = 0.0346 (watt-hr/gm)$^{-1}$ in Equation (4.7) to calculate G_γ^o. The value of G_γ^o thus calculated is 0.22 which results in

$$k_{R,omp,1.7} = 1.89 \times 10^{-2}\left[2.3f_N + 1\right] \ (wh/g)^{-1} \qquad (4.12)$$

4.3.3 Results from Other Laboratories

Irradiation results of ortho-rich terphenyl are scarce.
The few that are available from other laboratories were mea-
sured by transient irradiation in closed capsules and second-
order radiolytic kinetics was generally used in reported re-
sults. The experimental data of the irradiations to be des-
cribed below are presented in Appendix A6. The method of
calculating $k_{R,omp,n}$ using 1.7 order kinetics is also given
in that appendix.

4.3.3.1 Electron Irradiation of Santowax OM - Mackintosh
(4.3) reported the results of a series of electron irradiation
of Santowax OM at dose rate of 73 watts/gram. One series of
samples was irradiated at 375° C with total dose ranging from
4.4 to 105.8 watt-hr/gram. Another series involved samples
irradiated at constant dose of 8.8 watt-hr/gram at temperatures
ranging from 350° C to 450° C. An earlier M.I.T. report (4.4)
has also discussed the results of these irradiations.

The value of $k_{R,omp,1.7}$ of the 375° C irradiation series
calculated by least-square correlation (see Appendix A6) is
$0.020(wh/g)^{-1}$. Using $\Delta E_R = 1$ kcal /mole, $k_{R,omp,1.7}$ at 320° C
is calculated to be 0.019 $(wh/g)^{-1}$ from Equation (4.12).

The experimental data from the irradiation series at
fixed dose and variable temperature show the combined concen-
tration of terphenyl and biphenyl rather than terphenyl alone.
Therefore only the combined radiolytic rate constant of ter-
phenyl and biphenyl can be calculated. In such cases, the
value calculated is 0.026 $(wh/g)^{-1}$ at 350° C and 0.029 at
375° C.

4.3.3.2 Mixed Irradiation of Santowax OM

(1) AECL (4.5) reported irradiations of Santowax WR
    using NRX X-Rod Facility at a dose rate of 0.33 ±
    0.03 watts/gram and $f_N = 0.3$. Samples were ir-
    radiated from 230° C to 370° C with one sample

per given temperature. The $k_{R,omp,1.7}$ value cal-
culated between the temperature ranges of $305°$ C
and $330°$ C is about 0.028 $(wh/g)^{-1}$ (see Appendix A6).

(2) Tomlinson et al. (4.6) reported sealed capsule ir-
radiations of Santowax OM at $300° - 400°$ C up to 14
watt-hr/gram dose in the fast neutron enhanced
facility of the NRX reactor. The reported dose rate
was approximately 0.1 watt/gram with fast neutron
fraction f_N = 0.51. The experimental data appeared
to be quite scattered between $298°$ C and $325°$ C.
$k_{R,omp,1.7}$ calculated for these irradiations shows
a low of 0.0463 $(wh/g)^{-1}$ at $321°$ C to a high of
0.0587 at $298°$ C (See Appendix A6).

(3) Terrien and Mason (4.4) estimated the initial G
value from the irradiation of Santowax OM by Gercke
and Trilling (4.7) to be 0.27 at $600°$ F with f_N =
0.28 and a dose rate of 1.2 watts/grams based on
zero-order kinetics of HB formation. Using 1.7
order kinetics, the initial G calue is estimated to
be 0.32 which corresponds to $k_{R,omp,1.7}$ of 0.028
$(wh/g)^{-1}$.

(4) Tomlinson, et al. (4.8) reported in 1966 the ir-
radiation result of Santowax OM using an enriched
uranium neutron converter placed outside the calan-
dria tank of the NRX reactor. The averaged dose
rate was 0.1 to 0.15 watts/gram at f_N = 0.55 to
0.62. The reported initial decomposition rate was
0.035 gram/watt-hr at $350°$ C based on second-order
kinetics. This corresponded to a G value of 0.43
and a $k_{R,omp,2}$ of 0.040 at $350°$ C or 0.037 $(wh/g)^{-1}$
at $320°$ C.

Table 4.4 summarizes the results of these irradiations.
The value of $k_{R,omp,1.7}(320°$ C) for each irradiation based
on Equation (4.12) is also shown for comparison. The

Table 4.4

Summary of Low Temperature Irradiation of
Santowax OM[a]

Reference	Dose Rate watts/gm	f_N	$k_{R,omp,1.7}(320°)$, $(wh/g)^{-1}$	
			Experimental	Calculated[b]
(4.3)	73	0	0.019	0.019
(4.5)	0.33	0.3	0.028	0.032
(4.6)	0.1	0.51	0.46-0.059	0.041
(4.4)(4.7)	1.2	0.28	0.028[c]	0.031
(4.8)	0.1-0.15	0.55-0.62	0.037[d]	0.043-0.046
M.I.T. Runs 19A, 20A and 20B	0.06	0.36	0.035	0.035

[a]All results normalized to 320°C using ΔE_R = 1 kcal/mole and n = 1.7 except as noted

[b]Based on Equation (4.12)

[c]Based on initial decomposition rate

[d]Based on second-order kinetics.

agreement between the experimentally determined and the calculated values of $k_{R,omp,1.7}(320^\circ C)$ is quite good.

4.3.4 Comparison of Radiolytic Degradation of Santowax OM and Santowax WR

Results of irradiation of Santowax OM at low temperatures $(300^\circ C$ and $f_N = 0.36)$ show that within the measurement accuracy of the experiments,

(1) the apparent reaction order of radiolysis, $n = 1.7$ applies equally to Santowax OM and Santowax WR,

(2) the fast neutron effect ratio, G_N/G_γ, and the initial G value, G_γ^0, of the individual terphenyl isomers in a mixture of terphenyl remains essentially constant such that the G_N/G_γ and G_γ^0 of total terphenyl in a terphenyl mixture, either ortho- or meta-rich, can be estimated by weighting the corresponding value with the isomer concentration.

4.4 Relative Stabilities of Ortho and Meta Terphenyl Isomers at Low Temperatures

The degradation rate of individual isomers in a mixture of terphenyl isomers has been calculated in Appendix A3. The G* values for each isomer as well as for the total mixture have been shown in Table 4.1. Physically, $G*(-i)$ represents the number of molecules of the ith isomer degraded per 100 ev energy absorbed in the ith isomer. For the purpose of comparing the relative stability of the individual isomers, the ratio of the degradation rate of each isomer to that of the total mixture, $G*(-i)/G*(-omp)$, is used. Para terphenyl will not be included in this study since it represents only a small percentage (<2 w/o) of the total coolant and the irradiation time for each run was generally not long enough to yield results of significance for para terphenyl degradation.

Table 4.5 compares the relative degradation rates of the

Table 4.5

Relative Stabilities of Ortho and Meta Terphenyl
Isomers in Santowax OM Irradiated at 300°C[a]

Run No.	Terphenyl Conc. w/o				Relative Degradation Rates $G_R^*(-1)/G_R(omp)$ [b]	
	Ortho	Meta	Para	omp	Ortho	Meta
19A	41.5	20.1	1.53	63.1	1.04 ± 0.05	0.95 ± 0.05
20B	53.1	25.6	1.83	80.5	1.08 ± 0.06	0.87 ± 0.05
20A	57.7	26.6	1.77	86.1	1.01 ± 0.06	0.99 ± 0.06

[a]Steady-state irradiation at Fuel Position 1 (f_N = 0.36); 5 MW, nominal reactor power

[b]Error limits are 2σ

-4.15-

ortho and meta terphenyl isomers in Santowax OM for steady-state low temperature (300° C) runs at Fuel Position 1.

Returning to Equations (4.2) and (4.6), we can express the G^* values for the total terphenyl as

$$\frac{G_R^*(-omp)}{11.65} = k_{R,omp,n} C_{omp}^{n-1} \tag{4.13}$$

and for the terphenyl isomer as

$$\frac{G_R^*(-i)}{11.65} = k_{R,i,a+b} C_i^{a-1} C_{omp}^b \tag{4.14}$$

Dividing Equation (4.14) by Equation (4.13)

$$\frac{G_R^*(-i)}{G_R^*(-omp)} = \frac{k_{R,i,a+b} C_i^{a-1} C_{omp}^b}{k_{R,omp,} C_{omp}^{n-1}} \tag{4.15}$$

We note from Table 4.5 that the relative degradation rates, $G_R^*(-i)/G_R^*(-omp)$, of the ortho and meta terphenyl do not vary significantly with changes in individual isomer concentration. Mason and Timmins (4.1) reported the same observation from low temperature irradiations of Santowax WR. This suggests that in Equation (4.15), a = 1 and b = n-1 = 0.7 (with n = 1.7 from Section 4.3.1). We therefore have

$$\frac{G_R^*(-i)}{11.65} = k_{R,i,1.7} C_{omp}^{0.7} \tag{4.16}$$

Using the proposed calculation model of a = 1 and b = 0.7, Equation (4.15) thus states simply that the ratio of radiolytic rate constants of the individual isomer to the total terphenyl equals the ratio of the values of G_R^* for the two. We can then estimate the radiolytic rate constant of the isomers using the values of $G_R^*(-i)/G_R^*(-omp)$ from Table 4.5 and the value of $k_{R,omp,1.7}$ from Table 4.3. Table 4.6 summarizes the calculation of $k_{R,i,1.7}$.

Table 4.6

Radiolysis Rate Constants
for the Individual Terphenyl Isomers
in Santowax OM[a]

$k_{R,i,1.7}/k_{R,omp,1.7}$ [b]		$k_{R,omp,1.7}$ [c] $(watt-hr/gm)^{-1}$	$k_{R,i,1.7}$ $(watt-hr/gm)^{-1}$	
Ortho	Meta		Ortho	Meta
1.04	0.94	0.0346	0.0360	0.0326

[a] Fuel Position 1, f_N = 0.36, normalized to $320°C$

[b] Average value from Table 4.5

[c] Average value from Table 4.3

The above results indicate that the ortho terphenyl
may be slightly less stable than the meta terphenyl for
low temperature irradiation of Santowax OM at f_N = 0.36.
However, the significance of any difference in stability
is quite low.

Figure 4.2 shows the effect of the fast neutron
fraction, f_N, on the radiolysis rate constant, $k_{R,i,1.7}$,
normalized to $320°C$ according to Equation (4.5). The
values of G_γ^o and G_N/G_γ, as well as their sources, are
shown in the figure. The line for ortho in Santowax WR
intersects the line for meta in Santowax WR at an f_N
value of approximately 0.40. For f_N < 0.40, $k_{R,o,1.7}$ >
$k_{R,m,1.7}$ and for f_N > 0.40, $k_{R,o,1.7}$ < $k_{R,m,1.7}$. This is
a result of the relatively higher value of G_γ^o and lower
value of G_N/G_γ for ortho terphenyl relative to meta ter-
phenyl.

Mason and Timmins (4.1) reported the relative stabil-
ities of the terphenyl isomers for Santowax WR at $320°C$ and
at two values of f_N as follows:

	G_γ^0	G_N / G_γ	Reference
Ortho in SW-WR	0.25	2.7	(4.1)
Meta in SW-WR	0.18	4.5	(4.1)
SW-WR	0.19	3.9	(4.1)
SW-OM	0.22	3.3	Section 4.3.2
Pure Ortho	0.42	3.0	(4.9, 4.10)
Pure Meta	0.20	4.5	(4.9, 4.10)
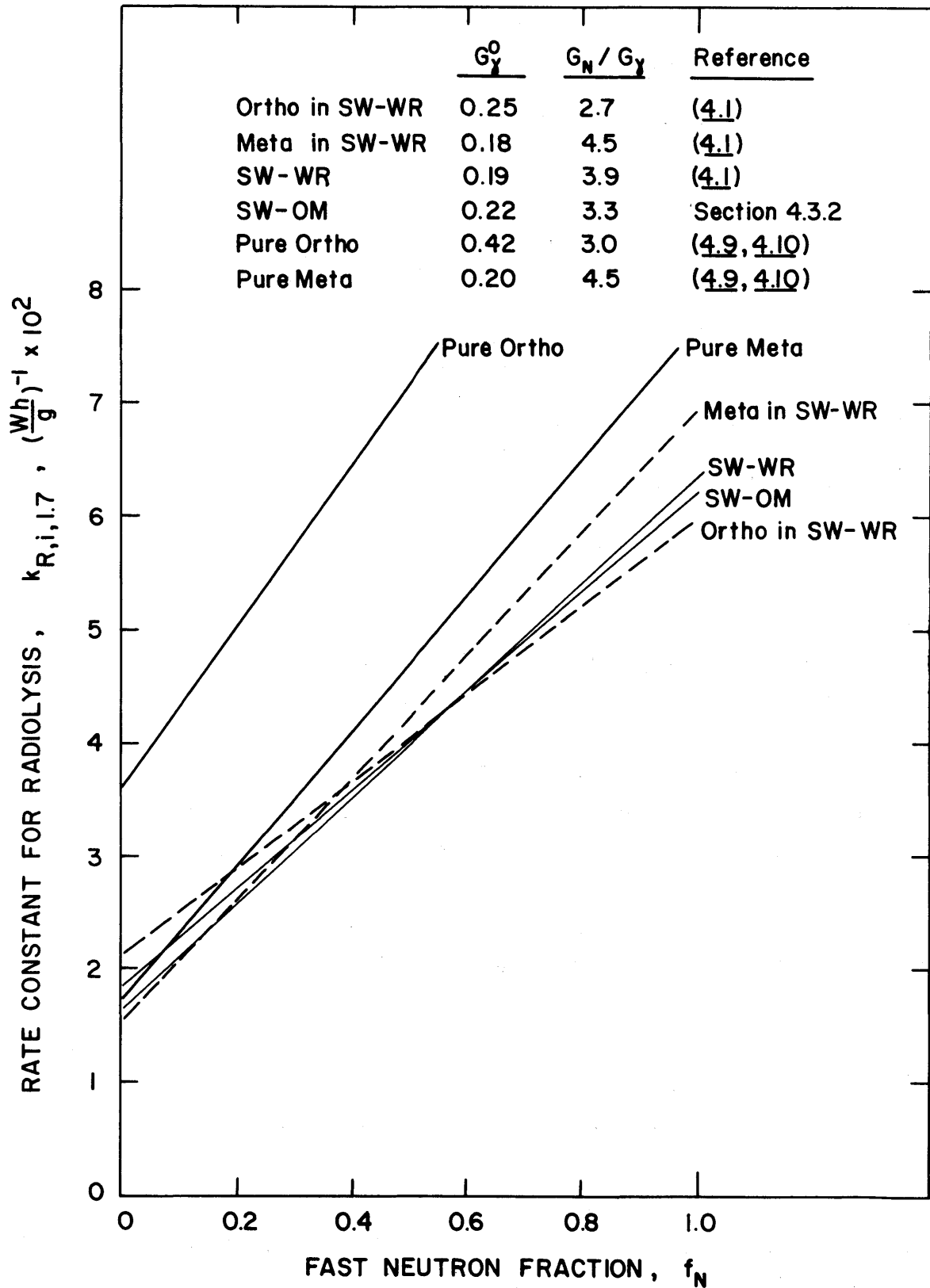
FIGURE 4.2   EFFECT OF FAST NEUTRON FRACTION, f_N, ON THE EMPIRICAL
RADIOLYSIS RATE CONSTANT FOR 1.7 ORDER APPARENT
KINETICS (NORMALIZED TO 320 °C)

f_N	$k_{R,i,1.7}/k_{R,omp,1.7}$ (Santowax WR)	
	Ortho	Meta
0.07	1.19	0.94
0.40	1.00	1.00

The values of $k_{R,i,1.7}/k_{R,omp,1.7}$ for the radiolysis of Santowax OM at $f_N = 0.36$ given in Table 4.6 are in agreement with these values for Santowax WR in indicating that the stability of ortho terphenyl decreases relative to meta terphenyl, as f_N decreases.

AECL (<u>4.9</u>,<u>4.10</u>) reported G_γ^O and G_N/G_γ values from low temperature (300°C) irradiations of pure terphenyl isomers as follows:

Ortho Terphenyl	Meta Terphenyl
$G_\gamma^O = 0.42$	$G_\gamma^O = 0.20$
$G_N/G_\gamma = 3$	$G_N/G_\gamma = 4.5$

Except for the value of G_γ^O for ortho terphenyl, these values of G_γ^O and G_N/G_γ for pure terphenyl isomers and the values obtained by Mason and Timmins (<u>4.1</u>) from irradiations of mixed terphenyls (see Section 4.3.2 or Figure 4.2) agree within 10%. Due to this higher value of G_γ^O for pure ortho terphenyl, the line for pure ortho in Figure 4.2 indicates substantially higher degradation rate constants ($k_{R,o,1.7}$) for pure ortho as compared to the rate constants for ortho in mixed terphenyls and for meta terphenyl either pure or in mixed terphenyl coolants. Further discussions on this point will be presented in Chapter 5.

CHAPTER 5

HIGH TEMPERATURE TERPHENYL DEGRADATION

5.1 Introduction

The principal objective of this study was to investigate the degradation rates of ortho-rich terphenyl (e.g. Santowax OM) and meta-rich terphenyl (e.g. Santowax WR) in the temperature range of 300°C (572°F) to 427°C (800°F), which covers the operating temperature range for large organic-cooled power reactors.

Figure 5.1 shows the terphenyl degradation rates measured in several irradiation facilities plotted in the form of an Arrhenius diagram. It includes irradiation of pure terphenyl isomers as well as ortho-rich and meta-rich terphenyl mixtures. The degradation rates are expressed in terms of initial G values, designated by $G^*(-1)$ or $G^o(-1)$, which represent the terphenyl degradation at 100% terphenyl concentration. In most cases, the data shown in Figure 5.1 were obtained from transient irradiations. In such cases, the original authors used correlation by first- and second-order kinetics (as well as by smooth curve fitting by eye) to obtain these values. The purpose of presenting this figure is to illustrate the effect of temperature on terphenyl degradation rates measured under a wide variety of experimental conditions and interpreted by the original authors with different techniques.

The interpretation of the high temperature terphenyl irradiation data, such as that shown in Figure 5.1, is complicated by the following facts:

    (1) Radiopyrolysis (thermal decomposition) becomes important at temperatures above 350°C expecially for those experiments with low average dose rates.
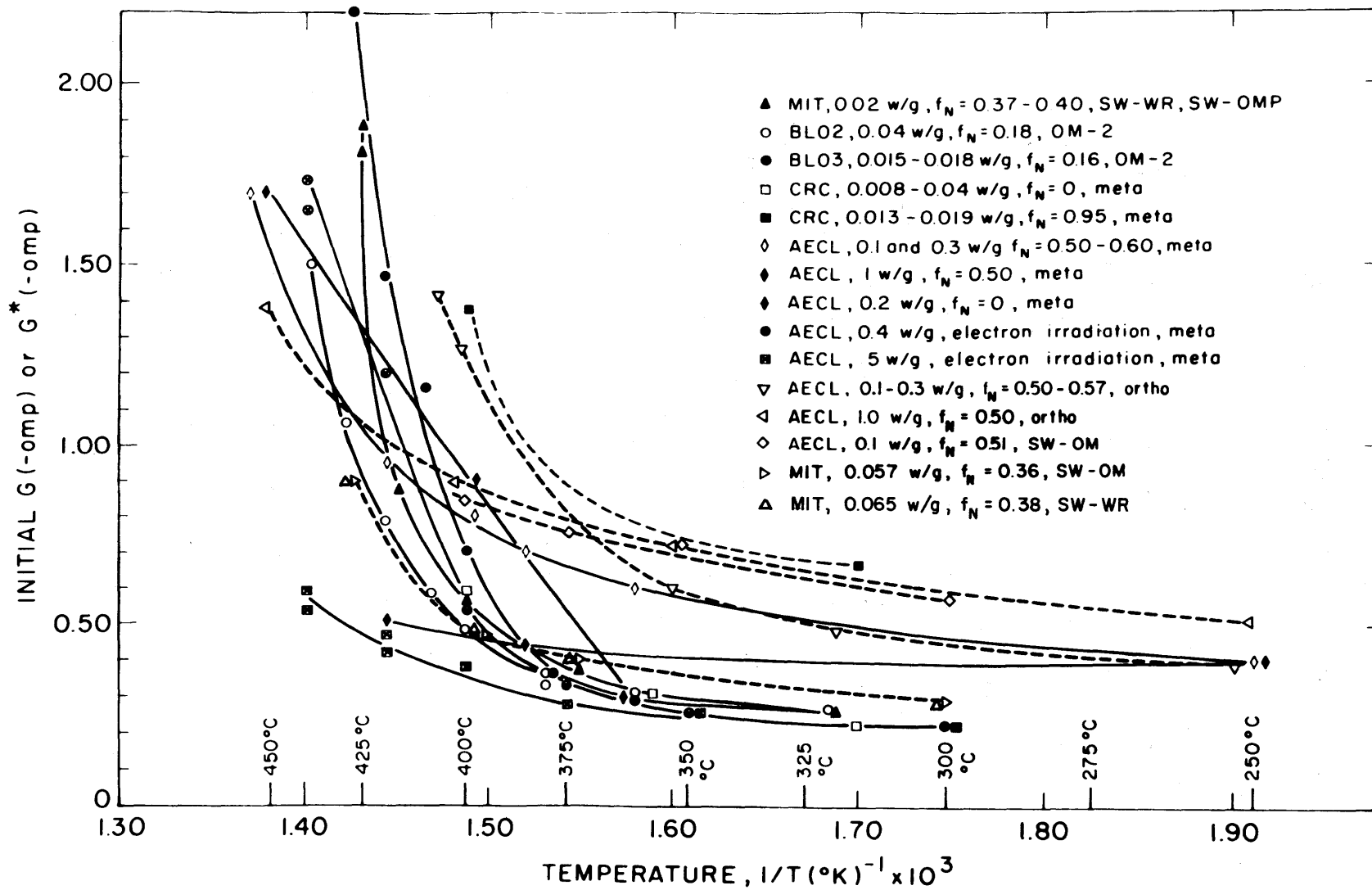
FIGURE 5.1 EFFECT OF TEMPERATURE ON TERPHENYL INITIAL DEGRADATION RATES

Determination of the relative contributions of
radiation and heat to the total degradation rates
is difficult.

(2) Based on the irradiation of pure ortho and meta
terphenyl, AECL (5.1) recently reported ortho ter-
phenyl to be less stable at high temperatures
than meta terphenyl. Therefore the total terphenyl
degradation rate for mixed terphenyl coolants may
vary with the relative concentration of the iso-
mers.

(3) AECL (5.1) also reported dose rate effects on
pure terphenyl isomers which become significant
at temperatures above 350°C.

Available data on ortho-rich terphenyl coolants are
scarce, and there have been no steady-state irradiation
data available except those presented in this chapter.

The overall objective of this chapter is to investi-
gate and compare the temperature and dose rate effects on
the degradation rates of ortho-rich Santowax OM and meta-
rich Santowax WR, at high temperatures (>350°C) and to
develop an empirical model which can be used to predict
the coolant degradation rates in organic-cooled power re-
actors.

To show how this model can be applied, the coolant
degradation rate of a conceptual Heavy Water Moderated
and Organic Cooled power reactor (HWOCR) will be calculated
as an example. Table 5.1 shows a comparison of the M.I.T.
in-pile loop irradiation conditions with those of a con-
ceptual 1000 MWe HWOCR.

5.2 Theory

5.2.1 Steady-State Irradiations

If the effects of radiation and heat are assumed to be
linearly additive, a general rate equation for the total ter-

Table 5.1

Comparison of M.I.T. In-Pile Loop and Conceptual 1000 Mwe HWOCR

Coolant Type	M.I.T. Loop Santowax OM (10% HB)	Conceptual Design[a] HWOCR Santowax OM (10% HB)
Inlet temperature	575°F - 800°F	575°F
Outlet temperature	575°F - 800°F	750°F
ΔT around coolant loop	$\sim 20^\circ$F	175°F
Total coolant mass, lbs	~ 12	$\sim 2,400,000$
Coolant mass in-core, lbs	0.6	23,000
Ratio, $\dfrac{\text{in-core coolant mass}}{\text{total coolant mass}}$	~ 0.05	~ 0.01
Coolant velocity, ft/sec	14 - 22	30 max
In-core residence time, sec	2.4	0.72
Out-of-core residence time, sec	48	77
Average dose rate in-core, watts/gm	0.51 - 1.45	1.3
Average dose rate (total coolant), watts/gm	0.023 - 0.066	0.012
Fast neutron fraction, f_N	0.36	0.66[b]

[a]Reference (5.9)

[b]Estimated from preliminary HWOCR core calculations (5.9).

phenyl degradation can be written as (See Appendix A3 for details):

$$\frac{G(-omp)}{11.65} = k_{R,omp,n} C_{omp}^n + \frac{k_{P,omp,m} C_{omp}^m}{\bar{r}} \qquad (5.1)$$

where

$k_{R,omp,n}$ = radiolysis rate constant of the total terphenyl for the nth kinetics order of radiolysis, $(watt\text{-}hr/gm)^{-1}$

$k_{P,omp,m}$ = radiopyrolysis rate constant of the total terphenyl for the mth kinetics order of radiolysis, $(hr)^{-1}$

$G(-omp)$ = G value of total terphenyl degradation, molecules degraded/100 ev absorbed

$\bar{r}$ = average dose rate to the total coolant, watts/gm

11.65 = conversion factor, (molecules)(watt-hr)/ (100 ev)(gram)

In accordance with earlier M.I.T. reports (5.2, 5.3) the term radiopyrolysis is applied to the thermal decomposition of the irradiated terphenyls whereas pyrolysis is applied to that of unirradiated terphenyls. In Chapter 4 radiolytic degradation rates have been obtained through the irradiation of terphenyl mixtures at low temperatures, where the effect of thermal decomposition is negligible. The method used in this report for the calculation of radiopyrolytic decomposition at higher temperatures is to employ Equation (5.1) by subtracting the radiolytic portion of degradation from the measured total degradation. Equation (5.1) can be rearranged to express the radiopyrolysis contribution as

$$k_{P,omp,m} c_{omp}^m = \left[\frac{G(-omp)}{11.65} - k_{R,omp,n} c_{omp}^n\right] \bar{r} \qquad (5.2)$$

At low temperatures (<320°C), it has been shown in Chapter 4 that the apparent reaction order for radiolysis, n, was equal to 1.7. This value of n is assumed to be applicable at higher temperatures also. At irradiation temperatures above 400°C where radiopyrolysis effects predominate, the values of radiopyrolysis reaction rate constant, $k_{P,omp,m}$, as calculated from Equation (5.2), are not significantly effected by the assumed value of n (see Section 5.8).

The value of m in Equation (5.2) is determined by correlation of the experimental data. Generally first-order kinetics (m = 1) are assumed for thermal decomposition of terphenyls by workers in this field.

The effect of temperature on the radiolysis rate constant can be expressed by the Arrhenius relation as

$$k_{R,omp,n}(T) = k_{R,omp,n}(T_o) \exp\left(\frac{-\Delta E_R}{R} \left[\frac{T_o - T}{T_o T}\right]\right) \qquad (5.3)$$

where ΔE_R is an activation energy of radiolysis, T is the irradidiation temperatures and R is the gas constant. $k_{R,omp,n}(T_o)$ is the radiolysis reaction rate constant determined at a reference temperature T_o.

5.2.2 Transient Irradiations

Although transient operation was not employed in any of the M.I.T. irradiations covered in this report, the irradiations made by other laboratories and discussed in this report consisted of transient runs with terphenyl coolant irradiated in capsules. In transient operation, the total terphenyl concentration and the G value (i.e., degradation rate) both decrease with time and dose. For transient operation with no fresh terphenyl feed (w_i = 0 in Equation (A3.4) of Appendix A3), we have

$$-\frac{dC_{omp}}{d\tau} = \frac{G(-omp)}{11.65} \qquad (5.4)$$

For the nth order kinetics, we can write

$$\left(-\frac{dC_{omp}}{d\tau}\right)_n = K_n(-omp) \, C_{omp}^n \qquad (5.5)$$

where $K_n(-omp)$ is the overall degradation rate constant for n^{th} order kinetics. Thus for zero-, first- and second-order kinetics, integration of Equation (5.5) yields

n = 0:
$$C_{omp} = C_o - K_o\tau \qquad (5.6)$$

n = 1:
$$\ln C_{omp} = \ln C_o - K_1\tau \qquad (5.7)$$

n = 2:
$$\frac{1}{C_{omp}} = \frac{1}{C_o} + K_2\tau \qquad (5.8)$$

where C_o is the initial (τ = 0) total terphenyl concentration. The total degradation rate constant K_n is determined by a least-square fit of the concentration, (C_{omp}), versus dose, (τ), data obtained from the transient run.

Mason and Timmins (5.3) have chosen to define a concentration $\bar{C}_{omp}$ of the transient run at which the value of $(dC_{omp}/d\tau)_1$ by first-order kinetics is equal to $(dC_{omp}/d\tau)_2$ by second-order kinetics, or simply

$$\bar{C}_{omp} = \frac{K_1(-omp)}{K_2(-omp)} \qquad (5.9)$$

Using this procedure to define the total degradation rate at the selected concentration $\bar{C}_{omp}$, in Equation (5.2), the expression for the radiopyrolysis rate constant (e.g., for n = 1.7) becomes

m = 1:

$$k_{P,omp,1} = \left[K_1(-omp) - k_{R,omp,1.7} \left[\bar{C}_{omp} \right]^{0.7} \right] \bar{r}$$

(5.10)

m = 0:

$$k_{P,omp,0} = k_{P,omp,1} \bar{C}_{omp}$$

(5.11)

5.3 Activation Energy of Radiolysis

Since the analysis of the effect of radiopyrolysis on terphenyl coolant at high temperatures depends on the results and extrapolation of the radiolytic degradation at low temperatures as shown by Equations (5.2) and (5.3), the activation energy of radiolysis will be investigated here before we proceed to analyse the experimental data obtained from irradiations at higher temperatures.

Only limited information is available on the radiolytic degradation of ortho-rich terphenyl coolant at different temperatures of irradiation. AECL (5.4) reported a series of electron irradiation ($f_n = 0$) on Santowax OM at temperature range of 350°C to 450°C. Another series of irradiation at AECL using the NRX - X Rod Facility (5.5) also provided irradiation results on Santowax OM at temperature range of 230°C to 370°C with $f_n = 0.33$. The experimental data and calculated results of $k_{R,omp,n}$ (using n = 1.7) for these two series of irradiation are presented in Appendix A6. Figures 5.2 and 5.3 are Arrhenius plots for these two series. The experimental values of the NRX irradiation fit quite well to the dashed line drawn with $\Delta E_R = 1$ kcal/mole within the temperature range of 230°C to about 370°C. For the electron irradiation data of AECL, the experimental points appear to follow $\Delta E_R = 1$ kcal/mole up to about 410°C.

Both these two irradiations used transient operation with the coolant contained in a capsule. Due to the high radiation dose rate and small volume of irradiation, the
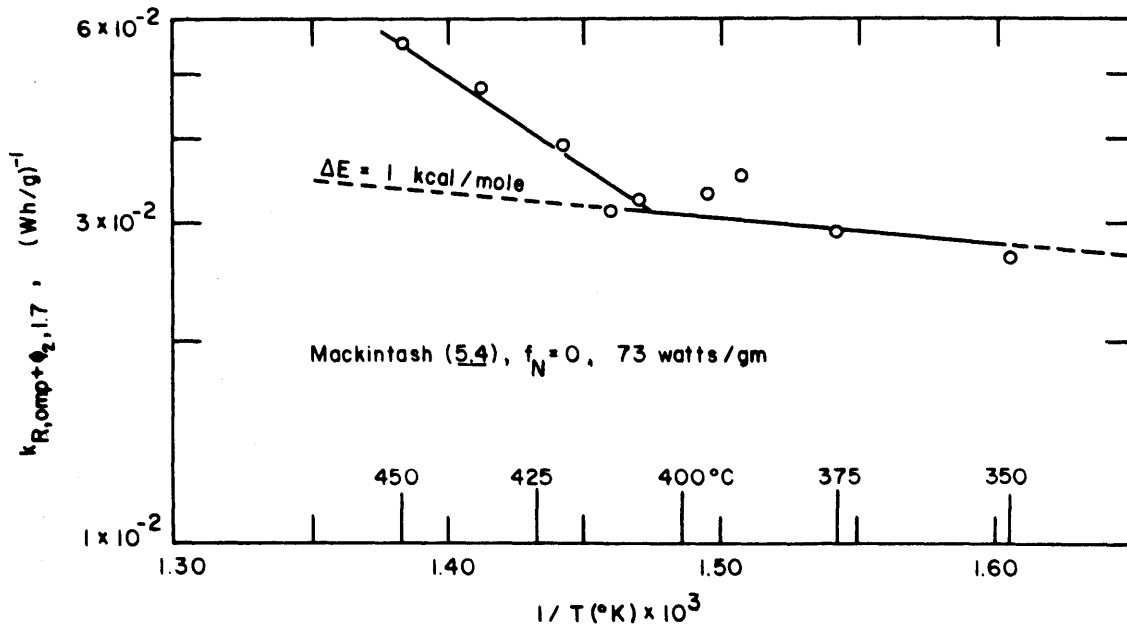
FIGURE 5.2   EFFECT OF TEMPERATURE ON TOTAL DEGRADATION RATE - SANTOWAX OM,
ELECTRON IRRADIATION
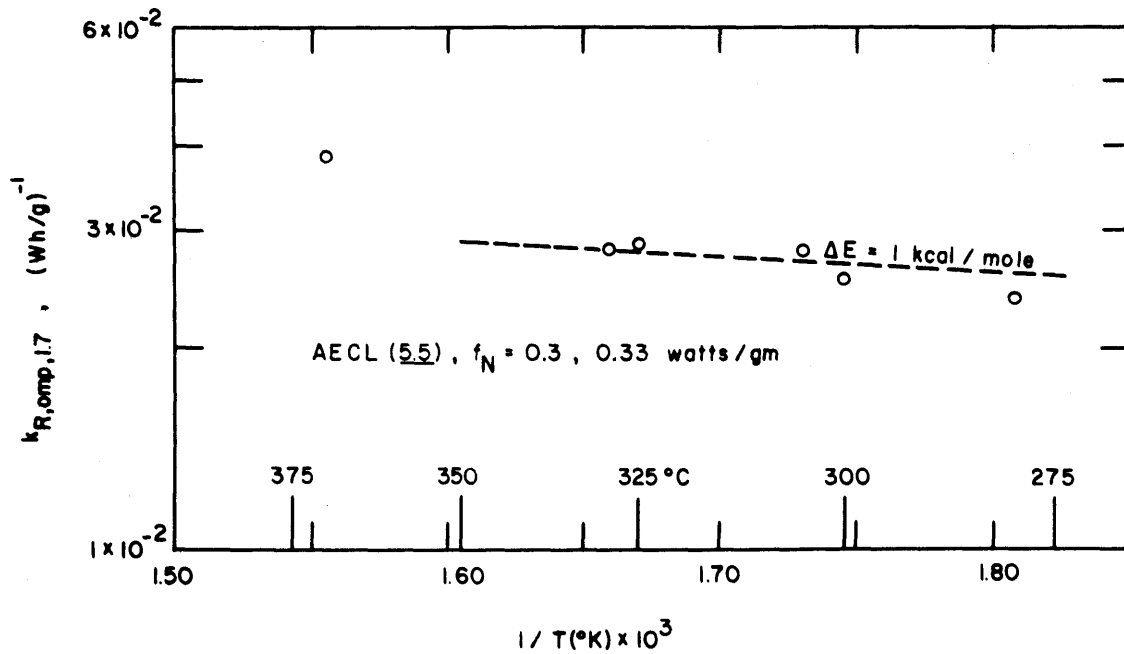
FIGURE 5.3   EFFECT OF TEMPERATURE ON TOTAL DEGRADATION RATE - SANTOWAX OM,
MIXED IRRADIATION

effect of radiopyrolysis on degradation was very small
compared to radiolytic degradation for this type of irradi-
ation. The points in Figures 5.2 and 5.3 have not been
adjusted for radiopyrolysis effects.

The best estimate of ΔE_R, based on these two series
of irradiation by AECL, appears to be about 1 kcal/mole
for temperatures up to about $400°C$. Earlier M.I.T. work
(5.2, 5.3) also indicated a value of ΔE_R = 1 kcal/mole for
meta-rich terphenyls for temperatures up to about $410°C$.
It is difficult to establish whether ΔE_R maintains this con-
stant value above $400°C$. In Section 5.8 it will be shown
that, at an irradiation temperature above $400°C$, the radio-
pyrolysis effect predominates (with a radiopyrolytic activa-
tion energy, ΔE_p, of about 50 kcal/mole), and that an in-
crease of ΔE_R by a factor of two or three would not appre-
ciably affect the calculated results of radiopyrolysis re-
action rates. Thus in the following section, the value of
ΔE_R will be assumed to be 1 kcal/mole for the purpose of
calculating the radiopyrolytic degradation rates.

5.4 M.I.T. Autoclave Pyrolysis Results For Santowax WR

The equipment and procedure of the autoclave pyro-
lysis experiments at M.I.T. have been described in Chap-
ter 2. Table 5.2 shows a summary of results of the six
transient autoclave pyrolysis experiments completed during
the period covered by this report. A detailed description
of these experiments is reported by Rigamonti (5.20).
Zero-, first- and second-order correlations of the disap-
pearance rates for the individual isomers as well as for
the total terphenyls are given in Appendix A4.

Figure 5.4 shows an Arrhenius plot of the first-order
pyrolysis rate constants for unirradiated meta terphenyl
and meta-rich terphenyl mixtures taken from several
sources. Curve I correlates the Euratom data points
(5.8, 5.19) and Curve II correlates both AECL (5.7) and

Table 5.2

Summary of MIT Autoclave Pyrolysis Results for Santowax WR

Run No.	Coolant	Temperature °F	°C	Range of Concentration-w/o DP	Total OMP	Total Terphenyl Disappearance Rate Constant, $k_{P\ omp,m}(hr)^{-1}$ Zero-Order	First-Order
1F	Fresh Santowax WR	796	425	9-30	91-70	1.33 ± 0.13 x 10^{-3}	1.68 ± 0.11 x 10^{-3}
2F	Fresh Santowax WR	833	445	9-43	91-57	3.77 ± 0.11 x 10^{-3}	5.27 ± 0.11 x 10^{-3}
3F	Fresh Santowax WR	769	410	9-31	91-69	4.01 ± 0.17 x 10^{-4}	5.07 ± 0.13 x 10^{-4}
4F	Irradiated[a] Santowax WR	772	411	20-44	80-56	8.32 ± 0.50 x 10^{-4}	1.21 ± 0.03 x 10^{-3}
5F	Irradiated[a] Santowax WR	828	443	21-60	79-40	4.65 ± 0.16 x 10^{-3}	7.97 ± 0.08 x 10^{-3}
6F	Irradiated[a] Santowax WR	798	426	20-51	80-49	1.85 ± 0.13 x 10^{-3}	3.00 ± 0.05 x 10^{-3}

[a] Mixture of irradiated coolant samples from steady-state Runs 26 and 27 which contained initially 9% HB

[b] Error limits are 2σ

-5.11-
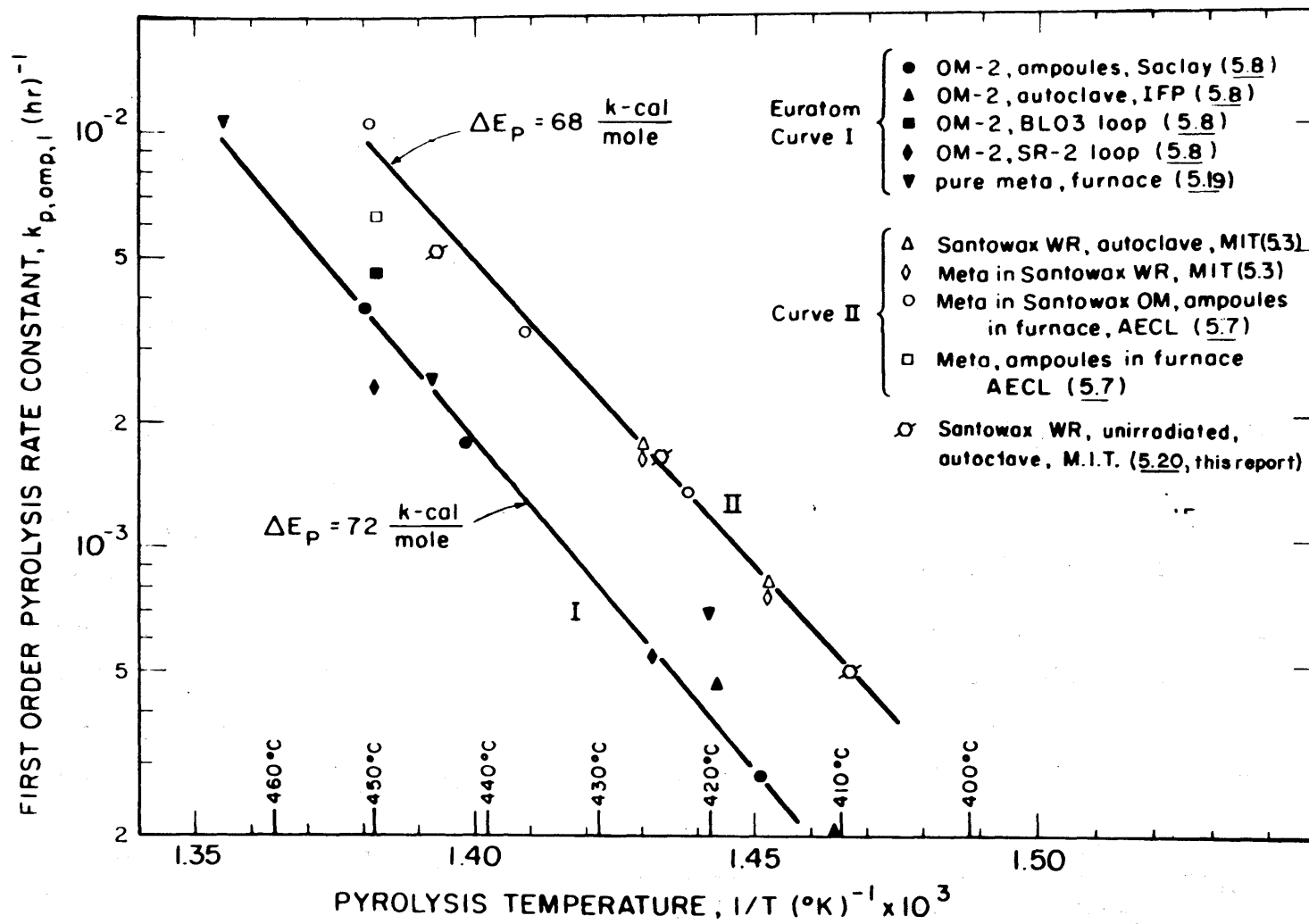
FIGURE 5.4 PYROLYSIS RATES OF META TERPHENYL AND META-RICH
TERPHENYL MIXTURES

previously reported M.I.T. (5.3) data points. The three
data points of the present autoclave runs for unirradiated
Santowax WR (Runs 1F, 2F and 3F) are also shown by the
flagged points. These points fit quite well on Curve II.

Note that the pyrolysis rate constants represented by
Curve II are about a factor of three higher than those obtained by Euratom data (Curve I). One hypothesis for the
difference between the results represented by Curves I and
II had been the possible presence of oxygen in the AECL and
earlier M.I.T. samples. In an attempt to eliminate this
possibility, the fresh coolant used for the autoclave experiments in the latest runs at M.I.T. was degassed repeatedly in several freezing and melting cycles under a
blanket of 2 mm Hg nitrogen before charging to the autoclave system under a blanket of nitrogen. Some of the Euratom pyrolysis experiments were carried out in metallic
loop systems and some in glass or silica ampoules; the AECL
results were obtained in silica ampoules while the M.I.T.
results were obtained by pyrolysis in a metallic autoclave.
At the present time it is not possible to explain the
difference in pyrolysis rates of unirradiated terphenyls
suggested by Curves I and II on the basis of either operating procedures or materials of construction (which might
have had a catalytic effect). The only known difference is
that the Euratom terphenyls were produced in France by
Progil and the AECL and M.I.T. terphenyls were produced
by the Monsanto Chemical Company in the U.S.A.

The first-order radiopyrolysis rate constants of
the irradiated Santowax WR determined from the autoclave
experiments (Runs 4F, 5F and 6F) are plotted in Figure
5.5. Curve III represents a least-square fit of these
three data points; $\Delta E_R = 59 \pm 2$ (2σ) kcal/mole. The
Euratom results (Curve I) and AECL and M.I.T. results
(Curve II) of unirradiated meta-rich terphenyls are also
shown in the figure. Included in the figure are radio-
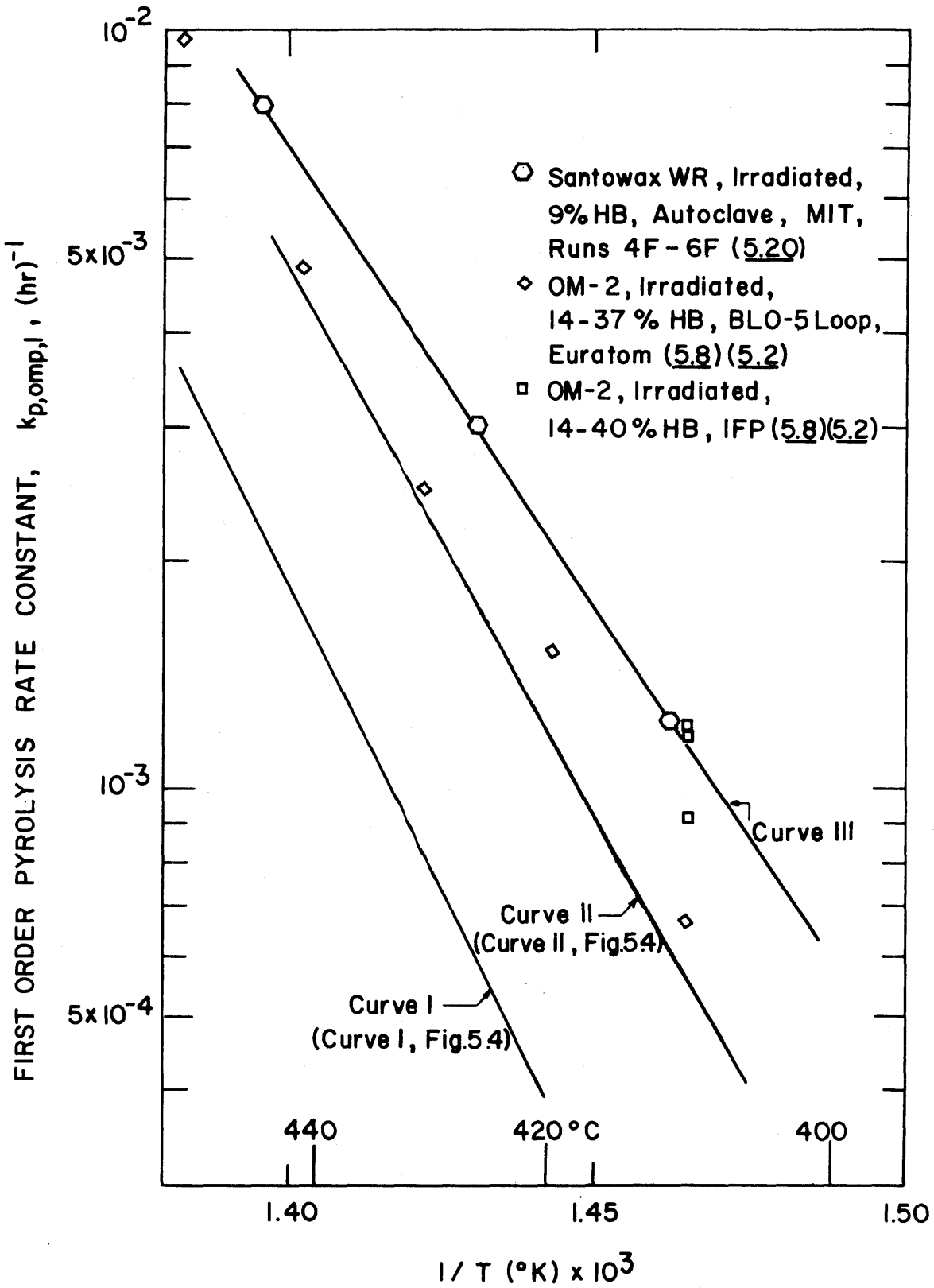
FIGURE 5.5   PYROLYSIS AND RADIOPYROLYSIS RATES
OF SANTOWAX WR AND OM-2

pyrolysis measurements by Euratom workers (5.8) using irrad-
iated OM-2 terphenyl coolant in the BLO-3 loop of the Mel-
usine reactor during week-end operation after the reactor
was shut down. Also, results from irradiated OM-2 coolant
from Melusine pyrolyzed in autoclaves by the Institute of
Petroleum Francais (IFP) (5.8) are presented in the
figure. It is noted that the M.I.T. radiopyrolysis rate
constants (Curve III) of irradiated Santowax WR show an
increase by a factor of two over the pyrolysis rate con-
stant (Curve II) of the unirradiated coolant. The Eur-
atom rate constants for the irradiated OM-2 are only
slightly higher than Curve II but significantly higher
(by a factor of four) than for unirradiated OM-2 (Curve I).
It should also be mentioned that the initial concentra-
tion of the irradiated coolant used in BLO-3 loop experi-
ments covered a wide range of HB concentration from 14%
to 37%. Mason and Timmins (5.3) have suggested that the
increased rate of radiopyrolysis may be due to the forma-
tion of free radical species through thermal decomposition
of the degradation products that are present in the irradi-
ated coolant. These "active species" react with terphenyls
to cause the increased rate of radiopyrolysis. A study
of free radical concentrations by such means as electron
spin resonance using irradiated and unirradiated ter-
phenyls at high temperatures may verify the above explan-
ations.

5.5 Pyrolysis of Santowax OM - AECL Results

Tomlinson, et.al. (5.6) and Mackintosh, et al.(5.7)
have reported the pyrolysis of unirradiated Santowax OM
using a pyrolysis furnace with silica sample ampoules accom-
odated in a massive brass block heated with heating coil.
Results of these experiments are shown in Figure 5.6 using
first-order kinetics.
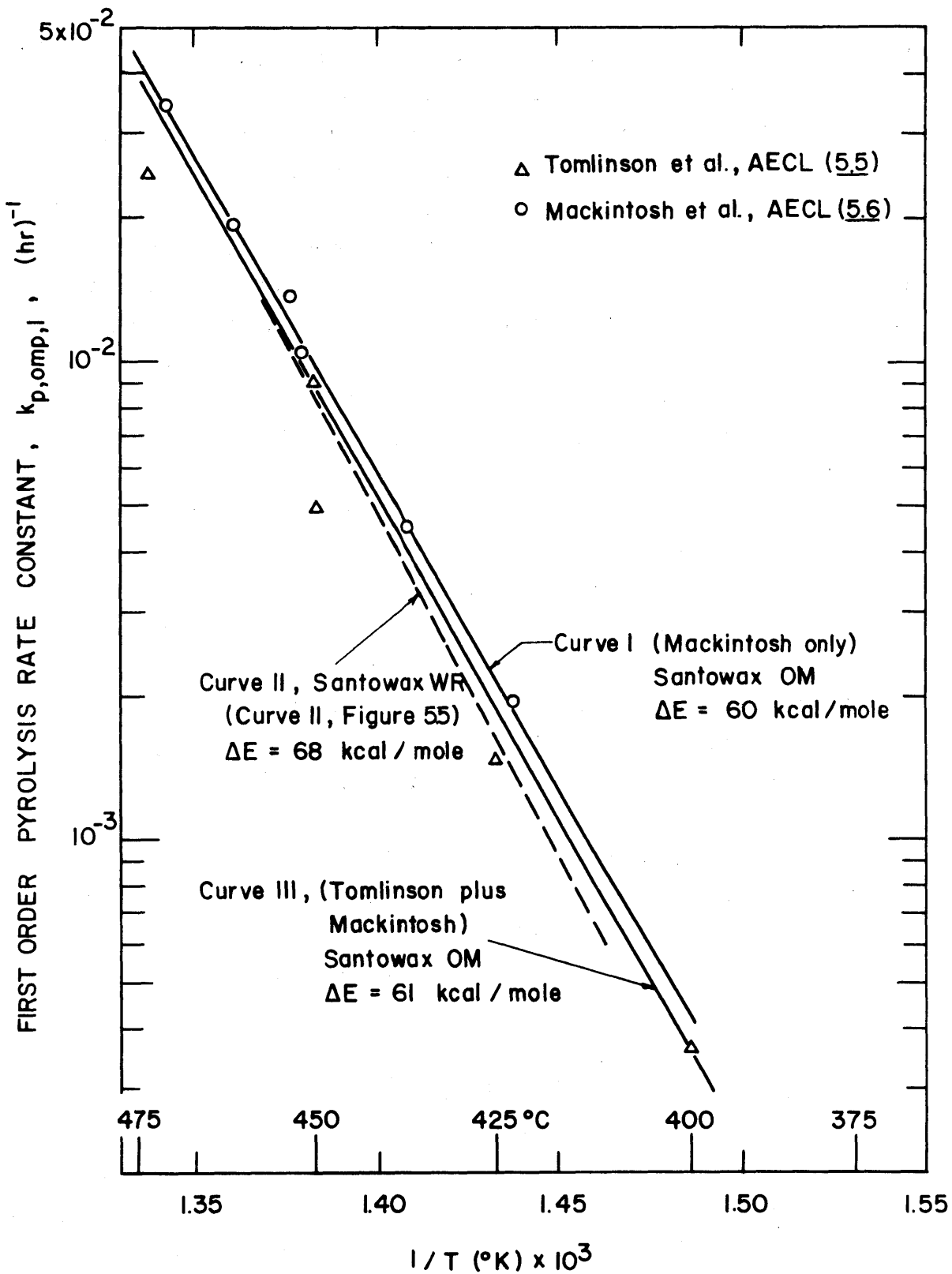
FIGURE 5.6 PYROLYSIS RATES OF UNIRRADIATED SANTOWAX

Curve I is a least-square fit of the data points by Mackintosh, which show little scatter; there is considerable scatter in the Tomlinson data. Curve III is a least-square fit of all the Mackintosh and Tomlinson data for Santowax OM. The pyrolysis results of Santowax WR from AECL and M.I.T. as presented in the last section are also given for comparison (Curve II, dashed line). Comparison of Curves I, II and III indicates that the rates of pyrolysis of unirradiated Santowax OM and WR are essentially the same.

5.6 M.I.T. Loop Irradiation Results - High Temperature Runs

A description of the irradiation conditions for those runs made during the period covered by this report has been presented in Chapter 2. The experimental results are given in Appendix A3. A total of six high temperature (>350°C) steady-state runs (Runs 21, 22, 23, 23A, 24 and 25) were made with Santowax OM as coolant and three (Runs 26, 27 and 28) with Santowax WR. Table 5.3 shows a summary of results for these runs. The first-order radiopyrolysis rate constant, $k_{P,omp,1}$ is also shown for each run. The value of $k_{P,omp,1}$ for Santowax OM runs was calculated according to Equation (5.2) using a value for $k_{R,omp,1.7}$ (320°C) of 0.0346 (wh/g)$^{-1}$, which was obtained from the low temperature irradiations (Runs 19A, 20A and 20B, see Chapter 4). For Santowax WR runs, the $k_{R,omp,1.7}$(320°C) value was calculated from Equation (4.5) using G_N/G_γ value of 3.9 and G_γ^{o} value of 0.19 as reported earlier by Mason and Timmins (5.3) for meta-rich terphenyls. $\Delta E_R = 1$ kcal/mole was assumed to apply over the entire temperature range for all runs. The LIB/HB ratios for these runs are also shown in Table 5.3. The ratios for the Santowax OM runs are appreciably higher than those for Santowax WR for a given temperature and total terphenyl concentration.

Table 5.3

Summary of Steady-State Irradiation Results
for High Temperature Runs in the M.I.T. Loop[a]

Run No.	Coolant	Temperature, °F — Irradiation Capsule	Loop Effective	Average[b] Dose Rate (watts/gm)	Concentration w/o OMP	DP	HB	Degradation Rates[c] G(-omp)	G*(-omp)	Radiopyrolysis[c][d] Rate Constants $k_{p,omp,1}$ (hr^{-1}) x 10^4	LIB/HB
21	Santowax - OM	750	734	0.024	78.0	22.0	9.0	0.48 ± 0.05	0.61 ± 0.06	4.8 ± 1.3	1.44
22	Santowax - OM	800	781	0.023	78.5	21.5	8.9	1.15 ± 0.09	1.47 ± 0.11	21.3 ± 1.6	1.42
23	Santowax - OM	700	684	0.022	80.6	19.4	7.7	0.36 ± 0.05	0.44 ± 0.06	1.4 ± 1.3	1.52
23A	Santowax - OM	700	685	0.057	81.8	18.2	6.5	0.33 ± 0.03	0.40 ± 0.04	1.1 ± 2.3	1.77
24	Santowax - OM	750	730	0.057	80.6	19.4	7.1	0.38 ± 0.03	0.47 ± 0.04	4.3 ± 2.3	1.78
25	Santowax - OM	800	781	0.056	76.0	24.0	7.7	0.68 ± 0.05	0.89 ± 0.06	24.5 ± 2.4	2.12
26	Santowax - WR	700	685	0.068	82.5	17.5	9.1	0.33 ± 0.02	0.40 ± 0.03	1.4 ± 2.8	0.92
27	Santowax - WR	750	739	0.065	79.3	20.7	8.2	0.39 ± 0.03	0.49 ± 0.04	6.4 ± 2.7	1.52
28	Santowax - WR	800	790	0.065	76.3	13.7	10.6	0.64 ± 0.04	0.89 ± 0.05	25.6 ± 2.8	1.24

March 3, 1967 to February 16, 1968

[a] Fuel Position 1, In-pile Section No. 4, f_N = 0.36, for Santowax OM; In-pile Section No. 5, f_N = 0.38, for Santowax WR

[b] Reactor Power was 2 MW for Runs 21, 22 and 23, 5 MW for Runs 23A, 24, 25, 26, 27 and 28

[c] Error limits are 2σ

[d] Assume ΔE_R = 1 kcal/mole, $k_{R,omp,1.7}$(320°C) = 0.0346(wh/g)$^{-1}$ for Santowax OM and $k_{R,omp,1.7}$ (320°C) = 0.0343 kcal/mole for Santowax WR

5.6.1 Radiopyrolysis Effect of Santowax OM

Figures 5.7 and 5.8 show the first-order and zero-
order radiopyrolysis calculated from the high temperature
irradiations of Santowax OM. The error limits on irradia-
tion Runs 23 and 23A, conducted at 700°F (371°C) (effective
loop temperature of 362°C), are large. This is because of
the extremely small radiopyrolysis effect at this tempera-
ture as compared to the radiolysis effect so that the
radiopyrolysis rate constant as calculated from Equation
(5.2) is the difference of two large and nearly equal quan-
tities.

Zero-and first-order kinetics appear to correlate
radiopyrolysis rate constants for Santowax OM equally well.
A similar conclusion was reached by Mason and Timmins (5.3)
regarding the radiopyrolysis of Santowax WR. First-order
kinetics (m = 1) has generally been adopted for the correl-
ation of pyrolysis rate constants for unirradiated coolants
(5.3, 5.5, 5.6, 5.8, 5.19). Mason and Timmins therefore
used first-order rate kinetics to report radiopyrolysis re-
sults for irradiated Santowax WR; to be consistent, first-
order kinetics will also be employed here for both irradiated
Santowax OM and WR.

The six data points as shown in Figures 5.7 and 5.8
belong to two groups irradiated at different dose rates.
The data points of Runs 21, 22, 23 were obtained from
irradiation at 1.95 MW reactor power (average dose rate =
0.023 watt/gm; in-core dose rate = 0.51 watt/gm), whereas
those of Runs 23A, 24 and 25 were obtained at 4.88 MW
reactor power (average dose rate = 0.057 watt/gm; in-core
dose rate = 1.25 watt/gm). No significant difference was
found in the calculated radiopyrolysis rate constants with
a change in dose rate of irradiation by a factor of about
2.5 over the temperature range of 360° to 420°C.

The effect of temperature on the pyrolysis rate con-
stants for the unirradiated Santowax OM as obtained from
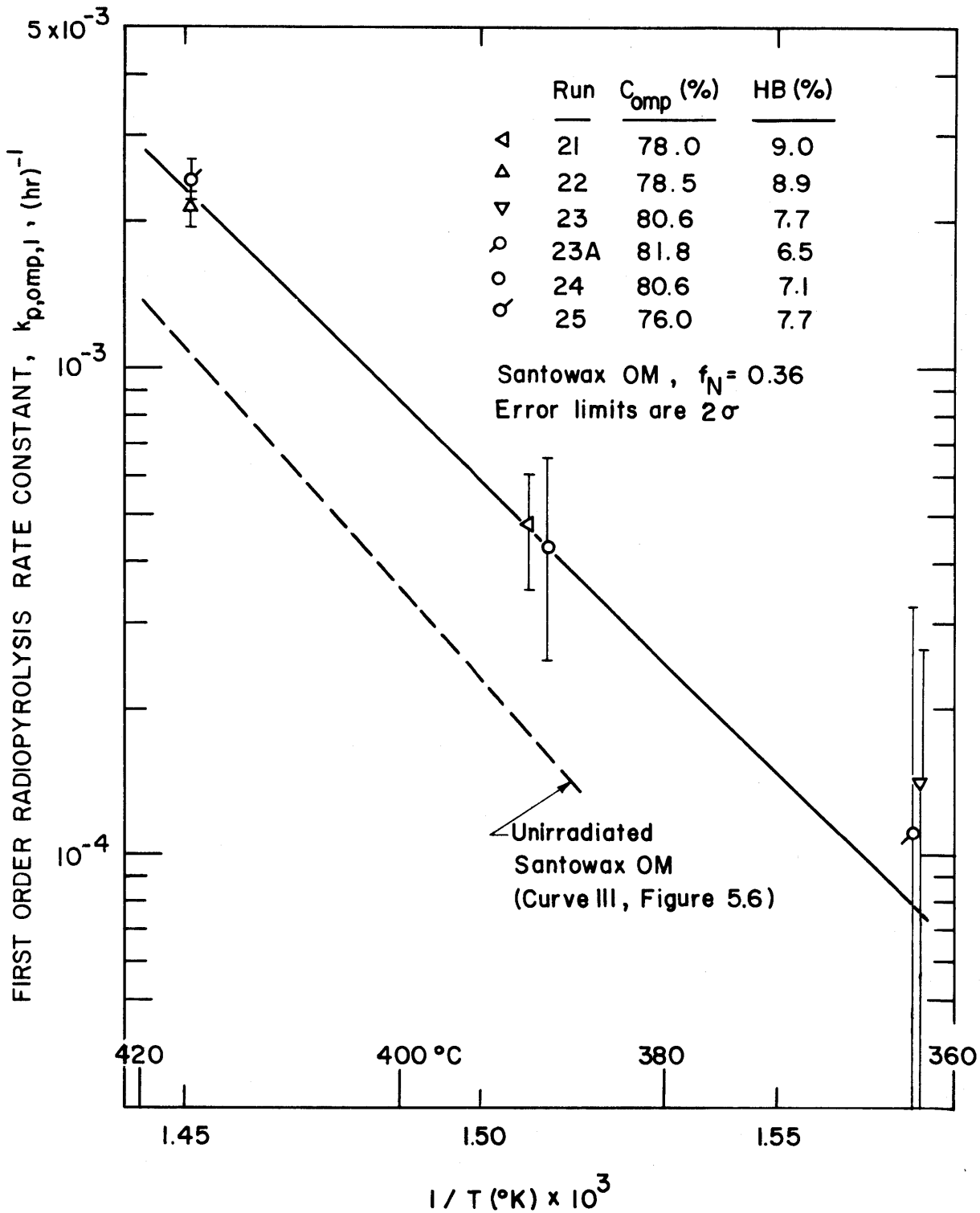
FIGURE 5.7   CORRELATION OF FIRST-ORDER RADIOPYROLYSIS RATE
CONSTANT FOR SANTOWAX OM
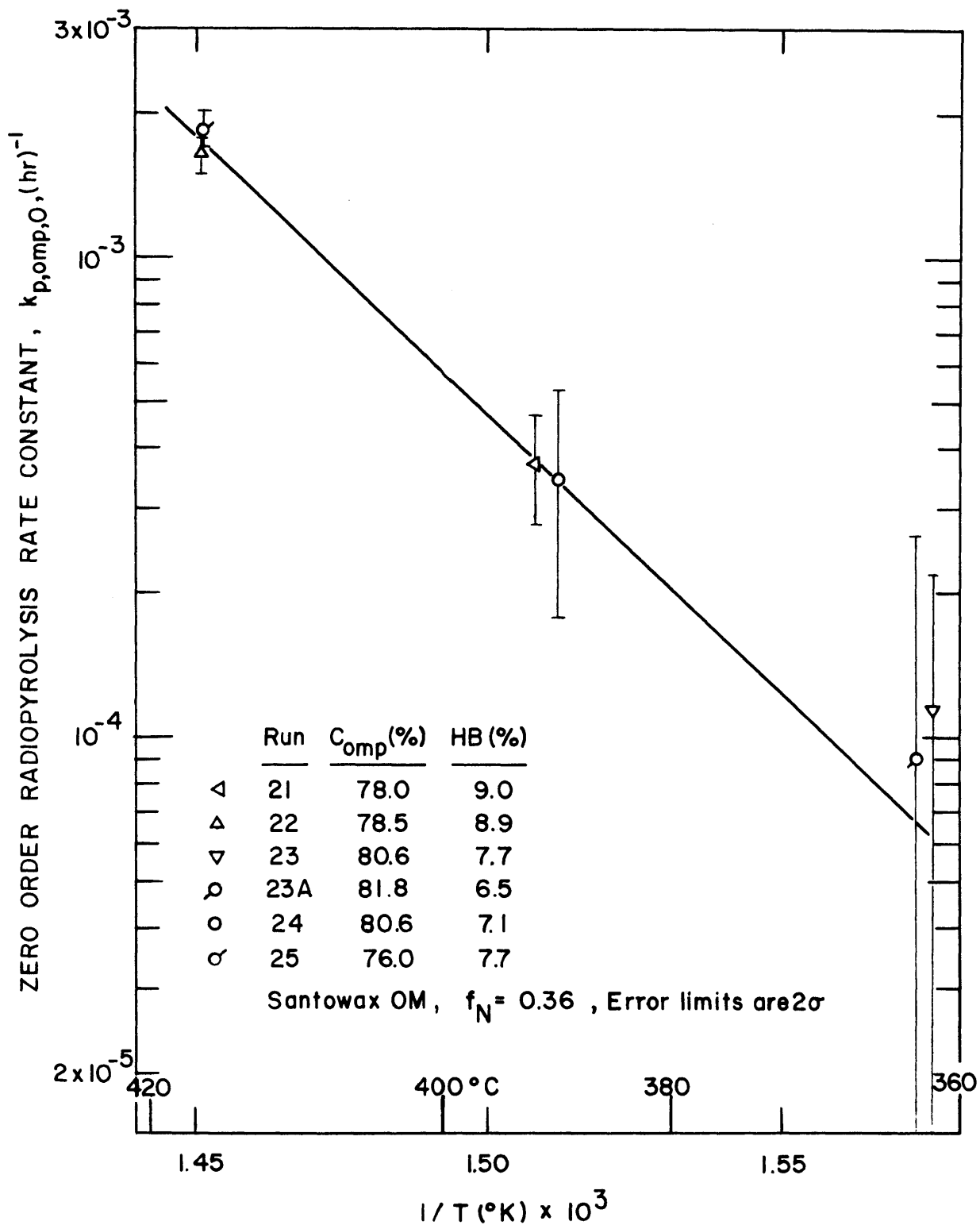
FIGURE 5.8   CORRELATION OF ZERO-ORDER RADIOPYROLYSIS RATE
CONSTANT FOR SANTOWAX OM

the AECL measurements (see Section 5.5, Figure 5.6, Curve III) is also shown (dashed line) in Figure 5.7. The rate constants for radiopyrolysis of the irradiated coolant are significantly greater than the pyrolysis rate constants for the unirradiated coolant.

Weighting the points inversely to their variances, the results of Figure 5.7 were correlated by a least-square fit. The equation obtained for first-order kinetics is

$$k_{P,omp,1}(T) = \exp\left(a - b\left[\frac{1}{T}\right]\right), \ (hr)^{-1} \qquad (5.12)$$

or

$$k_{P,omp,1}(T) = \exp\left(a - \Delta E_P\left[\frac{1}{RT}\right]\right), \ (hr)^{-1} \qquad (5.13)$$

where

$$a \ = 33.7 \pm 3.6 \ (2\sigma)$$
$$b \ = 27400 \pm 2400 \ (2\sigma)$$
$$\Delta E_P = 54.2 \pm 4.8 \ (2\sigma)$$

T is the temperature, $^\circ K$

R is the gas constant, 1.987×10^{-3} kcal/mole-$^\circ K$

The above equations (represented by the solid line in Figure 5.7) are considered to be the best estimate of the first-order radiopyrolytic reaction rate constant for Santowax OM based on steady-state irradiations at M.I.T. The activation energy of radiopyrolysis, ΔE_P, is 54 ± 5 (2σ) kcal/mole for Santowax OM.

5.6.2 Radiopyrolysis Effect of Santowax WR

The radiopyrolysis rate constants obtained from the current nine irradiations of Santowax WR and OM at temperatures greater than about $700^\circ F$ ($371^\circ C$) are shown in Fig-

ure 5.9. Also included in Figure 5.9 are three curves showing the results of autoclave pyrolysis experiments as presented in Figures 5.4, 5.5 and 5.6.

The first-order radiopyrolysis rate constants calculated from the Santowax WR irradiations (Runs 26, 27 and 28) are shown in Figure 5.9 by closed points. These runs were made at approximately the same conditions as Santowax OM Runs 23A, 24 and 25 in order to make direct comparison in degradation rates between the meta-rich terphenyl and the ortho-rich terphenyl. The error limits for Run 26 (700°C) again were large, due to the extremely small effect of radiopyrolysis in the presence of large radiolysis effects.

Although correlation of the radiopyrolysis rate constants shown on Figure 5.9 for Santowax WR alone (closed points) results in a slightly lower value of $\Delta E_{P,1}$, the rate constants for all nine irradiations of both Santowax OM and WR are correlated within the experimental limits by a single line with an activation energy, $E_{P,1} = 48 \pm 7$ (2σ) kcal/mole.

5.6.3 Comparison of Radiopyrolysis Effect of Santowax OM and Santowax WR

The following general conclusions are suggested, based on the results from the nine high temperature irradiations made in the M.I.T. loop and from the autoclave pyrolysis experiments (see Figure 5.9):

(1) Within the experimental accuracy, there appears to be no significant difference between the radiopyrolysis rate constants for Santowax OM and Santowax WR.

(2) Within the experimental accuracy, an activation energy for radiopyrolysis of 48 $\pm$ 7 (2σ) kcal/mole can be used for mixed terphenyl constants (either meta- or ortho-rich) containing about 80 w/o
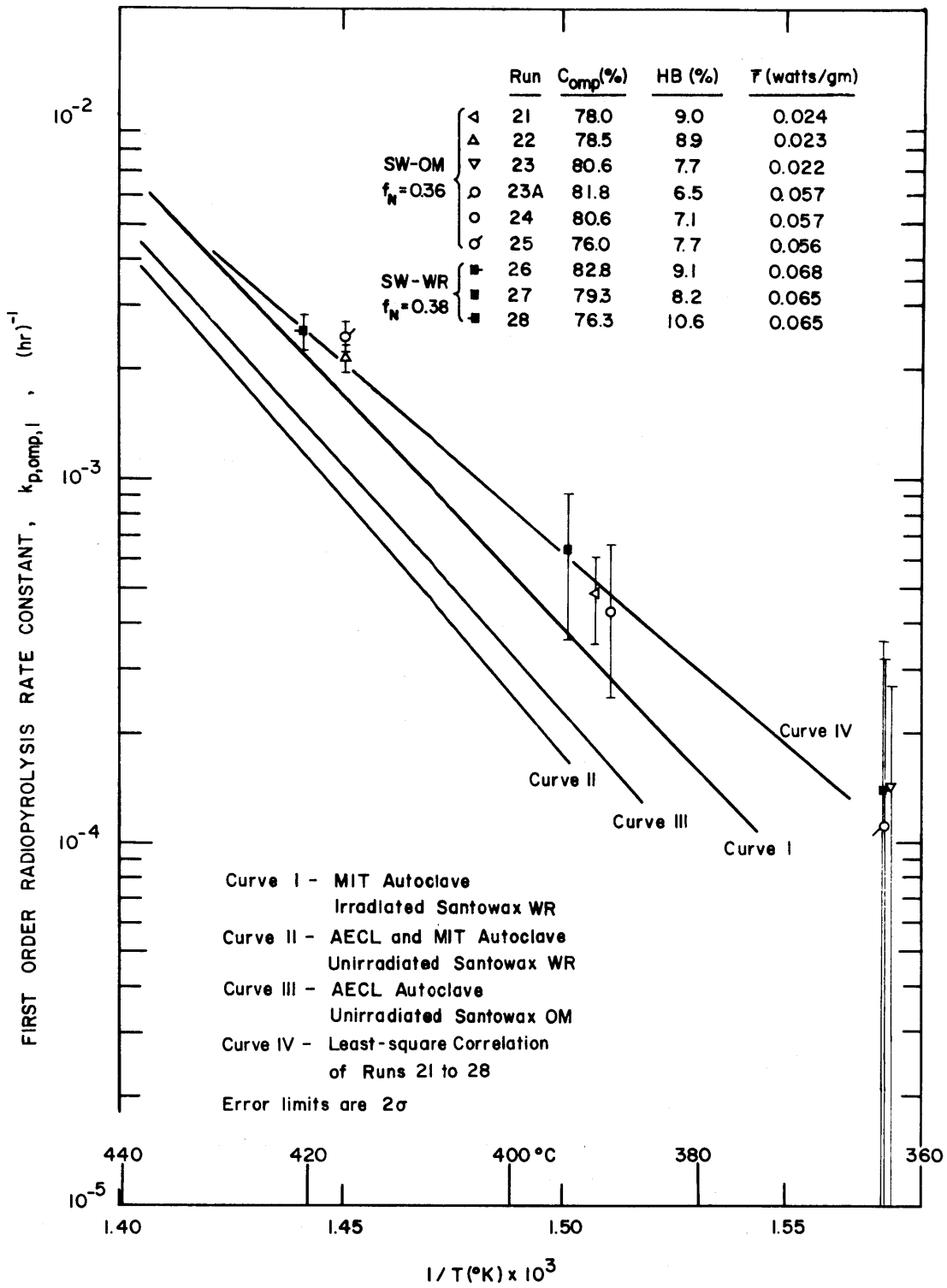
FIGURE 5.9   COMPARISON OF FIRST-ORDER RADIOPYROLYSIS RATE CONSTANTS OF SANTOWAX
OM AND SANTOWAX WR

terphenyl and about 6 to 11 w/o High Boilers. This
value for $E_{P,1}$ is the same as that suggested by
Mason and Timmins (5.3) for meta-rich coolants of
similar total terphenyl composition on the basis
of earlier irradiations.

(3) The radiopyrolysis rate constants of the irradiated
coolant are significantly higher at all tempera-
tures than the pyrolysis rate constants of unirradi-
ated coolant for both Santowax OM and Santowax WR

(4) The activation energy for pyrolysis of unirradiated
terphenyl (64 ± 7 kcal/mole) appears to be higher
than that for radiopyrolysis of the irradiated ter-
phenyl (48 ± 7 kcal/mole).

(5) The activation energy of radiopyrolysis from auto-
clave (post-irradiation) experiments (59 ± 2
kcal/mole) appears to be higher than that from
in-pile loop irradiation (48 ± 7 kcal/mole).

(6) There is no evidence of a dose rate effect on de-
gradation of mixed terphenyl coolants over the
range of coolant compositions, temperatures, and
dose rates in the range of interest for organic-
cooled nuclear reactors.

5.7 Correlation of First-Order Radiopyrolysis Rate Constants - M.I.T. Loop Irradiation

Figure 5.10 shows an Arrhenius plot of first-order
radiopyrolysis constants of all the high temperature (>350°C)
measurements made at M.I.T. In-pile Loop Facility since it
was established. The most recent nine irradiations, which
are described in detail in this report, are shown by
closed points. Three different mixed terphenyl coolants
are represented in this figure, namely Santowax OMP, Santo-
wax WR and Santowax OM. Also shown are four lines represent-
ing:

	Run	% omp	% Bottoms or % HB	
o	2-18B	52 - 90	12 - 35	SW-WR
◄	21	78	9	SW-OM
▲	22	79	9	SW-OM
▼	23	81	8	SW-OM
⬗	23A	82	7	SW-OM
●	24	81	7	SW-OM
◕	25	76	8	SW-OM
⬛	26	83	9	SW-WR
■	27	79	8	SW-WR
◧	28	76	11	SW-WR

Error Limits are 2σ

Curve I - MIT, Irradiated Santowax WR, Autoclave
Curve II - AECL and MIT, Unirradiated meta and Santowax WR
Curve III - Least Square Correlation of all data points
Curve IV - Least Square Correlation of Runs 21-28

FIGURE 5.10   CORRELATION OF FIRST ORDER RADIOPYROLYSIS
RATE CONSTANTS — MIT RUNS

Curve I   Radiopyrolysis from post-irradiation pyrolysis
                 of irradiated Santowax WR (from Curve III
                 Figure 5.5), $\Delta E_{P,1} = 59 \pm 2$ (2σ) kcal/mole

Curve II   Pyrolysis of unirradiated meta terphenyl
                 and Santowax WR (from Curve II Figure 5.4),
                 $\Delta E_{P,1} = 68 \pm 4$ (2σ) kcal/mole

Curve III   Radiopyrolysis - least-square fit of all
                 data points Santowax OM and WR (using
                 weighting inversely proportional to vari-
                 ance), $\Delta E_{P,1} = 54 \pm 9$ (2σ) kcal/mole

Curve IV   Radiopyrolysis from M.I.T. Runs 21-28,
                 Santowax OM and WR (from Curve IV Figure
                 5.9), $\Delta E_{P,1} = 48 \pm 7$ (2σ) kcal/mole.

Curves III and IV are only slightly different, but the
location of Curve IV above Curve III indicates that the re-
cent high temperature irradiations of Santowax WR (meta-
rich) resulted in greater radiopyrolysis rate constants than
the earlier meta-rich irradiations at M.I.T. The differences
in radiopyrolysis rate constants indicated by Curves III and
IV may be due, at least in part, to differences in the pro-
cessing methods used to remove the high boiling degradation
products during the steady-state runs. The recent steady-
state irradiations at M.I.T. utilized a "High Boiler Dis-
tillation" which cut off the distillation after para ter-
phenyl (and before High Boilers) had distilled over. All
but one (Run 2) of the earlier steady-state high temperature
irradiations had utilized a "Bottoms Distillation" which
permitted about 75 w/o of the quarterphenyls (considered a
High Boiler fraction) to distill over for recycle to the
loop makeup. The majority of the earlier M.I.T. irradia-
tions were made with coolant containing less than 70%

terphenyl and about 30% Bottoms.

On the basis of the results obtained from the few earlier irradiations which had relatively low Bottoms Content (Run 7 had 74% omp and 12% Bottoms; Run 6, 69% omp, 15% Bottoms; Run 10, 65% omp, 17% Bottoms), Mason and Timmins (5.3) tentatively suggested that radiopyrolysis constants for irradiated mixed terphenyl coolants, at any given temperature, increased with increasing Bottoms content (and decreasing terphenyl content). One of the objectives of the present series of irradiations (Runs 21-28) was to investigate this proposal, and the irradiations were operated at low High Boiler (7-11w/o HB) and high terphenyl (76-83w/o omp) contents. As shown in Figure 5.10 the radiopyrolysis constants were equal to or greater than those obtained earlier with 50-60w/o omp. In view of these additional recent results, rate constants for any given temperature do not appear to increase (or decrease) simply with High Boiler or Bottoms Content alone. The mechanism of the radiopyrolysis reaction is not understood at this time. Consequently, in the absence of further information regarding the effect of coolant composition, a single correlating line is now recommended for predicting the effect of radiopyrolysis degradation on either Santowax WR or OM. The recommended equation, (Curve III) derived from all the data can be expressed as

$$\ln k_{P,omp,1}(T) = a - b/T \tag{5.14}$$

or

$$k_{P,omp,1}(T) = \exp\left(a - \Delta E_p/RT\right) \tag{5.15}$$

where

$$a = 33.7 \pm 7.0 \ (2\sigma)$$
$$b = 27600 \pm 4800 \ (2\sigma), \ ^\circ K$$
$$\Delta E_p = 54.4 \pm 9.4 \ (2\sigma), \ kcal/mole$$

Note that the radiopyrolysis constants represented by Curve I, for the post-irradiation pyrolysis of Santowax WR, irradiated during Runs 26 and 27, lie below the radiopyrolysis rate constants obtained during the actual irradiation periods of Runs 26 and 27. This suggests that the (unknown) components in the coolant causing the increased radiopyrolysis degradation rates either disappear somewhat (but not completely) during the period of time between irradiation and the autoclave pyrolysis, and/or are consumed during the autoclave pyrolysis.

The magnitude of activation energies determined from the curves on Figure 5.10 are quite sensitive to the location of a few points, especially the high temperature values. There does not appear to be a significant difference in the activation energies for the three curves representing radiopyrolysis (Curves I, III and IV).

5.8 Radiopyrolysis Effect on Individual Isomers

Determination of the relative stabilities of the pure terphenyl isomers, especially in ortho-rich coolants, in high temperature irradiations, was one of the primary objectives of the latest series of irradiations at M.I.T. Before discussing the results obtained in these M.I.T. irradiations, a review of earlier studies of the stability of the pure isomer will be presented.

AECL has made capsule irradiations of ortho and meta terphenyls in the NRX reactor at f_N = 0.01 and f_N = 0.50-0.60 with dose rates ranging from 0.1 to 1 watts/gram at temperatures from 100° to 450°C (5.11, 5.12, 5.13). AECL has also made electron (Van de Graaf) irradiations of ortho and meta terphenyls as well as Santowax OM (5.4). Earlier M.I.T. reports (5.2, 5.10) have reviewed the results of these irradiations as well as the results of electron irradiations at Atomics International (5.14, 5.15) of ortho terphenyl from 752°F to 898°F at an average dose rate of

about 0.8 watts/gram. Figures 5.11 and 5.12 have been reproduced from an earlier M.I.T. report by Mason and Timmins
(5.3), which summarizes the results of the AECL and AI
radiolysis experiments with pure meta and meta-rich terphenyl and with pure ortho terphenyl. The ordinates of
Figures 5.11 and 5.12 represent the values of $k_{Total,1,2}$
(second-order total rate constant) normalized by
$k_{R,omp,1.7}$ calculated using Equation (4.7) in order to
account for wide variation in fast neutron fraction in these
experiments. Table 5.4 presents a review of the AECL
irradiations on pure ortho and pure meta terphenyls as summarized by Tomlinson, et al. (5.1).

These results are reported again here since the necessity to confirm them under conditions of steady-state inpile loop irradiation was one of the principal motivations
for the recent series of irradiations of Santowax OM and
WR at M.I.T.

The general conclusions reached from these AECL irradiations (5.1) in terms of radiolytic mechanism are summarized
as follows:

At temperatures below $350°C$, the radiolytic decomposition rates of pure terphenyl isomers:

(1) were independent of radiation intensity (or dose
rate)

(2) increased slightly with temperature

(3) were several times greater for recoil proton radiation (or fast neutrons) than for fast electrons
(or gamma radiation)

Above $350°C$, the decomposition rates during irradiation:

(1) were greater at low intensity than at high intensity

(2) increased more rapidly with temperature

(3) were independent of the type of radiation
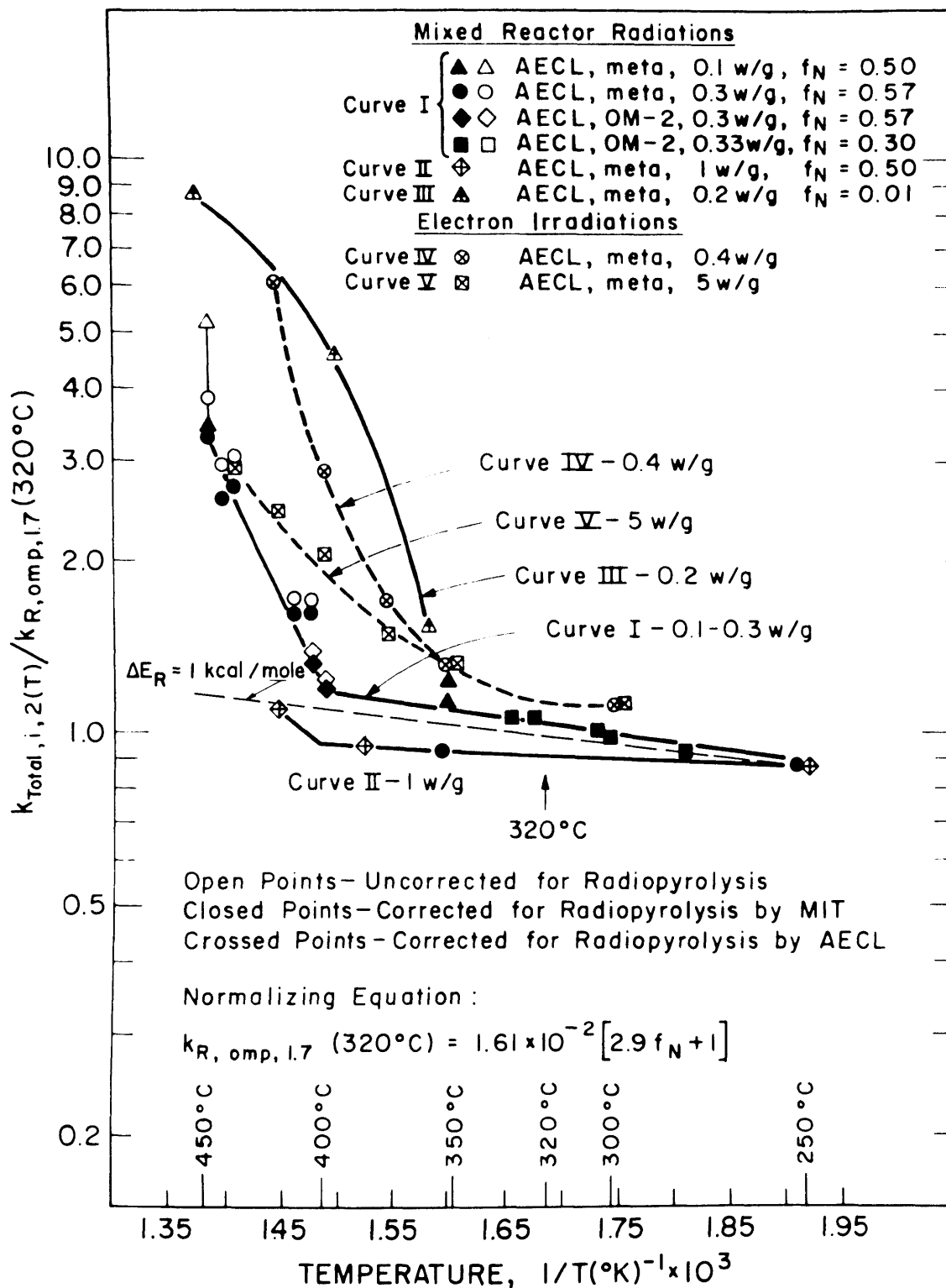
FIGURE 5.11 EFFECT OF TEMPERATURE ON THE RADIOLYSIS
RATE OF META-RICH TERPHENYLS (SECOND-
ORDER KINETICS)
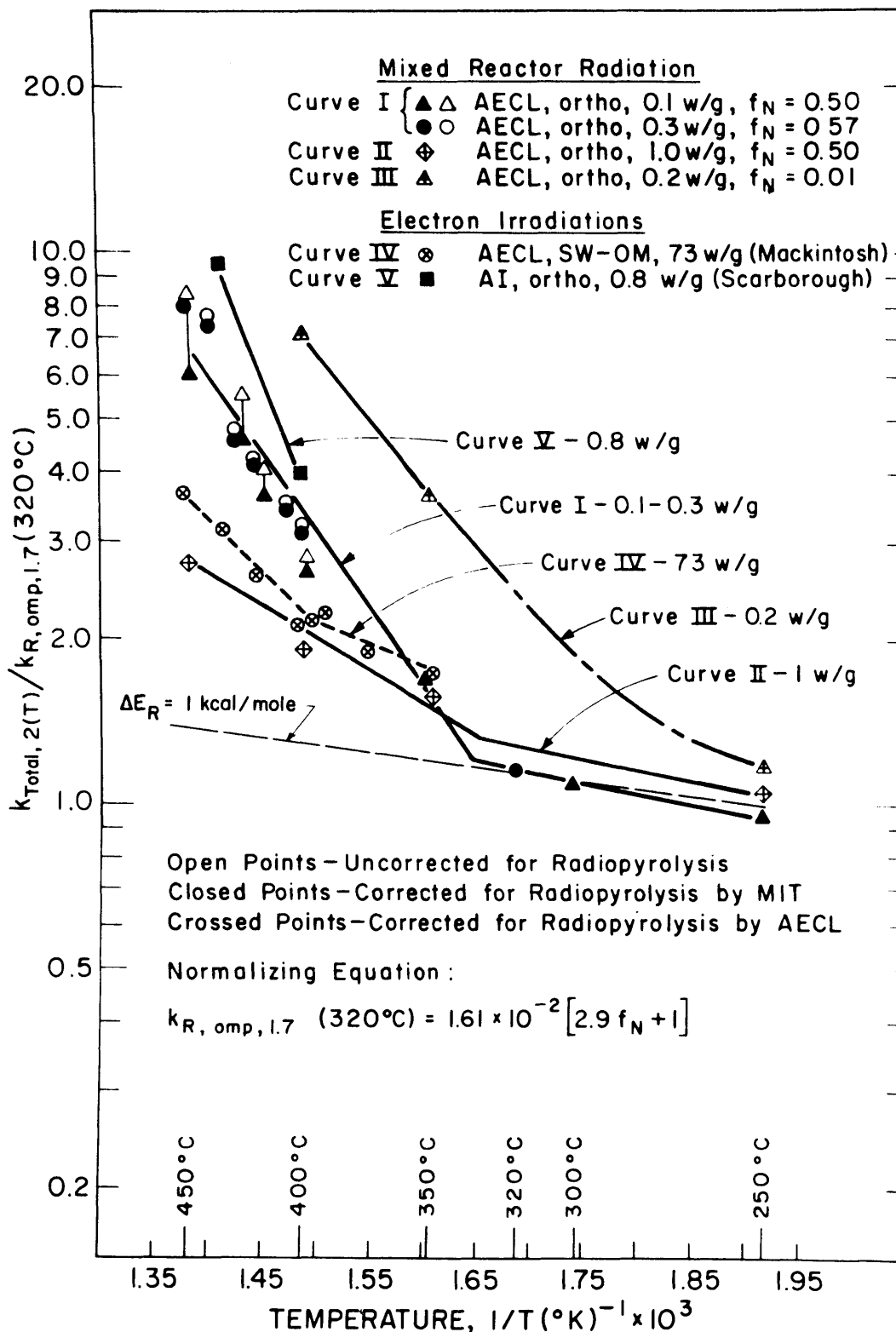
FIGURE 5.12 EFFECT OF TEMPERATURE ON THE RADIOLYSIS
RATE OF ORTHO-RICH TERPHENYLS (SECOND-
ORDER KINETICS)

Table 5.4

Initial Radiolytic Decomposition
Rates of Ortho- and Meta-Terphenyl[a]

| Temperature °C | | Initial G, molecules/100 ev[b] | | |
| | | γ rays (G_γ^0) | Mixed Irradiation Fast Neutron and γ-Rays[c] (G_T^*) | |
		0.2 watt/gm	0.1-0.3 watt/gm.	1 watt/gm
Ortho	250	0.23	0.5	0.5
	350	0.72	0.78	0.75
	400	1.5	1.5	0.9
	450	5	4	1.3
Meta	182	0.15		
	250		0.4	0.4
	360	0.3	0.6	
	385		0.7	0.44
	397	0.9	0.8	
	420		0.95	0.51
	455-458	1.7	1.7	

[a] Reported by Tomlinson, et al., Atomic Energy of Canada Limited, (5.1)

[b] Assuming second-order kinetics and corrected for thermal decomposition.

[c] $f_N = 0.50 - 0.57$

(4) increased with increasing radiation pulse fre-
    quency.

In order to compare the effects of irradiating various
ortho-rich coolants at different temperatures under mixed fast
neutron and gamma radiation, the total degradation rate con-
stants (grams degraded per watt-hour energy absorbed) from
AECL and M.I.T. irradiations having fast neutron fractions
of 0.3 to 0.57 and average dose rates from 0.06 to 1 watt/g
were normalized to a temperature of 320°C and plotted in
Figure 5.13. Second-order kinetics has been used because
the AECL results (5.1) were presented as initial G values
based on second-order kinetics, and information concerning
concentration versus dose was not reported. No corrections
for the effects of radiopyrolysis have been made. Except
for the irradiations at M.I.T., all data points were ob-
tained with capsule irradiation where the radiopyrolysis
effect is generally small (since the effects of radiopyroly-
sis in the low dose rate irradiation Runs 21, 22, 23 are
relatively more important, these runs are not shown in
Figure 5.13).

Several interesting observations are noted from Figure
5.13.

(1) At temperatures above 320°C, all the normalized
    second-order total reaction rate constants of
    Santowax OM are less than those for pure ortho
    terphenyl at 0.1-0.3 watts/gm dose rates.

(2) None of the AECL Santowax OM measurements show
    as rapid an increase in radiolysis rate with in-
    creasing temperature as do the AECL measurements
    with pure ortho terphenyl at dose rates of 0.1-
    0.3 watt/gm.

These conclusions suggest pure ortho terphenyl is more sen-
sitive to radiation than are ortho-rich mixed terphenyls.

Section 4.4 has considered the relative stabilities of
ortho and meta terphenyls under low temperature irradiations.
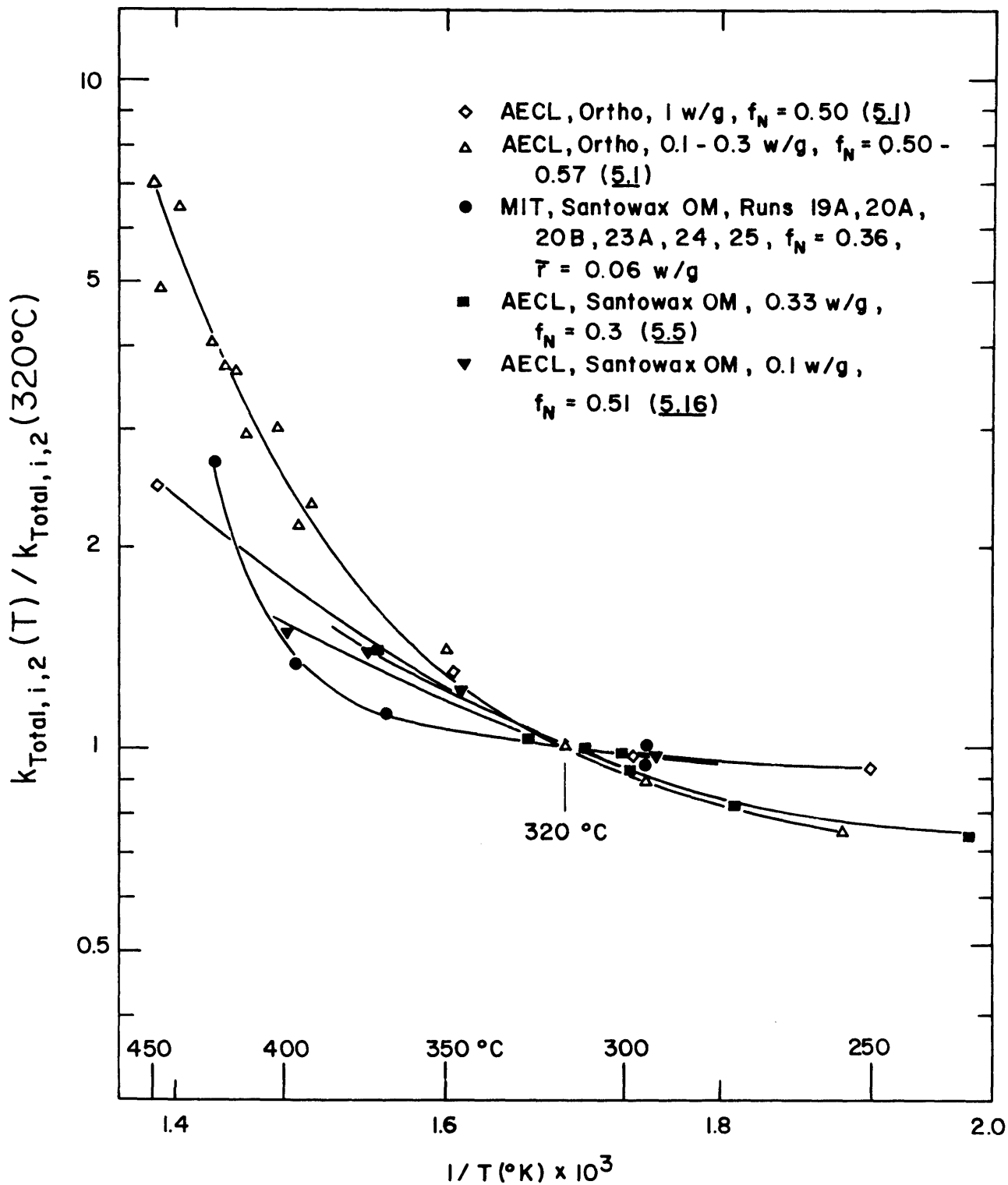
FIGURE 5.13 COMPARISON OF TOTAL DEGRADATION RATE BETWEEN
SANTOWAX OM AND PURE ORTHO TERPHENYL

The stabilities of these isomers will now be considered for high temperature radiations. From the general rate relation assumed in Equation (5.2), the radiopyrolysis rate of the terphenyl isomers may be written as

$$k_{P,i,c+d} \ c_i^c \ c_{omp}^d = \left[\frac{G(-i)}{11.65} - k_{R,i,a+b} \ c_i^a \ c_{omp}^b \right] \bar{r}$$

(5.16)

It has been shown in Chapter 4 that the best values for the constants a and b are a = 1.0 and b = 0.7. For lack of better information (see Section 5.3), we asssume at present that radiopyrolysis of Santowax OM follows a first-order mechanism depending only on the concentration of the component i which is being thermally decomposed. We therefore take c = 1 and d = 0 in Equation (5.16) and at steady state, we have

$$k_{P,i,1} = \left[\frac{G(-i)}{11.65 c_i} - k_{R,i,1.7} \ c_{omp}^{0.7} \right] \bar{r} \qquad (hr)^{-1}$$

(5.17)

Table 5.5 shows the calculated values of the radiopyrolysis rate constants for ortho and meta terphenyls in Santowax OM from the M.I.T. Runs 21-25 (see Table 5.3 for radiopyrolysis constants for total terphenyl). The values of $K_{R,i,1.7}$ at 320°C used in Equation (5.17) to obtain the radiopyrolysis rate constants for ortho and meta terphenyls are the values obtained from the M.I.T. irradiations of Santowax OM (see Section 4.4). The activation energy of radiolysis, ΔE_R, is assumed to be 1 kcal/mole for the calculation of radiopyrolysis rate constants at higher temperatures. Calculations have also been made for ΔE_R = 1 kcal/mole up to 350°C and ΔE_R = 2 kcal/mole for temperatures above 350°C, but the values of k_P changed insignificantly.

The first-order radiopyrolysis rate constants for ortho terphenyl in Santowax OM, $k_{P,o,1}$, shown in Table 5.5, are based on two different assumptions regarding radiolysis.

Table 5.5

Summary of Calculations of Radiopyrolysis Rate Constants
of Meta and Ortho Terphenyls in Santowax OM

Run No.	Temp. °F	°C	Concentration,% Ortho	Meta	G*(-i) Ortho	Meta	$\bar{r}$ watt/gm.	Meta[a]	Ortho Case I[b]	Case II[c]
23	700	371	51.7	26.6	0.524	0.311	0.022	-0.71×10^{-4}	2.63×10^{-4}	-1.64×10^{-3}
23A	700	371	52.3	27.3	0.440	0.342	0.057	-0.50×10^{-4}	2.41×10^{-4}	-1.20×10^{-3}
21	750	399	50.6	25.5	0.694	0.487	0.024	2.76×10^{-4}	6.24×10^{-4}	-1.35×10^{-4}
24	750	399	50.3	27.5	0.508	0.420	0.057	2.98×10^{-4}	5.42×10^{-4}	-2.38×10^{-3}
22	800	421	50.3	26.2	1.683	1.094	0.023	1.43×10^{-3}	2.52×10^{-3}	4.51×10^{-4}
25	800	421	46.4	26.8	1.013	0.728	0.056	1.77×10^{-3}	2.95×10^{-3}	-1.94×10^{-3}

Column header note: First-Order Radiopyrolysis Rate Constant, $(hr)^{-1}$

[a] Use $k_{R,m,1.7}$ (320°C) = 0.0326 $(wh/g)^{-1}$, (Table 4.3, Chapter 4), ΔE_R = 1 kcal/mole

[b] Use $k_{R,o,1.7}$ (320°C) = 0.0360 $(wh/g)^{-1}$, (Table 4.3, Chapter 4), ΔE_R = 1 kcal/mole

[c] Use Curve I of Figure 5.12

Case I assumes $k_{R,o,1.7}$ (320°C) = 0.0360 (as reported in Section 4.4). Case II uses the AECL radiolysis rate constants for pure ortho terphenyl according to Curve I (dose rate = 0.1-0.3 w/g) of Figure 5.12. Many of the calculated values of $k_{P,o,1}$ are negative for Case II assumptions. Similar results are obtained using Curve II (dose rate = 1 watt/gm) of Figure 5.12. This unrealistic result occurs because, in such cases, the _total_ degradation rates of ortho terphenyl in Santowax OM measured in the M.I.T. steady-state runs are less than the _radiolysis_ degradation rates of ortho terphenyl measured by AECL from pure ortho irradiation experiments. This suggests the possibility that the presence of other terphenyl isomers retards the radiolytic degradation rate of ortho terphenyl in terphenyl mixtures as compared to its radiolytic degradation rate in pure ortho terphenyl. It has been mentioned in Section 5.8 that the AECL results show a dose rate effect with pure isomer irradiated at higher temperatures (>350°C), but the M.I.T. irradiation of mixed terphenyl isomers, which was conducted at about the same in-core dose rates, do not show such a dose rate effect. Although the average dose rate to all the terphenyl coolant in the M.I.T. loop was 0.057 watts/gm at 5MW reactor power (0.023 watts/gm at 2MW), the in-core dose rate at the M.I.T. loop was 1.25 watts/gm at 5MW (0.51 watts/gm at 2MW) which is comparable to the dose rates in the AECL capsule.

Table 5.6 presents first-order radiopyrolysis rate constants, $k_{P,i,1}$ for total terphenyl, meta terphenyl and ortho terphenyl in Santowax WR for Runs 26, 27 and 28, calculated using Equation (5.17). Included in this table are values from earlier M.I.T. steady-state Santowax WR runs as reported by Mason and Timmins (5.3). The values of $k_{P,i,1}$ calculated for the present runs are consistent with those of earlier runs. For ortho terphenyl, unrealistic negative values are again obtained by using AECL results

Table 5.6

Calculation of Radiopyrolysis Rate Constants for Total Terphenyl, Meta Terphenyl, and Ortho Terphenyl in Santowax WR - M.I.T. Steady-State Runs

Run No.	Temperature °F	°C	$G^*(-i) = G(-1)/C_i$ total omp	meta	ortho	First-Order Radiopyrolysis Rate Constant, $k_{p,i,l}$ (hr)$^{-1}$ Total OMP Case I[a]	Case II[b]	Meta Curve I[b]	Ortho Curve I[c]
9	800	427	1.76	1.65	2.38	2.56×10^{-3}	2.16×10^{-3}	1.97×10^{-3}	1.84×10^{-3}
10	800	427	1.62	1.42	2.18	2.10×10^{-3}	1.63×10^{-3}	1.30×10^{-3}	1.06×10^{-3}
4	780	416	0.87	0.81	1.10	8.60×10^{-4}	6.25×10^{-4}	5.30×10^{-4}	-3.9×10^{-4}
3	750	399	0.63	0.59	1.00	6.50×10^{-4}	5.45×10^{-4}	4.78×10^{-4}	1.0×10^{-4}
6	750	399	0.45	0.45	0.54	1.51×10^{-4}	1.22×10^{-4}	1.22×10^{-4}	-9.3×10^{-4}
7	750	399	0.55	0.53	0.58	2.82×10^{-4}	2.48×10^{-4}	2.22×10^{-4}	-9.3×10^{-4}
2	750	399	0.53	0.52	0.79	4.20×10^{-4}	3.70×10^{-4}	3.52×10^{-4}	-2.2×10^{-4}
5	700	371	0.37	0.35	0.39	1.48×10^{-4}	1.0×10^{-4}	0.65×10^{-4}	-3.9×10^{-4}
18B	800	427	1.03	1.00	1.48	1.23×10^{-3}	1.01×10^{-3}	0.97×10^{-3}	1.02×10^{-3}
26	700	371	0.397	0.396	0.463	1.38×10^{-4}	1.16×10^{-4}	1.11×10^{-4}	-1.22×10^{-3}
27	750	399	0.491	0.487	0.608	6.42×10^{-4}	5.37×10^{-4}	5.15×10^{-4}	-2.26×10^{-3}
28	800	427	0.834	0.818	1.094	2.56×10^{-3}	1.46×10^{-3}	1.41×10^{-3}	-2.10×10^{-3}

[a] $\Delta E_R = 1$ kcal/mole, Equation (4.5) for radiolysis rate constant, with $G_N/G_\gamma = 3.9$ and $G_\gamma^0 = 0.19$

[b] Radiolysis contribution based on Curve I, Figure 5.11

[c] Radiolysis contribution based on Curve I, Figure 5.12

from pure ortho irradiations for the radiolytic rate constants.

5.9 Conclusion

The following conclusions can be made from the review of the results of terphenyl irradiation at high temperatures (above 350°C). These conclusions apply only to reactor irradiation of terphenyl mixtures. Conclusions reached earlier by Mason and Timmins (5.3) for meta-rich terphenyl coolants are also included.

(1) An activation energy of radiolysis, ΔE_R, of 1 kcal/mole appears to be applicable to either ortho-rich or meta-rich terphenyl coolants. Although AECL results suggest an increase in ΔE_R for temperatures above about 400°C, an increase by a factor of two or three in ΔE_R will have a negligible effect on the total estimated degradation since radiopyrolysis becomes the dominant mode of degradation above 400°C.

(2) Dose rate effects do not appear to be important for either ortho-rich or meta-rich mixed terphenyl coolants for the temperature range (575-800°F) and in-pile dose rates (1 watt/gm) that would be expected in organic-cooled reactors.

(3) The magnitudes of radiopyrolysis rate constants for ortho-rich terphenyl are not significantly different from those for meta-rich terphenyl. The radiopyrolysis constants for mixed terphenyl coolants (such as Santowax WR, OM and OMP) can be estimated from Equation (5.15), which fits all the M.I.T. in-pile irradiations to within ± 20%.

(4) Based on AECL irradiations, the radiolytic stability of pure ortho terphenyl is significantly less than that of pure meta terphenyl at temperatures

above $330°C$ and is strongly dose rate dependent above $350°C$. However, the difference between the stabilities of these two isomers in a terphenyl isomer mixture (either ortho-rich or meta-rich) appears to be much less than the differences indicated for the pure isomers. The stability of the individual isomers in ortho-rich terphenyl appears to be about the same as that in meta-rich terphenyl (Tables 5.5 and 5.6).

5.10 Recommendation For Future Work

Additional research and experiment in the following areas should improve the accuracy of predicting the rate of degradation of ortho-rich terphenyl coolant of organic-cooled reactors.

5.10.1 Activation Energy of Radiolysis, ΔE_R

It would be desirable to know more accurately the value of ΔE_R for ortho-rich terphenyl coolant in the range of temperature between $600°-700°F$ where radiolytic degradation rate is the predominating mode of degradation. Two or three steady-state irradiations covering a range of temperatures from $600°F$ to $700°F$ and preferably at a reduced value of f_N (such as $f_N = 0.07$ at Fuel Position 20 similar to that reported by Mason and Timmins (5.3) for the irradiation of Santowax WR) are recommended. The results of such irradiations could be combined with those presently completed on Santowax OM at $f_N = 0.36$ to determine the values of G_N/G_γ and G_γ^o for total terphenyl and terphenyl isomers in an ortho-rich terphenyl mixture as well as to determine ΔE_R.

5.10.2 Radiopyrolysis Rates

The effect of HB (or DP) concentration on radiopyroly-
sis rates has yet to be defined. A series of carefully con-
trolled irradiations at different temperatures will confirm
whether such an effect is present. A small increase in loop
temperature (20-30°F) and a longer irradiation time will
greatly enhance the radiopyrolytic rate and therefore im-
prove the uncertainty limits. A few irradiations at 750°F,
780°F and 800°F of Santowax OM with two or possibly three
steady-state concentrations (preferably around 60%, 80%
and/or 90%) is recommended to better define the effects
of coolant composition on radiopyrolysis.

5.11 Prediction of Coolant Degradation Rates For Organic-Cooled Reactors

5.11.1 Introduction

The ultimate use of the experimental results of the
terphenyl irradiations rests in the use of these data to
predict coolant degradation rates in organic-cooled reactors
under a variety of operating conditions. For reactors oper-
ating under steady-state coolant conditions,both the coolant
processing rate (for removal of HB) and the make-up rate
of fresh coolant depend on the degradation rate in the
irradiated coolant. Since the degradation rate depends on
coolant composition,radiation field, and the temperatuare dis-
tribution around the coolant loop, the equipment and operating
characteristics of the coolant system can be optimized to
minimize coolant-related costs. This section presents a
method for predicting the coolant makeup rates for an or-
ganic-cooled reactor and investigates the effects of such
parameters as coolant composition, temperature and coolant
mass distribution around the coolant system. The coolant
used in the calculation will be ortho-rich terphenyl such as
Santowax OM. The experimental data used for such coolant

have been presented early in this chapter and also in
Chapter 4.

5.11.2 Characterization of the Coolant

The circulating coolant in an organic-cooled reactor
will be a complex mixture of terphenyl isomers, low and in-
termediate boilers (LIB) and high boilers (HB). In the
course of steady-state operation, the irradiated coolant
must be continuously bled from the system and replaced by
fresh or processed coolant. HB is then removed from the
discharged coolant by means of distillation or other pro-
cesses; fresh coolant is added to make up for the HB. In
the M.I.T. loop, G(→HB) has always been less than G(-omp)
as shown in the calculations in Appendix A3 as well as
reported in earlier M.I.T. reports (5.2,5.3). The differ-
ence is due to the removal of LIB (plus small amount of gases)
from the coolant (retained in the cold trap of the distill-
ation apparatus or in the samples collected for coolant
analysis). During steady-state operation, the LIB and HB
concentrations in the coolant system reach constant val-
ues. Experimental results (5.4, 5.9) have showed the
G(→HB) values for ortho and meta terphenyl isomers are
about equal. Mackintosh (5.4) showed that the ortho
isomer tends to form biphenyl and triphenylene which are
generally less stable than the terphenyls and are themselves
degraded to HB while meta isomer tends to produce para
terphenyl or polymer (HB). The final product of the ter-
phenyls is therefore HB, with LIB as the intermediate
product. Mackintosh's report on the tendency of ortho
terpehnyl to produce LIB under irradiation is substan-
tiated by the present series of Santowax OM irradiation
(see Table 5.3).

5.11.3 Method of Calculating Coolant Degradation Rates

The degradation rates of terphenyl coolant can be calculated by making a terphenyl balance around the coolant system (refer to Equation A3.1, Appendix A3).

Assuming that the radiolytic and radiopyrolytic degradations are independent and additive

$$W_{omp} = W_R + W_P \qquad (5.18)$$

where

W_{omp} is the total terphenyl degradation rate, gms/hr

W_R is the radiolytic degradation rate, gms/hr

W_P is the radiopyrolytic degradation rate, gms/hr

Considering radiolytic degration rate first, W_R can then be written as

$$W_R = \frac{G_R(-omp)}{11.65} \, \bar{r} \, M_C = k_{R,omp,n} \, C_{omp}^n \, \bar{r} M_C \qquad (5.19)$$

where

C_{omp} is the concentration of total terphenyl in the well mixed coolant system, w/o

$\bar{r}$ is the dose rate to the coolant averaged over all the coolant, watts/gm

M_C is the mass of circulating coolant in coolant system, gm

In the case of organic-cooled reactors, $\bar{r}M_C$ represents a fraction of the total thermal power of the reactor, depending on the design of the fuel element and the coolant channel. The best value of n is given as 1.7 ± 0.1 as shown in Chapter 4 and $k_{R,omp,n}$ is calculated according to Equation (4.12). The activation energy of radiolysis, ΔE_R is assumed to be 1 kcal/mole.

The rate of degradation due to radiopyrolysis W_P, depends on the temperature and mass distribution around the coolant system. For calculation purposes, a simplified cool-

ant flow diagram as shown in Figure 5.14 for an organic-cooled reactor similar to that of a 750MWe HWOCR (5.9) will be used as an example. Mason and Timmins (5.3) have shown the procedures to calculate the radiopyrolytic degradation rate, W_P, for such a system. Only a brief summary will be presented in this report.

The coolant system as shown in Figure 5.14 is divided into N zones each of which is characterized by a coolant mass, M_N, an inlet temperature to that zone, T_1, and outlet temperature, T_2. Steady-state operation is assumed with constant terphenyl concentration, C_{omp}. The radiopyrolytic degradation rate of zone N, $W_P(N)$, can be expressed as (assuming first-order radiopyrolysis rate constant)

$$W_P(N) = \frac{M_N \, C_{omp}}{T_2 - T_1} \int_{T_1}^{T_2} k_{P,omp,1}(T) \, dT \qquad (5.20)$$

where $k_{P,omp,1}(T)$ can be expressed by Equation (5.15). Equation (5.20) can be integrated stepwise over small temperature increments, ΔT_j,

$$W_P(N) = \frac{M_N C_{omp}}{T_2 - T_1} \sum_{T_1}^{T_2} k_{P,omp,1}(T_j) \Delta T_j \qquad (5.21)$$

where

$k_{P,omp,1}$ is the first-order radiopyrolysis rate constant for irradiated coolant evaluated at temperature T_j

ΔT_j is a small temperature increment with average temperature T_j

5.11.4 Example of Coolant Degradation Calculations

The values used for the fast neutrons and gamma radiation dose rates to the coolant for the example reac-
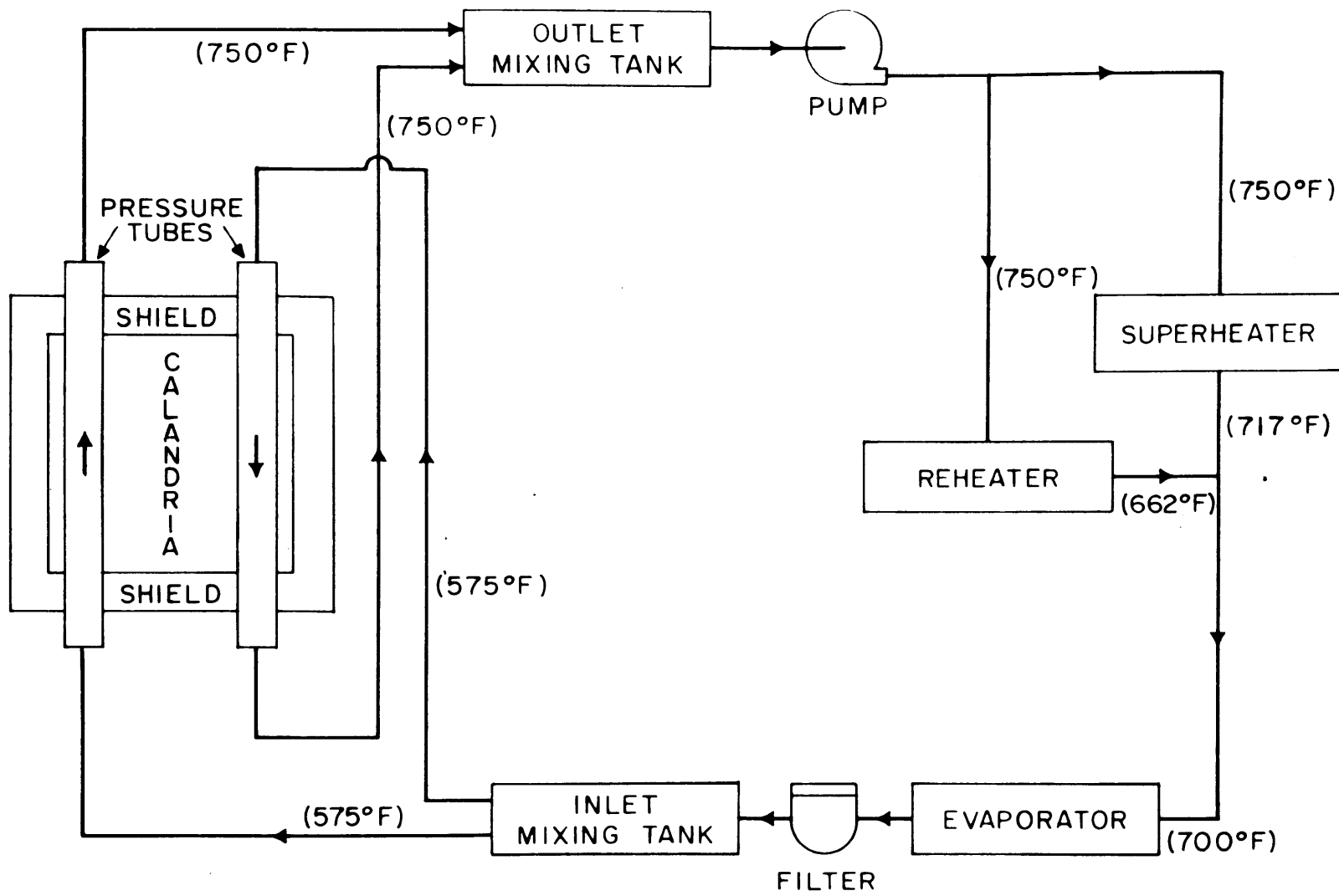
FIGURE 5.14 SIMPLIFIED ORGANIC COOLANT FLOW DIAGRAM – 750 MWE HWOCR

tor are those of Combustion Engineering ($\underline{5.3}$, $\underline{5.9}$, $\underline{5.18}$) and
are 5.9 MW for fast neutrons and 3.0 MW for gamma radia-
tion. The fast neutron fraction of the dose rate is there-
fore 0.66.

Table 5.7 shows the calculated radiolysis, radiopyroly-
sis and total rates for Santowax OM operating at core outlet
temperature of 750°F and 800°F in such a demonstration plant
at C_{omp} = 0.9. The temperature profile around the coolant
loop for the 800°F case was estimated simply by raising all
temperatures in the 750°F case by 50°F; no change in the
mass of coolant in the various zones was made. Table 5.7
shows that most of the radiopyrolytic degradation occurs
in the outlet header and hot leg where coolant heldup is
large at high temperatures. This is especially true for
the 800°F case. Substantial lowering in coolant makeup
cost would result if the coolant holdup in this zone can
be reduced. The rate and cost of coolant degradation are
significantly greater for the reactor operating with 800°F
coolant temperature at the core outlet than for a tempera-
ture of 750°F. Bulk coolant temperature in organic-
cooled reactor designs is therefore normally limited to
temperatures of 750°F or less.

Figure 5.15 shows the effect of terphenyl concen-
tration on the degradation rate of the reactor plant used
as example. Two cases, namely 750°F and 800°F coolant
temperatures at core outlet, are shown. The total degrad-
ation rate of the coolant increases with increasing ter-
phenyl concentration. As far as coolant makeup cost is con-
cerned, lower terphenyl concentrations (higher DP content)
would be desirable. However in the design of organic-
cooled reactors, the selection of optimum coolant concentra-
tion and temperature depends on additional factors such as
pumping power, pressure drop and heat transfer characteris-
tics. Lower terphenyl concentrations (higher HB) and lower
temperatures increase both the viscosity and density of the

Table 5.7

Calculated Coolant Makeup Rates for 750 Mwe HWOCR Demonstration Plant

$(C_{omp} = 0.90)$

Zone	Description	Coolant Mass (lbs)	750°F Core Outlet Coolant Temperature		800°F Core Outlet Coolant Temperature	
			Temp. (°F)	Total Terphenyl Degradation Rate (lbs/hr)	Temp. (°F)	Total Terphenyl Degradation Rate (lbs/hr)
Radiopyrolysis						
I	Cold leg, inlet header	536,000	575	-	625	4
II	Decay heat loop	43,000	650	1	700	6
III	Reactor core	64,000	575-750	6	625-800	33
IV	Outlet header, hot leg	690,000	750	517	800	2648
V	Superheater	73,000	750-717	38	800-767	189
VI	Evaporator	49,000	700-574	1	750-624	8
VII	Reheater	52,000	750-662	14	800-712	75
	Sub-total (Radiopyrolysis)			577		2963
Radiolysis	(Radiolysis)			902		930
	Total Makeup Rate			1479		3893
	Coolant Makeup Cost (mills/kwhe)			0.27		0.62

(@$0.12/lb coolant cost)
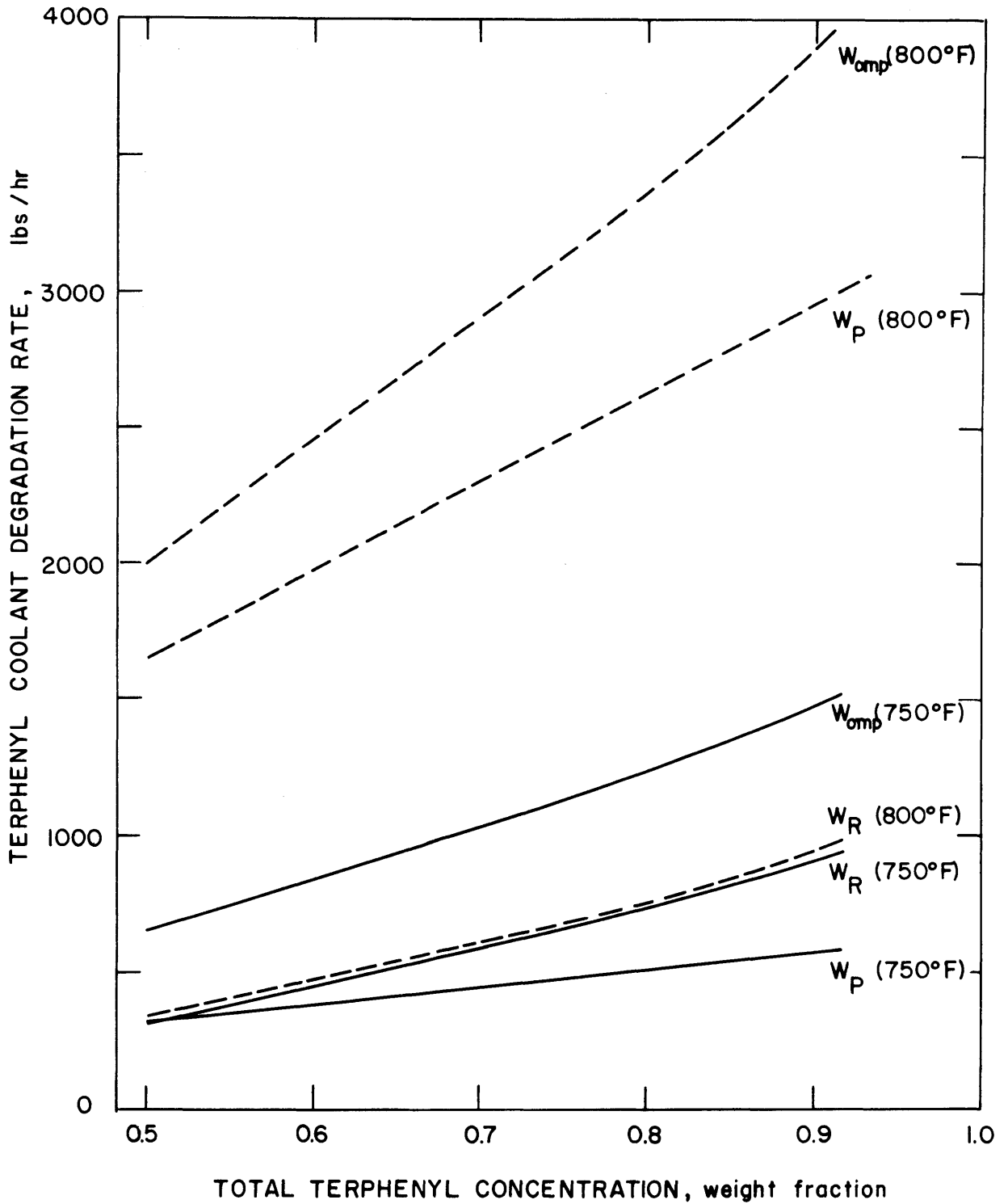
FIGURE 5.15   EFFECT OF COOLANT COMPOSITION AND CORE OUTLET
TEMPERATURE ON TERPHENYL DEGRADATION RATE FOR
ORGANIC-COOLED REACTOR - DEMONSTRATION PLANT

coolant (Chapter 3) and therefore increase pumping power and reduce heat transfer coefficient with raising pumping and capital costs. An optimization between these various factors is required to arrive at coolant operating conditions leading to minimum total cost for the energy produced by the reactor system.

APPENDIX A1

CALORIMETRY AND FOIL DOSIMETRY

A1.1 Introduction

In previous work (A1.1, A1.2) as well as in Section 4.3.2, it has been shown that fast neutrons are more effective than gamma rays in causing degradation in the terphenyl. Therefore, the total energy deposition rate to the terphenyl as well as its fractional dose rates due to fast neutrons and gamma radiation must be known accurately.

At the Organic Loop Project at M.I.T., adiabatic calorimetry was undertaken to determine the dose rates in the in-pile section due to fast neutrons and gamma radiation. Measurements of the neutron spectrums by means of foil dosimetry were also made to aid in defining the fast neutron contribution and to monitor possible changes in dose rates during an irradiation. Theory and procedures of both the adiabatic calorimetry and the foil dosimetry have been well described in earlier M.I.T. reports (A1.1, A1.2). Therefore, only a brief description will be given here.

A1.2 Adiabatic Calorimetry

A total of five series of calorimetry were made in a stainless steel thimble to mockup the in-pile assembly at Fuel Position 1 between the period of September 1, 1966 and March 8, 1968 for the purpose of calculating the dose rate factors. Three series were made on In-pile Section No. 4 which was used for the irradiations of Santowax OM and the remaining two on In-pile Section No. 5, which was used for the high temperature irradiations of Santowax WR. Table A1.1 shows a summary of the five series of calorimetry.

Table A1.1

Summary of Calorimetry in
Fuel Position 1 for In-pile Sections
No. 4 and No. 5

Calorimetry Series	Date (mo/day/yr.)	Calorimetry[a] (Model)
XXII	August 17, 1966	SW(E-1),PE(E-1),PS(E-3) C(E-1),Al(E-3),Be(c-4)
XXIII	October 8, 1966	SW(E-1),PE(E-1),PS(E-3) C(E-1),Al(E-3)
XXV	August 3, 1967	SW(E-1),PE(E-2),PS(E-4), C(E-1),Al(E-3)
XXVI	September 7, 1967	SW(E-1),PE(E-2),PS(E-4), C(E-1), Al(E-3)
XXVIII,XXIX, XXX	February 26, 1968 to March 8, 1968	SW(E-1),PE(E-2),PS(E-4) C(E-1),Al(E-3)

(a)   See reference (A1.5, A1.8) for specification on diff-
erent models of calorimeter; SW-Santowax, PE-Poly-
ethylene, PS-Polystyrene, C-Carbon, Al-Aluminum, Be-
Beryllium.

The use of beryllium as a calorimeter material was dis-
continued after Calorimetry Series XXII because of inconsis-
tent results.

A1.2.1   Theory of Measurement

The various calorimeters are made of materials of
widely varying energy absorption rates in a field of mixed
neutron and gamma radiation. Before one was lowered to the
desired axial position inside a stainless steel thimble lo-
cated along the axis of the special fuel element at the
Fuel Position 1 (See Figures 2.1 and 2.3, Chapter 2), it was
cooled in the cooling plug so that the temperature of the
aluminum jacket (or can) of the calorimeter was about 20°F

lower than that of the sample. As soon as the calorimeter
is inserted into the reactor core region, both the jacket and
the sample begin to heat up due to energy deposition. Tem-
peratures of the calorimeter jacket and the sample are mea-
sured continuously by means of thermocouples connected to
recording potentiometers. The jacket temperature normally
rises faster than that of the sample due to its contact with
the D_2O-cooled stainless steel thimble. In a few moments
the jacket temperature is equal to the sample temperature,
at which time the adiabatic condition is fulfilled. Follow-
ing each such measurement the calorimeter is pulled back to
the cooling plug position. The procedure is repeated at
each desired axial position.

At or near the adiabatic point, the dose rate to which
the sample has been exposed can be expressed as

$$R_T^j = KC_p(T_a)\left[\frac{dT}{dt}\right]_a \qquad (A1.1)$$

where

R_T^j is the total dose rate in sample j, watts/gm

K is a conversion factor = 0.0387
     (watt)(min)(lb)/(Btu)(gm)

$C_p(T_a)$ is the specific heat capacity of the sample
     j at the temperature T_a of the adiabatic
     point, Btu/lb-°F

$\left[\frac{dT}{dt}\right]_a$ is the rate of temperature rise of the
     sample j at the adiabatic point, °F/min

In the reactor, the dose rate in the irradiated sample
as calculated by Equation (A1.1) results from the absorp-
tion of fast neutron and gamma ray energy in the sample.

$$R_T^j = R_\gamma^j + R_N^j \qquad \text{watts/gm} \qquad (A1.2)$$

With samples of low atomic number, Sawyer and Mason (A1.2) reported that only the Compton effect is of significance in gamma ray attenuation. Therefore, we will express the dose rate due to gamma radiation in any sample in terms of the gamma dose rate in carbon by the following relationship:

$$R_\gamma{}^j = \frac{(Z/A)_j}{(Z/A)_C} R_\gamma{}^C \qquad \text{watts/gm} \qquad (A1.3)$$

where

   $(Z/A)_j$ is the ratio of atomic number to that of the mass number of the sample j.

For compounds, (Z/A) is the weighted average of Z/A.

   The dose rate due to fast neutrons in an absorber j can be represented by

$$R_N{}^j = \sum_i N_i I_i \qquad \text{watts/gm} \qquad (A1.4)$$

where

   N_i is the number of atoms/gm of ith nuclei of the sample j

   I_i is the neutron scattering integral for the ith nuclei in the absorber j, watts/atom

   If the neutrons scattering integrals are normalized by the neutron scattering integral for hydrogen, I_H, Equation (A1.4) can be written as:

$$R_N{}^j = \sum_i N_i \left[\frac{I_i}{I_H}\right] I_H \qquad \text{watts/gm} \qquad (A1.5)$$

   For absorbers consisting of elements of low Z numbers, we assume that the fast neutron dose rate is due to elastic scattering by the absorber nuclei. An earlier M.I.T. report (A1.2) has shown that the ratios of neutron scattering integral of light nuclei, such as C, to that of hydro-

gen are essentially independent of the neutron spectra due to the fact that the elastic scattering cross section of the samples have the same general energy dependency. This ratio can be calculated from

$$\frac{I_i}{I_H} = \frac{Sg_i \int_0^\infty \sigma_s^i(E)\emptyset(E)dE}{Sg_H \int_0^\infty \sigma_s^H(E)\emptyset(E)dE} \qquad (A1.5a)$$

where

g_i is the average fraction of neutron energy transferred to the ith nuclide, equal to $2A_i/(A_i + 1)^2$

S is a conversion factor, 1.6×10^{-43} $(cm^2)(watt)(sec)/(barn)(ev)$

$\sigma_s^i(E)$ is the elastic scattering cross section of the ith nuclei at neutron energy E, barns

$\emptyset(E)$ is the differential neutron flux, neutrons/ cm^2-sec-ev.

The differential flux, $\emptyset(E)$, is measured by foil dosimetry (Section A1.4).

Combining Equations (A1.2) (A1.3) and (A1.5), we have for the total dose rate

$$R_T^j = a_j R_\gamma^C + b_j I_H \qquad (A1.6)$$

where a_j and b_j are constants for any sample j, calculated according to Equations (A1.3) and (A1.5). Thus, by measuring the total dose R_T^j in at least two different materials, the value of R_γ^C and I_H can be determined. From these known values of R_γ^C and I_H, the total dose in the same radiation field can be calculated for any desired material,

(e.g. terphenyl coolant) using Equation (A1.6) with values
of a_j and b_j corresponding to the desired material. The val-
ues of a_j and b_j used for calorimetry measurements at M.I.T.
in Fuel Position 1 are shown in Table A1.2

Table A1.2

Constants a_j and b_j Used for Calorimetry Measurements

Sample	a_j	b_j x 10^{-22} atoms/gm
Polyethylene	1.142	9.374
Polystyrene	1.076	5.471
Carbon	1.000	0.913
Santowax OMP	1.060	4.520
Aluminum	0.963	0.248

Due to the comparatively larger thermal neutron cross
section of aluminum, a correction to Equation (A1.6) must be
made for the resulting β-decay heating. For an aluminum
calorimeter, we have

$$R_T^{Al} = a_{Al}R_\gamma^C + b_{Al}I_H + R_{th}^{Al} \tag{A1.7}$$

where

R_{th}^{Al} is the dose rate in aluminum due to the induced
β-decay heating

R_{th}^{Al} is calculated with the following expression reported
by Sawyer and Mason (A1.2) according to a method described
by Morgan and Mason (A1.1)

$$R_{th}^{Al} = \emptyset_{2200} \times 10^{-16} \left[3.2 + 9.3 \left[1 - e^{-0.3t} \right] \right] \text{ watts/gm} \tag{A1.8}$$

where

$\emptyset_{2200}$ is the thermal neutron flux, neutrons/$(cm^2)(sec)$

t is the length of time the calorimeter has been
exposed to the thermal flux, min.

A1.2.2 Results of Calorimetric Measurements

With known a_j and b_j of Equation (A1.6) for any par-
ticular calorimeter and with measured value of R_T^j accord-
ing to Equation (A1.1), Equation (A1.6) can be plotted as
a straight line with R_γ^C and I_H as coordinates. One such
line is thus developed for each of several different cal-

orimeters. These lines should intercept at a common point
which determines the R_γ^C and I_H values of the position at
which these calorimeters were irradiated. However, due
to uncertainties in measurements and physical and nuclear
properties of the calorimeter materials, a unique point of
intersection may not be obtained if more than 2 different
absorbers are employed. Instead, the intersections of
lines spread within a small area of the plot. For this
reason, a least-square error analysis is performed to ob-
tain the best values of R_γ^C and I_H. A computer program,
MNCAL, described by Sawyer and Mason (A1.2) is used for such
analysis. The output of the program gives the values of
R_γ^C, I_H and R_T^{SW} (and their variances) which result in min-
imum variance in the calculated total dose in the organic
coolant, R_T^{SW}. Figure A1.1 shows a graphical example of
the measured dose rates in Fuel Position 1 selected from
Calometry Series XXIII. Table A1.3 shows the results for
the various Calorimeter Series. Figures A1.2 and A1.3
show the neutron, gamma, and total dose rate to the or-
ganic coolant at various axial positions from the center
of reactor core normalized to 1MW of reactor power for
In-pile Sections No.4 and No.5 respectively. The results
shown in Table A1.3 and Figures A1.2 and A1.3, and used
in determining the dose rates for the coolant irradiations
reported here,are based on measurements from the five
calorimeter absorbers shown in Table A1.2. Calculations
were also carried out omitting the measurements made with
the aluminum absorber (due to the uncertainty introduced
by the absorption of the induced β-particles); the resulting
values of R_T^{SW} and f_N were not significantly different from
the values shown for these variables in Figures A1.2 and
A1.3 (Agreement within ±3%).

Knowing the total dose rate distribution, the speci-
fic dose rate to the organic coolant in the in-pile sec-
tion can be calculated by the following equation:
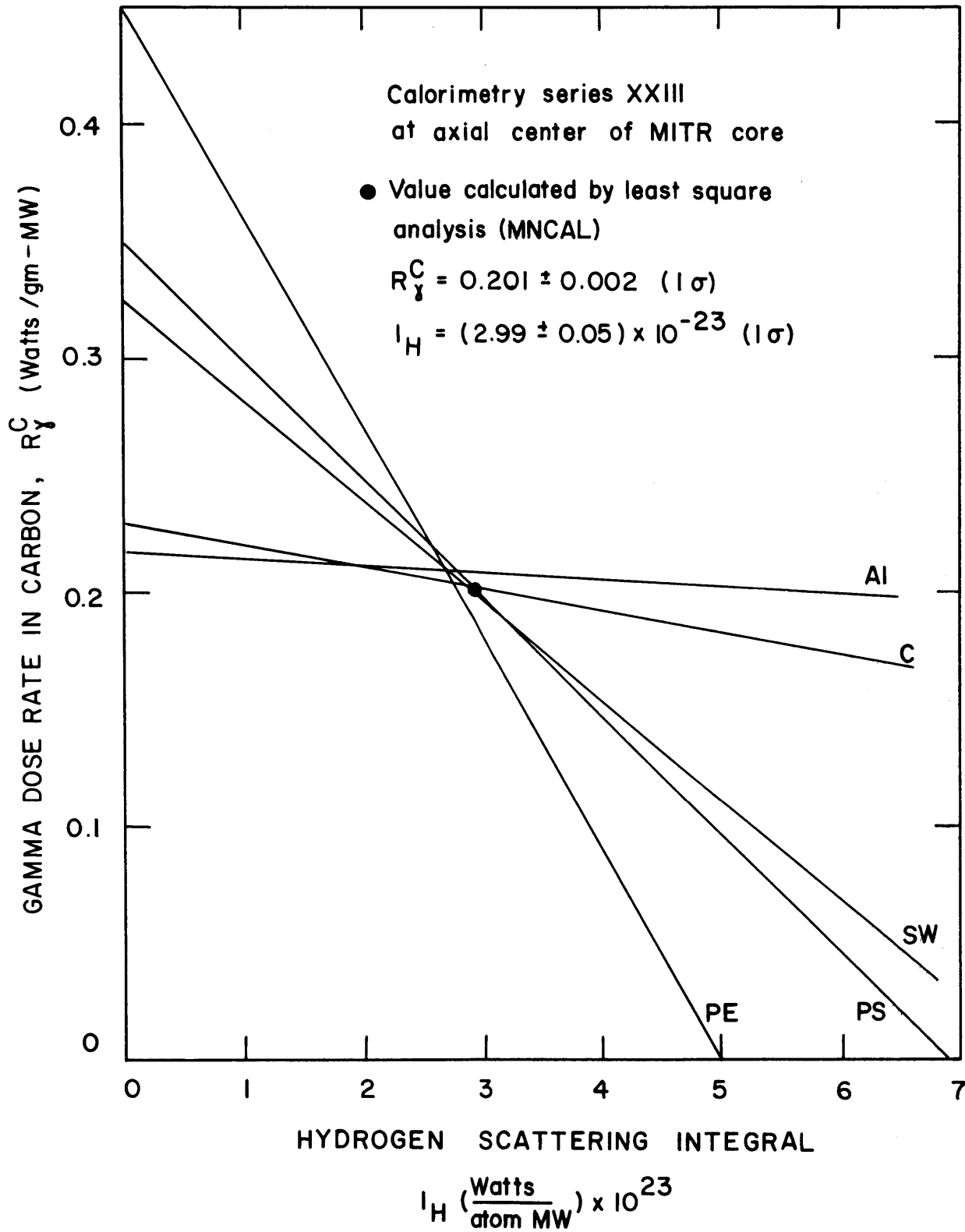
FIGURE A1.1 GRAPHICAL REPRESENTATION OF MEASURED DOSE RATE
IN FUEL POSITION 1 - CALORIMETRY SERIES XXIII

Table A1.3

Results of Least-Square Analysis

Computer Program MNCAL

Calorimetry Series XXII, XXIII, XXV, XXVI, XXVIII, XXIX, XXX

Calorimetry Series	Position (Inch)	R_γ^C (a) (watts/gm-MW)	$I_H \times 10^{-24}$ (a) (watts/atom-MW)	R_T^{SW} (a) (watts/gm-MW)
XXII	-14	0.071 + 0.001	0.574 + 0.023	0.101 + 0.002
	-9	0.161 ∓ 0.002	2.404 ∓ 0.055	0.279 ∓ 0.003
	-4	0.200 ∓ 0.001	2.842 ∓ 0.036	0.341 ∓ 0.002
	0	0.211 ∓ 0.002	2.896 ∓ 0.057	0.354 ∓ 0.003
	4	0.200 ∓ 0.002	2.687 ∓ 0.030	0.333 ∓ 0.003
	9	0.152 ∓ 0.002	2.066 ∓ 0.068	0.255 ∓ 0.004
	14	0.067 ∓ 0.001	0.347 ∓ 0.024	0.087 ∓ 0.002
	19	0.030 ∓ 0.003	0.123 ∓ 0.073	0.037 ∓ 0.004
XXIII	-14	0.063 + 0.002	0.704 + 0.050	0.099 + 0.003
	-9	0.168 ∓ 0.005	2.438 ∓ 0.114	0.288 ∓ 0.007
	0	0.201 ∓ 0.002	2.989 ∓ 0.047	0.349 ∓ 0.003
	9	0.135 ∓ 0.006	2.051 ∓ 0.154	0.236 ∓ 0.010
	14	0.060 ∓ 0.001	0.360 ∓ 0.019	0.080 ∓ 0.001
XXV	-14	0.079 + 0.001	0.959 + 0.151	0.127 + 0.008
	-6	0.161 ∓ 0.003	2.463 ∓ 0.074	0.282 ∓ 0.005
	0	0.173 ∓ 0.003	2.418 ∓ 0.061	0.293 ∓ 0.004
	6	0.147 ∓ 0.004	2.009 ∓ 0.085	0.247 ∓ 0.003
	14	0.058 ∓ 0.001	0.166 ∓ 0.014	0.069 ∓ 0.001
XXVI	-14	0.077 + 0.003	0.693 + 0.077	0.113 + 0.005
	-9	0.164 ∓ 0.002	2.370 ∓ 0.017	0.281 ∓ 0.002
	-6	0.193 ∓ 0.002	2.741 ∓ 0.039	0.329 ∓ 0.003
	0	0.213 ∓ 0.002	3.021 ∓ 0.040	0.362 ∓ 0.003
	6	0.183 ∓ 0.002	2.789 ∓ 0.050	0.320 ∓ 0.003
	9	0.152 ∓ 0.004	2.359 ∓ 0.086	0.268 ∓ 0.005
	14	0.076 ∓ 0.004	1.039 ∓ 0.088	0.128 ∓ 0.006
	16	0.053 ∓ 0.001	0.475 ∓ 0.027	0.077 ∓ 0.002
XXVIII, XXIX, XXX	-14	0.076 + 0.002	0.428 + 0.009	0.099 + 0.002
	-9	0.152 ∓ 0.003	2.207 ∓ 0.081	0.261 ∓ 0.005
	-4	0.188 ∓ 0.005	2.791 ∓ 0.150	0.325 ∓ 0.008
	0	0.194 ∓ 0.004	2.965 ∓ 0.121	0.338 ∓ 0.007
	4	0.183 ∓ 0.004	2.804 ∓ 0.092	0.321 ∓ 0.006
	9	0.140 ∓ 0.004	2.210 ∓ 0.103	0.248 ∓ 0.006
	14	0.059 ∓ 0.004	1.157 ∓ 0.116	0.114 ∓ 0.007
	19	0.033 ∓ 0.001	0.109 ∓ 0.028	0.040 ∓ 0.002
	25	0.023 ∓ 0.003	0.012 ∓ 0.101	0.025 ∓ 0.006

(a) Error limits are 1σ
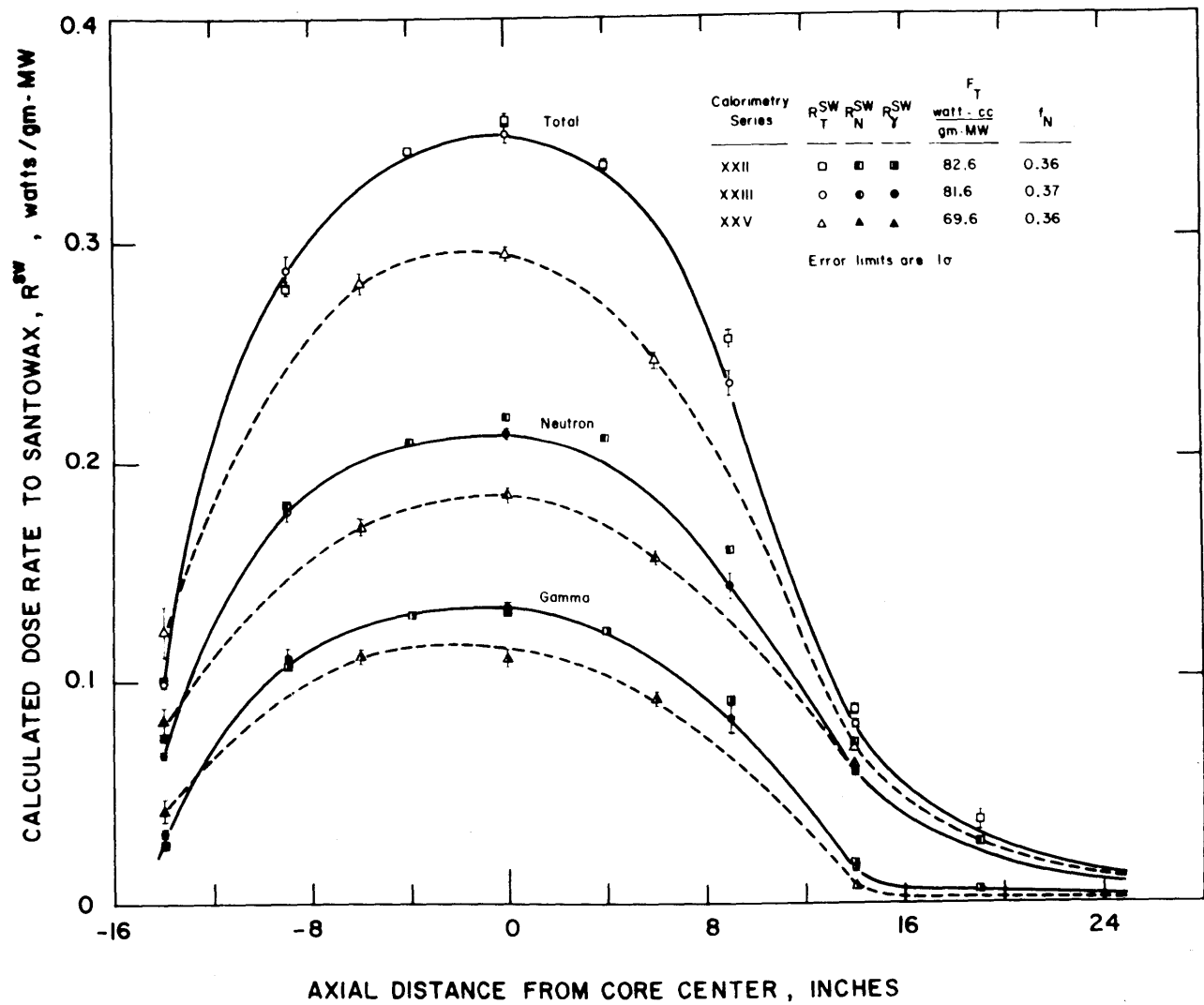
FIGURE AI.2   AXIAL VARIATION OF THE TOTAL, NEUTRON AND GAMMA DOSE RATES IN FUEL POSITION I
BEFORE THE INSTALLATION AND AFTER THE REMOVAL OF IN-PILE SECTION NO. 4

0.4

CALCULATED DOSE RATE TO SANTOWAX, R^{sw}, watts/gm - MW

0.3

0.2

0.1

0

Calorimetry Series	R$_T^{SW}$	R$_N^{SW}$	R$_\gamma^{SW}$	F$_T$ watt-cc gm MW	f$_N$
XXVI	o	●	●	89.1	0.38
XXVIII, XXIX, XXX	△	▲	▲	80.5	0.38

Error limits are in

Total

Neutron

Gamma

-16   -8   0   8   16   24

AXIAL DISTANCE FROM CORE CENTER, INCHES
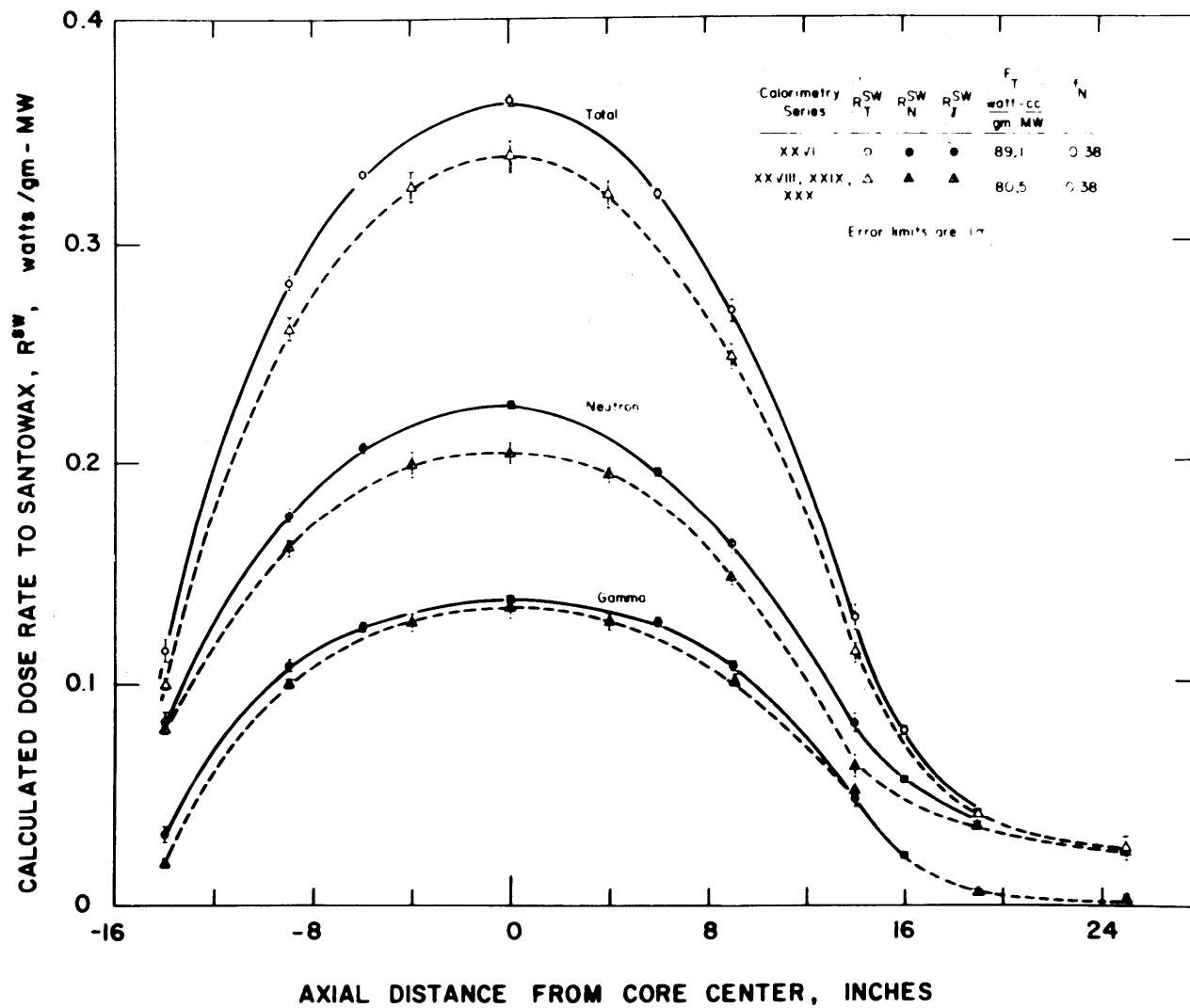
FIGURE AI.3   AXIAL VARIATION OF THE TOTAL, NEUTRON AND GAMMA DOSE RATES IN FUEL POSITION I BEFORE THE INSTALLATION AND AFTER THE REMOVAL OF IN-PILE SECTION NO. 5

$$F_T^{SW} = \int_{L_L}^{L_T} \frac{R_T^{SW}}{P_o} \, x dL \qquad (A1.9)$$

where

F_T^{SW} is the total in-pile specific dose rate factor to the organic coolant, watt-cc/gm-MW

L_L is the bottom of the in-pile capsule relative to the center of reactor core, inches

L_T is the top of the in-pile capsule relative to the center of reactor core, inches

P_o is the operating power level of the reactor at the time of calorimetry measurements, mega-watts

x is the volume per unit length of the in-pile capsule, cc/inch

For calorimetry series XXII, XXIII, XXV, XXVIII, XXIX and XXX, (In-pile Sections No. 4 and No. 5), the x values used in Equation (A1.9) are tabulated in Table A1.4.

Table A1.4

Volume per Unit Length of

In-pile Capsules No. 4 and No. 5

x (cc/in)	Position of Capsule Relative to Reactor Core Center (in)	
	In-pile Capsule No. 4	In-pile Capsule No. 5
10.57	-13.06 to +13.69	-13.34 to +13.41
5.85	+13.69 to +25.00	+13.41 to +25.00

A planimeter was used to measure the areas under the total dose rate curves of Figures A1.2 and A1.3.

The specific dose rate factors due to fast neutrons and gamma radiation ($F_N{}^{SW}$ and $F_\gamma{}^{SW}$) are calculated in the same manner using $R_N{}^{SW}$ and $R_\gamma{}^{SW}$ in place of $R_T{}^{SW}$ in Equation (A1.9).

The standard deviation of the dose rate factor is determined from the standard deviation of the dose rates, calculated from MNCAL, in the following manner.

$$\frac{\sigma(F)}{F} = \frac{\sqrt{\sum_i \sigma^2(R_i)}}{\sum_i R_i} \qquad (A1.10)$$

Table A1.5 shows the in-pile dose rate factors to Santowax OM before the installation and after the removal of In-pile Section No. 4. Table A1.6 shows the same for Santowax WR in In-pile Section No. 5. The In-pile dose rate factor at any time during the run is calculated by means of linear interpolation of the measured dose rate factors against accumulated megawatt-hours of reactor operation. The dose rate factor for each run is listed in Appendix A3.

The percentage standard error of the total in-pile dose rate factor, $F_T{}^{SW}$, as shown in Tables A1.5 and A1.6 is approximately one percent. In view of the uncertainties in physical properties of the calorimeters (e.g. the specific heat, c_p) and the nuclear properties (e.g. the scattering cross-sections), the percentage standard error on the calculated $F_T{}^{SW}$ is taken to be 0.03 in the degradation calculation of Appendix A3. This error limit is consistent with earlier M.I.T. reports (A1.2, A1.5).

Table A1.5

Results of Calorimetry Measurements in Fuel Position 1
Before Installation and After Removal of In-pile Section No. 4[a]

| Calorimetry Series | Date | In-pile Dose Rate Factors, watt-cc/MW-gm[b] | | | Fast Neutron Fraction f_N |
		Total, F_T^{SW}	Gamma, F_γ^{SW}	Neutron, F_N^{SW}	
XXII	August 17, 1966	82.6 ± 0.4	52.7 ± 0.3	29.9 ± 0.3	0.36
XXIII	October 8, 1966	81.6 ± 1.0	51.4 ± 0.7	30.2 ± 0.7	0.37
XXV	August 3, 1967	69.6 ± 0.7	44.5 ± 0.5	25.1 ± 0.6	0.36

[a] In-pile Section No. 4 was installed on October 30, 1966 and removed on July 28, 1967

[b] Error limits are 1σ

Table A1.6

Results of Calorimetry Measurements in Fuel Position 1
Before Installation and After Removal of In-pile Section No. 5[a]

Calorimetry Series	Date	In-pile Dose Rate Factors, watt-cc/MW-gm[b]			Fast Neutron Fraction f_N
		Total, F_T^{SW}	Gamma, F_γ^{SW}	Neutron, F_N^{SW}	
XXVI	September 7, 1967	89.1 ± 0.5	55.6 ± 0.4	33.5 ± 0.4	0.38
XXVIII XXIX and XXX	February 26, 1968 to March 8, 1968	80.5 ± 0.8	49.7 ± 0.5	30.8 ± 0.6	0.38

[a] In-pile Section No. 5 was installed on October 8, 1967 and removed on February 24, 1968

[b] Error limits are 1σ

A1.3 Foil Dosimetry

A1.3.1 Introduction

The foil activation program for the measurement of thermal neutron flux, differential resonance and fast neutron fluxes, and the neutron elastic scattering integral was initially developed by Sefchovich (A1.3). It has subsequently been modified and described in other M.I.T. reports (A1.1, A1.2, A1.4, A1.5). Therefore, only a brief outline of the theory and method will be described in this report.

A1.3.2 Theory

In the thermal energy range, high purity cobalt-aluminum wires (0.595 w/o Co) were irradiated at different axial positions of the reactor. The 2200 m/sec flux was calculated from the relationship.

$$\emptyset_{2200} = \frac{1}{\sigma_{2200}} \left[\frac{(Act)_B}{(1 - e^{-\lambda t_B})} - \frac{(Act)_{Cd}}{(1 - e^{-\lambda t_{Cd}})} \right] \quad (A1.11)$$

where

σ_{2200} is the 2200 m/sec cross-section for Co^{59}, barns

λ is the disintegration constant for Co^{60}, min.$^{-1}$

t_B is the irradiation time of the bare wire, min.

t_{Cd} is the irradiation time of the cadmium covered wire, min.

$(Act)_B$ is the bare absolute activity per atom, disintegration/sec

$(Act)_{Cd}$ is the cadmium covered absolute activity per atom, disintegration/sec.

The activity of the activated sample was determined by

$$Act = \frac{[C - C_b] \, A e^{-\lambda t}}{w N_o \varepsilon}$$
(A1.12)

where

C   is the measured counting rate of the Co-Al wire, counts/sec

C_b is the background counting rate of the counting equipment, counts/sec

A   is the atomic weight of the Co^{59} sample,

w   is the weight of the Co^{59} sample, grams,

N_o is the Avogadro's Number,

t   is the waiting time between irradiation and counting, min.

ε is the overall counting efficiency of the Counter

The Co-Al wires were counted in a well-type NaI scintillation system.

The neutron flux in the resonance or epithermal region was determined also by Co-Al measurements since Co^{59} has a resonance at 120 ev. The flux between 120 ev and 1.51 Mev was assumed to have $1/E^q$ behavior, i.e.

$$\emptyset(E) = \emptyset_o / E^q$$
(A1.13)

where

$\emptyset_o$ is a constant, n/cm^2-sec

E   is the neutron energy, ev

q   is a joining function for the energy dependence of the differential flux, $\emptyset(E)$, between the Co^{59} resonance at 120 ev and the fast spectrums at 1.51 Mev as determined by threshhold foils (See Equation A1.18).

$\emptyset_O$ was determined by the following expression

$$\emptyset_O = \frac{\emptyset_{2200}\sigma_{2200}}{[R_{Cd} - 1][T.R.I.]} \qquad (A1.14)$$

where

$$R_{Cd} = (Act)_B/(Act)_{Cd} \text{ is the cadmium ratio}$$

$$T.R.I. = \int_{E_c}^{\infty} \left[\sigma_{res} + \sigma_{1/v}\right]\frac{dE}{E} \qquad (A1.15)$$

where

T.R.I.	is the total resonance integral, barns
E_c	is the cadmium cut-off energy, assumed to be 0.5 ev
σ_{res}	is the resonance cross-section, barns
$\sigma_{1/v}$	is the 1/v cross-section, barns.

For the measurements of the fast neutron flux, threshhold detectors were used (A1.6). The integral flux for such a detector can be determined from

$$\emptyset(\geqslant E_{eff}) = \frac{Act}{\overline{\sigma_{eff}}\left[1-e^{-\lambda t}\right]} \qquad (A1.16)$$

where

$\emptyset(\geqslant E_{eff})$	is the integral flux for energy larger than or equal to E_{eff}
E_{eff}	is the effective threshold energy of the detector
$\overline{\sigma_{eff}}$	is the effective cross section of the detector

The differential flux was determined from a set of measure-

ments of the integral flux using different detectors having different values of E_{eff}. The technique applied was to use first a fast fission spectrum of Watt (A1.7) to obtain a first approximation to the flux shape and then to fit the integral flux by means of the relation

$$\ln \emptyset(\geq E) = a + bE \qquad (A1.17)$$

by the method of least squares. The fast differential flux is then determined by differentiating Equation (A1.17).

$$\emptyset(E) = b\left[e^{a + bE}\right] \qquad (A1.18)$$

Equation (A1.18) is used above 1.51 Mev and Equation (A1.13) is used between 120 ev and 1.51 Mev.

The threshold detectors employed for this work were nickel (E_{eff} = 2.9 Mev), magnesium (E_{eff} = 6.3 Mev) and aluminum (E_{eff} = 8.1 Mev).

Sawyer and Mason (A1.2) have developed the computer program, MNFOIL, to determine the differential flux $\emptyset(E)$ from the foil activitation measurements. This program has been used extensively in this report. The output of the program gives $\overline{\sigma_{eff}}$, $\emptyset(\geq E_{eff})$, $\emptyset(E)$ for the threshold foils and the constant a and b of Equation (A.18), the cadmium ratio R_{Cd} and $\emptyset_o$ for the resonance flux and the thermal neutron flux, $\emptyset_{2200}$.

With the differential flux spectrum determined, the elastic scattering integral, I_i, can then be calculated according to Equation (A1.5a) using published data for elastic cross-sections. Sawyer and Mason (A1.2) have also developed the computer program MNDOS, for this purpose. The output of this program gives the value of q of the joining function between resonance and fast flux of Equation (A1.13), the scattering integrals of hydrogen, I_H, and other samples of interest, I_i, as well as the ratio of I_i/I_H.

In the measurement of resonance flux using Co-Al wire, Mason and Timmins (A1.5) have reported a value of resonance integral of Co^{59} of 52 barns at 0.595 weight percent cobalt in Co-Al wire based on measurements reported by Vidal (A1.8). This value has been used throughout the foil dosimetry measurements covered in this report.

A1.3.3 Results of Foil Dosimetry

The chronology of foil measurements at Fuel Position 1 for the period covered in this report has been shown in Chapter 2.

The primary application of foil dosimetry results was in the determination of the ratio of neutron scattering integral, I_i/I_H, for use in the determination of the in-pile neutron dose rate, R_N^J, of Equation (A1.5).

The results of Foil Runs 47 and 52C will be discussed to illustrate the procedures employed. It should be noted that these two runs were made in two different central fuel elements into which In-pile Sections No. 4 and No. 5 were fitted.

Table A1.7 shows, at various axial positions of Fuel Position 1, the calculated values of

(1) thermal neutron flux, $\emptyset_{2200}$

(2) $\emptyset_o$ and q of Equation (A1.13) for the differential resonance flux

(3) constant a and b of Equation (A1.18) for the differential fast flux

(4) neutron elastic scattering integral, I_H

(5) ratio of neutron elastic scattering integral of carbon and aluminum to that of hydrogen I_C/I_H and I_{Al}/I_H.

Figure A1.4 plots the axial variation of the thermal neutron fluxes for both Foil Runs 47 and 52C. The thermal fluxes are normalized to 1MW of reactor power.

Table A1.7

Summary of Results of Foil Dosimetry

Foil Runs 47 and 52C

Foil Run 52c

Axial Position	ϕ_{2200} n/cm²-S-MW x10⁻¹²	ϕ_0 n/cm²-s x10⁻¹²	q (Eq.A1.13)	b(Mev⁻¹) (Eq.A1.18)	a	I_H watts/atom/MW x10⁻²⁶	I_C/I_H	I_{Al}/I_H
-16	9.77	0.490	-1.093	-0.611	27.04	0.291	0.1786	0.1149
-12	9.67	0.880	-0.964	-0.645	28.85	1.538	0.1838	0.1193
-8	9.66	1.42	-0.959	-0.658	29.37	2.564	0.1832	0.1188
-4	10.73	1.60	-0.981	-0.632	29.28	2.721	0.1837	0.1192
0	10.42	1.62	-0.960	-0.658	29.49	2.891	0.1831	0.1188
3	9.62	1.54	-0.959	-0.658	29.45	2.780	0.1832	0.1189
6	8.65	1.27	-0.952	-0.657	29.32	2.433	0.1836	0.1192
9	7.88	0.993	-0.951	-0.663	29.08	1.904	0.1833	0.1189
15	6.31	0.335	-1.117	-0.600	26.44	0.164	0.1780	0.1144
19	4.30	0.090	-1.131	-0.530	25.01	0.041	0.1824	0.1181
25	1.49	0.022	-1.211	-0.436	22.87	0.0055	0.1861	0.1209

Foil Run 47

Axial Position	ϕ_{2200} n/cm²-S-MW x10⁻¹²	ϕ_0 n/cm²-s x10⁻¹²	q (Eq.A1.13)	b(Mev⁻¹) (Eq.A1.18)	a	I_H watts/atom/MW x10⁻²⁶	I_C/I_H	I_{Al}/I_H
-12 3/4	9.66	0.768	-1.016	-0.640	28.21	0.856	0.1812	0.1171
-9 3/4	9.39	1.06	-0.949	-0.663	29.17	2.064	0.1834	0.1190
-6 3/4	9.74	1.38	-0.965	-0.655	29.29	2.368	0.1830	0.1187
-2 3/4	10.76	1.52	-0.973	-0.653	29.30	2.427	0.1828	0.1185
1 1/4	10.18	1.52	-0.975	-0.653	29.28	2.376	0.1827	0.1184
5 1/4	8.63	1.26	-0.959	-0.654	29.26	2.288	0.1835	0.1190
9 1/4	7.34	0.885	-0.959	-0.633	29.00	1.624	0.1849	0.1202
16 1/4	4.84	0.237	-1.117	-0.609	26.09	0.115	0.1770	0.1137
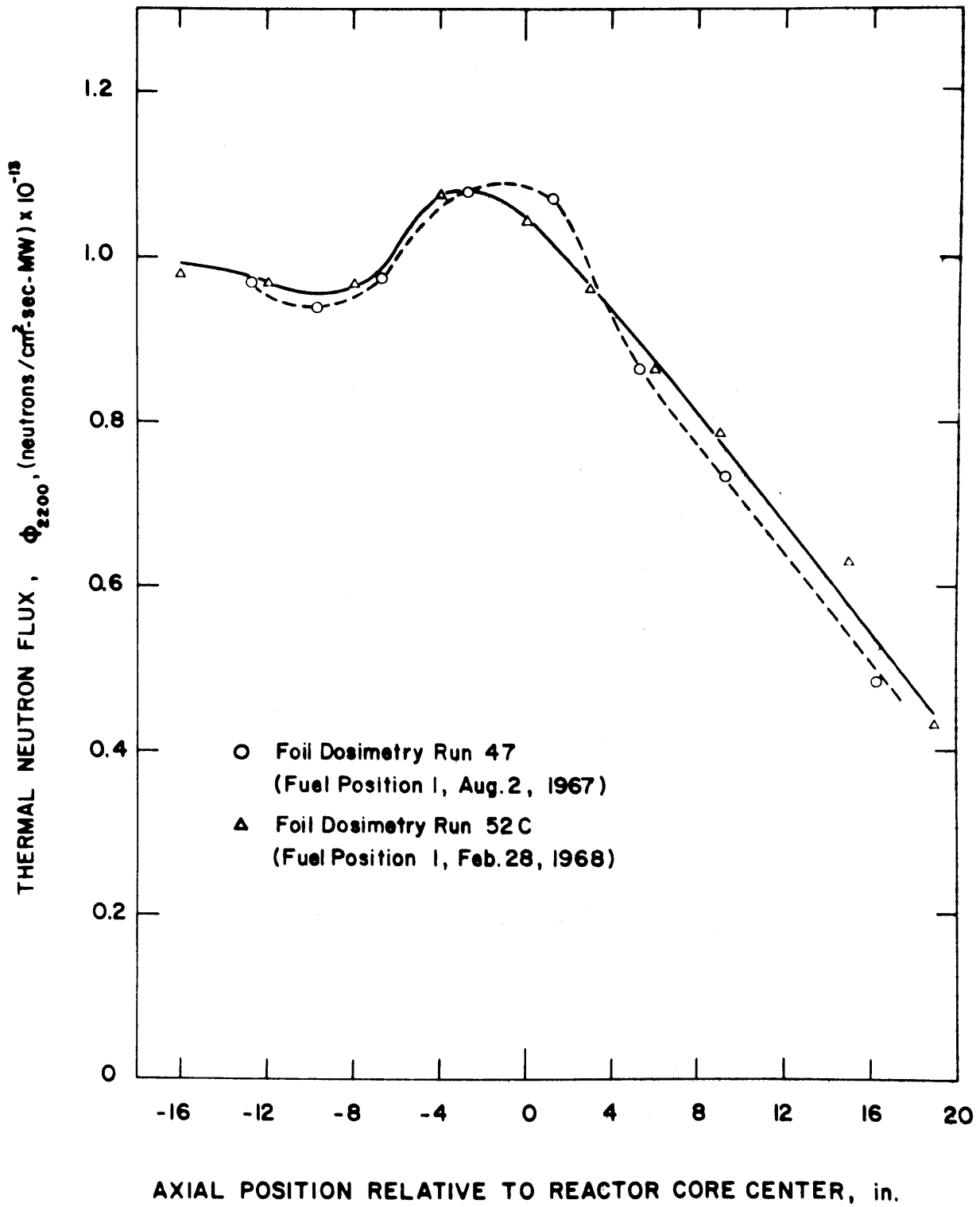
FIGURE A1.4 AXIAL DISTRIBUTION OF THERMAL NEUTRON FLUX AT FUEL
POSITION I

Figure Al.5 shows the neutron energy spectrum near the mid-plane of Fuel Position 1.

Figure Al.6 shows the neutron scattering ratio, I_C/I_H and I_{Al}/I_H at various positions of the Fuel Position 1.

Within the region from -14 inches to +14 inches of the axial position in Fuel Position 1 where nearly 80% of the active volume of the in-pile section lies, the maximum variation of I_i/I_H, as shown in Table Al.7 or Figure Al.6, is less than 2% between two data points from either foil run. This confirms the earlier assumption that the ratios of neutron scattering integrals, I_i/I_H, are essentially independent of the neutron spectra and the axial position of the reactor core (see Section Al.2.1). The b_j values tabulated in Table Al.2 were calculated using the average value of I_C/I_H and I_{Al}/I_H obtained from the foil runs.

A comparison of the I_H values presented in Table Al.3, which were determined by adiabatic dosimetry, and in Table Al.7, which were determined by foil dosimetry, will be of interest. Since Foil Run 47 was made at approximately the same time as the Calorimetry Series XXV and Foil Run 52 as Calorimetry Series XXVIII-XXX, comparison at each axial position is shown in Table Al.8. Except for the end positions where the neutron dose rate is only a very small fraction of the total dose rate, the difference in I_H between these two different measurements is generally less than 5%.

The fast neutron dose rate factors to the organic coolant, F_N^{SW}, have also been calculated based on I_H data from Foil Runs 47 and 52C and are shown in Table Al.8 together with those calculated from the Calorimetry Series. The fast neutron dose rate factors, F_N^{SW}, calculated using foil dosimetry agree quite well with those using adiabatic calorimetry.

Mason and Bley (Al.8) have made foil measurements of the flux spectrum through the aluminum monitoring tube mounted outside the in-pile assembly (see Figure 2.1) during the per-
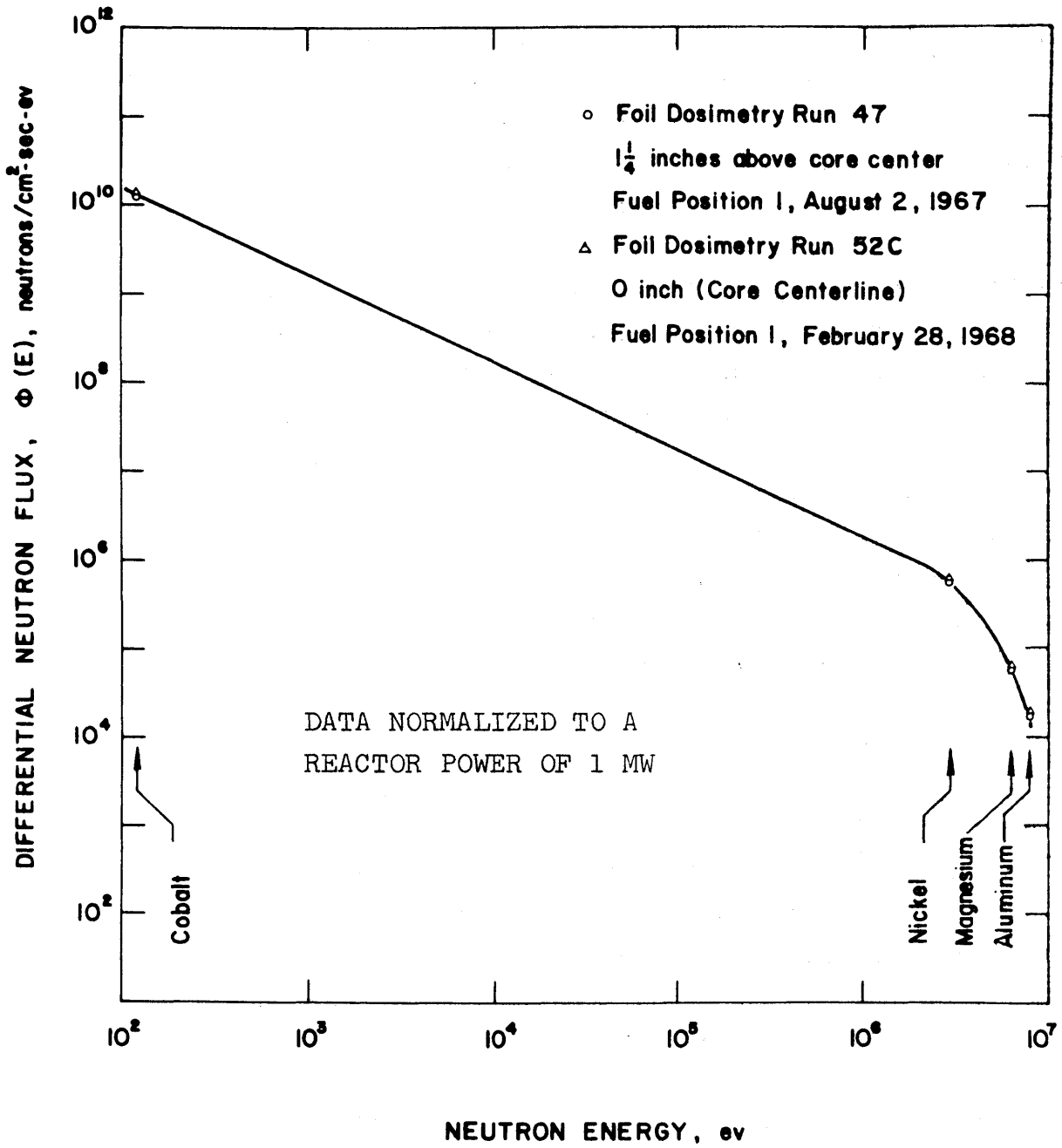
FIGURE AI.5 NEUTRON ENERGY SPECTRUM IN FUEL POSITION I
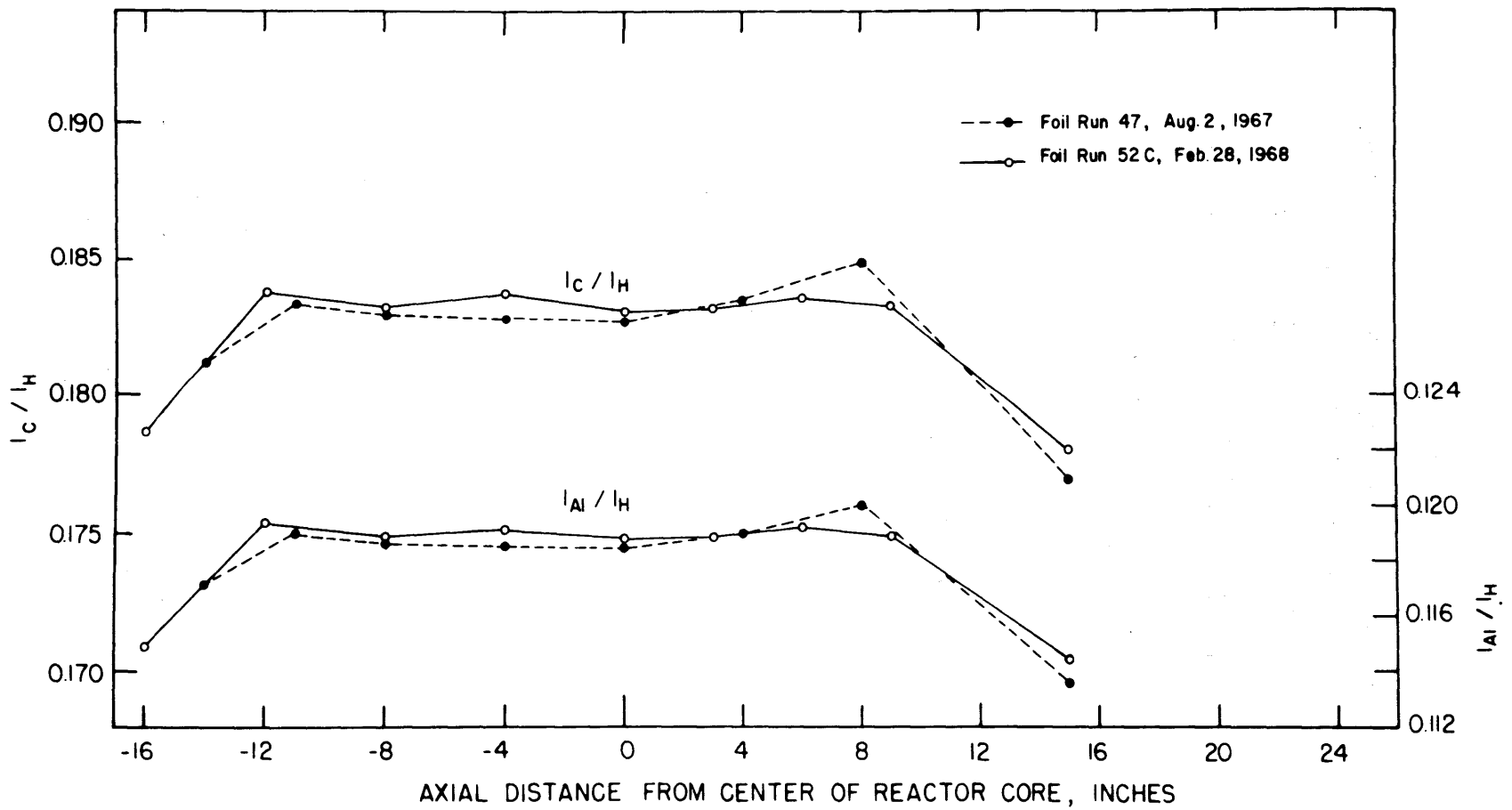
FIGURE A1.6   NEUTRON SCATTERING INTEGRAL RATIO ALONG AXIAL POSITION AT   FUEL   POSITION   I

Table A1.8

Comparison of Neutron Scattering Integral

of Hydrogen from Calorimetric

and Foil Dosimetric Measurements

I_H, (watts/atom - MW) x 10^{-24}

Axial Position	Calorimetry Series XXV	Foil Run 47	Axial Position	Calorimetry Series XXVIII-XXX	Foil Run 52
			-16		0.291
-14	0.959				
-12 3/4		0.856	-14	0.428	
-9 3/4		2.064	-12		1.538
-6 3/4		2.368	-9	2.207	
-6	2.463		-8		2.564
			-4	2.791	2.721
-2 3/4		2.427	0	2.965	2.891
0	2.418		3		2.780
1 1/4		2.376	4	2.804	
			6		2.433
5 1/4		2.288	9	2.210	1.904
6	2.009		14	1.157	
9 1/4		1.624	15		0.164
14	0.166		19	0.109	0.041
16 1/4		0.115	25	0.012	0.006
F_N^{SW} $\frac{watt-cc}{MW - gm}$	25.1	24.5		30.0	29.2

iod the in-pile section was installed at Fuel Position 1
(Foil Dosimetry Nos. 43C through 45C for In-pile Section
No. 4 and Nos. 49C through 51C for In-pile Section No. 5).
The neutron dose rate factors, F_N^{SW}, obtained from these
measurements decreased with accumulated reactor exposure
so as to support the use of linear interpolation between
the measured calorimetric dose rate factors as functions
of accumulated reactor exposure (i.e., MWH of reactor
energy).

APPENDIX A2

CIRCULATING COOLANT MASS AND

TEMPERATURE PROFILES AROUND LOOP

A2.1 Calculations of Mass of Circulating Coolant in the Loop

In the calculations of coolant degradation (see Appendix A3) and in the determination of average dose rate (watt/gm) to the coolant in the loop, the circulating mass of the coolant must be known. A tritium dilution method is used at M.I.T. for the determination of circulating mass of the coolant in the loop. Since the volumes and temperatures of various sections of the loop are known, the mass of coolant in the loop can also be calculated and compared to the circulating mass of the loop as determined by the tritium dilution method.

A2.2 Tritium Dilution Method

The tritium dilution method consists of introducing a sample of tritiated terphenyl of known tritium concentration and known weight into the loop in which the circulating coolant mass is to be determined. After sufficient time of mixing in the loop, samples are taken from the loop and analyzed to determine the tritium concentration. A tritium balance in the loop yields the loop circulating mass as shown in Equation (A2.1)

$$M_C = \frac{M_0 [C_0 - C_L]}{C_L - C_b} \qquad (A2.1)$$

where

M_C is the circulating mass of the organic coolant in the loop before the tritiated terphenyl was added, grams

C_0 is the tritium concentration of the tritiated ter-
phenyl sample added to the loop, microcurie (μ c/gm)

C_L is the tritium concentration of the coolant sample
removed from the loop after mixing, μ c/gm

C_b is the background tritium concentration of the cool-
ant in the loop before tritiated terphenyl is added,
μ c/gm

M_0 is the weight of tritiated terphenyl added to the
loop, grams

At M.I.T., the tritium dilution was carried out either
at the beginning or at the end of a steady-state run. 100 to
200 millicuries of tritiated terphenyl prepared by the Tracer-
lab Inc. was mixed with approximately 200 grams of fresh ter-
phenyl. The concentration, C_0, of Equation (A2.1) was deter-
mined from this mixture. The mixture was then used to fill a
150 gram makeup capsule. The net amount, M_0, of the mixture
in the capsule was weighted and the capsule was connected to
the loop. After mixing of the tritiated terphenyl in the
loop, a sample was taken by means of the Sampling Capsule from
which the concentration, C_L, was determined. The concentra-
tion, C_b, of Equation (A2.1) was determined from the coolant
sample taken immediately before the tritiated terphenyl was
added to the loop.

The tritium concentrations (C_0, C_L and C_b) of Equation
(A2.1) were determined by means of liquid scintillation count-
ings at two laboratories, namely The Tracerlab Inc. (Waltham,
Massachusetts) and The New England Nuclear Corporation (Boston,
Massachusetts). In order to minimize errors in sample pre-
parations prior to liquid scintillation counting, the count-
ing solution (sample dissolved in scintillating solution) was
prepared at M.I.T. Between 0.2 to 2 grams of each sample,
depending on the color and estimated tritium concentration,
was weighed and dissolved in 200 ml to 600 ml scintillation
solution consisting of 77% toluene and 23% denatured ethyl
alcohol. At least two preparations of each sample were made

of different sample concentration. In each of the two labora-
tories, three aliquots from each preparation were counted both
with and without internal spiking using a toluene solution con-
taining tritium standard. The volume of the spiking solution,
0.1 ml to 0.2 ml,was small as compared to the counting solution
so that its effect on the counting geometry, coloration and
efficiency was negligbile. However the activity of the spike
was sufficiently large, relative to the activity of the count-
ing solution, so that the counting efficiency could be accu-
rately determined.

By collecting coolant samples successively from the loop
after the introduction of the tritiated terphenyl, the effect
of mixing of tritiated terphenyl with the coolant was investi-
gated. We first assume that an approximately equal amount of
makeup terphenyl is added to the loop preceding the removal of
each sample. A tritium balance on the loop shows that the
circulating coolant mass can be calculated from the jth sample
as

$$M_{C,j} = \frac{\sum_{i=0}^{i=j-1} D_i[C_{D,i} - C_{L,j}] - \sum_{i=1}^{i=j-1} L_i[C_{L,i} - C_{L,j}]}{C_{L,j} - C_b} \qquad (A2.2)$$

where

$M_{C,j}$ is the circulating coolant mass of the loop deter-
mined from the jth sample, grams

D_i is the weight of the makeup coolant preceding the
i^{th} sample taken from the loop (D_0 = the weight of
the tritiated terphenyl), grams

L_i is the weight of the ith sample taken from the loop,
grams,

$C_{D,i}$ is the tritium concentration of the makeup coolant
preceding the ith sample taken from the loop, $\mu c/gm$

$C_{L,i}$ is the tritium concentration of the ith sample taken
from the loop, $\mu c/gm$

C_b is the background tritium concentration of the cool-
ant in the loop before the tritiated terphenyl is
added, $\mu c/gm$

Variation in $M_{c,j}$ would be expected if complete mixing was slow.

For Run 23A, the tritium dilution method was carried out at the end of the steady-state run so that no makeup terphenyl was added. Equation (A2.2) can then be simplified with $D_i(i > 0) = 0$, and

$$M_{C,j} = \frac{D_0[C_{D,0} - C_{L,j}] - \sum_{i=1}^{i=j-1} L_i[C_{L,i} - C_{L,j}]}{C_{L,j} - C_b} \qquad (A2.3)$$

The statistical error in the determination of coolant circulating mass using the tritium dilution method can be calculated as follows.

For the first sample taken after the dilution, we apply the variance propagation rule to Equation (A2.1),

$$\sigma^2(M_C) = \left[\frac{C_0 - C_L}{C_L - C_b}\right]^2 \sigma^2(M_0) + \left[\frac{M_0}{C_L - C_b}\right]^2 \sigma^2(C_0)$$

$$+ \left[\frac{M_0(C_0 - C_L)}{(C_L - C_b)^2}\right]^2 \sigma^2(C_b) + \left[\frac{M_0(C_0 - C_b)}{(C_L - C_b)^2}\right]^2 \sigma^2(C_L)^2 \qquad (A2.4)$$

Similarly, the variance of the circulating coolant mass after the removal of the jth coolant sample is obtained from Equation (A2.3) as

$$\sigma^2(M_{C,j}) = \sum_{i=0}^{i=j-1}\left[\frac{C_{L,i} - C_{L,j}}{C_{L,j} - C_b}\right]^2 \sigma^2(L_i) + \sum_{i=0}^{i=j-1}\left[\frac{L_i}{C_{L,j} - C_b}\right]^2 \sigma^2(C_{L,i})$$

$$+ \sum_{i=0}^{i=j-1}\left[\frac{L_i(C_{L,i} - C_{L,j})}{(C_{L,j} - C_b)^2}\right]^2 \sigma^2(C_b)$$

$$+ \sum_{i=0}^{i=j-1}\left[\frac{L_i(C_{L,i} - C_b)}{(C_{L,j} - C_b)^2}\right]^2 \sigma^2(C_{L,j}) \qquad (A2.5)$$

with $C_{L,0} = C_{D,0}$ and $L_0 = D_0$.

The error in the weighing of coolant samples, ranging from 20 grams to 150 grams, is estimated to be 0.5 grams. As mentioned earlier in this section that at least four analyses were made on tritium concentration for each sample added or removed from the loop by means of liquid scintillation counting, the variance in concentration, $\sigma^2(C_j)$ in Equation (A2.5) is calculated as follows:

$$\sigma^2(C_{L,j}) = \frac{\sum\limits_{j=1}^{Z}[C_{L,j} - \overline{C}_{L,j}]^2}{Z[Z - 1]} \tag{A2.6}$$

where

$C_{L,j}$ is the measured tritium concentration of the jth sample

$\overline{C}_{L,j}$ is the average tritium concentration of the jth sample

Z is the number of tritium analyses performed on the jth sample.

A2.2.1   Tritium Dilution-Run 23A

Table A2.1 shows the results of tritium counting from samples taken during tritium dilution of Run 23A.

Table A2.2 summarizes the circulating coolant mass of Run 23A at various times after dilution as calculated from the counting data tabulated in Table A2.1. A total of nine samples were taken within 26 hours after the addition of tritiated terphenyl. Both the Tracerlab and New England Nuclear results were shown. Figure A2.1 plots the measured circulating coolant mass as a function of time after tritium dilution. The solid line is an empirical fit to the data points using two exponential terms as expressed by

$$M_C = 4940 - 4200e^{-3.0t} - 740e^{-0.154t} \text{ grams} \tag{A2.7}$$

where t is time after tritium dilution in hours. Equation (A2.7) appears to show that the coolant in the loop may be

Table A2.1

Summary of Tritium Counting

Tritium Dilution - Run 23A

Sample No.	Weight of Sample Removed From Loop (gm)	Sample[b] Conc. (gm/ml) x10³	Aliquot No.	Tracerlab Analysis				New England Nuclear Analysis			
				Activity[c] per Unit Volume (nc/ml)	Specific Activity (µc/gm)	Avg.Sp.[d] Activity (µc/gm)	Std.Error Sp.Activity (±µc/gm)	Activity[c] per Unit Volume (nc/ml)	Specific Activity (µc/gm)	Avg.Sp.[d] Activity (µc/gm)	Std.Error Specific Activity (± µc/gm)
23A-L16A		0.8725	1	9.308	10.668			12.372	14.180		
			2	9.533	10.926			12.089	13.856		
			3	9.237	10.587			12.062	13.825		
						10.773 $(c_{L,9})$	0.051			13.875 $(c_{L,9})$	0.096
23A-L16B		0.5820	1	6.297	10.820			8.130	13.968		
			2	6.320	10.857			7.837	13.466		
			3	6.275	10.782			8.122	13.955		
23A-L15A	21.4(L_8)	0.5050	1	5.655	11.197			7.287	14.431		
			2	5.694	11.275			7.406	14.665		
			3	5.693	11.273			7.203	14.263		
						11.221 $(c_{L,8})$	0.017			14.560 $(c_{L,8})$	0.082
23A-L15B	21.4(L_8)	0.9915	1	11.095	11.190			14.091	14.211		
			2	11.090	11.185			14.575	14.700		
			3	11.109	11.204			14.343	14.466		
23A-L14A	21.4(L_7)	0.6015	1	6.743	11.210			8.842	14.700		
			2	6.850	11.389			8.712	14.484		
			3	6.815	11.330			8.803	14.635		
						11.301 $(c_{L,7})$	0.025			14.491 $(c_{L,7})$	0.063
23A-L14B	21.4(L_7)	1.0815	1	12.184	11.265			15.510	14.340		
			2	12.223	11.302			15.482	14.315		
			3	12.230	11.308			15.642	14.473		
23A-L13A	22.7(L_6)	0.9465	1	10.684	11.288			13.085	13.825		
			2	10.605	11.205			13.704	14.479		
			3	10.651	11.253			13.891	14.676		
						11.372 $(c_{L,6})$	0.057			14.522 $(c_{L,6})$	0.167
23A-L13B	22.7(L_6)	0.5635	1	6.471	11.483			8.111	14.394		
			2	6.464	11.470			8.475	15.039		
			3	6.499	11.534			8.293	14.718		
23A-L12A	19.4(L_5)	0.9655	1	10.973	11.366			14.492	15.010		
			2	11.146	11.544			14.500	15.019		
			3	11.210	11.610			14.450	14.966		
						11.397 $(c_{L,5})$	0.059			14.802 $(c_{L,5})$	0.095
23A-L12B	19.4(L_5)	0.5090	1	5.747	11.290			7.367	14.474		
			2	5.748	11.293			7.430	14.597		
			3	5.740	11.278			7.505	14.744		

Table A2.1 (Cont.)

Sample No.	Weight of Sample Removed From Loop (gm)	Sample[b] Conc. (gm/ml) x 10³	Aliquot No.	Tracerlab Analysis				New England Nuclear Analysis			
				Activity[c] per Unit Volume (nc/ml)	Specific Activity (uc/gm)	Avg.Sp.[d] Activity (uc/gm)	Std.Error Sp.Activity (± uc/gm)	Activity[c] per Unit Volume (nc/ml)	Specific Activity (uc/gm)	Avg.Sp.[d] Activity (uc/gm)	Std. Error Specific Activity (± uc/gm)
23A-L11A	21.4(L_4)	0.9440	1	11.109	11.768			14.275	15.121		
			2	11.024	11.678			14.150	14.989		
			3	11.135	11.795			14.448	15.305		
23A-L11B	21.4(L_4)	0.5110	1	6.061	11.860	11.787 ($c_{L,4}$)	0.038	7.660	14.990	15.177 ($c_{L,4}$)	0.069
			2	6.092	11.921			7.864	15.390		
			3	5.978	11.699			7.801	15.267		
23A-L10A	22.1(L_3)	1.0350	1	12.412	11.992			16.183	15.636		
			2	12.540	12.116			15.813	15.278		
			3	12.379	11.960			15.978	15.438		
23A-L10B	22.1(L_3)	0.6115	1	7.280	11.905	12.011 ($c_{L,3}$)	0.030	9.365	15.283	15.380 ($c_{L,3}$)	0.076
			2	7.349	12.017			9.491	15.520		
			3	7.363	12.041			9.251	15.128		
23A-L9A	16.4(L_2)	0.5100	1	6.227	12.210			8.070	15.824		
			2	6.256	12.267			7.953	15.593		
			3	6.179	12.116			8.134	15.949		
23A-L9B	16.4(L_2)	1.0870	1	12.992	11.952	12.088 ($c_{L,2}$)	0.054	17.219	15.841	15.662 ($c_{L,2}$)	0.103
			2	13.005	11.964			16.602	15.290		
			3	13.062	12.016			16.822	15.476		
23A-L8A	131.4(L_1)	1.4455	1	18.392	12.724			23.321	16.134		
			2	18.296	12.657			23.548	16.291		
			3	18.264	12.635						
23A-L8B	131.4(L_1)	0.5125	1	6.366	12.421	12.618 ($c_{L,1}$)	0.050	8.223	16.044	16.088 ($c_{L,1}$)	0.093
			2	6.419	12.525			8.310	16.215		
			3	6.531	12.743			8.075	15.755		
23A-L7A		9.1285	1	9.964	1.092			12.488	1.368		
			2	9.928	1.088			12.693	1.390		
			3	9.916	1.086			13.038	1.428		
23A-L7B		6.0320	1	6.638	1.101	1.092 (c_b)	0.002	8.710	1.444	1.417 (c_b)	0.013
			2	6.668	1.097			8.668	1.437		
			3	6.573	1.090			8.655	1.435		
23A-D1A	159.4(D_0)	0.2218	1	69.082	311.460			86.071	388.058		
			2	68.738	309.911			91.435	412.239		
			3	69.206	312.021			87.054	392.488		
23A-D1B	159.4(D_0)	0.2670	1	84.954	318.180	313.530 ($c_{D,0}$)	1.222	109.063	408.475	405.250 ($c_{D,0}$)	4.894
			2	83.954	314.434			110.378	413.401		
			3	84.152	315.175			111.297	416.841		

(a) Symbols in brackets correspond to the notations used in Equation (A2.3)
(b) Weight of sample per unit volume of counting solution as prepared at M.I.T. Organic Loop Project
(c) Tritium activity counted in sample per unit volume of counting solution
(d) Tritium activity counted per gram of sample. Symbols in brackets correspond to the notations used in Equation (A2.3)
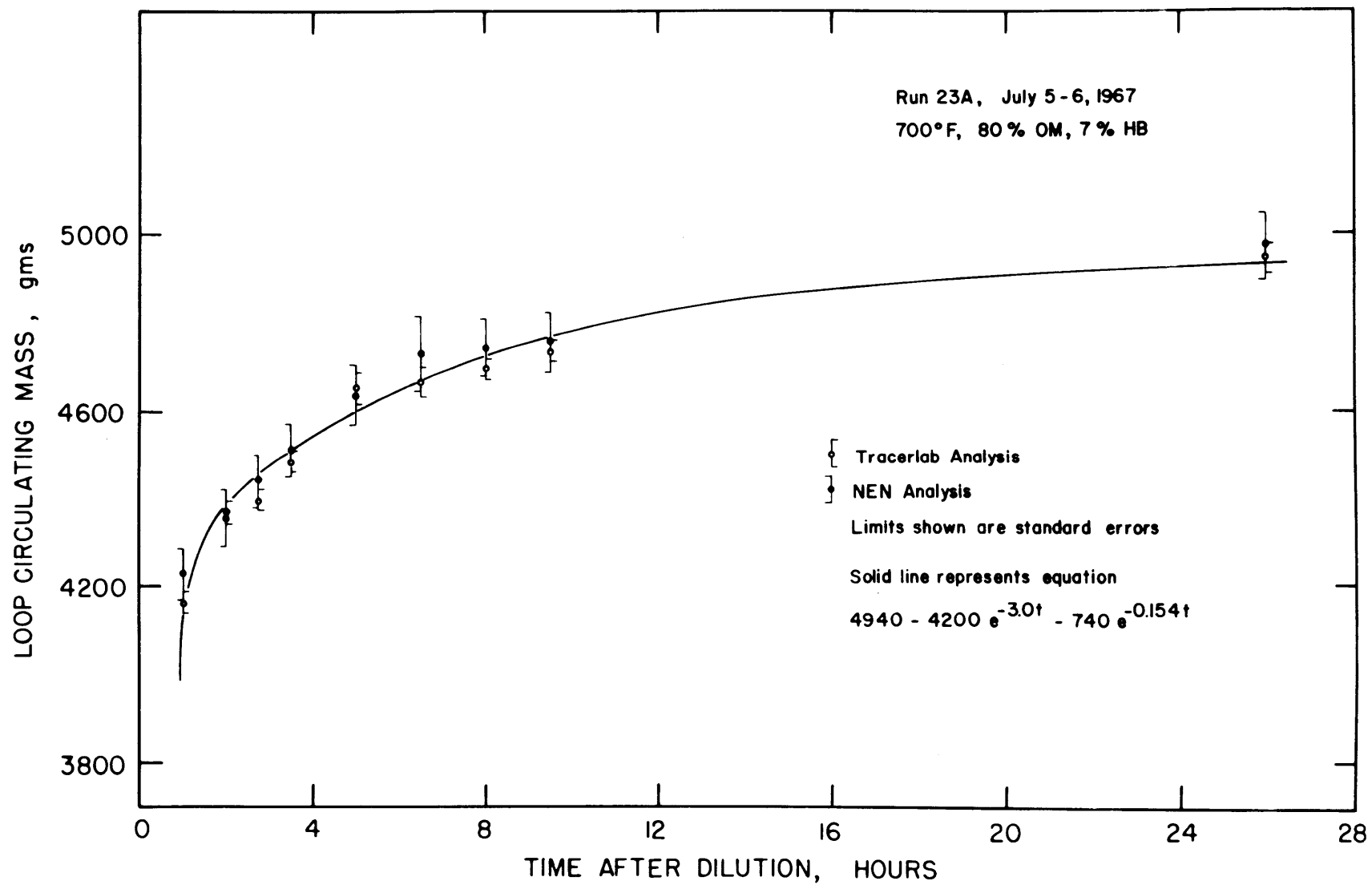
FIGURE A2.I LOOP CIRCULATING MASS AFTER TRITIUM DILUTION — RUN 23A

described as consisting of two circulating components, one of
which, approximately 4200 grams in mass, circulates rapidly
with mixing time constant of 1/3 hour and the other, approxi-
mately 740 grams, is slowly mixing with mixing time constant
of 6.5 hours. We also noted that the mixing was essentially
complete 26 hours after the dilution. The above results are
consistent with the earlier M.I.T. report (A2.1) in estimating
the volume of circulating coolant in the M.I.T. loop based on
the assumption that the coolant in some sections of the loop
in which dead-end spaces exist was not well mixed. The estima-
tion of circulating coolant volumes presented in Section A2.3
of this report is based on the original estimate of that report
(A2.1).

Table A2.2

Summary of Tritium Dilution[a]

Run 23A

Time After Tritium Dilution (hr)	Circulating Coolant Mass[b] (gm)	
	Tracerlab	NEN
1	4162 ± 52	4229 ± 120
2	4364 ± 72	4356 ± 128
2-3/4	4396 ± 44	4444 ± 124
3-1/2	4486 ± 50	4509 ± 124
5	4655 ± 68	4635 ± 136
6-1/2	4666 ± 68	4733 ± 174
8	4698 ± 46	4743 ± 130
9-1/2	4735 ± 44	4756 ± 136
26	4948 ± 72	4973 ± 150

[a] Surge Tank gage-glass level at dilution = 7 inches
[b] Error limits are 2σ

A2.2.2 Tritium Dilution - Run 20B

The tritium dilution made during Run 20B was somewhat different from the rest. The first coolant sample was taken two hours after the tritiated terphenyl was introduced and the second sample two and one-half hours after the first. Meanwhile, the process system (Makeup and Sampling System) was turned off. Therefore, Equation (A2.2) is still applicable to calculate the circulating loop mass from these first two samples. However, after the second sample was taken, the processing system was turned on in order to maintain steady-state condition of the coolant concentration in the loop. During this period, a portion of the loop coolant was pumped into the Sampling Tank and replaced by the processed ter-phenyl pumped from the Makeup Tank. The processed terphenyl pumped from the Makeup Tank into the circulating loop con-tained no tritium except its background activity from loop irradiation. A tritium balance around the loop after the third sample was taken shows

$$
\begin{aligned}
M_{C,3}C_b &+ D_1C_{D,1} + D_2C_{D,2} - L_1C_{L,1} - L_2C_{L,2} \\
&+ [M_1 - M_2]C_M - [S_1C_{S,1} - S_2C_{S,2}] \\
&- H_S[C_{L,3} - C_{S,1}] = \Big[M_{C,3} + D_1 + D_2 - L_1 - L_2 \\
&+ [M_1 - M_2] - [S_1 - S_2] \Big]C_{L,3}
\end{aligned}
\tag{A2.8}
$$

where

S_1 and S_2 are the initial and final masses of the coolant in the Sampling Tank from the time the processing sys-tems are turned on to the time the third sample is taken, grams

M_1 and M_2 are the initial and final masses of coolant in the Makeup Tank, grams

$C_{S,1}$ and $C_{S,2}$ are the initial and final tritium concen-trations of the coolant in the Sampling Tank, μ c/gm

C_M is the background tritium concentration of the cool-
ant in the Makeup Tank, μ c/gm

H_S is the mass of the coolant held-up in the line between
the loop and the 0" level of the Sampling Tank, grams

All other notations are similar to those used in Equation (A2.2)

Rearranging Equation (A2.8), the circulating coolant mass
in the loop can be calculated from the third sample taken with
processing systems running as

$$
M_{C,3} = \frac{1}{[C_{L,3} - C_b]} \, D_0 \Big[C_{D,0} - C_{L,3} + D_1 [C_{D,1} - C_{L,3}]
$$
$$
+ D_2 [C_{D,2} - C_{L,3}] - L_1 [C_{L,1} - C_{L,3}] - L_2 [C_{L,2} - C_{L,3}]
$$
$$
+ [M_1 - M_2][C_M - C_{L,3}] + [S_1 + H_S]C_{S,1} - [S_1 - S_2]C_{L,3}
$$
$$
- S_2 C_{S,2} - H_S C_{L,3} \Big] \tag{A2.9}
$$

Tables A2.3 and A2.4 summarize the results of tritium dilution
made during Run 20B. The effect of incomplete mixing is again
noted.

Table A2.3

Summary of Tritium Dilution[a]

Run 20B

Time After Tritium Dilution (hr)	Circulating Coolant Mass[b] (gm)	
	Tracerlab	NEN
2	4656 ± 68	4474 ± 286
4-1/2	4818 ± 82	4417 ± 384
25	5180 ± 170	5111 ± 394

[a] Surge Tank gage-glass level at dilution = 7-7/8 inches

[b] Error limits are 2σ

Table A2.4

Summary of Tritium Analysis
Tritium Dilution - Run 20B

Sample No.[a]	Weight of Sample[a] (gm)	Tritium Concentration[b] (μc/gm)			
		Tracerlab		NEN	
20B-D2 ($c_{D,0}$)	158.6 (D_0)	796.3 $\pm$ 5.1		995.3 $\pm$ 22.2	
20B-L5 (c_b)		0.158 $\pm$ 0.001		0.273 $\pm$ 0.001	
20B-L6 ($c_{L,1}$)	136.7 (L_1)	26.4 $\pm$ 0.1		34.3 $\pm$ 0.7	
20B-L7 ($c_{L,2}$)	136.3 (L_2)	24.7 $\pm$ 0.1		33.6 $\pm$ 1.1	
20B-L8 ($c_{L,3}$)	137.5 (L_3)	16.1 $\pm$ 0.10		21.0 $\pm$ 0.2	
20B-D3 ($c_{D,1}$)	152.8 (D_1)	0		0	
20B-D4 ($c_{D,2}$)	130.6 (D_2)	0		0	
20B-M7 (c_M)	1828.8 (M_1-M_2)	0.111 $\pm$ 0.001		0.163 $\pm$ 0.001	
20B-S7 ($c_{S,1}$)	1310.0 (S_1)	0.147 $\pm$ 0.002		0.513 $\pm$ 0.015	
20B-S8 ($c_{S,2}$)	3070.0 (S_2)	9.92 $\pm$ 0.04		11.95 $\pm$ 0.12	
	320.0 (H_S)				

[a] Symbols in brackets correspond to notation used in Equations (A2.2) and (A2.9)

[b] Error limits are 1σ

A2.2.3 Tritium Dilution - Runs 26, 27 and 28

The tritium dilution for each of the steady-state irradiation Runs 26, 27 and 28 consisted of only one sampling taken about 60 hours after the addition of tritiated terphenyl to the loop. The tritiated terphenyl was added prior to the shutdown of reactor and the lowering of loop operating temperature on Friday. The sample was taken on Monday morning prior to the startup of the reactor. The circulating coolant mass was then calculated according to Equation (A2.1).

Tables A2.5 and A2.6 summarize the results of tritium dilution for Runs 26, 27 and 28.

Table A2.5

Summary of Tritium Dilution

Runs 26, 27 and 28

Run No.	Surge Tank Level, inches	Circulating Coolant Mass[a] (gm)	
		Tracerlab	NEN
26	15	5144 ± 56	5104 ± 78
27	15-1/4	4859 ± 80	4916 ± 208
28	13-3/8	4776 ± 50	4744 ± 134

[a]Error Limits are 2σ

A2.2.4 Summary

A total of five tritium dilutions were made from November 1, 1966 (beginning of Run 19) to February 16, 1968 (end of Run 28). Two of the dilutions were made during the irradiation runs of Santowax OM (Runs 20B and 23A) and the rest during the irradiation runs of Santowax WR (Runs 26, 27 and 28). The circulating coolant masses for these runs have been shown in Tables A2.2,

Table A2.6

Summary of Tritium Analysis
Tritium Dilution - Runs 26, 27 and 28

Sample No.[a]	Weight of Sample[a] (gm)	Tritium Concentration[b] (μc/gm)			
		Tracerlab		NEN	
26-D1 (C_O)	142.5 (M_O)	174.3	$\pm$ 0.4	209.3	$\pm$ 1.00
26-L10 (C_b)	----------	0.345	$\pm$ 0.001	0.378	$\pm$ 0.001
26-L11 (C_L)	----------	5.04	$\pm$ 0.02	6.05	$\pm$ 0.03
27-D1 (C_O)	157.3 (M_O)	169.0	$\pm$ 1.0	211.9	$\pm$ 2.2
27-S12 (C_b)	----------	1.12	$\pm$ 0.001	1.69	$\pm$ 0.03
27-L10 (C_L)	----------	6.39	$\pm$ 0.03	8.21	$\pm$ 0.11
28-D1 (C_O)	148.1 (M_O)	235.1	$\pm$ 0.4	281.1	$\pm$ 0.5
28-S17 (C_b)	----------	0.995	$\pm$ 0.004	1.32	$\pm$ 0.02
28-L1 (C_L)	----------	8.03	$\pm$ 0.02	9.60	$\pm$ 0.11

[a] Symbols in bracket correspond to the notations used in Equation (A2.1)

[b] Error limits are 1σ

A2.3 and A2.5. There was no significant difference between the Tracerlab and the NEN values. Only the values from Tracerlab were used for the degradation caculation (see Appendix A3) since these represented less statistical fluctuations in tritium analyses.

For each dilution run, the coolant level in the Surge Tank was taken from the gage-glass level readings. The gage-glass temperature was also monitored and recorded. The Surge Tank volume was measured and reported by Morgan and Mason (A2.1) to be 61.1 cc/inch. To allow for the difference in coolant temperature between the tank and the gage-glass, the coolant mass in the Surge Tank based on the gage-glass level reading can be calculated as

$$M_{ST} = 61.1 y \rho_g \qquad (A2.10)$$

or

$$k_{ST} = 61.1 \rho_g \qquad (A2.11)$$

where

M_{ST} is the mass of coolant in the Surge Tank, grams

y is the coolant level on the gage-glass, inches

ρ_g is the density of the coolant at the gage-glass temperature, grams/cc

k_{ST} is the Surge Tank calibration factor based on gage-glass level reading, grams/inch

In the degradation calculation (Appendix A3), the circulating coolant masses at the beginning and at the end of a steady-state irradiation run must be known. Since at each point the level of coolant in the gage-glass of the Surge Tank was known, the circulating coolant mass at that point could be calculated from the circulating mass determined from tritium dilution adjusted by the mass change in the Surge Tank as calculated from Equation (A2.10). Such a calculation can be expressed by the following equation

$$M_{C,1} = M_{C,a} \frac{\rho_{C,1}}{\rho_{C,a}} + 61.1 \left[y_1 \rho_{g,1} - y_a \rho_g a \right] \qquad (A2.12)$$

where

$M_{C,1}$ is the circulating coolant mass at point "1" of a steady-state run, grams

$M_{C,a}$ is the circulating coolant mass at point "a" of a steady-state run determined from tritium dilution, grams

$\rho_{C,1}$ is the density of the coolant in the loop at point "1", grams/cc

$\rho_{C,a}$ is the density of the coolant in the loop during tritium dilution, grams/cc

$\rho_{g,1}$ is the density of the coolant at gage-glass temperature at point "1", grams/cc

$\rho_{g,a}$ is the density of the coolant at gage-glass temperature during tritium dilution, grams/cc

y_1 is the gage-glass reading at point "1", inches

y_a is the gage-glass reading at tritium dilution, inches

This is correct only if the volume occupied by the circulating mass in the loop (excluding the Surge Tank) did not change. In other words, the only change in the circulating mass between two points during irradiation runs would appear in the change of level of the Surge Tank. In order to verify this, the volumes of the circulating mass calculated from the tritium dilution measurements at 0" Surge Tank level can be compared. The coolant mass in the Surge Tank during each run is calculated from Equation (A2.10). This mass is then subtracted from the circulating mass as determined in the last section. The normalized volume of the circulating mass (0" surge tank) is then calculated with the average coolant density in the loop Table A2.7 shows the comparison between Runs 20B and 23 of the Santowax OM irradiations. Table A2.8 presents the results for Santowax WR irradiations. No significant difference is noted in the measurements of normalized volume of the circulating mass shown in Tables A2.7 and A2.8. However, the volume calculated for the Santowax OM runs (Table A2.7) is approximately 5% higher than that of Santowax WR

Table A2.7

Comparison of the Volume of Circulating Mass and Volume
Normalized to 0" Surge Tank - Runs 20B and 23A

Run No.	Temperature, °F		Gage-glass level at dilution, (inch)	Coolant Density, gm/cc		Circ.Mass[a] at 0" Surge Tank (gm)	Normalized[a] Volume of Circ. Coolant, (cc)
	Gage-glass	Loop Average		Gage-glass	Loop Average		
20B	340	560	7-7/8	0.991	0.888	4704 $\pm$ 174	5299 $\pm$ 197
23A	475	675	7	0.925	0.830	4552 $\pm$ 82	5482 $\pm$ 99

[a] Error limits are 2σ

Table A2.8

Comparison of the Volume of Circulating Mass and Volume
Normalized to 0" Surge Tank - Runs 26,27 and 28

Run No.	Temperature, °F		Gage-glass level at dilution, (inch)	Coolant Density, gm/cc		Circ.Mass[a] at 0" Surge Tank (gm)	Normalized[a] Volume of Circ. Coolant, (cc)
	Gage-glass	Loop Average		Gage-glass	Loop Average		
26	475	675	15	0.937	0.844	4286 $\pm$ 68	5079 $\pm$ 81
27	515	730	15-1/4	0.917	0.817	4005 $\pm$ 89	4902 $\pm$ 109
28	550	780	13-3/8	0.903	0.797	4038 $\pm$ 64	5064 $\pm$ 80

[a] Error limits are 2σ

(Table A2.8) reflecting changes in the flow system. Further
discussion on this point will be given in the following sec-
tion.

A2.3 Circulating Coolant Mass Based on Volume and Temperature of Loop Sections

Several modifications of the M.I.T. Organic Coolant Loop
had taken place since it was reported earlier (A2.2, A2.3).
The modifications are listed as follows: (see Figures 2.4,
and 2.5, Chapter 2)

(1) Removal of one of the coolers
(2) Addition of processing system connected to valves 6
    and 8 (S & M I), valves 14 and 16 (S & M II).
(3) Removal of coolant circulating pump No. 2
(4) Removal of AECL Fouling Probe
(5) Relocation of DP Cell to the Surge Tank

Only the first three items of modification will directly
effect the volume of circulating coolant in the system.

In-pile Sections No. 4 and No. 5 have identical dimen-
sions as In-pile Section No. 3 (A2.2). The volume of the ir-
radiation capsule and the connecting line up to the reactor
top has been recalculated to be 765 cc after correcting for
thermocouples, spacers, and heaters. The volume of one cooler
plus connecting lines is 215 cc based on ᵗhe report by Morgan
and Mason (A2.1). The liquid sample capsule is not included
in this calculation but the coolant in the lead lines up to
valves 14 and 16, (see Figure 2.4, Chapter 2), amounting to
173 grams, is included since the lead lines are permanent
parts of the circulating system. Volume above 0" Surge Tank
is excluded in order to compare with the results of tritium
dilution method using 0" Surge Tank as reference. Although
the AECL Fouling Probe and the associated flow meter have been
removed, the connecting lines between valve 12 and valve 27
remain in the system with valves 50 and 51 closed off. The

line was not heated and therefore no contribution to the circulating volume is assumed. The connection of the processing system (S & M I) to valves 6 and 8 adds additional volume from valve M3 to valve 6 and valve S2 to valve 8. All these valves are open during normal operation. The volume of the four valves is 150 cc and the lines 60 cc (total 6 feet). It is assumed that the volume beyond value M3 and S2 (see Figure 2.4, Chapter 2) towards the pump is non-mixing. However, this additional 210 cc does not apply to Runs 26, 27 and 28, in which the processing system (S & M II) was relocated and the connections to the circulating loop were made at valve 14 and valve 16 Figure 2.5, (See Chapter 2). During normal operation, these valves are closed and therefore no additional circulating volume is introduced to the loop.

Table A2.9 shows the circulating volumes and the average temperature of each of the sections of the loop for various runs. The circulating volumes are obtained from earlier M.I.T. reports (A2.1, A2.2, A2.3). The average temperatures are obtained using thermocouples attached to the various sections of the loop. The total circulating volume of 5316 cc checks quite well with the volume determined by tritium dilution method of Runs 20B and 23A (Table A2.7). The circulating volume of 5106 cc excluding the valves and leads to the processing system also checks quite well with the volume determined by tritium dilution method of Runs 26, 27 and 28 (Table A2.8).

Table A2.10 shows the circulating masses of the various runs calculated section by section from the known volume, temperature and density of each section. The density is calculated using Equations (3.2) and (3.3). Again there are good agreements with the mass determined by the tritium dilution method.

A2.4 Calculation of the Effective Loop Temperature

The M.I.T. loop for the irradiation of terphenyl coolant has a temperature distribution around the loop as indicated in Table A2.9. Since the radiopyrolytic degradation rate has been

Table A2.9

Volume of Circulating Coolant and Temperatures in Various Sections of the Loop

Section	Circulating Volume (cc)	Run 20B	Run 23A	Run 26	Run 27	Run 28
(1) In-pile Irradiation Capsule (up to right-angle bend)	765	572	702	700	750	800
(2) Right-angle bend to Surge Tank	446	558	672	673	730	780
(3) 0" Surge Tank to Pump (excluding Trim Heater)	788	558	675	675	733	783
(4) Trim Heater	300	572	700	700	750	800
(5) Pump Impeller through upstream half of Test Heater	1320	560	680	680	736	785
(6) Pump Motor Section	370	300	380	370	410	440
(7) Downstream half of Test Heater to Cooler	444	578	702	704	762	812
(8) Liquid Sampler leads	173	560	675	670	740	785
(9) Cooler	215	575	701	703	755	805
(10) Cooler to right-angle bend	285	573	703	702	753	802
(11) Processing System leads	210	500	600	---	---	---
Total	5316 ± 200 [a]					
Total - (11)	5106 ± 200					

[a] Standard error according to Morgan and Mason (A2.1)

Table A2.10

Calculated Circulating Coolant Mass in Various
Sections of the Loop Normalized to O" Surge Tank

(Based on known volume and temperature)[a]

Section[a]	Coolant Mass, grams				
	20B	23A	26	27	28
(1)	675	626	637	618	603
(2)	396	370	377	364	356
(3)	700	654	666	644	628
(4)	265	246	250	242	236
(5)	1172	1093	1114	1076	1049
(6)	374	359	365	357	353
(7)	390	361	367	356	347
(8)	154	144	146	141	138
(9)	189	176	178	173	169
(10)	251	233	237	230	224
(11)	192	182	---	---	---
Total[b]	4758	4444	4337	4203	4103

[a]See Table A2.9 for descriptions of each section and
volume and average temperature of each section.

[b]Error of approximately 200 gms has been estimated
by Morgan and Mason (A2.1)

shown to be strongly dependent on temperature (see Chapter 5), its contribution to the total degradation rate would be significantly different for each section of the loop. An effective loop temperature must be calculated which accounts for the temperature variation between different sections of the loop and the terphenyl mass holdup in each section.

Mason, Timmins et al. (A2.3) have described a method used to determine the effective loop temperature for M.I.T. loop irradiations at high temperature. This method is briefly described in the following.

It is assumed that the radiopyrolysis rate constant, $k_{P,i,m}$, for each approximately isothermal section j of the loop fits an Arrhenius type relation as expressed in Equation (A2.13).

$$k_{P,i,m}(T_j)/k_{P,i,m}(T_o) = \exp\left(-\frac{\Delta E_{P,i}}{R}\left[\frac{T_o - T_j}{T_o T_j}\right]\right) \qquad (A2.13)$$

where

   j   refers to a section of the loop

   T_j is the average coolant temperature of the jth section, ^oK

   T_o is an arbitrarily chosen temperature, ^oK

   $\Delta E_{P,i}$ is the pyrolytic activation energy of the ith isomer of the irradiated terphenyl coolant, kcal/ mole

   R   is the gas constant, kcal/mole ^oK

A mass-averaging procedure is then performed on the radiopyolytic rate constant as

$$\frac{[k_{P,i,m}(T_j)]_{avg}}{k_{P,i,m}(T_o)} = \frac{\sum_j M_j \frac{k_{P,i,m}(T_j)}{k_{P,i,m}(T_o)}}{\sum_j M_j} \qquad (A2.14)$$

where

M_j is the mass of terphenyl coolant in the jth section of the loop, grams

Substituting Equation (A2.13) into Equation (A2.14),

$$\frac{[k_{P,i,m}(T_j)]_{avg}}{k_{P,i,m}(T_o)} = \frac{\sum_j M_j \exp\left(-\frac{\Delta E_{P,i}}{R}\left[\frac{T_o-T_j}{T_o T_j}\right]\right)}{\sum_j M_j} \qquad (A2.15)$$

The average temperature of each section, T_j, is known by thermocouples attached along the section. T_o is an arbitrary reference temperature generally chosen to be the temperature of the coolant in the Surge Tank in this report. The mass of coolant in each section is calculated with known circulating volume (as shown in Table A2.9) and density (using Equations (3.2) and (3.3) of Chapter 3). It is necessary to assume an activation energy of radiopyrolysis, $\Delta E_{P,i}$. However a small error in the assumed value of $\Delta E_{P,i}$ does not significantly affect the calculation of the effective loop temperature since the chosen reference temperature, T_o, at the Surge Tank represent very closely the average coolant temperature. Once the value of $[k_{P,i,m}(T_j)]_{avg}/k_{P,i,m}(T_o)$ has been calculated from Equation (A2.15) for an irradiation run, it is used in Equation (A2.13) to calculate the temperature T_j which is designated as the "effective" loop temperature of that run. It is possible to obtain the value of $\Delta E_{P,i}$ by means of an iteration procedure using Equation (A2.15). In applying this technique, values of $k_{P,i,m}(T_o)$ and $\Delta E_{p,i}$ (presumably applicable to all runs at different temperatures but otherwise same conditions) are assumed using known values of M_j and T_j in Equation (A2.15). A value of the $[k_{P,i,m}(T_j)]_{avg}$ is calculated and compared to the experimental value found in Chapter 5. Successively better estimates of $k_{P,i,m}(T_o)$ and $\Delta E_{P,i}$ are employed by iteration until the calculated values of $[k_{P,i,m}(T_j)]_{avg}$ equals the experimental value.

The value of $\Delta E_{P,i}$, used in this report has been taken as 50 kcal/mole for all runs. This assumed value is in close agreement with the experimentally determined values of $\Delta E_{P,i}$ = 54 kcal/mole as presented in Chapter 5. Table A2.11 shows the calculations using Equation (A2.15) at various sections of the loop for all the high temperature irradiations covered by this report. The effective loop temperature of each run is also shown.

Table A2.11

Calculations of the Effective Loop Temperature[a]
for the High Temperature Irradiations

Section[b]	Run 21 ($T_O = 658°K$) T_j (°F)	M_j	$\dfrac{k_p(T_j)}{k_p(T_O)}M_j$	Run 22 ($T_O = 683°K$) T_j (°F)	M_j	$\dfrac{k_p(T_j)}{k_p(T_O)}M_j$	Run 23 ($T_O = 639°K$) T_j (°F)	M_j	$\dfrac{k_p(T_j)}{k_p(T_O)}M_j$
1	750	612	1592	797	594	1311	700	627	1494
2	730	360	428	770	351	351	675	371	371
3[c]	726	1213	1213	770	1155	1155	676	1304	1304
4	750	240	624	800	233	570	700	246	586
5	726	1068	1132	771	1033	1033	680	1093	1321
6	400	357	0	450	348	0	380	359	0
7	750	353	469	798	343	819	700	363	865
8	727	140	157	770	137	137	670	144	98
9	749	171	359	797	166	366	698	176	395
10	748	228	452	796	221	643	697	234	494
11	650	178	8	700	173	18	600	182	9
Loop Total		4920	6434		4754	7777		5099	6937
$\overline{T}_j$	734°F(390°C)			781°F(416°C)			684°F(362°C)		

Section[b]	Run 23A ($T_O = 630°K$)			Run 24 ($T_O = 657°K$)			Run 25 ($T_O = 684°K$)		
	T_J (°F)	M_J	$\frac{k_P(T_J)}{k_P(T_O)}M_J$	T_J (°F)	M_J	$\frac{k_P(T_J)}{k_P(T_O)}M_J$	T_J (°F)	M_J	$\frac{k_P(T_J)}{k_P(T_O)}M_J$
1	702	626	1585	748	609	1354	798	593	1305
2	672	370	326	722	359	338	773	350	350
3[c]	675	1162	1162	724	1124	1124	773	1127	1127
4	700	246	586	750	239	562	800	232	538
5	680	1093	1321	722	1067	1006	770	1037	982
6	380	359	0	400	356	0	450	347	0
7	702	361	914	748	352	783	799	342	753
8	675	144	144	725	140	148	775	136	151
9	701	176	419	746	171	360	797	166	347
10	700	233	555	745	227	451	795	221	439
11	600	182	8	650	177	14	700	172	18
Loop Total		4952	7020		4821	6140		4723	6010
$\overline{T}_J$	685°F(363°C)			730°F(388°C)			781°F(416°C)		

Section[b]	Run 26 ($T_O = 630°K$)			Run 27 ($T_O = 662°K$)			Run 28 ($T_O = 690°K$)		
	T_j (°F)	M_j	$\dfrac{k_P(T_j)}{k_P(T_O)}M_j$	T_j (°F)	M_j	$\dfrac{k_P(T_j)}{k_P(T_O)}M_j$	T_j (°F)	M_j	$\dfrac{k_P(T_j)}{k_P(T_O)}M_j$
1	700	637	1517	750	618	1088	800	603	1015
2	673	377	354	730	364	344	780	356	338
3[c]	675	1282	1282	733	1296	1296	783	1217	1217
4	700	250	596	750	242	426	800	236	397
5	680	1114	1346	736	1076	1207	785	1049	1106
6	370	365	0	410	357	0	440	353	0
7	704	367	987	762	356	874	812	347	793
8	670	146	99	740	141	177	785	138	145
9	703	178	478	755	173	360	805	169	315
10	702	237	600	753	230	453	802	224	397
11	-	-	-	-	-	-	-	-	-
Loop Total		4925	7259		4853	6225		4692	5723
$\overline{T}_j$	685°F(363°C)			739°F(393°C)			790°F(421°C)		

[a] Assuming $\Delta E_{P,1} = 50$ kcal/mole

[b] See Table A2.9 for description of section

[c] Mass of coolant in Section 3 based on Surge Tank level averaged throughout the run

APPENDIX A3

CALCULATION OF DEGRADATION RESULTS AND STATISTICS

A3.1 General Degradation Rate Equation

From a terphenyl material balance as illustrated in the following diagram,
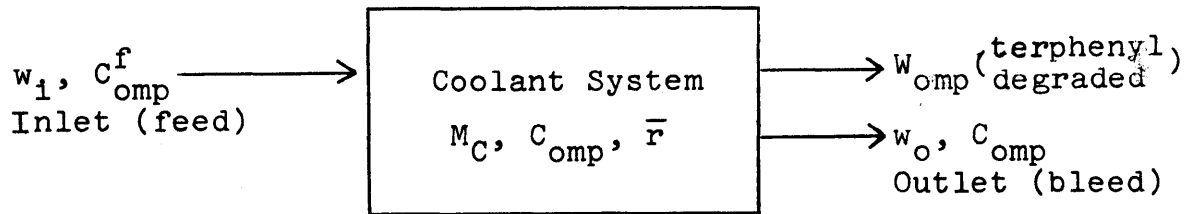
Mason, Timmins, et. al. (A3.1) arrive at the following general degradation rate equation,

$$\frac{d(M_C C_{omp})}{dt} = M_C(\frac{dC_{omp}}{dt}) + C_{omp}(\frac{dM_C}{dt}) \qquad (A3.1)$$

$$= w_i C^f_{omp} - w_o C_{omp} - W_{omp}$$

where

w_i = inlet coolant feed rate, gms/hr

w_o = outlet coolant bleed rate, gms/hr

C^f_{omp} = total terphenyl concentration in the feed, weight fraction

C_{omp} = total terphenyl concentration in the coolant system, weight fraction

W_{omp} = terphenyl degradation rate, gms/hr

M_C = total coolant mass, gms

According to the degradation model assumed here, W_{omp} can be expressed as

$$W_{omp} = [k_{R,omp,n} C_{omp}^n \left(\frac{d\tau}{dt}\right) + k_{p,omp,m} C_{omp}^m] M_C$$

$$\text{(A3.2)}$$

or in terms of a G value

$$\frac{W_{omp}}{\bar{r} M_C} = \frac{G(-omp)}{11.65} \quad \text{(gms/watt-hr)} \qquad \text{(A3.3)}$$

where

$G(-omp)$ = molecules of terphenyl degraded/100ev

11.65 = conversion factor, (molecules) (watt-hr)/ (gram)(100ev)

$\bar{r}$ = $\frac{d\tau}{dt}$ = average specific dose rate in M_C, watts/gm

τ = specific dose, watt-hr/gm

$\bar{r} M_C$ = rate of energy deposition in the total coolant, watts

Combining Equations (A3.1), (A3.2) and (A3.3) and neglecting small amount of terphenyl converted into gases, the general degradation rate equation is obtained as Equation (A3.4)

$$\frac{w_1}{\bar{r} M_C} (C_{omp}^f - C_{omp}) - \frac{dC_{omp}}{d\tau} = k_{R,omp,n} C_{omp}^n \qquad \text{(A3.4)}$$

$$+ \frac{k_{P,omp,m}}{\bar{r}} C_{omp}^m = \frac{G(-omp)}{11.65}$$

For steady-state runs, we have therefore

$$\frac{w_1}{\bar{r} M_C} (C_{omp}^f - C_{omp}) = k_{R,omp,n} C_{omp}^n \qquad \text{(A3.5)}$$

$$+ \frac{k_{P,omp,m}}{\bar{r}} C_{omp}^m = \frac{G(-omp)}{11.65}$$

For transient runs, we have therefore

$$-\left(\frac{dC_{omp}}{d\tau}\right) = k_{R,omp,n} C_{omp}^n + \frac{k_{P,omp,m}}{\bar{r}} C_{omp}^m \qquad \text{(A3.6)}$$

$$= \frac{G(-omp)}{11.65}$$

A3.2 Method of Calculating Degradation Rates for Steady-State Runs

A3.2.1 Calculation of G and G* Values

For steady-state runs at M.I.T., the G and G* values are determined as follows:

$$G(-i) = \frac{11.65W_i}{F\rho(MWH)} \quad \frac{\text{molecules of } i^{th} \text{ isomer degraded}}{100ev \text{ absorbed in total coolant}} \quad (A3.7)$$

$$G^*(-i) = \frac{G(i)}{C_i} \quad \frac{\text{molecules of } i^{th} \text{ isomer degraded}}{100ev \text{ absorbed in } i^{th} \text{ isomer}} \quad (A3.8)$$

where

$G(-i)$ = G value for the disappearance of total terphenyl, terphenyl isomer or for the production of HB

W_i = total mass of terphenyl or terphenyl isomer degraded, or HB produced, gms

F = total in-pile dose rate factor, watt-cc/MW-gm

ρ = density of coolant at irradiation temperature, gms/cc

(MWH) = length of steady-state irradiation, reactor megawatt-hours

C_i = average concentration of total terphenyl or terphenyl isomer, or HB, weight fraction

A3.2.2 Calculation of Total Mass Degraded

A schematic flow diagram of the organic coolant loop at M.I.T. during steady-state operation is shown in the following:
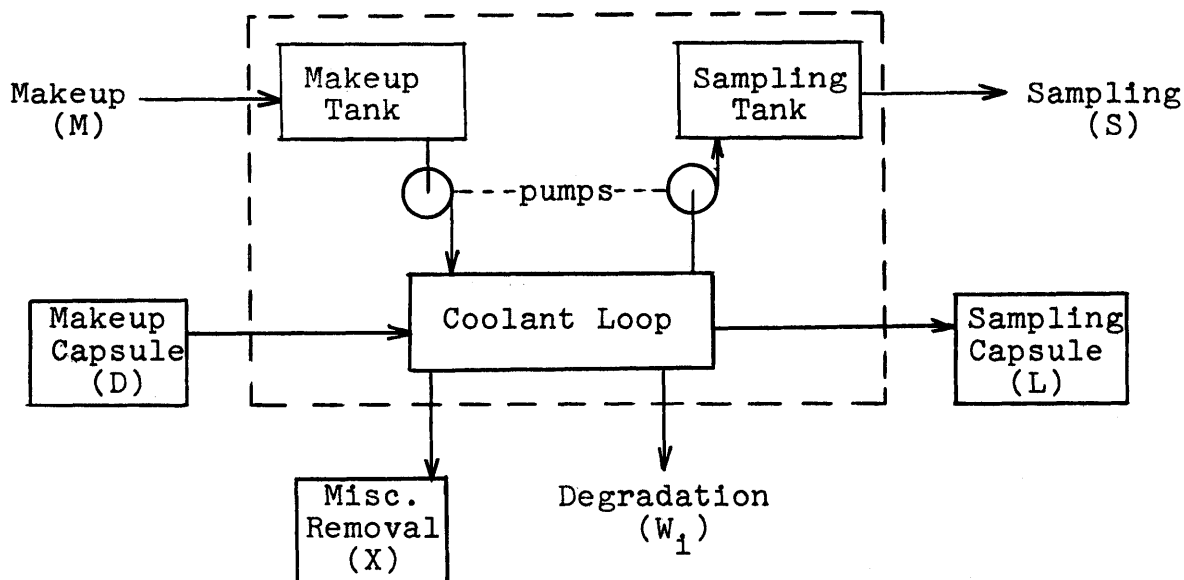
During steady-state operation, the circulating coolant was continuously removed by pumping into the Sampling Tank and was continuously replenished by processed terphenyl pumped from the Makeup Tank. When the Sampling Tank was nearly full, the contents were transferred in batches and distilled to remove the high boiler constituents. Fresh makeup terphenyl, approximately equal to the weight of high boiler removed, was added to the distillate and the distillate plus the fresh makeup was returned to the Makeup Tank. The pumping or processing rates of the makeup system and the sampling system were adjusted to obtain a desired terphenyl concentration and were set constant to insure steady-state condition after initial transients. The makeup processing rate was set generally at a slightly higher rate than the sampling processing rate by the adjustment of the pump stroke so that the coolant mass could be controlled by manual transfer from the loop to the Sampling Tank. Sampling Capsule (L) was used to sample coolant for the determination of coolant concentration at any given instant. Makeup Capsule (D) was used primarily for tritium dilution to determine the coolant mass. Miscellaneous sampling (X) consisted of sampling from the pumping system (e.g. degassing of the pump degasifiers) and losses or hold-ups

in the process of transfer to and from the Makeup and
Sampling tanks. Each coolant sample removed from the loop
and each returned to the loop was analyzed by vapor phase
chromatography (VPC) for the biphenyl, ortho, meta, and para
terphenyl concentrations. The concentration of high boiler
(HB) in the sample removed was determined by distillation.
The LIB concentration was then defined as (100 - %omp - %HB).

The total mass of terphenyl (or any terphenyl isomer)
degraded, or HB produced, was the sum of the net terphenyl
mass added (net transfer across the dashed lines of the sche-
matic flow diagram), or HB removed, and the change in the mass
(net accumulation within the system enclosed by the dashed
lines of the schematic flow diagram) of terphenyl, or HB, in
the system during the steady-state run. Making a terphenyl
balance around the dashed lines of the schematic flow diagram
between two specified times of a steady-state run, we have

$$\text{Total mass degraded } (W_i) = (\text{Net Transfer})_i + (\text{Net Accumulation}, \Delta_i)$$

$$(A3.9)$$

The net transfer is expressed by the following equation:

$$(\text{Net Transfer})_i = \sum_j M_j C_{M,i,j} + \sum_j D_j C_{D,i,j} \qquad (A3.10)$$

$$- \sum_j S_j C_{S,i,j} - \sum_j L_j C_{L,i,j} - \sum_j X_j C_{X,i,j}$$

where M_j, D_j, S_j, L_j and X_j denotes the mass of the jth sample
returned to the Makeup Tank, returned to the Makeup Capsule,
removed from the Sampling Tank, removed from the Sampling
Capsule, and removed from the loop respectively; and $C_{M,i,j}$,
$C_{D,i,j}$, $C_{S,i,j}$, $C_{L,i,j}$, and $C_{X,i,j}$ denotes concentration of
the ith component of M_j, D_j, S_j, L_j and X_j samples respec-
tively.

The change in mass in the system during the steady-
state run (the net accumulation) is expressed by the follow-
ing equation:

$$\Delta_i = \Delta_{M,i} + \Delta_{S,i} + \Delta_{C,i} \qquad (A3.11)$$

where

Δ_i = net accumulation

= (initial mass of ith component in the system)
- (final mass of ith component in the system)

$\Delta_{M,i}$ = (initial mass of ith component in the Makeup Tank) - (final mass of ith component in the Makeup Tank)

$\Delta_{S,i}$ = (initial mass of ith component in the Sampling Tank) - (final mass of ith component in the Sampling Tank)

$\Delta_{C,i}$ = (initial mass of ith component in the loop) - (final mass of ith component in the loop)

The accumulations in the Makeup Tank, Sampling Tank and the loop can be obtained by the following equations:

$$\Delta_{M,i} = (C_{M,i,1}J_{M,1} - C_{M,i,2}J_{M,2})k_M + (C_{M,i,1} - C_{M,i,2})H_M$$
(A3.12)

$$\Delta_{S,i} = (C_{S,i,1}J_{S,1} - C_{S,i,2}J_{S,2})k_S + (C_{S,i,1} - C_{S,i,2})H_S$$
(A3.13)

$$\Delta_{C,i} = C_{C,i,1}M_{C,1} - C_{C,i,2}M_{C,2}$$
(A3.14)

where

J_M = Makeup Tank level, inches

J_S = Sampling Tank level, inches

k_M = average Makeup Tank level calibration, gms/in

k_S = average Sampling Tank level calibration, gms/in

H_M = mass of coolant holdup below 0" Makeup Tank level, grams

H_S = mass of coolant holdup below 0" Sampling Tank level, grams

$C_{C,i}$ = concentration of the ith component of the coolant in the loop, weight fraction

M_C = mass of the circulating coolant in the loop, gms

and the subscripts "1" and "2" denote the initial and final conditions of the steady-state run.

Combining Equations (A3.11), (A3.12), (A3.13) and (A3.14), we obtain

$$\Delta_i = (C_{M,i,1}J_{M,1} - C_{M,i,2}J_{M,2})k_M \qquad (A3.15)$$

$$+ (C_{M,i,1} - C_{M,i,2})H_M + (C_{S,i,1}J_{S,1} - C_{S,i,2}J_{S,2})k_S$$

$$+ (C_{S,i,1} - C_{S,i,2})H_S + (C_{C,i,1}M_{C,1} - C_{C,i,2}M_{C,2})$$

Combining Equations (A3.9), (A3.10), and (A3.15), total mass of the ith component degraded is obtained in Equation (A3.16)

$$W_i = \sum_j M_j C_{M,i,j} + \sum_j D_j C_{D,i,j} - \sum_j S_j C_{S,i,j} \qquad (A3.16)$$

$$- \sum_j L_j C_{L,i,j} - \sum_j X_j C_{x,i,j} + (C_{M,i,1}J_{M,1} - C_{M,i,2}J_{M,2})k_M$$

$$+ (C_{M,i,1} - C_{M,i,2})H_M + (C_{S,i,1}J_{S,1} - C_{S,i,2}J_{S,2})k_S$$

$$+ (C_{S,i,1} - C_{S,i,2})H_S + (C_{C,i,1}M_{C,1} - C_{C,i,2}M_{C,2})$$

Equation (A3.16) is applicable even if the degradation process is not at steady-state.

Except for the concentration of the makeup, the concentrations of terphenyl used in Equation (A3.16) are calculated by a least-square fit of all vapor phase chromatograph (VPC) analyses for coolant samples removed from the loop during the steady-state portion of the run by the following equation:

$$C_{i,j} = a_i + b_i Y_j \qquad (A3.17)$$

where

$C_{i,j}$ = calculated concentration of the ith component of the jth sample determined by the least-square-error analysis

Y_j = accumulated megawatt-hours at which the jth sample was taken.

Computer program, MNDEG, developed by Sawyer and Mason (A3.2) had been used for the least-square fit for all the coolant samples removed from the loop during the steady-state run.

Since both the makeup and sampling pumps pumped only inter-
mittently and since fresh makeups added to the distillates
varied to some extent, small variation in concentration existed
between sampling. The calculated concentrations from the
least-square fit using Equation (A3.17) represented the best
estimates of the sample concentrations at any time during the
steady-state run. The HB concentration was also calculated
with the same type of least-square fit using Equation (A3.17).

As mentioned earlier in this section, fresh makeup,
approximately equal to the weight of high boiler removed,
was added to the distillate and the distillate plus the fresh
makeup was returned to the Makeup Tank. The relative pro-
portions of distillate and the fresh makeup varied to some
extent. Therefore no attempt had been made to apply a least-
square fit to the makeup concentrations. The average value
of at least four VPC analyses from at least two aliquots of
each makeup sample was used for the makeup concentration in
Equation (A3.16).

The level readings J_M and J_S represented gage-glass
readings on the Makeup and Sampling tanks. H_M and H_S repre-
sented total amount of holdup of coolant from 0" level of
the Makeup and Sampling tanks to the circulating loop.

The level calibrations k_M and k_S were determined from
the average of at least four transfers to the Makeup Tank
or from the Sampling Tank. At each transfer, the total amount
transferred was weighed and the change of gage-glass level
was recorded.

The loop circulating mass, M_C, was determined by means
of tritium dilution (see Appendix A2).

A3.3 Statistical Errors in G Values for Steady-State Runs

The statistical errors in the calculation of G values
according to Equation (A3.7) are due to uncertainties in the
mass of coolant degraded, W_i, the dose rate factor, F, the
density of the coolant, ρ and the length of steady-state

irradiation, (MWH). The variance of G can be written as

$$\frac{\sigma^2(G_i)}{G_i^2} = \frac{\sigma^2(W_i)}{W_i^2} + \frac{\sigma^2(F)}{F^2} + \frac{\sigma^2(\rho)}{\rho^2} + \frac{\sigma^2(MWH)}{(MWH)^2}$$

However, the uncertainties in ρ and (MWH) are negligible as compared to those of W_i and F. Therefore,

$$\frac{\sigma^2(G_i)}{G_i^2} \cong \frac{\sigma^2(W_i)}{W_i^2} + \frac{\sigma^2(F)}{F^2} \qquad (A3.18)$$

From Equation (A3.8), with uncertainties of concentrations to be much smaller than those of G, the variance of G* is then

$$\frac{\sigma^2(G_i^*)}{G_i^{*2}} = \frac{\sigma^2(G_i)}{G_i^2} + \frac{\sigma^2(C_i)}{C_i^2} \cong \frac{\sigma^2(G_i)}{G_i^2} \qquad (A3.19)$$

From Equation (A3.9), the variance in W_i may be expressed as

$$\sigma^2(W_i) = \sigma^2(\text{Net Transfer})_i + \sigma^2(\Delta_i) \qquad (A3.20)$$

Applying variance propagational rule (A3.3) to Equation (A3.10), the variance of the net transfer terms is expressed as

$$\sigma^2(\text{Net Transfer})_i = \sum_j M_j^2 \sigma^2(C_{M,i,j}) + \qquad (A3.21)$$

$$\sum_j C_{M,i,j}^2 \sigma^2(M_j) + \sum_j D_j^2 \sigma^2(C_{D,i,j})$$

$$+ \sum_j C_{D,i,j}^2 \sigma^2(D_j) + \sum_j S_j^2 \sigma^2(C_{S,i,j})$$

$$+ \sum_j C_{S,i,j}^2 \sigma^2(S_j) + \sum_j L_j^2 \sigma^2(C_{L,i,j}) + \sum_j C_{L,i,j}^2 \sigma^2(L_j)$$

$$+ \sum_j X_j^2 \sigma^2(C_{X,i,j}) + \sum_j C_{X,i,j}^2 \sigma^2(X_j)$$

From Equations (A3.11), (A3.12) and (A3.13) we have

$$\sigma^2(\Delta_i) = \sigma^2(\Delta_{M,i}) + \sigma^2(\Delta_{S,i}) + \sigma^2(\Delta_{C,i}) \qquad (A3.22)$$

$$\sigma^2(\Delta_{M,i}) = k_M^2 [C_{M,i,1}^2 \sigma^2(J_{M,1}) + J_{M,1}^2 \sigma^2(C_{M,i,1}) \quad (A3.23)$$

$$+ C_{M,i,2}^2 \sigma^2(J_{M,2}) + J_{M,2}^2 \sigma^2(C_{M,i,2})]$$

$$+ (C_{M,i,1} J_{M,1} - C_{M,i,2} J_{M,2})^2 \sigma^2(k_M)$$

$$+ H_M^2 [\sigma^2(C_{M,i,1}) + \sigma^2(C_{M,i,2})] + (C_{M,i,1} -$$

$$C_{M,i,2})^2 \sigma^2(H_M)$$

$$\sigma^2(\Delta_{S,i}) = k_S^2 [C_{S,i,1}^2 \sigma^2(J_{S,1}) + J_{S,1}^2 \sigma^2(C_{S,i,1}) \quad (A3.24)$$

$$+ C_{S,i,2}^2 \sigma^2(J_{S,2}) + J_{S,2}^2 \sigma^2(C_{S,i,2})]$$

$$+ (C_{S,i,1} J_{S,1} - C_{S,i,2} J_{S,2})^2 \sigma^2(k_S)$$

$$+ H_S^2 [\sigma^2(C_{S,i,1}) + \sigma^2(C_{S,i,2})]$$

$$+ (C_{S,i,1} - C_{S,i,2}) \sigma^2(H_S)$$

The variance of the accumulation term of loop mass, $\Delta_{C,i}$ is treated in a different way. The loop circulating mass was determined at one point during the steady-state run by means of tritium dilution method. The initial and final loop circulating mass, $M_{C,1}$, and $M_{C,2}$, were then calculated by means of a mass balance of the coolant in the system between that point and the initial and the final points. In other words, $M_{C,1}$ and $M_{C,2}$ were not completely independent. For this reason, the variance propagation rule cannot be applied directly here. Let

$M_{C,a}$ = loop circulating mass determined by some method (e.g. tritium dilution) at a certain time, a, during the steady-state run.

$\sigma(M_{C,a})$ = standard deviation of loop circulating mass as determined at time a.

$\delta_{1,a}$ = net change of coolant in the loop between the initial time and time a.

$\delta_{2,a}$ = net change of coolant in the loop between the final time and time a.

Therefore

$$M_{C,1} = M_{C,a} + \delta_{1,a} \tag{A3.25}$$

$$M_{C,2} = M_{C,a} + \delta_{2,a} \tag{A3.26}$$

Substituting Equations (A3.25) and (A3.26) into (A3.14),

$$\Delta_{C,i} = C_{C,i,1}(M_{C,a} + \delta_{1,a}) - C_{C,i,2}(M_{C,a} + \delta_{2,a}) \tag{A3.27}$$

Since $C_{C,i,1}$, $C_{C,i,2}$, $M_{C,a}$, $\delta_{1,a}$ and $\delta_{2,a}$ are now all independent of each other, the variance propagational rule (A3.3) can be applied to Equation (A3.27) to calculate the variance of the net accumulation term, $\sigma^2(\Delta_{C,i})$.

$$\sigma^2(\Delta_{C,i}) = (M_{C,a} + \delta_{1,a})^2 \sigma^2(C_{C,i,1}) \tag{A3.28}$$

$$+ (M_{C,a} + \delta_{2,a})^2 \sigma^2(C_{C,i,2})$$

$$+ (C_{C,i,1} - C_{C,i,2})^2 \sigma^2(M_{C,a})$$

$$+ C_{C,i,1}^2 \sigma^2(\delta_{1,a}) - C_{C,i,2}^2 \sigma^2(\delta_{2,a})$$

The last two terms involving $\sigma^2(\delta_{1,a})$ and $\sigma^2(\delta_{2,a})$ were found to be negligible compared to the other terms, and Equation (A3.28) becomes

$$\sigma^2(\Delta_{C,i}) = M_{C,1}^2 \sigma^2(C_{C,i,1}) + M_{C,2}^2 \sigma^2(C_{C,i,2}) \tag{A3.29}$$

$$+ (C_{C,i,1} - C_{C,i,2})^2 \sigma^2(M_{C,a})$$

From Equations (A3.22), (A3.23), (A3.24) and (A3.29) the variance of the accumulation term in Equation (A3.20) can now be expressed as

$$\sigma^2(\Delta_i) = k_M^2[C_{M,i,1}^2\sigma^2(J_{M,1}) + J_{M,1}^2\sigma^2(C_{M,i,1}) \qquad (A3.30)$$

$$+ C_{M,i,2}^2\sigma^2(J_{M,2}) + J_{M,2}^2\sigma^2(C_{M,i,2})]$$

$$+ (C_{M,i,1}J_{M,1} - C_{M,i,2}J_{M,2})^2\sigma^2(k_M)$$

$$+ H_M^2[\sigma^2(C_{M,i,1}) + \sigma^2(C_{M,i,2})]$$

$$+ (C_{M,i,1} - C_{M,i,2})^2\sigma^2(H_M)$$

$$+ k_S^2[C_{S,i,1}^2\sigma^2(J_{S,1}) + J_{S,1}^2\sigma^2(C_{S,i,1})$$

$$+ C_{S,i,2}^2\sigma^2(J_{S,2}) + J_{S,2}^2\sigma^2(C_{S,i,2})]$$

$$+ (C_{S,i,1}J_{S,1} - C_{S,i,2}J_{S,2})^2\sigma^2(k_S)$$

$$+ H_S^2[\sigma^2(C_{S,i,1}) + \sigma^2(C_{S,i,2})]$$

$$+ (C_{S,i,1} - C_{S,i,2})^2\sigma^2(H_S)$$

$$+ M_{C,1}^2\sigma^2(C_{C,i,1}) + M_{C,2}^2\sigma^2(C_{C,i,2})$$

$$+ (C_{C,i,1} - C_{C,i,2})^2\sigma^2(M_{C,a})$$

According to Equation (A3.20), the variance in W_i is then the sum of all the terms as expressed in Equation (A3.21) and Equation (A3.30).

The methods for determining the variance of each of the parameters of Equations (A3.21) and (A3.30) will now be discussed.

The variance of concentration of the jth sample returned to the loop, $\sigma(C_{M,i,j})$ was calculated as

$$\sigma^2(C_{M,i,j}) = \frac{\sum_{j=1}^{N}(C_{M,i,j} - \bar{C}_{M,i,j})^2}{N(N - 1)} \qquad (A3.31)$$

where N is the number of VPC chromatographic analyses made on the jth sample.

In Section A3.2.2, it was noted that the best values of the coolant concentration, namely $C_{S,i,j}$ and $C_{C,i,j}$ (or $C_{L,i,j}$) were determined by a least-square fit of the chromatographic analyses of the coolant samples. Earlier M.I.T. reports (A3.1, A3.2) described a computer program, MNDEG, which had been used for the least-square error analysis of the coolant sample removed from the loop. The concentration variance, $\sigma^2(C_{i,j})$, for either the Sampling Tank or the loop, was approximated by the expression

$$\sigma^2(C_{i,j}) = \sigma^2(a_i) + Y_j(Y_j - 2\overline{Y})\sigma^2(b_i) \qquad (A3.32)$$

where

$C_{i,j}$ = calculated concentration of the ith component of the jth sample determined by the least-square fit, weight fraction.

$\sigma^2(a_i)$ = variance of the intercept, a_i, (refer to Equation (A3.17)).

$\sigma^2(b_i)$ = variance of the slope, b_i, (refer to Equation (A3.17)).

Y_j = accumulated megawatt-hours at which the jth sample was taken

$\overline{Y}$ = weighted mean of the Y_j values.

The weighted mean of the Y_j values was calculated as

$$\overline{Y} = \frac{\sum W_{i,j} Y_j}{W_{i,j}} \qquad (A3.33)$$

where $W_{i,j}$ is the weighting factor for each data point taken to be the reciprocal of the variance of the measured concentration of the jth sample from the least-square calculated concentration

$$W_{i,j} = \frac{1}{\sigma^2(c_{i,j})} \qquad (A3.34)$$

where

$c_{i,j}$ = measured concentration of the ith component of the jth sample at Y_j

$\sigma^2(c_{i,j})$ is calculated as

$$\sigma^2(c_{i,j}) = \frac{\sum\limits_{j=1}^{j=N}(C_{i,j} - c_{i,j})^2}{N - 2} \qquad (A3.35)$$

where

N is the number of separate chromatographic analyses of the jth sample.

The computer program, MNDEG, determined the constants a_i, b_i, $\sigma(a_i)$, $\sigma(b_i)$, $\overline{Y}$ and the 95% confidence limits on $C_{i,j}$ calculated with the aid of Student's t for (N - 2) degrees of freedom (A3.4).

Both the Makeup Tank and the Sampling Tank had gage-glasses graduated to the smallest division of one-eighth of an inch. Therefore the standard deviations in gage-glass reading, namely $\sigma(J_M)$ and $\sigma(J_S)$ in Equation (A3.30) were assumed to be one-sixteenth of an inch. The standard deviations in gage-glass calibration, namely $\sigma(k_M)$ and $\sigma(k_S)$ in Equation (A3.30) were calculated as the standard deviation of all the experimentally determined gage-glass calibrations from the average value as shown by the following Equation

$$\sigma^2(k) = \frac{\sum\limits_{j=1}^{j=Q}(k_j - \overline{k})^2}{Q(Q - 1)} \qquad (A3.36)$$

where

k_j is the gage-glass level calibration of the jth sample in gms/in (the weight of the jth sample transferred divided by the change of levels on the gage-glass)

$\overline{k}$ is the average of k_j

Q is the number of batches transferred during the steady-state run.

The loop circulating mass M_C and the variance $\sigma^2(M_C)$ were determined by tritium dilution method as discussed in Appendix A2.

For the uncertainty in weighing the amount of organic coolant transferred, the following errors were estimated. For large batches of transfer such as the transfer to the Makeup Tank and from the Sampling Tank in the amount of about 3000 gram per transfer, a balance graduated to the smallest scale of 1 gram was used. A weighing error of $\pm$ 3 grams was assumed for each weighing of the Transfer Tank. An error of $\pm$ 5 grams was assumed for the net amount of coolant transferred which was obtained from the difference in weights of the Transfer Tank before and after transferring. For the capsules (D and L), an error of ± 0.5 grams was assumed using a balance graduated to the smallest division of one-tenth of a gram. For the miscellaneous sample (X), an error of $\pm$ 2 grams was assumed. For the coolant holdups (H_M and H_S), an error of $\pm$ 10 grams was assumed.

A3.4 Estimation of Statistical Error During a Steady-State Irradiation

A knowledge of the statistical error of the amount of total coolant degraded (W_T) in a steady-state run is essential since this will determine the length of the run in order to obtain data of significance.

The following calculations give a close estimation of the standard deviation of W_{omp} for the length of steady-state run expressed in terms of the number of batches of coolant processed through the Makeup Tank or the Sampling Tank.

The values tabulated below are used in Equations (A3.21) and (A3.30) for this calculation. These values are typical for the Santowax OM irradiation between November 1966 and

July 1967. Subscripts "i" will be left out since only total
terphenyl will be dealt with.

Makeup Tank (M): M_j = 3000 gm/batch, $\sigma(M_j)$ = 5 gm

$\overline{C}_{M,j}$ = 0.90

$C_{M,1}$ = 0.91, $C_{M,2}$ = 0.89

J_M = 10 inches, $\sigma(J_M)$ = 1/16 inch

k_M = 220 gm/inch, $\sigma(k_M)$ = 1 gm/inch

H_M = 550 gm, $\sigma(H_M)$ = 10 gm.

Sampling Tank (S): S_j = 3000 gm/batch, $\sigma(S_j)$ = 5 gm

$\overline{C}_{S,j}$ = 0.80, $\sigma(C_{S,j})$ = 10^{-3}

$C_{S,1}$ = 0.81, $C_{S,2}$ = 0.79

J_S = 10 inches, $\sigma(J_S)$ = 1/16 inch

k_S = 220 g/inch, $\sigma(k_S)$ = 1 gm/inch

H_S = 550 gm, $\sigma(H_S)$ = 10 gm

Loop: $M_{C,1}$ = 5000 gm, $M_{C,2}$ = 4900 gm

$\sigma(M_C)$ = 150 gm

$C_{C,1}$ = 0.81, $C_{C,2}$ = 0.79

$\sigma(C_C)$ = 10^{-3}

Makeup Capsule (D): D = 20 gm/capsule, $\sigma(D)$ = 0.5 gm

C_D = 0.90, $\sigma(C_D)$ = 10^{-3}

Sampling Capsule (L): L = 20 gm/capsule, $\sigma(L)$ = 0.5 gm

C_L = 0.80, $\sigma(C_L)$ = 10^{-3}

Miscellaneous Sampling (X): X_j = 40 gm, $\sigma(X_j)$ = 2 gm

C_X = 0.80, $\sigma(C_{X,j})$ = 10^{-3}

Two values of $\sigma(M_j)$ are used, namely 3×10^{-3} and 10^{-3}
which bracket the standard deviation from at least four VPC
analyses of the concentration of the processed coolant that
is returned to the loop. Table A3.1 presents the variance of
the "net transfer" term of Equation (A3.21) per 3000 gram
batch of transfer of both the Makeup and Sampling tanks, and
Table A3.2 presents that of the "net accumulation" term of
Equation (A3.30).

Table A3.1

Variance of Net Transfer per
3000 gm Batch Processed

	Variance of Net Transfer σ^2(Net Transfer), $(\text{grams})^2$	
	$\sigma(C_M) = 3 \times 10^{-3}$	$\sigma(C_M) = 10^{-3}$
$M^2\sigma^2(C_M)$	81	9
$C_M^2\sigma^2(M)$	20	20
$S^2\sigma^2(C_S)$	9	9
$C_S^2\sigma^2(S)$	16	16
$D^2\sigma^2(C_D)$	~ 0	~ 0
$C_D^2\sigma^2(D)$	~ 0	~ 0
$L^2\sigma^2(C_L)$	~ 0	~ 0
$C_L^2\sigma^2(L)$	~ 0	~ 0
$X^2\sigma^2(C_X)$	~ 0	~ 0
$C_X^2\sigma^2(X)$	3	3
σ^2(Net Transfer)/Batch	129	57

Table A3.2

Variance of Net Accumulation

	Variance of Net Accumulation $\sigma^2(\Delta)$, (grams)^2	
	$\sigma(C_M) = 3 \times 10^{-3}$	$\sigma(C_M) = 10^{-3}$
Δ_M:		
$k_M^2 C_{M,1}^2 \sigma^2(J_M)$	157	157
$k_M^2 J_M^2 \sigma^2(C_{M,1})$	44	5
$k_M^2 C_{M,2}^2 \sigma^2(J_M)$	150	150
$k_M^2 J_M^2 \sigma^2(C_{M,2})$	44	5
$(C_{M,1}J_M - C_{M,2}J_M)^2 \sigma^2(k_M)$	~0	~0
$H_M^2[\sigma^2(C_{M,1}) + \sigma^2(C_{M,2})]$	5	1
$(C_{M,1} - C_{M,2})^2 \sigma^2(H_M)$	~0	~0
Δ_S:		
$k_S^2 C_{S,1}^2 \sigma^2(J_S)$	124	124
$k_S^2 J_S^2 \sigma^2(C_{S,1})$	5	5
$k_S^2 C_{S,2}^2 \sigma^2(J_S)$	118	118
$k_S^2 J_S^2 \sigma^2(C_{S,2})$	5	5
$(C_{S,1}J_S - C_{S,2}J_S)\sigma^2(k_S)$	~0	~0
$H_S^2[\sigma^2(C_{S,1}) + \sigma^2(C_{S,2})]$	1	1
$(C_{S,1} - C_{S,2})^2 \sigma^2(H_S)$	~0	~0
Δ_C:		
$M_{C,1}^2 \sigma(C_{C,1})^2$	25	25
$M_{C,2}^2 \sigma^2(C_{C,2})^2$	24	24
$(C_{C,1} - C_{C,2})^2 \sigma^2(M_C)$	9	9
$\sigma^2(\Delta)$	711	629

For Santowax OM irradiations between 572° F and 800° F at approximately 80% loop coolant concentration, the processed coolant returned to the loop varied approximately between 87% and 90%. Thus the average amount of degradation of the total terphenyl was about 240 grams per 3000 gram batch of transfer. For Q batches of transfer during a steady-state run, the total degradation is then 240Q grams. The variance of the net transfer term (Table A3.1) also increases with the number of batches processed, whereas the variance of the net accumulation term is independent of the number of batches. We have therefore:

for $\sigma(C_M) = 3 \times 10^{-3}$ (A3.37)

$$\sigma^2(W_{omp}) = 129Q + 711 \quad \text{gram}^2$$

for $\sigma(C_M) = 10^{-3}$ (A3.38)

$$\sigma^2(W_{omp}) = 57Q + 629 \quad \text{gram}^2$$

Table A3.3 shows the percentage standard error of the total terphenyl degraded for different lengths of irradiation period expressed in terms of the number of 3000 gram batches processed. It is noted that at least eight batches of 3000 gram coolant must be processed in order to obtain a standard error of about 2%.

Table A3.3

Percentage Standard Error of Total Terphenyl
Degraded Per Number of Batches Processed

No. of Batches (Q)	Total Terphenyl Degraded (W_{omp})	Percentage Standard Error, %	
		$\sigma(C_M) = 3 \times 10^{-3}$	$\sigma(C_M) = 10^{-3}$
1	240	12.0	10.9
2	480	6.5	5.7
3	720	4.6	3.9
4	960	3.6	3.1
5	1200	3.1	2.5
6	1440	2.7	2.2
7	1680	2.4	1.9
8	1920	2.2	1.7
9	2160	2.0	1.6
10	2400	1.9	1.4

A3.5 Degradation Rates Measured in Fuel Position 1

The terphenyl degradation rates of both Santowax OM and Santowax WR during the period covered by this report are presented in this section using the calculation methods as described in Sections A3.2 and Section A3.3. A summary of the irradiation conditions and experimental results is shown in Table A3.4.

Figures A3.1 through A3.12 show the terphenyl and HB concentration as a function of irradiation time (MWH) for the steady-state period of each run.

Tables A3.5 through A3.16 show for each run:

(1) a summary of irradiation and pertinent chromatography results, and

(2) the values of G and G* and the statistics.

Table A3.4

Summary of Irradiation Conditions and Experimental Results
of Steady-State Run at Fuel Position 1

Dec. 19, 1966 to Feb. 16, 1968

Run No.	Irrad. Temp. (Coolant)	Average Dose_Rate r (watts/gm)	Concentration - w/o					$G(-1)$ or $G(\to HB)$ molecules/100ev					$G^*(-1) = G(-1)/C_1$				LIB/HB	f_N
			C_o	C_m	C_p	C_{omp}	HB	$G(-o)$	$G(-m)$	$G(-p)$	$G(-omp)$	$G(HB)$	$G^*(-o)$	$G^*(-m)$	$G^*(-p)$	$G^*(-omp)$		
19A	572°F (SW-OM)	0.060	41.5	20.1	1.5	63.1	26.4	0.122	0.054	0.003	0.178	0.160	0.293	0.266	0.183	0.282	0.40	0.36
20A	572°F (SW-OM)	0.065	57.7	26.6	1.8	86.1	6.1	0.207	0.094	0.005	0.307	0.232	0.359	0.354	0.297	0.357	1.28	0.36
20B	572°F (SW-OM)	0.061	53.1	25.6	1.8	80.5	8.5	0.193	0.074	0.003	0.270	0.205	0.363	0.290	0.180	0.336	1.29	0.36
21	750°F (SW-OM)	0.024	50.6	25.5	1.9	78.0	9.0	0.351	0.124	0.001	0.476	0.405	0.694	0.487	0.046	0.611	1.44	0.36
22	800°F (SW-OM)	0.023	50.3	26.2	2.0	78.5	8.9	0.846	0.287	0.020	1.153	0.674	1.683	1.094	0.990	1.469	1.42	0.36
23	700°F (SW-OM)	0.022	51.4	26.9	2.3	80.6	7.7	0.271	0.083	0.003	0.357	0.348	0.524	0.311	0.149	0.443	1.52	0.36
23A	700°F (SW-OM)	0.057	52.0	27.3	2.5	81.8	6.5	0.230	0.093	0.003	0.326	0.298	0.440	0.342	0.112	0.398	1.77	0.36
24	750°F (SW-OM)	0.057	50.6	27.5	2.6	80.6	7.1	0.255	0.115	0.005	0.376	0.349	0.508	0.420	0.213	0.468	1.78	0.36
25	800°F (SW-OM)	0.056	46.5	26.8	2.7	76.0	7.7	0.470	0.195	0.013	0.678	0.553	1.013	0.728	0.479	0.893	2.12	0.36
26	700°F (SW-WR)	0.068	14.0	61.9	6.6	82.5	9.1	0.065	0.245	0.018	0.328	0.289	0.463	0.396	0.266	0.397	0.92	0.38
27	750°F (SW-WR)	0.065	12.4	60.4	6.5	79.3	8.2	0.076	0.294	0.020	0.389	0.324	0.608	0.487	0.302	0.491	1.52	0.38
28	800°F (SW-WR)	0.065	11.1	59.2	6.1	76.3	10.6	0.121	0.484	0.031	0.636	0.584	1.094	0.818	0.515	0.834	1.24	0.38

FIGURE A3.I   TERPHENYL AND HIGH BOILER CONCENTRATION
DURING RUN 19A AT 572°F (300°C)

Summary of Irradiation of Santowax OM - Run 19A

Sample No.	Sample Wt. (gram)	Accum. Run Time (MWH)	Terphenyl Concentration - w/o				Concentration Variance x10^8				HB w/o	σ^2(HB)x10^8
			O	M	P	OMP	σ^2(O)	σ^2(M)	σ^2(P)	σ^2(OMP)		
L-1	305	0	42.4	20.2	1.5	64.1	158	86	12	256	24.5	1935
L-2	301	92	41.5	20.5	1.6	63.6	125	69	10	204	27.2	1528
L-3	314	175	41.2	20.0	1.6	62.8	101	56	8	165	27.2	1231
L-4	301	258	40.8	20.0	1.7	62.5	82	45	6	133	27.2	965
L-5	307	342	41.4	20.4	1.7	63.5	67	37	5	109	27.2	768
L-6	307	428	41.6	20.3	1.5	63.4	57	31	4	93	26.9	627
L-7	311	508	41.3	19.8	1.5	62.6	52	28	4	84	26.6	542
L-8	303	594	41.6	20.0	1.7	63.2	52	28	4	83	26.4	512
L-9	313	682	41.2	19.8	1.6	62.6	57	30	4	91	26.4	548
L-10	308	761	41.6	20.2	1.5	63.3	66	35	4	105	26.0	627
L-11	311	855	41.9	20.4	1.5	63.8	83	43	5	131	25.5	792
L-12	305	928	41.7	20.4	1.4	63.5	99	52	7	158	26.0	968
L-13	309	1010	41.4	20.3	1.6	63.3	123	64	8	195	26.2	1231
L-14	311	1093	41.4	20.3	1.5	63.2	151	79	10	240	26.7	1525
L-15	308	1176	41.3	20.0	1.6	62.9	184	96	12	293	26.7	1891
D-2	304	12	60.2	29.3	2.1	91.6	396	31	3	430	0	
D-3	346	117	63.8	29.7	2.0	95.5	171	160	4	335	0	
D-4	297	228	62.0	29.1	1.9	93.0	218	61	11	289	0	
D-5	311	261	63.8	29.7	2.0	95.5	171	160	4	335	0	
D-6	245	345	61.3	28.3	1.9	91.5	393	144	1	438	0	
D-7	299	507	62.0	29.1	1.8	92.9	381	78	2	460	0	
D-8	312	520	61.6	28.4	1.9	91.9	157	175	4	336	0	
D-9	306	597	61.1	28.5	2.0	91.7	84	48	12	144	0	
D-10	319	742	61.9	29.4	2.1	93.4	155	248	14	417	0	
D-11	341	826	61.2	29.0	2.2	92.4	805	78	3	885	0	
D-12	324	826	61.2	29.0	2.2	92.4	805	78	3	885	0	
D-13	308	938	60.6	28.7	2.2	91.5	364	140	8	512	0	
D-14	315	1024	60.3	28.9	2.2	91.3	284	100	6	391	0	
D-15	307	1140	59.5	28.4	2.2	90.1	554	123	4	682	0	
D-16	302	1257	59.5	28.3	2.2	90.0	375	38	11	424	0	

Note: (1) Concentrations and Variances of L Sample were calculated from least-square analysis

Table A3.5b

Degradation Rate Calculation

Run No. __19A__

Santowax OM

Summary:

Date: From___12/9/66___   To___12/30/66___

Irradiation Temp.___572___ °F   Type of Distillation___HB___

Terphenyl Concentration _63.1_ w/o   HB Concentration ___0.40___ w/o

Terphenyl Degraded___1369___ gms   LIB/HB___0.40___

Averaged Dose Rate, $\bar{r}$___0.060___Watts/gm

Density, ρ___0.911___gms/cc   Length of Run___1257___MWH

In Pile Dose Rate Factor, F_T^{SW}___78.2___Watt-cc/MW-gm

Reactor Power___4.88___MW   Fast Neutron Fraction, f_N_0.36_

G(-omp)___0.178___ $\sigma(G)$___0.006___

Calculation of G:

	Total Coolant	$O-\emptyset_3$	$M-\emptyset_3$	$P-\emptyset_3$	omp	HB
1. Coolant Sample (L)						
(a) Avg. Conc.	1.000	0.415	0.201	0.015	0.631	0.264
(b) Grams Removed	4615	1914	925	71	2914	1217
2. Sample Tank (S)						
Tank Calib. (k_S) =	gm/in					
(a) Avg. Conc.						
(b) Grams Removed	0					
3. Misc. Removals (X)						
(a) Avg. Conc.						
(b) Grams Removed	0					
4. Makeup Sample (D)						
(a) Avg. Conc.	1.000	0.613	0.289	0.021	0.923	0
(b) Grams Removed	4636	2844	1342	95	4281	0

Degradation Rate Calculation, Cont'd.

	Total Coolant	$O\text{-}\emptyset_3$	$M\text{-}\emptyset_3$	$P\text{-}\emptyset_3$	omp	HB
5. Makeup Tank (M) Tank Calib. $(k_M) =$ gm/in						
(a) Avg. Conc.						
(b) Grams Returned	0					
6. Net Transferred (5.+4.-3.-2.-1.)	21	930	413	24	1367	-1217
7. Initial Conc.						
(a) Coolant		0.416	0.202	0.015	0.633	0.263
(b) Sample Tank						
(c) Makeup Tank						
8. Initial Mass						
(a) Coolant	5748	2391	1159	87	3637	1512
(b) Sample Tank	0					
(c) Makeup Tank	0					
9. Final Conc.						
(a) Coolant		0.414	0.201	0.015	0.630	0.264
(b) Sample Tank						
(c) Makeup Tank						
10. Final Mass						
(a) Coolant	5769	2387	1159	89	3635	1524
(b) Sample Tank	0					
(c) Makeup Tank	0					
11. Δ Correction (8.-10.)						
(a) Coolant	-21	4	0	-2	2	-12
(b) Sample Tank	0					
(c) Makeup Tank	0					
(d) Total Δ Corr.	-21	4	0	-2	2	-12
12. Total Mass Degraded, W (6.+11.(d))	0	934	413	22	1369	-1229
13. G(-omp), G(-i), G(HB)		0.122	0.054	0.003	0.178	0.160
14. G*(-omp) = G(-omp)/C, G*(-i) = G(-i)/C$_1$		0.293	0.266	0.183	0.282	----

Degradation Rate Calculation, Cont'd.

Statistics of G Calculation:

$(MWH)_1 = $ _____0_____ , $(MWH)_2 = $ _____1257_____

$\sigma(F)/F = $ _____0.03_____

	$O-\emptyset_3$	$M-\emptyset_3$	$P-\emptyset_3$	omp	HB
15. Intercept, a_i	0.416	0.202	0.015	0.634	0.263
16. Slope, b_i x 10^5	-0.200	-0.058	0.029	-0.249	0.102
17. $\sigma(a_i)$ x 10^2	0.126	0.093	0.035	0.190	0.440
18. $\sigma(b_i)$ x 10^5	0.185	0.136	0.051	0.275	0.636
19. $\sigma^2(C_{initial})$ x 10^8					
(a) Coolant	158	86	12	256	1935
(b) Sample Tank					
(c) Makeup Tank (Return)	396	31	3	430	----
20. $\sigma^2(C_{final})$ x 10^8					
(a) Coolant	184	96	12	293	1891
(b) Sample Tank					
(c) Makeup Tank (Return)	375	38	11	424	----
21. $\sigma^2(\Delta$ Correction)					
(a) Coolant	114	61	8	182	1268
(b) Sample Tank					
(c) Makeup Tank					
(d) Total	114	61	8	182	1268
22. $\sigma^2($Net Transfer)					
(a) Loop (D,L and X)	4	1	0	8	16
(b) Sample Tank					
(c) Makeup Tank					
(d) Total	4	1	0	8	16
23. $\sigma(W)/W$	0.012	0.020	0.133	0.011	0.029
24. $\sigma(G)/G$	0.032	0.036	0.137	0.032	0.042
25. $\sigma(G)$	0.004	0.002	0.001	0.006	0.007
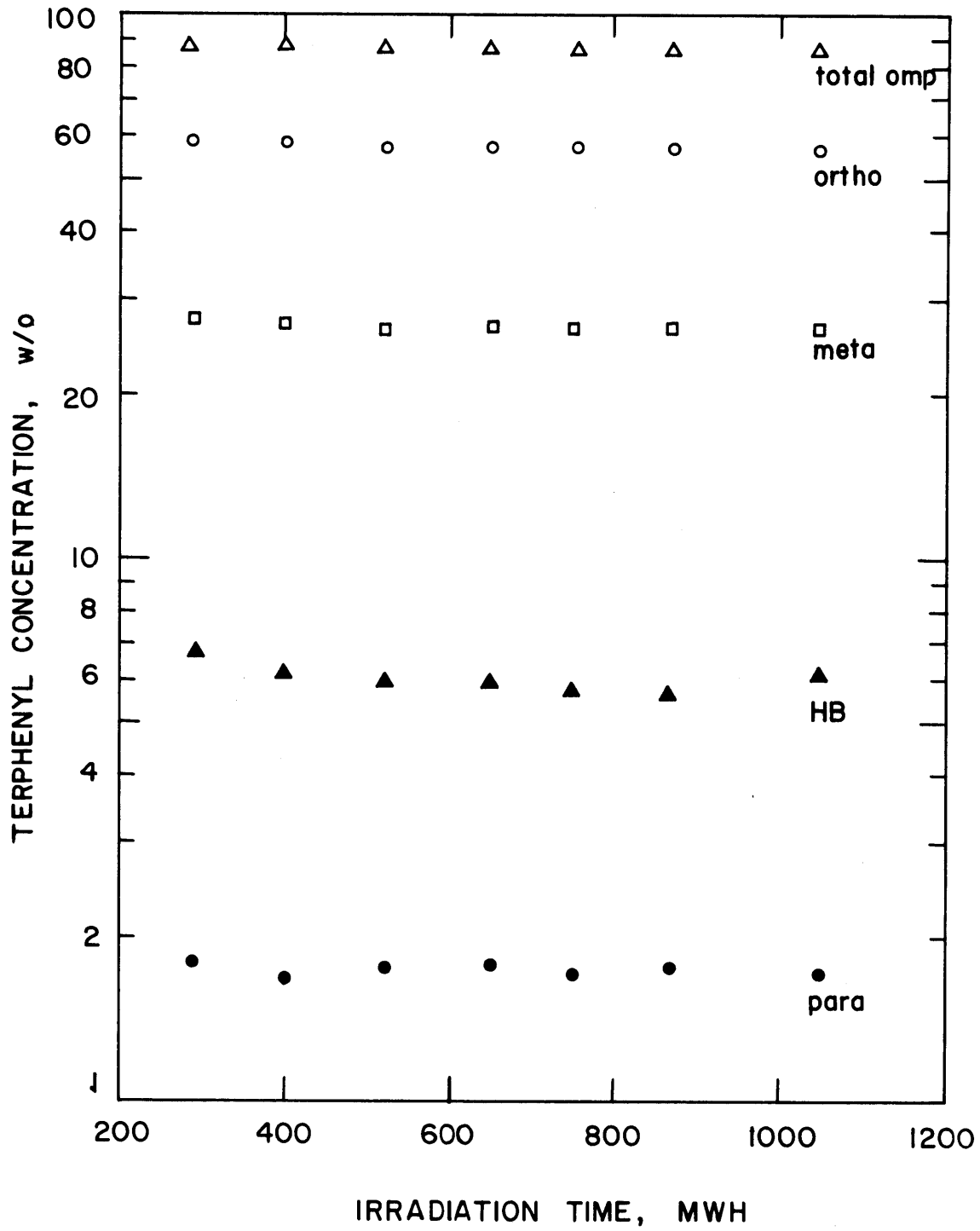
FIGURE A3.2   TERPHENYL AND HIGH BOILER CONCENTRATION
DURING RUN 20A AT 572°F (300°C)

Table A3.6a

Summary of Irradiation of Santowax OM - Run 20A

Sample No.	Sample Wt. (gram)	Accum. Run Time (MWH)	Terphenyl Concentration - w/o				Concentration Variance x10^8				HB w/o	σ^2(HB)x10^8
			O	M	P	OMP	σ^2(O)	σ^2(M)	σ^2(P)	σ^2(OMP)		
S-5	3284	283	58.8	27.1	1.8	87.7	184	71	3	310	6.3	308
S-6	2962	400	58.5	26.9	1.8	87.2	118	45	2	199	6.2	200
S-7	3059	518	58.1	26.8	1.8	86.7	78	31	1	131	6.1	130
S-8	2684	644	57.7	26.6	1.8	86.1	64	27	1	108	6.1	98
S-9	2530	756	57.3	26.4	1.8	85.5	77	34	1	130	6.0	107
S-10	2433	870	57.0	26.3	1.7	85.0	115	52	2	193	5.9	153
S-11	3123	1042	56.4	26.0	1.7	84.1	217	97	4	366	5.9	326
M-5A	592	175	64.5	29.5	1.8	95.8	297	51	1	348	0	
M-6	3764	269	61.1	29.2	1.8	92.1	119	249	3	370	0	
M-7	3357	408	61.8	29.1	1.9	92.8	1047	101	5	1153	0	
M-8	2860	548	62.3	29.0	1.9	93.2	769	75	10	854	0	
M-9	3302	663	61.1	28.7	1.9	91.7	527	226	17	769	0	
M-10	2548	780	62.1	28.4	1.8	92.3	698	24	5	727	0	
M-11	2539	891	61.1	28.7	2.0	91.8	514	21	1	535	0	
M-12	2508	1006	60.0	28.6	2.0	90.6	33	127	2	162	0	
L-2	19	404	58.1	26.9	1.8	86.8	23	11	2	36	6.2	200
L-3	18	775	56.6	26.2	1.8	84.6	89	225	9	323	6.0	107
X-1	556	670	57.7	26.6	1.8	86.1	72	40	1	150	6.1	130

Note: (1) Concentrations and Variances of S Samples were calculated from least square analysis

(2) Makeup Tank Calibration = 216.9 ± 0.7 gms/in; Sample Tank Calibration = 219.8 ± 1.6 gms/in

Table A3.6b

Degradation Rate Calculation

Run No. __20A__

Santowax OM

Summary:

Date: From ___1/10/67___   To ___1/24/67___

Irradiation Temp.___572___ °F   Type of Distillation___HB___

Terphenyl Concentration_86.1_ w/o   HB Concentration ___6.1___ w/o

Terphenyl Degraded___1711___ gms   LIB/HB ___1.28___

Averaged Dose Rate, $\bar{r}$ ___0.065___ Watts/gm

Density, ρ ___0.878___ gms/cc   Length of Run___964___ MWH

In Pile Dose Rate Factor, F_T^{SW} ___76.8___ Watt-cc/MW-gm

Reactor Power___4.86___ MW   Fast Neutron Fraction, f_N _0.36_

G(-omp)___0.307___ $\sigma(G)$ ___0.012___

Calculation of G:

	Total Coolant	$O-\emptyset_3$	$M-\emptyset_3$	$P-\emptyset_3$	omp	HB
1. Coolant Sample (L)						
(a) Avg. Conc.	1.000	0.574	0.265	0.018	0.858	0.061
(b) Grams Removed	37	21	10	1	32	2
2. Sample Tank (S)						
Tank Calib. (k_S) =	219.8gm/in					
(a) Avg. Conc.	1.000	0.577	0.266	0.018	0.861	0.061
(b) Grams Removed	20075	11587	5341	351	17279	1218
3. Misc. Removals (X)						
(a) Avg. Conc.	1.000	0.618	0.286	0.019	0.922	0
(b) Grams Removed	556	343	159	11	513	0
4. Makeup Sample (D)						
(a) Avg. Conc.						
(b) Grams Removed	0					

Degradation Rate Calculation, Cont'd.

	Total Coolant	$O-\phi_3$	$M-\phi_3$	$P-\phi_3$	omp	HB
5. Makeup Tank (M)						
Tank Calib. (k_M) = 216.9gm/in						
(a) Avg. Conc.	1.000	0.618	0.286	0.019	0.922	0
(b) Grams Returned	21469	13261	6132	406	19799	0
6. Net Transferred						
(5.+4.-3.-2.-1.)	801	1310	622	44	1976	-1220
7. Initial Conc.						
(a) Coolant	1.000	0.588	0.271	0.018	0.877	0.063
(b) Sample Tank	1.000	0.588	0.271	0.018	0.877	0.063
(c) Makeup Tank	1.000	0.645	0.295	0.019	0.958	0
8. Initial Mass						
(a) Coolant	4996	2939	1354	88	4381	313
(b) Sample Tank	1201	706	325	21	1052	75
(c) Makeup Tank	2655	1711	782	49	2542	0
9. Final Conc.						
(a) Coolant	1.000	0.565	0.263	0.017	0.844	0.059
(b) Sample Tank	1.000	0.565	0.263	0.017	0.844	0.059
(c) Makeup Tank	1.000	0.611	0.287	0.020	0.912	0
10. Final Mass						
(a) Coolant	5056	2853	1316	88	4257	296
(b) Sample Tank	2863	1615	745	49	2409	168
(c) Makeup Tank	1734	1041	497	35	1573	0
11. Δ Correction						
(8.-10.)						
(a) Coolant	-60	86	38	0	124	17
(b) Sample Tank	-1662	-909	-420	-29	-1358	-93
(c) Makeup Tank	921	670	285	14	969	0
(d) Total Δ Corr.	-801	-153	-97	-15	-265	-76
12. Total Mass Degraded, W						
(6.+11.(d))	0	1157	525	29	1711	-1296
13. G(-omp), G(-1), G(HB)		0.207	0.094	0.005	0.307	0.232
14. G*(-omp) = G(-omp)/C,						
G*(-1) = G(-1)/C_1		0.359	0.354	0.297	0.357	----

Degradation Rate Calculation, Cont'd.

Statistics of G Calculation:

$(MWH)_1 = \underline{\hspace{1em} 172 \hspace{1em}}$, $(MWH)_2 = \underline{\hspace{1em} 1136 \hspace{1em}}$

$\sigma(F)/F = \underline{\hspace{1em} 0.03 \hspace{1em}}$

	O-$\emptyset_3$	M-$\emptyset_3$	P-$\emptyset_3$	omp	HB
15. Intercept, a_1	0.600	0.275	0.018	0.890	0.064
16. Slope, b_1 x 10^5	-3.208	-1.402	-0.020	-4.571	-0.543
17. $\sigma(a_1)$ x 10^2	0.212	0.133	0.026	0.275	0.270
18. $\sigma(b_1)$ x 10^5	0.307	0.200	0.039	0.399	0.374
19. $\sigma^2(C_{initial})$ x 10^8					
(a) Coolant	184	71	3	310	309
(b) Sample Tank	184	71	3	310	309
(c) Makeup Tank	297	51	1	349	----
20. $\sigma^2(C_{final})$ x 10^8					
(a) Coolant	217	97	4	366	326
(b) Sample Tank	217	97	4	366	326
(c) Makeup Tank	33	127	2	162	----
21. $\sigma^2(\Delta$ Correction)					
(a) Coolant	118	46	2	206	180
(b) Sample Tank	248	56	0	546	31
(c) Makeup Tank	229	54	1	509	----
(d) Total	595	156	3	1261	211
22. σ^2(Net Transfer)					
(a) Loop (D,L and X)	8	2	0	24	0
(b) Sample Tank	133	44	1	256	118
(c) Makeup Tank	413	105	3	599	----
(d) Total	554	151	4	879	118
23. $\sigma(W)/W$	0.029	0.033	0.091	0.027	0.014
24. $\sigma(G)/G$	0.042	0.045	0.096	0.040	0.033
25. $\sigma(G)$	0.009	0.004	0.001	0.012	0.008
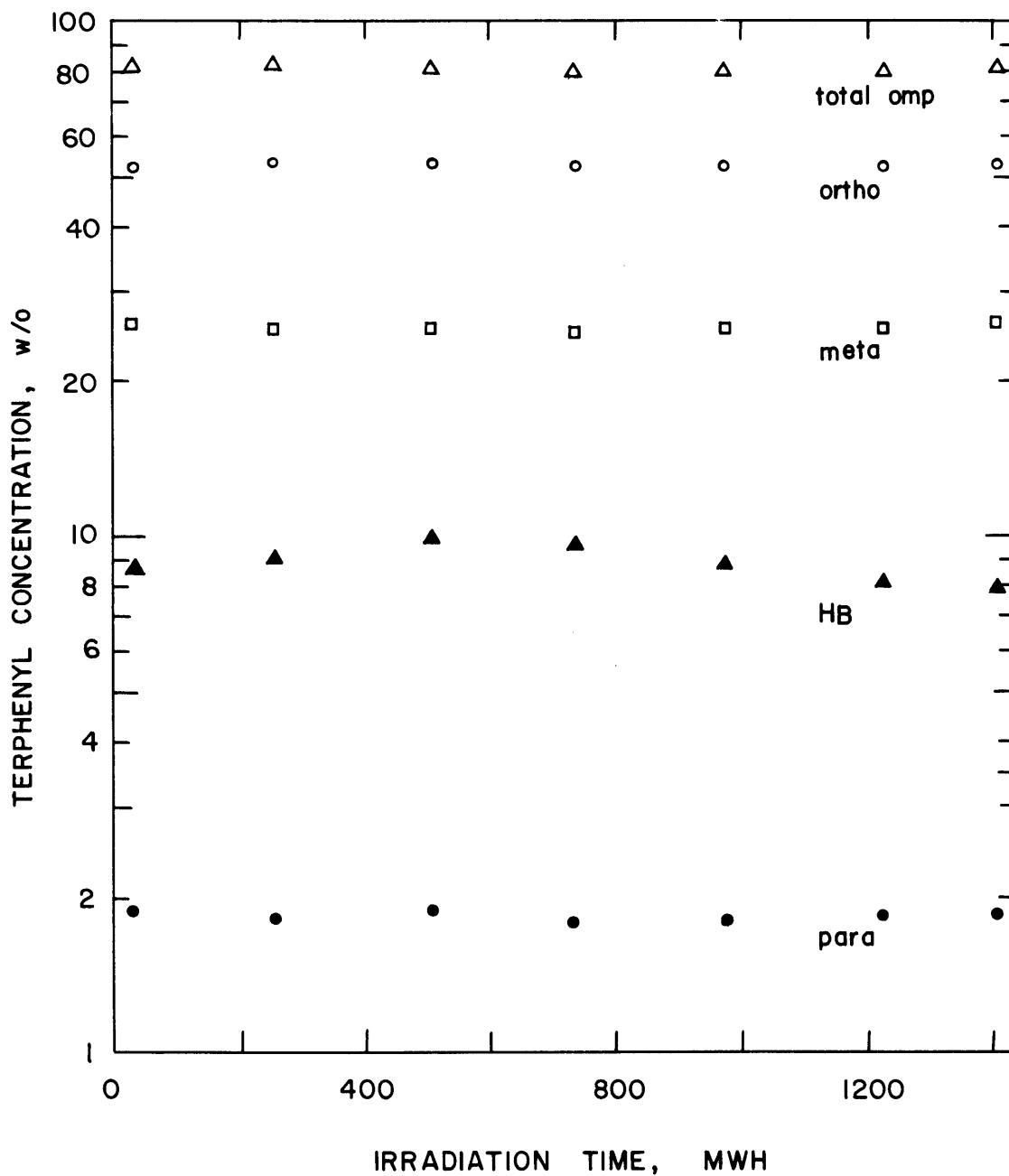
FIGURE A3.3   TERPHENYL AND HIGH BOILER CONCENTRATION
DURING RUN 20B AT 572 °F (300 °C)

Table A3.7a

Summary of Irradiation of Santowax OM - Run 20B

Sample No.	Sample Wt. (gram)	Accum. Run Time (MWH)	Terphenyl Concentration - w/o				Concentration Variance x10^8				HB w/o	σ^2(HB)x10^8
			O	M	P	OMP	σ^2(O)	σ^2(M)	σ^2(P)	σ^2(OMP)		
S-1	3628	16	53.7	25.9	1.9	81.5	103	76	3	324	9.6	2529
S-2	3752	254	53.8	25.6	1.8	81.2	66	49	2	209	9.3	1605
S-3	2359	509	53.4	25.5	1.9	80.8	46	34	2	145	9.1	985
S-4	3671	730	52.5	25.1	1.8	79.4	44	33	2	140	8.9	760
S-5	3670	977	52.9	25.6	1.8	80.3	66	50	2	210	8.6	856
S-6	4271	1224	52.6	25.6	1.9	80.1	93	70	3	295	8.4	1306
S-7	3171	1452	52.7	25.7	1.9	80.3	140	107	5	446	8.2	2050
M-1	2567	0	61.3	29.0	2.2	92.5	679	135	7	820	0	
M-2	3610	155	59.6	28.4	1.9	89.9	167	300	7	474	0	
M-3	3839	498	59.9	28.1	1.9	89.9	110	122	1	233	0	
M-4	2343	722	60.2	28.6	1.9	90.7	142	210	4	356	0	
M-5	3726	878	59.8	28.1	1.9	89.8	80	198	14	292	0	
M-6	3739	1109	59.6	28.3	2.0	89.9	160	260	13	432	0	
M-7	4222	1352	59.3	27.9	2.0	89.2	496	113	6	614	0	
L-2	19	351	53.5	25.4	1.8	80.7	196	4	4	204	9.2	1605
L-3	17	513	51.7	24.4	1.7	77.8	60	57	1	118	9.1	985
L-4	19	740	52.6	25.1	1.8	79.6	26	63	3	91	8.7	852
D-1	303	1380	64.1	30.9	2.4	97.4	101	356	8	664	0	
X-1	132	727	53.1	25.6	1.8	80.5	160	50	3	213	0.848	980

Note: (1) Concentrations and Variances of S Sample were calculated from least square analysis

(2) Makeup Tank Calibration = 220.2 ± 0.5 gms/in; Sample Tank Calibration = 221.6 ± 0.9 gms/in

Table A3.7b

Degradation Rate Calculation

Run No. ___20B___

Santowax OM

Summary:

Date: From ___1/30/67___   To ___2/17/67___

Irradiation Temp. ___572___ °F   Type of Distillation___HB___

Terphenyl Concentration ___80.5___ w/o   HB Concentration ___8.5___ w/o

Terphenyl Degraded ___2246___ gms   LIB/HB ___1.29___

Averaged Dose Rate, $\bar{r}$ ___0.0613___ Watts/gm

Density, ρ ___0.882___ gms/cc   Length of Run ___1454___ MWH

In Pile Dose Rate Factor, F_T^{SW} ___75.5___ Watt-cc/MW-gm

Reactor Power ___4.88___ MW   Fast Neutron Fraction, f_N ___0.36___

G(-omp) ___0.270___ $\sigma(G)$ ___0.010___

Calculation of G:

	Total Coolant	$O-\phi_3$	$M-\phi_3$	$P-\phi_3$	omp	HB
1. Coolant Sample (L)						
(a) Avg. Conc.	1.000	0.526	0.250	0.018	0.794	0.091
(b) Grams Removed	55	29	14	1	44	5
2. Sample Tank (S) Tank Calib. (k_S) = 221.6gm/in						
(a) Avg. Conc.	1.000	0.531	0.256	0.018	0.805	0.085
(b) Grams Removed	24547	13033	6284	449	19766	2081
3. Misc. Removals (X)						
(a) Avg. Conc.	1.000	0.531	0.256	0.018	0.805	0.085
(b) Grams Removed	132	70	34	2	106	11
4. Makeup Sample (D)						
(a) Avg. Conc.	1.000	0.641	0.309	0.024	0.974	0
(b) Grams Removed	303	194	94	7	295	0

Degradation Rate Calculation, Cont'd.

	Total Coolant	$O-\phi_3$	$M-\phi_3$	$P-\phi_3$	omp	HB
5. Makeup Tank (M)						
Tank Calib. $(k_M) = 220.2$ gm/in						
(a) Avg. Conc.	1.000	0.598	0.283	0.020	0.901	0
(b) Grams Returned	24045	14392	6800	472	21664	0
6. Net Transferred						
(5.+4.-3.-2.-1.)	-387	1454	562	27	2043	-2097
7. Initial Conc.						
(a) Coolant	1.000	0.537	0.257	0.018	0.812	0.096
(b) Sample Tank	1.000	0.537	0.257	0.018	0.812	0.096
(c) Makeup Tank	1.000	0.613	0.290	0.022	0.925	0
8. Initial Mass						
(a) Coolant	5278	2836	1356	95	4287	505
(b) Sample Tank	3955	2125	1016	71	3212	378
(c) Makeup Tank	902	553	261	20	834	0
9. Final Conc.						
(a) Coolant	1.000	0.525	0.255	0.019	0.799	0.082
(b) Sample Tank	1.000	0.525	0.255	0.019	0.799	0.082
(c) Makeup Tank	1.000	0.593	0.279	0.020	0.892	0
10. Final Mass						
(a) Coolant	5327	2795	1359	99	4253	436
(b) Sample Tank	693	364	177	13	554	57
(c) Makeup Tank	3728	2209	1041	73	3323	0
11. Δ Correction						
(8.-10.)						
(a) Coolant	-49	41	-3	-4	34	69
(b) Sample Tank	3262	1761	839	58	2658	321
(c) Makeup Tank	-2826	-1656	-780	-53	-2489	0
(d) Total Δ Corr.	387	146	56	1	203	390
12. Total Mass Degraded, W						
(6.+11.(d))	0	1600	618	28	2246	-1707
13. G(-omp), G(-i), G(HB)		0.193	0.074	0.003	0.270	0.205
14. $G^*(-omp) = G(-omp)/C$,						
$G^*(-i) = G(-i)/C_i$		0.363	0.290	0.180	0.336	----

Degradation Rate Calculation, Cont'd.

Statistics of G Calculation:

(MWH)$_1$ = _____0_____ , (MWH)$_2$ = _____1454_____

$\sigma(F)/F$ = _____0.03_____

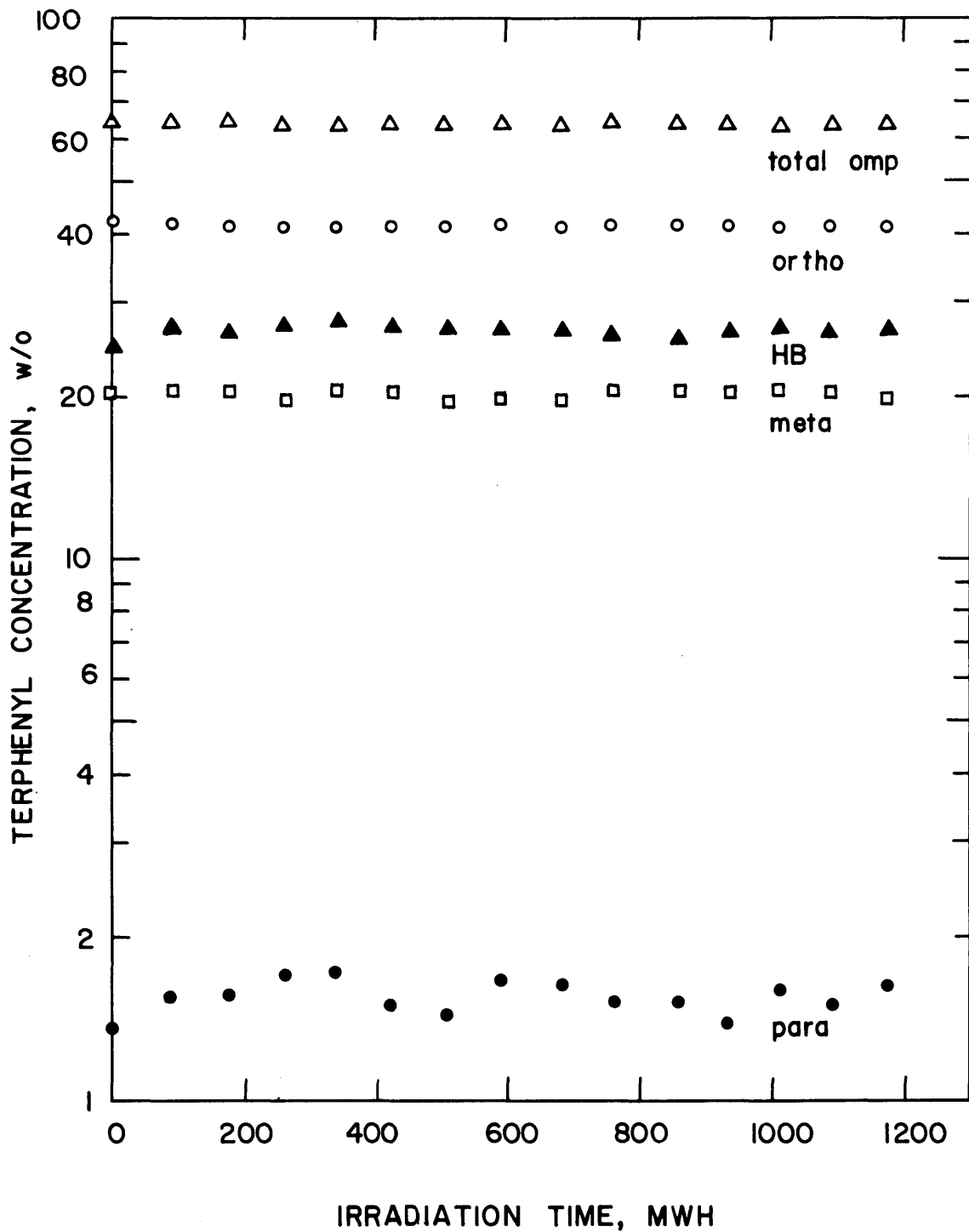|	$O-\emptyset_3$	$M-\emptyset_3$	$P-\emptyset_3$	omp	HB
15. Intercept, a_1	0.537	0.257	0.018	0.812	0.096
16. Slope, b_1 x 10^5	-0.877	-0.117	0.046	-0.954	-0.955
17. $\sigma(a_1)$ x 10^2	0.103	0.089	0.019	0.183	0.510
18. $\sigma(b_1)$ x 10^5	0.122	0.106	0.023	0.218	0.545
19. $\sigma^2(C_{initial})$ x 10^8					
(a) Coolant	102	76	3	324	2529
(b) Sample Tank	103	76	4	324	2529
(c) Makeup Tank	679	135	7	821	----
20. $\sigma^2(C_{final})$ x 10^8					
(a) Coolant	139	106	5	445	2050
(b) Sample Tank	140	107	5	446	2050
(c) Makeup Tank	496	113	6	614	----
21. $\sigma^2(\Delta$ Correction)					
(a) Coolant	71	52	2	220	1290
(b) Sample Tank	193	51	1	454	324
(c) Makeup Tank	311	69	1	646	----
(d) Total	575	172	4	1320	1614
22. σ^2(Net Transfer)					
(a) Loop (D,L and X)	7	2	0	21	0
(b) Sample Tank	121	65	3	340	1278
(c) Makeup Tank	275	176	6	523	----
(d) Total	403	241	9	884	1278
23. $\sigma(W)/W$	0.020	0.033	0.129	0.021	0.032
24. $\sigma(G)/G$	0.036	0.045	0.132	0.036	0.044
25. $\sigma(G)$	0.007	0.003	0.001	0.010	0.009
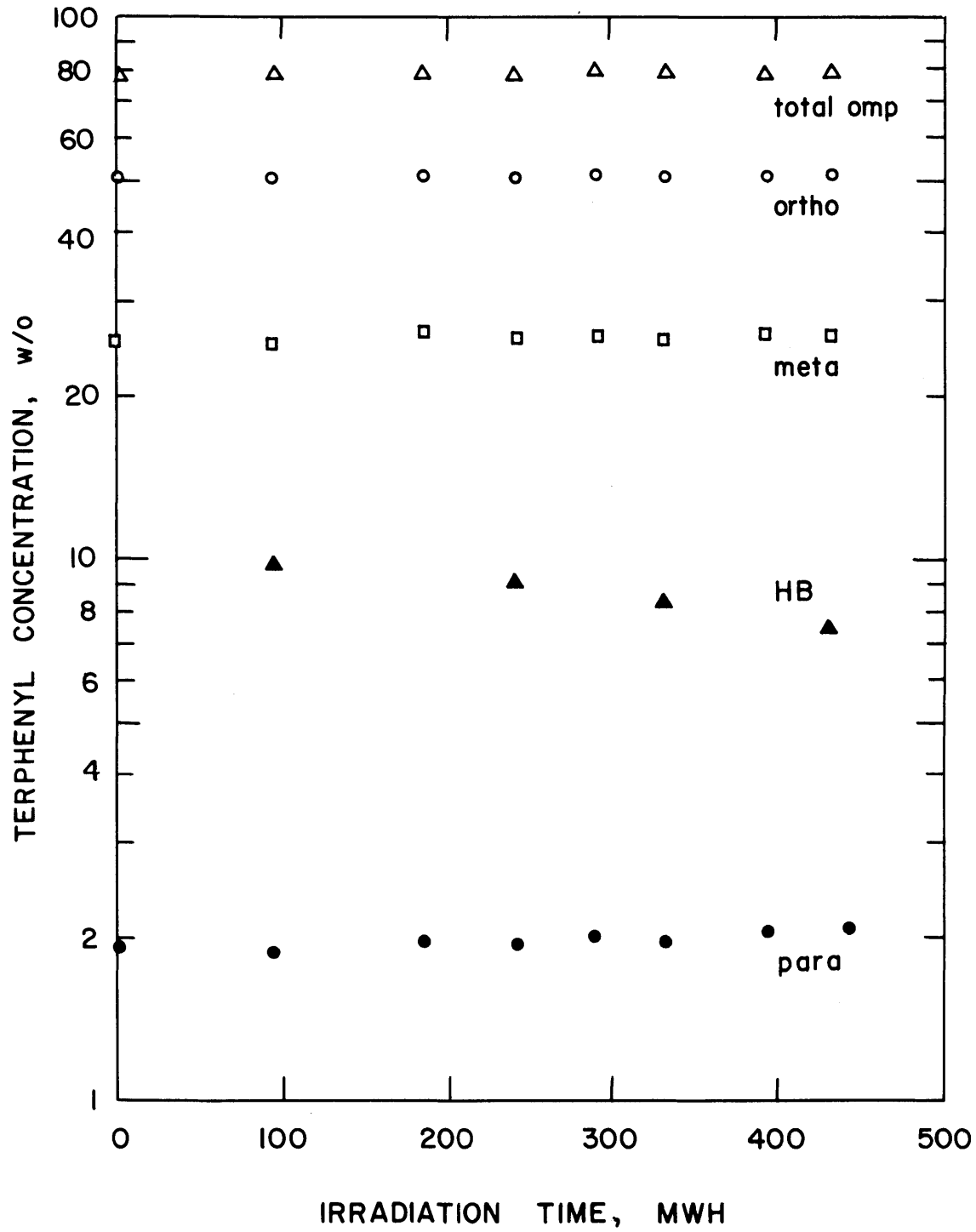
FIGURE A3.4   TERPHENYL AND HIGH BOILER CONCENTRATION
DURING RUN 21 AT 750°F (399°C)

Table A3.8a

Summary of Irradiation of Santowax OM - Run 21

Sample No.	Sample Wt. (gram)	Accum. Run Time (MWH)	Terphenyl Concentration - w/o				Concentration Variance x10^8				HB w/o	σ^2(HB)x10^8
			O	M	P	OMP	σ^2(O)	σ^2(M)	σ^2(P)	σ^2(OMP)		
S-1	3018	97	50.6	25.5	1.9	78.0	123	48	3	309	10.0	329
S-2	3602	241	50.7	25.7	2.0	78.4	43	17	1	108	8.9	106
S-3	3168	332	50.9	25.9	2.1	78.8	48	19	1	123	8.2	89
M-1	3675	8	58.5	28.2	2.1	88.8	226	29	1	257	0	
M-2	3022	202	56.9	28.0	2.1	87.0	139	109	1	250	0	
M-3	3601	285	56.7	28.5	2.1	87.3	124	140	9	273	0	
M-4	3258	388	56.8	28.4	2.1	87.3	53	16	3	72	0	
L-2	19	97	50.7	25.6	2.0	78.3	86	110	1	227	10.0	329
L-3	19	185	51.1	25.8	2.0	78.9	95	68	1	252	8.9	106
L-4	21	290	51.3	25.9	2.0	79.2	146	76	1	386	8.9	106
X-1	19	87	58.5	28.2	2.1	88.8	226	29	1	257	0	
X-2	35	287	56.7	28.5	2.1	87.3	124	140	9	250	0	
X-3	46	293	56.8	28.5	2.1	87.4	124	140	9	250	0	
X-4	238	215	50.6	25.5	1.9	78.0	139	110	1	366	9.0	150

Note: (1) Concentrations and Variances of S and L Samples were calculated from least square analysis

(2) Makeup Tank Calibration = 221.0 ± 0.8 gms/in; Sample Tank Calibration = 219.5 ± 0.7 gms/in

Table A3.8b

Degradation Rate Calculation

Run No. __21__

Santowax OM

Summary:

Date: From ___3/13/67___   To ___3/28/67___

Irradiation Temp. __750__ ^{O}F Type of Distillation __HB__

Terphenyl Concentration __78.0__ w/o   HB Concentration __9.0__ w/o

Terphenyl Degraded __1028__ gms   LIB/HB __1.44__

Averaged Dose Rate, $\bar{r}$ __0.024__ Watts/gm

Density, ρ __0.780__ gms/cc   Length of Run __423__ MWH

In Pile Dose Rate Factor, F_T^{SW} __74.2__ Watt-cc/MW-gm

Reactor Power __1.93__ MW   Fast Neutron Fraction, f_N __0.36__

G(-omp) __0.476__ $\sigma(G)$ __0.023__

Calculation of G:

	Total Coolant	$O-\emptyset_3$	$M-\emptyset_3$	$P-\emptyset_3$	omp	HB
1. Coolant Sample (L)						
(a) Avg. Conc.	1.000	0.511	0.258	0.020	0.789	0.085
(b) Grams Removed	144	73	37	3	113	12
2. Sample Tank (S)						
Tank Calib. (k_S) =	219.5gm/in					
(a) Avg. Conc.	1.000	0.506	0.255	0.019	0.780	0.090
(b) Grams Removed	9788	4949	2497	189	7635	880
3. Misc. Removals (X)						
(a) Avg. Conc.	1.000	0.525	0.264	0.020	0.808	0.063
(b) Grams Removed	338	178	89	7	274	21
4. Makeup Sample (D)						
(a) Avg. Conc.						
(b) Grams Removed	0					

Degradation Rate Calculation, Cont'd.

	Total Coolant	$O\text{-}\phi_3$	$M\text{-}\phi_3$	$P\text{-}\phi_3$	omp	HB
5. Makeup Tank (M)						
Tank Calib. (k_M) = 221.0gm/in						
(a) Avg. Conc.	1.000	0.573	0.283	0.021	0.876	0
(b) Grams Returned	13556	7762	3831	283	11876	0
6. Net Transferred						
(5.+4.-3.-2.-1.)	3286	2562	1208	84	3854	-913
7. Initial Conc.						
(a) Coolant	1.000	0.501	0.253	0.019	0.773	0.100
(b) Sample Tank	1.000	0.504	0.253	0.019	0.776	0.100
(c) Makeup Tank	1.000	0.591	0.286	0.020	0.897	0
8. Initial Mass						
(a) Coolant	4800	2406	1215	92	3713	481
(b) Sample Tank	1968	992	497	36	1525	197
(c) Makeup Tank	1785	1054	510	36	1600	0
9. Final Conc.						
(a) Coolant	1.000	0.514	0.260	0.021	0.795	0.074
(b) Sample Tank	1.000	0.508	0.259	0.021	0.788	0.082
(c) Makeup Tank	1.000	0.568	0.284	0.022	0.874	0
10. Final Mass						
(a) Coolant	4741	2439	1233	97	3769	349
(b) Sample Tank	3546	1800	919	73	2792	289
(c) Makeup Tank	3552	2017	1010	76	3103	0
11. Δ Correction						
(8.-10.)						
(a) Coolant	59	-33	-18	-5	-56	132
(b) Sample Tank	-1578	-808	-422	-37	-1267	-92
(c) Makeup Tank	-1767	-963	-500	-40	-1503	0
(d) Total Δ Corr.	-3286	-1804	-940	-82	-2826	40
12. Total Mass Degraded, W						
(6.+11.(d))	0	758	268	2	1028	-873
13. G(-omp), G(-1), G(HB)		0.351	0.124	0.001	0.476	0.405
14. G*(-omp) = G(-omp)/C,						
G*(-1) = G(-1)/C_1		0.694	0.487	0.046	0.611	----

Degradation Rate Calculation, Cont'd.

Statistics of G Calculation:

$(MWH)_1 = \underline{\hspace{1cm} 3 \hspace{1cm}}$, $(MWH)_2 = \underline{\hspace{1cm} 426 \hspace{1cm}}$

$\sigma(F)/F = \underline{\hspace{1cm} 0.03 \hspace{1cm}}$

	$0\text{-}\phi_3$	$M\text{-}\phi_3$	$P\text{-}\phi_3$	omp	HB
15. Intercept, a_1	0.503	0.251	0.018	0.772	0.108
16. Slope, $b_1 \times 10^5$	1.084	1.939	0.651	3.686	-7.923
17. $\sigma(a_1) \times 10^2$	0.154	0.096	0.024	0.245	0.247
18. $\sigma(b_1) \times 10^5$	0.511	0.322	0.082	0.813	0.758
19. $\sigma^2(C_{initial}) \times 10^8$					
(a) Coolant	262	207	2	692	329
(b) Sample Tank	123	48	3	309	329
(c) Makeup Tank	304	249	5	558	0
20. $\sigma^2(C_{final}) \times 10^8$					
(a) Coolant	193	153	2	511	180
(b) Sample Tank	105	42	3	267	89
(c) Makeup Tank	53	16	3	72	0
21. $\sigma^2(\Delta \text{ Correction})$					
(a) Coolant	108	83	1	285	132
(b) Sample Tank	165	44	0	397	20
(c) Makeup Tank	219	57	1	504	0
(d) Total	492	184	2	1186	152
22. $\sigma^2(\text{Net Transfer})$					
(a) Loop (D,L and X)	3	1	0	7	0
(b) Sample Tank	41	14	0	100	53
(c) Makeup Tank	98	42	2	177	0
(d) Total	142	57	2	284	53
23. $\sigma(W)/W$	0.033	0.058	1.000	0.037	0.016
24. $\sigma(G)/G$	0.045	0.065	1.000	0.048	0.034
25. $\sigma(G)$	0.016	0.008	0.001	0.023	0.014
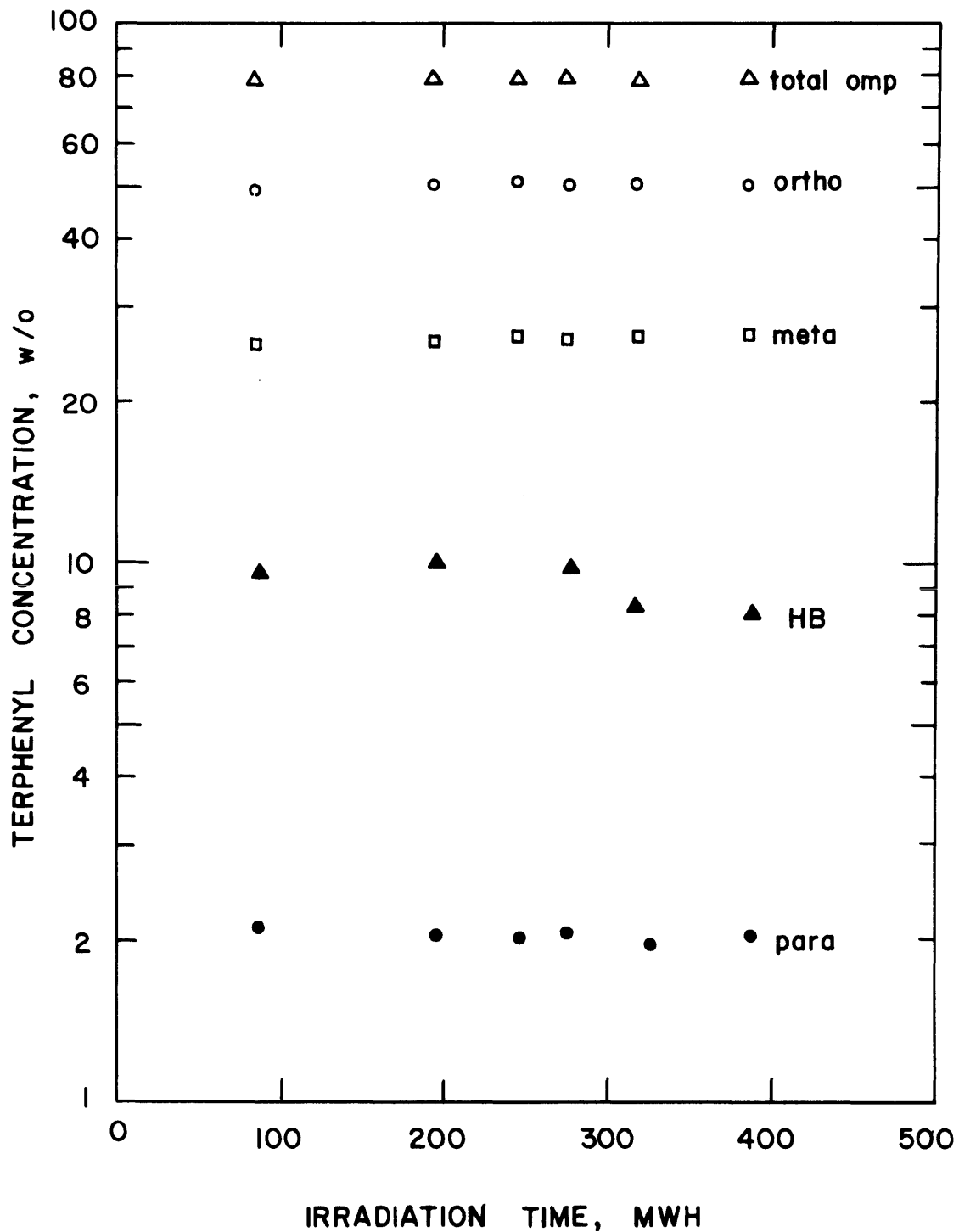
FIGURE A3.5   TERPHENYL AND HIGH BOILER CONCENTRATION
DURING RUN 22 AT 800°F (427°C)

Table A3.9a

Summary of Irradiation of Santowax OM - Run 22

Sample No.	Sample Wt. (gram)	Accum. Run Time (MWH)	Terphenyl Concentration - w/o				Concentration Variance x10³				HB w/o	$\sigma^2(HB) \times 10^8$
			O	M	P	OMP	$\sigma^2(O)$	$\sigma^2(M)$	$\sigma^2(P)$	$\sigma^2(OMP)$		
S-2	3219	196	50.1	25.9	2.0	78.0	156	29	2	249	9.4	2282
S-3	3021	276	50.3	26.2	2.0	78.5	128	25	1	205	8.8	1520
S-4	4103	318	50.4	26.4	2.0	78.8	171	33	2	280	8.5	1844
M-3	4067	196	56.8	29.0	2.2	88.0	22	86	3	111	0	
M-4	3328	245	57.4	29.8	2.2	89.4	37	214	7	259	0	
M-5	3027	289	57.4	29.6	2.2	89.2	73	51	2	126	0	
M-6	4140	366	55.8	29.2	2.2	87.2	20	8	1	29	0	
L-3	21	98	51.7	26.5	2.0	80.2	1488	335	8	3448	9.9	2400
L-4	24	196	51.0	26.4	2.0	79.4	824	184	4	1917	9.4	2282
L-5	18	243	50.7	26.4	2.0	79.1	504	111	2	1179	8.9	1600
L-6	17	332	50.1	26.4	2.0	78.5	708	148	3	1673	8.5	1844
X-1	77	158	50.3	26.2	2.0	78.5	140	28	2	230	8.9	1600
X-2	761	209	56.8	29.4	2.2	88.4	73	51	2	126	0	

Note: (1) Concentrations and Variances of S and L Samples were calculated from least square analysis

(2) Makeup tank Calibration = 220.6 ± 1.2 gms/in; Sample Tank Calibration = 221.0 ± 1.0 gms/in

Table A3.9b

Degradation Rate Calculation

Run No. __22__

Santowax OM

Summary:

Date: From __4/5/67__ To __4/18/67__

Irradiation Temp. __800__ °F Type of Distillation __HB__

Terphenyl Concentration __78.5__ w/o HB Concentration __8.9__ w/o

Terphenyl Degraded __1644__ gms LIB/HB __1.42__

Averaged Dose Rate, $\bar{r}$ __0.023__ Watts/gm

Density, ρ __0.776__ gms/cc Length of Run __290__ MWH

In Pile Dose Rate Factor, F_T^{SW} __73.8__ Watt-cc/MW-gm

Reactor Power __1.92__ MW Fast Neutron Fraction, f_N __0.36__

G(-omp) __1.153__ $\sigma(G)$ __0.044__

Calculation of G:

	Total Coolant	$O-\emptyset_3$	$M-\emptyset_3$	$P-\emptyset_3$	omp	HB
1. Coolant Sample (L)						
(a) Avg. Conc.	1.000	0.509	0.264	0.020	0.793	0.093
(b) Grams Removed	80	41	21	2	64	7
2. Sample Tank (S)						
Tank Calib. (k_S) =	221.0 gm/in					
(a) Avg. Conc.	1.000	0.503	0.262	0.020	0.785	0.089
(b) Grams Removed	10343	5201	2710	209	8120	921
3. Misc. Removals (X)						
(a) Avg. Conc.	1.000	0.562	0.291	0.022	0.874	0.089
(b) Grams Removed	838	471	244	18	733	7
4. Makeup Sample (D)						
(a) Avg. Conc.						
(b) Grams Removed	0					

Degradation Rate Calculation, Cont'd.

	Total Coolant	$O-\phi_3$	$M-\phi_3$	$P-\phi_3$	omp	HB
5. Makeup Tank (M)						
Tank Calib. (k_M) = 220.6 gm/in						
(a) Avg. Conc.	1.000	0.568	0.293	0.022	0.883	0
(b) Grams Returned	14562	8267	4274	322	12863	0
6. Net Transferred						
(5.+4.-3.-2.-1.)	3301	2555	1300	92	3947	-935
7. Initial Conc.						
(a) Coolant	1.000	0.499	0.255	0.021	0.775	0.102
(b) Sample Tank	1.000	0.499	0.255	0.021	0.775	0.102
(c) Makeup Tank	1.000	0.635	0.301	0.024	0.960	0
8. Initial Mass						
(a) Coolant	4592	2374	1216	91	3680	469
(b) Sample Tank	1163	581	297	24	902	119
(c) Makeup Tank	4194	2663	1262	102	4027	0
9. Final Conc.						
(a) Coolant	1.000	0.505	0.266	0.020	0.791	0.081
(b) Sample Tank	1.000	0.504	0.264	0.020	0.788	0.085
(c) Makeup Tank	1.000	0.558	0.292	0.022	0.872	0
10. Final Mass						
(a) Coolant	4388	2181	1157	90	3428	353
(b) Sample Tank	3042	1537	810	61	2407	260
(c) Makeup Tank	5820	3247	1699	130	5076	0
11. Δ Correction						
(8.-10.)						
(a) Coolant	204	193	59	1	252	116
(b) Sample Tank	-1879	-956	-513	-36	-1505	-141
(c) Makeup Tank	-1626	-585	-437	-28	-1050	0
(d) Total Δ Corr.	-3301	-1348	-891	-63	-303	-25
12. Total Mass Degraded, W						
(6.+11.(d))	0	1207	409	29	1644	-960
13. G(-omp), G(-1), G(HB)		0.846	0.287	0.020	1.153	0.674
14. G*(-omp) = G(-omp)/C,						
G*(-1) = G(-1)/C_1		1.683	1.094	0.990	1.469	----

Degradation Rate Calculation, Cont'd.

Statistics of G Calculation:

$(MWH)_1 =$ _____94_____ , $(MWH)_2 =$ _____384_____

$\sigma(F)/F =$ _____0.03_____

|	$O-\emptyset_3$	$M-\emptyset_3$	$P-\emptyset_3$	omp	HB
15. Intercept, a_1	0.497	0.252	0.021	0.770	0.108
16. Slope, b_1 x 10^5	2.048	3.644	-0.286	5.572	-7.254
17. $\sigma(a_1)$ x 10^2	0.287	0.124	0.033	0.363	1.084
18. $\sigma(b_1)$ x 10^5	1.054	0.461	0.116	1.337	3.750
19. $\sigma^2(C_{initial})$ x 10^8					
(a) Coolant	433	80	6	678	6186
(b) Sample Tank	433	80	6	678	6186
(c) Makeup Tank	42	102	8	152	0
20. $\sigma^2(C_{final})$ x 10^8					
(a) Coolant	320	62	3	517	3374
(b) Sample Tank	171	33	2	276	1844
(c) Makeup Tank	20	8	1	29	0
21. $\sigma^2(\Delta$ Correction)					
(a) Coolant	154	31	2	249	1964
(b) Sample Tank	197	52	1	467	249
(c) Makeup Tank	230	73	1	552	0
(d) Total	581	156	4	1268	2113
22. $\sigma^2(Net\ Transfer)$					
(a) Loop (D,L and X)	4	1	0	10	0
(b) Sample Tank	75	16	1	137	686
(c) Makeup Tank	50	53	1	142	0
(d) Total	129	70	2	289	686
23. $\sigma(W)/W$	0.022	0.037	0.084	0.024	0.055
24. $\sigma(G)/G$	0.037	0.047	0.090	0.038	0.063
25. $\sigma(G)$	0.032	0.014	0.002	0.044	0.042
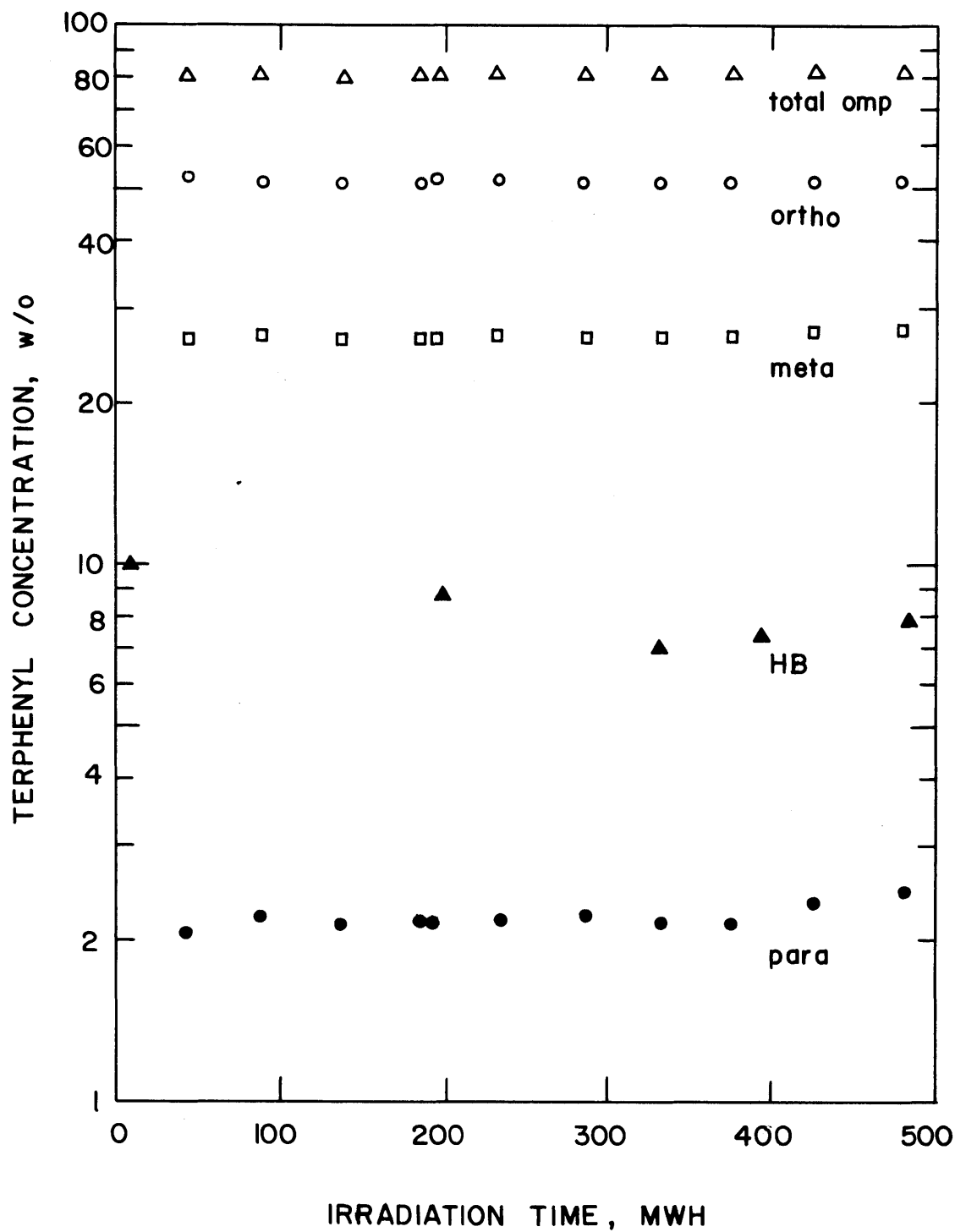
FIGURE A3.6   TERPHENYL AND HIGH BOILER CONCENTRATION
DURING RUN 23 AT 700°F (371 °C)

Table A3.10a

Summary of Irradiation of Santowax OM - Run 23

Sample No.	Sample Wt. (gram)	Accum. Run Time (MWH)	Terphenyl Concentration - w/o				Concentration Variance x10^8				HB w/o	σ^2(HB)x10^8
			O	M	P	OMP	σ^2(O)	σ^2(M)	σ^2(P)	σ^2(OMP)		
S-7	3190	198	51.2	26.5	2.2	79.9	184	100	16	654	8.0	8218
S-8	3128	332	51.4	26.9	2.3	80.6	56	31	6	214	7.7	2312
S-9	1819	394	51.5	27.0	2.3	80.8	66	37	7	244	7.6	2487
S-10	2100	482	51.7	27.3	2.4	81.3	157	87	17	545	7.4	5952
M-8	4192	136	57.1	29.1	2.6	88.8	31	20	16	66	0	
M-9	3197	284	57.3	29.4	2.4	89.1	97	119	9	225	0	
M-10	3156	392	57.2	29.6	2.5	89.3	412	64	10	485	0	
L-13	22	137	51.8	26.2	2.1	80.1	51	28	5	101	8.1	8300
L-14	23	183	51.8	26.4	2.1	80.3	36	20	3	71	8.0	8200
L-15	22	194	51.8	26.4	2.2	80.4	33	18	3	66	8.0	8200
L-16	20	231	51.8	26.5	2.2	80.5	26	14	2	51	7.9	6500
L-17	23	285	51.8	26.6	2.2	80.6	21	12	2	43	7.8	4300
L-18	21	333	51.8	26.7	2.2	80.7	23	13	3	49	7.7	2300
L-19	22	376	51.7	26.9	2.3	80.9	30	17	4	65	7.6	2400
L-20	19	427	51.7	27.0	2.3	81.0	44	25	5	95	7.5	3800
L-21	20	479	51.7	27.1	2.3	81.1	65	37	7	139	7.4	5900
X-1	23	138	57.2	29.3	2.4	88.9	90	109	9	215	0	
X-2	82	285	57.3	29.4	2.4	89.1	97	119	9	225	0	
X-3	169	340	51.4	26.9	2.3	80.6	40	22	3	70	7.7	2300
X-4	13	423	57.2	29.7	2.5	89.4	430	70	11	490	0	

Note: (1) Concentrations and Variances of S and L Samples were calculated from least square analysis

(2) Makeup Tank Calibration = 217.7 ± 0.4 gms/in; Sample Tank Calibration = 219.9 ± 0.6 gms/in

Table A3.10b

Degradation Rate Calculation

Run No. __23__

Santowax OM

Summary:

Date: From ____5/17/67____   To ____6/2/67____

Irradiation Temp. ___700___ ^{o}F   Type of Distillation ___HB___

Terphenyl Concentration _80.6_ w/o   HB Concentration ___7.7___ w/o

Terphenyl Degraded ___701___ gms   LIB/HB _____1.52_____

Averaged Dose Rate, $\bar{r}$ ___0.022___ Watts/gm

Density, ρ ___0.821___ gms/cc   Length of Run ___382___ MWH

In Pile Dose Rate Factor, F_T^{SW} __72.8__ Watt-cc/MW-gm

Reactor Power ___1.93___ MW   Fast Neutron Fraction, f_N _0.36_

G(-omp) ____0.357____ $\sigma(G)$ ____0.023____

Calculation of G:

	Total Coolant	O-$\emptyset_3$	M-$\emptyset_3$	P-$\emptyset_3$	omp	HB
1. Coolant Sample (L)						
(a) Avg. Conc.	1.000	0.517	0.266	0.022	0.806	0.078
(b) Grams Removed	192	99	51	4	154	15
2. Sample Tank (S)						
Tank Calib. (k_S) =	219.9gm/in					
(a) Avg. Conc.	1.000	0.514	0.269	0.023	0.806	0.077
(b) Grams Removed	10237	5263	2750	234	8247	790
3. Misc. Removals (X)						
(a) Avg. Conc.	1.000	0.538	0.279	0.024	0.841	0.046
(b) Grams Removed	288	155	80	7	242	13
4. Makeup Sample (D)						
(a) Avg. Conc.						
(b) Grams Removed	0					

Degradation Rate Calculation, Cont'd.

	Total Coolant	$O-\phi_3$	$M-\phi_3$	$P-\phi_3$	omp	HB
5. Makeup Tank (M)						
Tank Calib. (k_M) = 217.7 gm/in						
(a) Avg. Conc.	1.000	0.572	0.293	0.025	0.890	0
(b) Grams Returned	10545	6028	3093	265	9386	0
6. Net Transferred						
(5.+4.-3.-2.-1.)	-172	511	212	20	743	-818
7. Initial Conc.						
(a) Coolant	1.000	0.518	0.261	0.021	0.800	0.080
(b) Sample Tank	1.000	0.512	0.265	0.022	0.799	0.080
(c) Makeup Tank	1.000	0.569	0.294	0.025	0.888	0
8. Initial Mass						
(a) Coolant	5211	2702	1361	108	4171	417
(b) Sample Tank	1985	1016	525	44	1585	159
(c) Makeup Tank	1752	997	516	44	1567	0
9. Final Conc.						
(a) Coolant	1.000	0.517	0.271	0.023	0.811	0.074
(b) Sample Tank	1.000	0.517	0.273	0.024	0.814	0.074
(c) Makeup Tank	1.000	0.572	0.296	0.025	0.893	0
10. Final Mass						
(a) Coolant	5257	2719	1425	123	4267	390
(b) Sample Tank	665	344	182	16	542	49
(c) Makeup Tank	2854	1631	844	71	2546	0
11. Δ Correction						
(8.-10.)						
(a) Coolant	-46	-17	-64	-15	-96	27
(b) Sample Tank	1320	672	343	28	1043	110
(c) Makeup Tank	-1102	-634	-328	-27	-989	0
(d) Total Δ Corr.	172	21	-49	-14	-42	137
12. Total Mass Degraded, W						
(6.+11.(d))	0	532	163	6	701	-681
13. G(-omp), G(-1), G(HB)		0.271	0.083	0.003	0.357	0.348
14. G*(-omp) = G(-omp)/C,						
G*(-1) = G(-1)/C_1		0.524	0.311	0.149	0.443	----

Degradation Rate Calculation, Cont'd.

Statistics of G Calculation:

$(MWH)_1$ = _____ 102 _____ , $(MWH)_2$ = _____ 484 _____

$\sigma(F)/F$ = _____ 0.03 _____

	$O-\emptyset_3$	$M-\emptyset_3$	$P-\emptyset_3$	omp	HB
15. Intercept, a_1	0.519	0.259	0.020	0.798	0.084
16. Slope, $b_1 \times 10^5$	-0.316	2.555	0.674	3.011	-2.046
17. $\sigma(a_1) \times 10^2$	0.113	0.084	0.036	0.160	1.801
18. $\sigma(b_1) \times 10^5$	0.354	0.264	0.117	0.509	4.904
19. $\sigma^2(C_{initial}) \times 10^8$					
(a) Coolant	73	40	7	145	8218
(b) Sample Tank	184	100	16	654	8218
(c) Makeup Tank	90	97	0	187	0
20. $\sigma^2(C_{final}) \times 10^8$					
(a) Coolant	65	37	8	139	5952
(b) Sample Tank	157	87	17	545	5952
(c) Makeup Tank	412	64	10	485	0
21. $\sigma^2(\Delta \text{ Correction})$					
(a) Coolant	94	53	9	333	3878
(b) Sample Tank	160	45	1	398	185
(c) Makeup Tank	211	55	1	485	0
(d) Total	465	153	11	1216	4265
22. $\sigma^2(\text{Net Transfer})$					
(a) Loop (D,L and X)	3	1	0	10	0
(b) Sample Tank	60	26	8	185	1408
(c) Makeup Tank	81	28	5	142	0
(d) Total	144	55	13	337	1408
23. $\sigma(W)/W$	0.046	0.089	0.762	0.056	0.110
24. $\sigma(G)/G$	0.055	0.093	0.763	0.064	0.115
25. $\sigma(G)$	0.015	0.008	0.002	0.023	0.040
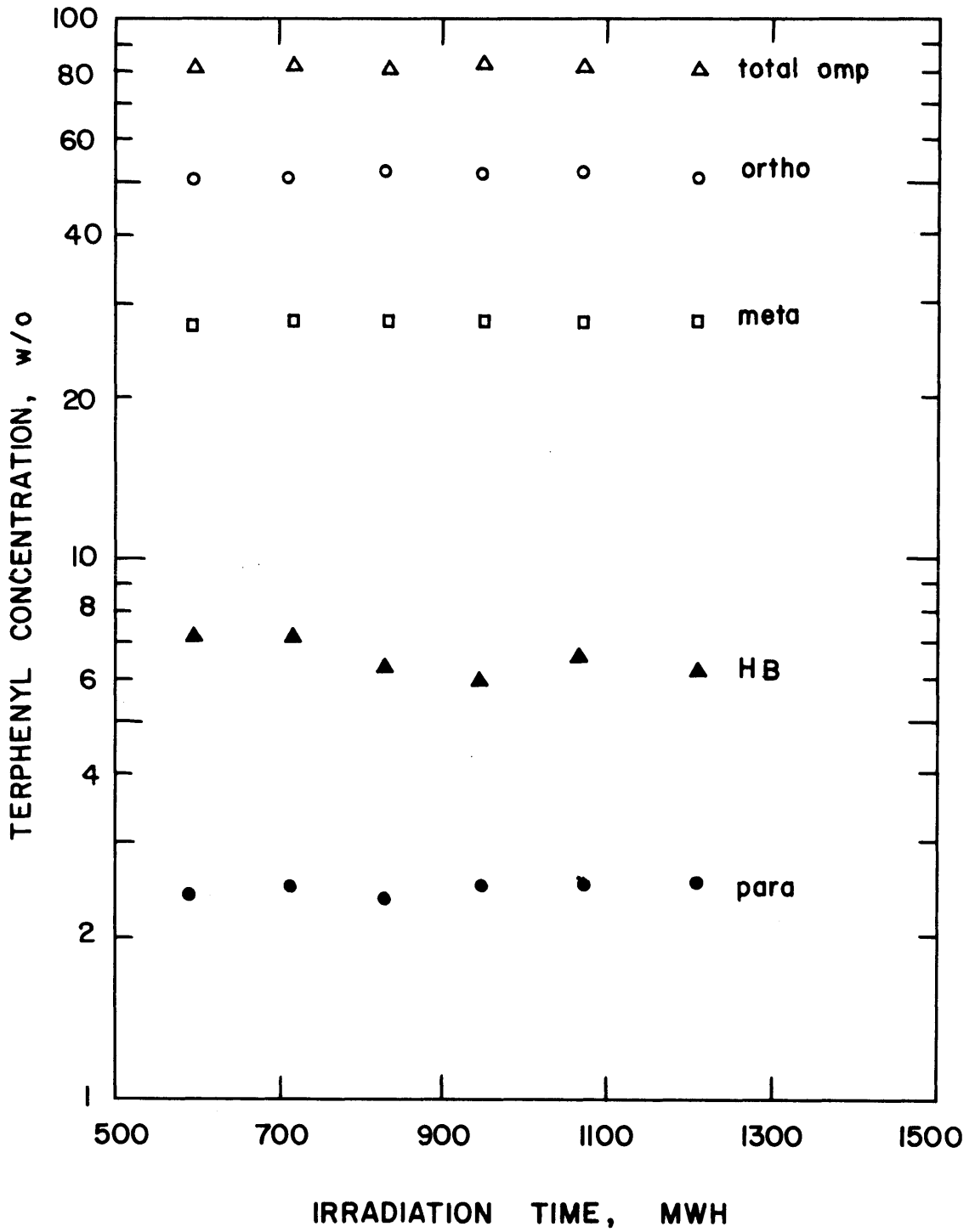
FIGURE A3.7　　TERPHENYL AND HIGH BOILER CONCENTRATION
DURING RUN 23A AT 700°F (371°C)

Table A3.11a

Summary of Irradiation of Santowax OM - Run 23A

Sample No.	Sample Wt. (gram)	Accum. Run Time (MWH)	Terphenyl Concentration - w/o				Concentration Variance x10^8				HB w/o	σ^2(HB)x10^8
			O	M	P	OMP	σ^2(O)	σ^2(M)	σ^2(P)	σ^2(OMP)		
S-2	2855	714	52.0	27.2	2.5	81.7	93	31	2	179	6.7	793
S-3	2932	831	52.0	27.3	2.5	81.8	57	19	2	110	6.5	467
S-4	2388	944	52.0	27.3	2.5	81.8	55	18	1	106	6.4	407
S-5	2829	1065	52.0	27.4	2.5	81.9	87	29	2	168	6.2	616
M-3	3178	650	56.6	29.4	2.6	88.6	299	125	2	427	0	
M-4	2886	758	57.2	29.6	2.6	89.4	372	62	1	435	0	
M-5	2920	875	56.2	29.5	2.6	88.3	306	183	3	492	0	
M-6	2379	997	56.2	29.3	2.7	88.2	4	27	1	32	0	
M-7	2878	1099	56.5	29.3	2.7	88.5	156	35	5	195	0	
L-2	21	621	52.4	27.1	2.5	82.0	163	69	4	310	6.8	850
L-3	20	737	52.3	27.2	2.5	82.0	96	41	2	182	6.6	681
L-4	19	846	52.3	27.3	2.5	82.1	62	26	1	118	6.6	432
L-5	19	958	52.2	27.4	2.5	82.1	56	24	1	107	6.4	512
L-6	21	1060	52.1	27.4	2.5	82.1	76	33	2	147	6.2	620
X-1	28	620	56.6	29.4	2.6	88.6	300	130	2	450	0	
X-2	35	782	57.2	29.5	2.6	89.1	350	60	1	425	0	
X-3	132	950	52.0	27.3	2.5	81.8	60	21	1	110	6.5	425
X-4	62	962	56.2	29.4	2.7	88.3	95	55	2	215	0	
X-5	15	1201	52.1	27.4	2.5	82.0	60	32	1	120	6.4	390

Note: (1) Concentrations and Variances of S and L Samples were calculated from least square analysis

(2) Makeup Tank Calibration = 216.2 ± 0.4 gms/in; Sample Tank Calibration = 218.1 ± 0.5 gms/in

Table A3.11b

Degradation Rate Calculation

Run No. ___23A___

Santowax OM

Summary:

Date: From ___6/6/67___   To ___6/14/67___

Irradiation Temp. ___700___ °F   Type of Distillation ___HB___

Terphenyl Concentration ___82.0___ w/o   HB Concentration ___6.5___ w/o

Terphenyl Degraded ___961___ gms   LIB/HB ___1.77___

Averaged Dose Rate, $\bar{r}$ ___0.057___ Watts/gm

Density, ρ ___0.819___ gms/cc   Length of Run ___580___ MWH

In Pile Dose Rate Factor, F_T^{SW} ___72.3___ Watt-cc/MW-gm

Reactor Power ___4.85___ MW   Fast Neutron Fraction, f_N ___0.36___

G(-omp) ___0.326___ $\sigma(G)$ ___0.016___

Calculation of G:

	Total Coolant	$0-\phi_3$	$M-\phi_3$	$P-\phi_3$	omp	HB
1. Coolant Sample (L)						
(a) Avg. Conc.	1.000	0.523	0.273	0.025	0.820	0.065
(b) Grams Removed	100	52	27	3	82	7
2. Sample Tank (S)						
Tank Calib. (k_S) =	216.2 gm/in					
(a) Avg. Conc.	1.000	0.520	0.273	0.025	0.818	0.065
(b) Grams Removed	11004	5718	3004	273	8995	710
3. Misc. Removals (X)						
(a) Avg. Conc.	1.000	0.533	0.279	0.025	0.837	0.046
(b) Grams Removed	272	145	76	7	228	13
4. Makeup Sample (D)						
(a) Avg. Conc.						
(b) Grams Removed	0					

Degradation Rate Calculation, Cont'd.

	Total Coolant	$O\text{-}\varnothing_3$	$M\text{-}\varnothing_3$	$P\text{-}\varnothing_3$	omp	HB
5. Makeup Tank (M)						
Tank Calib. (k_M) = 218.1gm/in						
(a) Avg. Conc.	1.000	0.566	0.294	0.026	0.886	0
(b) Grams Returned	14241	8054	4189	373	12616	0
6. Net Transferred						
(5.+4.-3.-2.-1.)	2866	2139	1082	90	3311	-730
7. Initial Conc.						
(a) Coolant	1.000	0.524	0.272	0.025	0.820	0.067
(b) Sample Tank	1.000	0.520	0.272	0.024	0.816	0.067
(c) Makeup Tank	1.000	0.563	0.290	0.025	0.878	0
8. Initial Mass						
(a) Coolant	4958	2598	1346	122	4066	333
(b) Sample Tank	1141	593	310	28	931	77
(c) Makeup Tank	3446	1939	999	87	3025	0
9. Final Conc.						
(a) Coolant	1.000	0.520	0.275	0.025	0.821	0.059
(b) Sample Tank	1.000	0.520	0.274	0.025	0.820	0.059
(c) Makeup Tank	1.000	0.565	0.293	0.027	0.885	0
10. Final Mass						
(a) Coolant	5337	2777	1467	136	4380	317
(b) Sample Tank	4072	2117	1116	103	3336	242
(c) Makeup Tank	3000	1696	880	80	2656	0
11. Δ Correction (8.-10.)						
(a) Coolant	-379	-179	-121	-14	-314	16
(b) Sample Tank	-2931	-1524	-806	-75	-2405	-165
(c) Makeup Tank	446	243	119	7	369	0
(d) Total Δ Corr.	-2866	-1460	-808	-82	-2350	-149
12. Total Mass Degraded, W						
(6.+11.(d))	0	679	274	8	961	-879
13. G(-omp), G(-1), G(HB)		0.230	0.093	0.003	0.326	0.298
14. G*(-omp) = G(-omp)/C,						
$G*(-1) = G(-1)/C_i$		0.440	0.342	0.112	0.398	----

Degradation Rate Calculation, Cont'd.

Statistics of G Calculation:

$(MWH)_1$ = _____ 621 _____ , $(MWH)_2$ = _____ 1201 _____

$\sigma(F)/F$ = _____ 0.03 _____

|	$O\text{-}\emptyset_3$	$M\text{-}\emptyset_3$	$P\text{-}\emptyset_3$	omp	HB
15. Intercept, a_1	0.528	0.268	0.023	0.820	0.079
16. Slope, $b_1 \times 10^5$	-0.638	0.581	0.145	0.088	-1.576
17. $\sigma(a_1) \times 10^2$	0.326	0.213	0.050	0.450	0.925
18. $\sigma(b_1) \times 10^5$	0.344	0.225	0.053	0.475	0.987
19. $\sigma^2(C_{initial}) \times 10^8$					
(a) Coolant	163	69	4	310	793
(b) Sample Tank	163	54	4	315	793
(c) Makeup Tank	518	72	2	592	----
20. $\sigma^2(C_{final}) \times 10^8$					
(a) Coolant	156	68	4	299	616
(b) Sample Tank	178	60	5	345	616
(c) Makeup Tank	156	35	5	195	----
21. $\sigma^2(\Delta \text{ Correction})$					
(a) Coolant	62	27	1	118	371
(b) Sample Tank	188	53	1	454	178
(c) Makeup Tank	235	57	1	503	----
(d) Total	485	137	3	1075	549
22. $\sigma^2(\text{Net Transfer})$					
(a) Loop (D,L and X)	4	1	0	11	0
(b) Sample Tank	50	15	1	110	178
(c) Makeup Tank	140	49	1	237	----
(d) Total	194	65	2	358	178
23. $\sigma(W)/W$	0.038	0.052	0.275	0.039	0.031
24. $\sigma(G)/G$	0.049	0.060	0.277	0.050	0.043
25. $\sigma(G)$	0.011	0.006	0.001	0.016	0.013
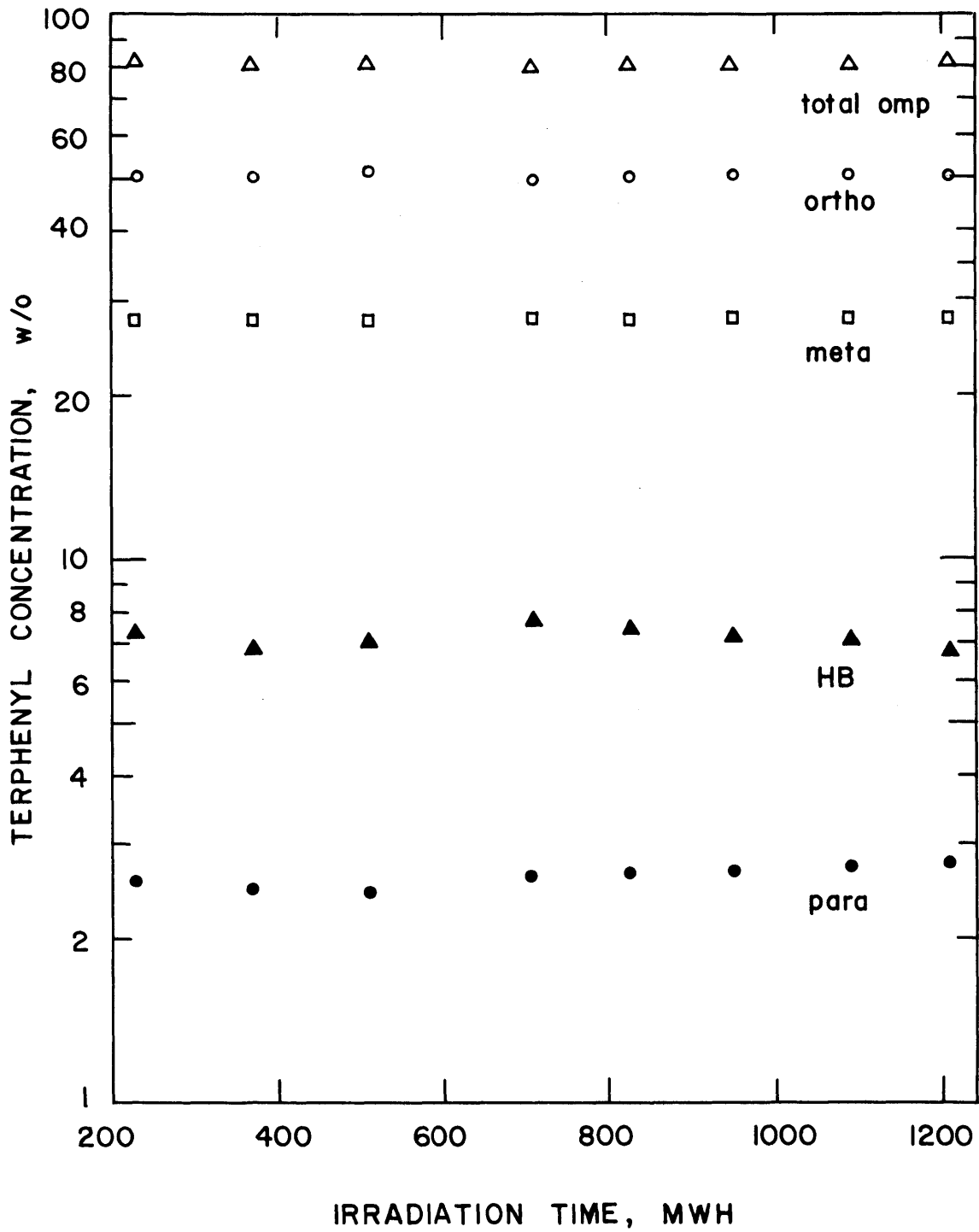
FIGURE A3.8   TERPHENYL AND HIGH BOILER CONCENTRATION
DURING RUN. 24 AT 750°F (399°C)

Table A3.12a

Summary of Irradiation of Santowax OM - Run 24

Sample No.	Sample Wt. (gram)	Accum Run Time (MWH)	Terphenyl Concentration - w/o				Concentration Variance x10^8				HB w/o	σ^2(HB)x10^8
			O	M	P	OMP	σ^2(O)	σ^2(M)	σ^2(P)	σ^2(OMP)		
S-2	2889	234	50.8	27.3	2.5	80.6	179	27	5	236	7.3	545
S-3	2914	367	50.7	27.3	2.5	80.6	122	19	3	161	7.2	372
S-4	3370	503	50.7	27.4	2.6	80.6	81	12	2	106	7.2	249
S-5	3151	712	50.6	27.4	2.6	80.6	51	8	1	67	7.1	164
S-6	3034	830	50.5	27.5	2.6	80.6	52	8	1	69	7.1	172
S-7	3032	947	50.5	27.5	2.7	80.7	66	10	2	88	7.1	221
S-8	3028	1091	50.4	27.6	2.7	80.7	101	16	3	135	7.0	336
S-9	3047	1214	50.3	27.6	2.7	80.7	146	22	4	195	7.0	482
M-2	1890	244	56.0	29.8	2.8	88.6	105	41	3	149	0	
M-3	2920	347	56.4	30.0	2.7	89.1	447	51	5	503	0	
M-4	2914	485	54.7	29.7	2.7	87.1	270	57	10	337	0	
M-5	3350	619	55.0	29.9	2.7	87.6	173	96	4	274	0	
M-6	3202	737	55.8	30.0	2.7	88.5	104	35	4	143	0	
M-7	3070	854	56.0	30.1	2.8	88.9	806	99	2	906	0	
M-8	2981	991	55.1	29.9	2.8	87.8	64	343	1	408	0	
M-9	3036	1112	55.0	29.6	2.8	87.4	274	230	4	508	0	
L-3	18	221	50.4	27.3	2.5	80.2	62	19	1	79	7.3	545
L-4	21	358	50.4	27.3	2.5	80.2	39	12	1	51	7.3	545
L-5	20	461	50.3	27.4	2.5	80.2	28	9	1	36	7.2	372
L-6	19	508	50.3	27.4	2.5	80.2	24	8	1	30	7.2	372
L-7	20	600	50.3	27.4	2.5	80.2	19	6	1	24	7.2	249
L-8	20	718	50.3	27.5	2.5	80.3	17	5	1	22	7.1	164
L-9	18	836	50.3	27.5	2.6	80.4	22	7	1	28	7.1	172
L-10	20	968	50.2	27.6	2.6	80.4	33	11	1	43	7.1	221
L-11	20	988	50.2	27.6	2.6	80.4	35	11	1	46	7.0	336
L-12	19	1078	50.2	27.6	2.7	80.4	48	16	1	62	7.0	375
L-13	16	1196	50.2	27.7	2.7	80.4	70	22	2	90	7.0	482
X-1	23	342	56.0	29.9	2.7	88.6	120	45	4	180	0	
X-2	28	493	54.9	29.8	2.7	88.4	315	65	10	450	0	
X-3	728	710	50.6	27.5	2.6	80.7	155	32	4	230	7.1	600
X-4	23	848	55.9	30.1	2.7	89.0	502	74	3	672	0	

Note: (1) Concentrations and Variances of S and L Samples were calculated from least square analysis

(2) Makeup Tank Calibration = 217.3 ± 0.5 gms/in; Sample Tank Calibration = 217.8 ± 0.6 gms/in

Table A3.12b

Degradation Rate Calculation

Run No. ___24___

Santowax OM

Summary:

Date: From ___6/20/67___   To ___7/7/67___

Irradiation Temp. ___750___ $^{\circ}$F   Type of Distillation ___HB___

Terphenyl Concentration ___80.3___ w/o   HB Concentration ___7.1___ w/o

Terphenyl Degraded ___1955___ gms   LIB/HB ___1.78___

Averaged Dose Rate, $\bar{r}$ ___0.057___ Watts/gm

Density, ρ ___0.796___ gms/cc   Length of Run ___1068___ MWH

In Pile Dose Rate Factor, F_T^{SW} ___71.3___ Watt-cc/MW-gm

Reactor Power ___4.88___ MW   Fast Neutron Fraction, f_N ___0.36___

G(-omp) ___0.376___ $\sigma(G)$ ___0.014___

Calculation of G:

	Total Coolant	$O\text{-}\emptyset_3$	$M\text{-}\emptyset_3$	$P\text{-}\emptyset_3$	omp	HB
1. Coolant Sample (L)						
(a) Avg. Conc.	1.000	0.503	0.275	0.025	0.803	0.071
(b) Grams Removed	210	106	58	5	169	15
2. Sample Tank (S)						
Tank Calib. (k_S) =	217.8 gm/in					
(a) Avg. Conc.	1.000	0.506	0.275	0.026	0.806	0.071
(b) Grams Removed	24465	12367	6720	639	19726	1743
3. Misc. Removals (X)						
(a) Avg. Conc.	1.000	0.510	0.277	0.026	0.813	0.065
(b) Grams Removed	826	421	228	22	671	54
4. Makeup Sample (D)						
(a) Avg. Conc.						
(b) Grams Removed	0					

Degradation Rate Calculation, Cont'd.

	Total Coolant	O-$\emptyset_3$	M-$\emptyset_3$	P-$\emptyset_3$	omp	HB
5. Makeup Tank (M)						
Tank Calib. (k_M) = 217.3gm/in						
(a) Avg. Conc.	1.000	0.555	0.299	0.027	0.881	0
(b) Grams Returned	23363	12961	6983	638	20582	0
6. Net Transferred						
(5.+4.-3.-2.-1.)	-2138	68	-23	-28	17	-1811
7. Initial Conc.						
(a) Coolant	1.000	0.504	0.272	0.025	0.801	0.073
(b) Sample Tank	1.000	0.508	0.273	0.025	0.806	0.073
(c) Makeup Tank	1.000	0.560	0.298	0.028	0.886	----
8. Initial Mass						
(a) Coolant	4964	2502	1350	123	3975	361
(b) Sample Tank	1398	710	382	35	1127	102
(c) Makeup Tank	5063	2834	1510	143	4487	----
9. Final Conc.						
(a) Coolant	1.000	0.502	0.277	0.026	0.804	0.070
(b) Sample Tank	1.000	0.503	0.276	0.027	0.807	0.070
(c) Makeup Tank	1.000	0.550	0.296	0.027	0.873	----
10. Final Mass						
(a) Coolant	5203	2610	1440	134	4184	364
(b) Sample Tank	1494	752	413	41	1206	104
(c) Makeup Tank	2592	1424	768	70	2262	----
11. Δ Correction (8.-10.)						
(a) Coolant	-239	-108	-90	-11	-208	-3
(b) Sample Tank	96	-41	-31	-6	-79	-3
(c) Makeup Tank	2471	1409	743	73	2225	0
(d) Total Δ Corr.	2138	1260	622	56	1938	-6
12. Total Mass Degraded, W						
(6.+11.(d))	0	1328	599	28	1955	-1817
13. G(-omp), G(-1), G(HB)		0.255	0.115	0.005	0.376	0.349
14. G*(-omp) = G(-omp)/C,						
G*(-1) = G(-1)/C_1		0.508	0.420	0.213	0.468	----

Degradation Rate Calculation, Cont'd.

Statistics of G Calculation:

$(MWH)_1$ = _____ 147 _____ , $(MWH)_2$ = _____ 1215 _____

$\sigma(F)/F$ = _____ 0.03 _____

|	$0\text{-}\varnothing_3$	$M\text{-}\varnothing_3$	$P\text{-}\varnothing_3$	omp	HB
15. Intercept, a_1	0.504	0.272	0.025	0.801	0.073
16. Slope, b_1 x 10^5	-0.219	0.417	0.082	0.268	-0.290
17. $\sigma(a_1)$ x 10^2	0.107	0.060	0.018	0.121	0.312
18. $\sigma(b_1)$ x 10^5	0.143	0.081	0.024	0.162	0.382
19. $\sigma^2(C_{initial})$ x 10^8					
(a) Coolant	62	19	2	79	545
(b) Sample Tank	179	27	5	236	545
(c) Makeup Tank	105	41	3	149	----
20. $\sigma^2(C_{final})$ x 10^8					
(a) Coolant	70	22	2	90	482
(b) Sample Tank	146	22	4	195	482
(c) Makeup Tank	274	230	4	508	----
21. $\sigma^2(\Delta \text{ Correction})$					
(a) Coolant	35	11	1	45	260
(b) Sample Tank	149	44	1	375	18
(c) Makeup Tank	221	72	1	524	----
(d) Total	405	127	3	944	277
22. $\sigma^2(\text{Net Transfer})$					
(a) Loop (D,L and X)	6	2	0	15	0
(b) Sample Tank	124	27	2	227	234
(c) Makeup Tank	264	104	3	447	----
(d) Total	394	133	5	689	234
23. $\sigma(W)/W$	0.021	0.027	0.100	0.021	0.013
24. $\sigma(G)/G$	0.037	0.040	0.104	0.037	0.033
25. $\sigma(G)$	0.009	0.005	0.001	0.014	0.011
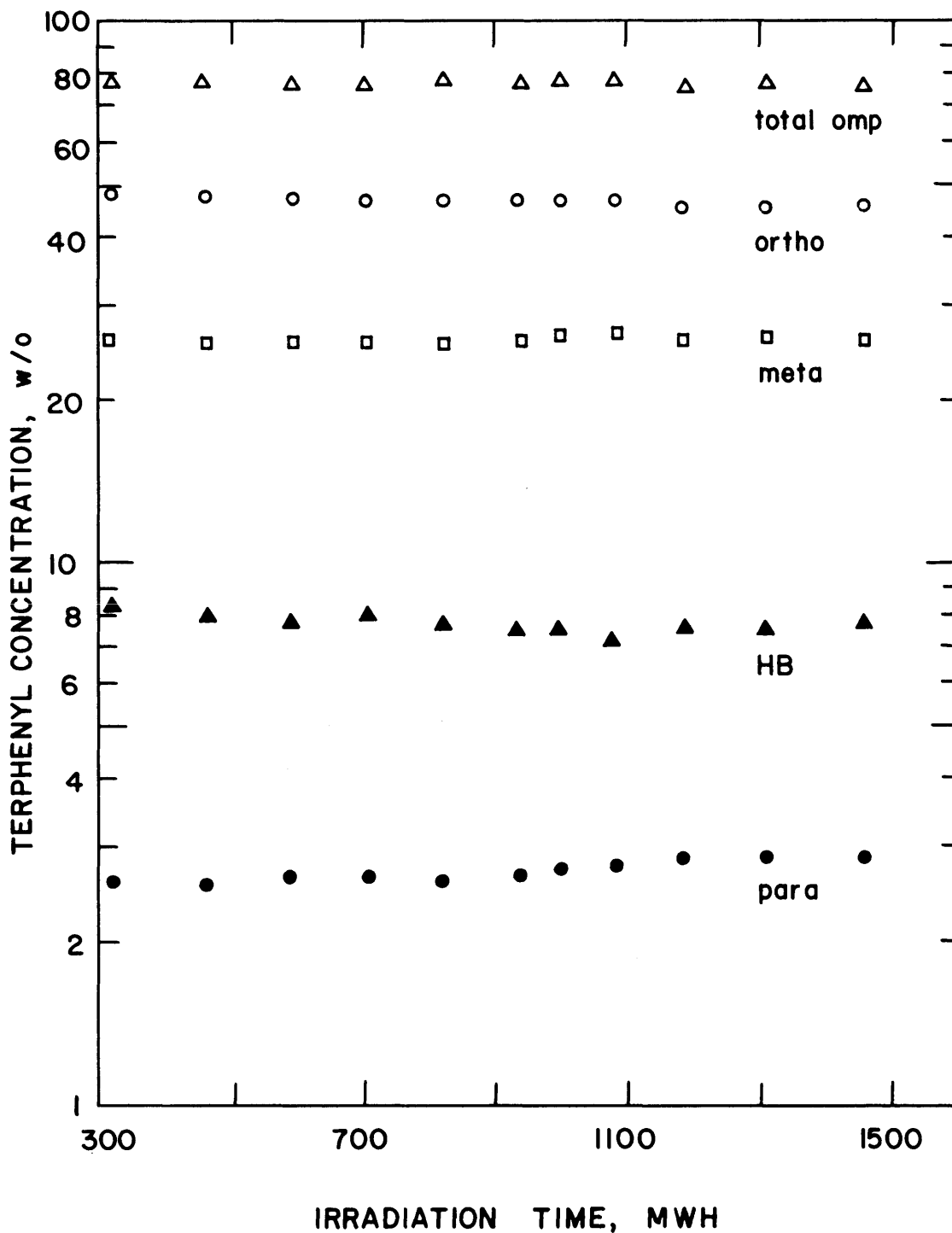
FIGURE A3.9   TERPHENYL AND HIGH BOILER CONCENTRATION
DURING RUN 25 AT 800°F (427 °C)

Table A3.13a

Summary of Irradiation of Santowax OM - Run 25

Sample No.	Sample Wt. (gram)	Accum. Run Time (MWH)	Terphenyl Concentration - w/o				Concentration Variance x10^8				HB w/o	σ^2(HB)x10^8
			O	M	P	OMP	σ^2(O)	σ^2(M)	σ^2(P)	σ^2(OMP)		
S-4	3861	593	47.3	26.6	2.6	76.5	85	46	2	185	7.8	141
S-5	3180	702	47.0	26.6	2.7	76.3	63	35	2	138	7.8	102
S-6	3929	824	46.8	26.7	2.7	76.2	48	27	1	107	7.7	77
S-7	3890	942	46.5	26.8	2.7	76.0	44	25	1	99	7.7	72
S-8	2280	1000	46.4	26.8	2.7	75.9	46	27	1	103	7.6	77
S-9	3272	1080	46.2	26.8	2.8	75.8	52	31	2	118	7.6	91
S-10	3993	1196	46.0	26.9	2.8	75.7	68	41	2	156	7.5	126
S-11	4005	1314	45.8	26.9	2.8	75.5	95	56	3	216	7.5	181
M-4	3864	517	52.9	29.6	2.9	85.3	329	95	5	429	0	
M-5	3839	622	53.4	29.7	3.0	86.1	273	218	3	494	0	
M-6	3181	741	52.2	29.2	2.9	84.3	312	153	7	471	0	
M-7	3967	858	52.8	29.3	2.9	85.1	1328	3	11	1341	0	
M-8	3861	967	52.6	29.5	3.0	85.1	729	172	7	909	0	
M-9	2349	1075	52.8	29.5	3.0	85.2	407	142	2	551	0	
M-10	3339	1114	51.6	29.5	3.0	84.0	71	41	4	115	0	
M-11	4050	1225	51.6	29.6	2.9	84.0	570	104	15	688	0	
M-12	4015	1342	51.3	29.6	2.9	83.8	338	158	7	503	0	
L-6	19	599	47.0	26.7	2.8	76.5	79	39	2	212	7.9	210
L-7	24	718	46.8	26.7	2.8	76.3	56	27	2	149	7.8	141
L-8	23	835	46.6	26.8	2.8	76.2	43	21	1	115	7.7	77
L-9	18	953	46.4	26.8	2.8	76.0	40	20	1	107	7.7	72
L-10	17	995	46.3	26.8	2.8	75.9	41	21	1	110	7.6	77
L-11	20	1100	46.1	26.8	2.8	75.8	49	25	1	134	7.6	91
L-12	19	1216	46.0	26.9	2.8	75.6	68	35	2	186	7.5	126
L-13	20	1323	45.8	26.9	2.8	75.4	94	48	3	256	7.5	181
X-1	298	953	46.5	26.8	2.7	76.0	47	26	2	120	7.7	220

Note: (1) Concentrations and Variances of S and L Samples were calculated from least square analysis

(2) Makeup Tank Calibration = 217.1 ± 0.4 gms/in; Sample Tank Calibration = 217.3 ± 0.4 gms/in

Table A3.13b

Degradation Rate Calculation

Run No. ___25___

Santowax OM

Summary:

Date: From ___7/17/67___   To ___7/28/67___

Irradiation Temp.___800___°F   Type of Distillation___HB___

Terphenyl Concentration ___76.0___ w/o   HB Concentration ___7.7___ w/o

Terphenyl Degraded ___2866___ gms   LIB/HB ___2.12___

Averaged Dose Rate, $\bar{r}$ ___0.056___ Watts/gm

Density, ρ ___0.774___ gms/cc   Length of Run ___908___ MWH

In Pile Dose Rate Factor, F_T^{SW} ___70.1___ Watt-cc/MW-gm

Reactor Power ___4.86___ MW   Fast Neutron Fraction, f_N ___0.36___

G(-omp) ___0.678___ $\sigma(G)$ ___0.023___

Calculation of G:

	Total Coolant	$O-\emptyset_3$	$M-\emptyset_3$	$P-\emptyset_3$	omp	HB
1. Coolant Sample (L)						
(a) Avg. Conc.	1.000	0.464	0.268	0.028	0.760	0.077
(b) Grams Removed	160	74	43	4	121	12
2. Sample Tank (S)						
Tank Calib. (k_S) =	217.3gm/in					
(a) Avg. Conc.	1.000	0.465	0.268	0.027	0.760	0.077
(b) Grams Removed	28410	13209	7602	772	21582	2174
3. Misc. Removals (X)						
(a) Avg. Conc.	1.000	0.465	0.268	0.027	0.760	0.077
(b) Grams Removed	298	139	80	8	227	23
4. Makeup Sample (D)						
(a) Avg. Conc.						
(b) Grams Removed	0					

Degradation Rate Calculation, Cont'd.

	Total Coolant	O-ϕ_3	M-ϕ_3	P-ϕ_3	omp	HB
5. Makeup Tank (M)						
Tank Calib. (k_M) = 217.1gm/in						
(a) Avg. Conc.	1.000	0.523	0.295	0.029	0.848	0
(b) Grams Returned	32465	16986	9579	953	27518	0
6. Net Transferred						
(5.+4.-3.-2.-1.)	3597	3564	1854	169	5587	-2209
7. Initial Conc.						
(a) Coolant	1.000	0.471	0.267	0.027	0.765	0.079
(b) Sample Tank	1.000	0.474	0.266	0.026	0.766	0.079
(c) Makeup Tank	1.000	0.532	0.294	0.029	0.855	----
8. Initial Mass						
(a) Coolant	4672	2194	1248	129	3571	368
(b) Sample Tank	2646	1254	703	69	2026	209
(c) Makeup Tank	1355	720	399	39	1158	----
9. Final Conc.						
(a) Coolant	1.000	0.456	0.269	0.028	0.753	0.074
(b) Sample Tank	1.000	0.456	0.270	0.028	0.753	0.074
(c) Makeup Tank	1.000	0.513	0.296	0.029	0.839	----
10. Final Mass						
(a) Coolant	5038	2298	1355	141	3794	373
(b) Sample Tank	4493	2045	1212	128	3384	333
(c) Makeup Tank	2739	1404	812	81	2297	----
11. Δ Correction						
(8.-10.)						
(a) Coolant	-366	-104	-107	-12	-223	-5
(b) Sample Tank	-1847	-791	-509	-59	-1358	-124
(c) Makeup Tank	-1384	-684	-413	-42	-1139	----
(d) Total Δ Corr.	-3597	-1579	-1029	-113	-2720	-129
12. Total Mass Degraded, W						
(6.+11.(d))	0	1985	825	56	2866	-2338
13. G(-omp), G(-1), G(HB)		0.470	0.195	0.013	0.678	0.553
14. G*(-omp) = G(-omp)/C,						
G*(-1) = G(-1)/C_1		1.013	0.728	0.479	0.893	----

Degradation Rate Calculation, Cont'd.

<u>Statistics of G Calculation:</u>

$(MWH)_1 =$ ____517____ , $(MWH)_2 =$ ____1425____

$\sigma(F)/F =$ ____0.03____

|	$O-\emptyset_3$	$M-\emptyset_3$	$P-\emptyset_3$	omp	HB
15. Intercept, a_i	0.479	0.266	0.027	0.774	0.081
16. Slope, b_i x 10^5	-1.614	0.233	0.029	-1.466	-0.516
17. $\sigma(a_i)$ x 10^2	0.187	0.131	0.031	0.307	0.252
18. $\sigma(b_i)$ x 10^5	0.189	0.134	0.032	0.311	0.261
19. $\sigma^2(C_{initial})$ x 10^8					
(a) Coolant	105	51	3	281	210
(b) Sample Tank	85	46	2	185	210
(c) Makeup Tank	86	136	1	224	----
20. $\sigma^2(C_{final})$ x 10^8					
(a) Coolant	126	65	4	344	253
(b) Sample Tank	130	77	4	296	253
(c) Makeup Tank	338	158	7	503	----
21. $\sigma^2(\Delta$ Correction)					
(a) Coolant	61	30	2	162	119
(b) Sample Tank	151	57	1	393	47
(c) Makeup Tank	175	59	1	440	----
(d) Total	387	146	4	995	166
22. σ^2(Net Transfer)					
(a) Loop (D,L and X)	8	2	0	20	0
(b) Sample Tank	110	53	2	266	118
(c) Makeup Tank	678	162	9	930	---
(d) Total	796	217	11	1216	118
23. $\sigma(W)/W$	0.017	0.023	0.069	0.016	0.007
24. $\sigma(G)/G$	0.035	0.038	0.075	0.034	0.031
25. $\sigma(G)$	0.016	0.007	0.001	0.023	0.017
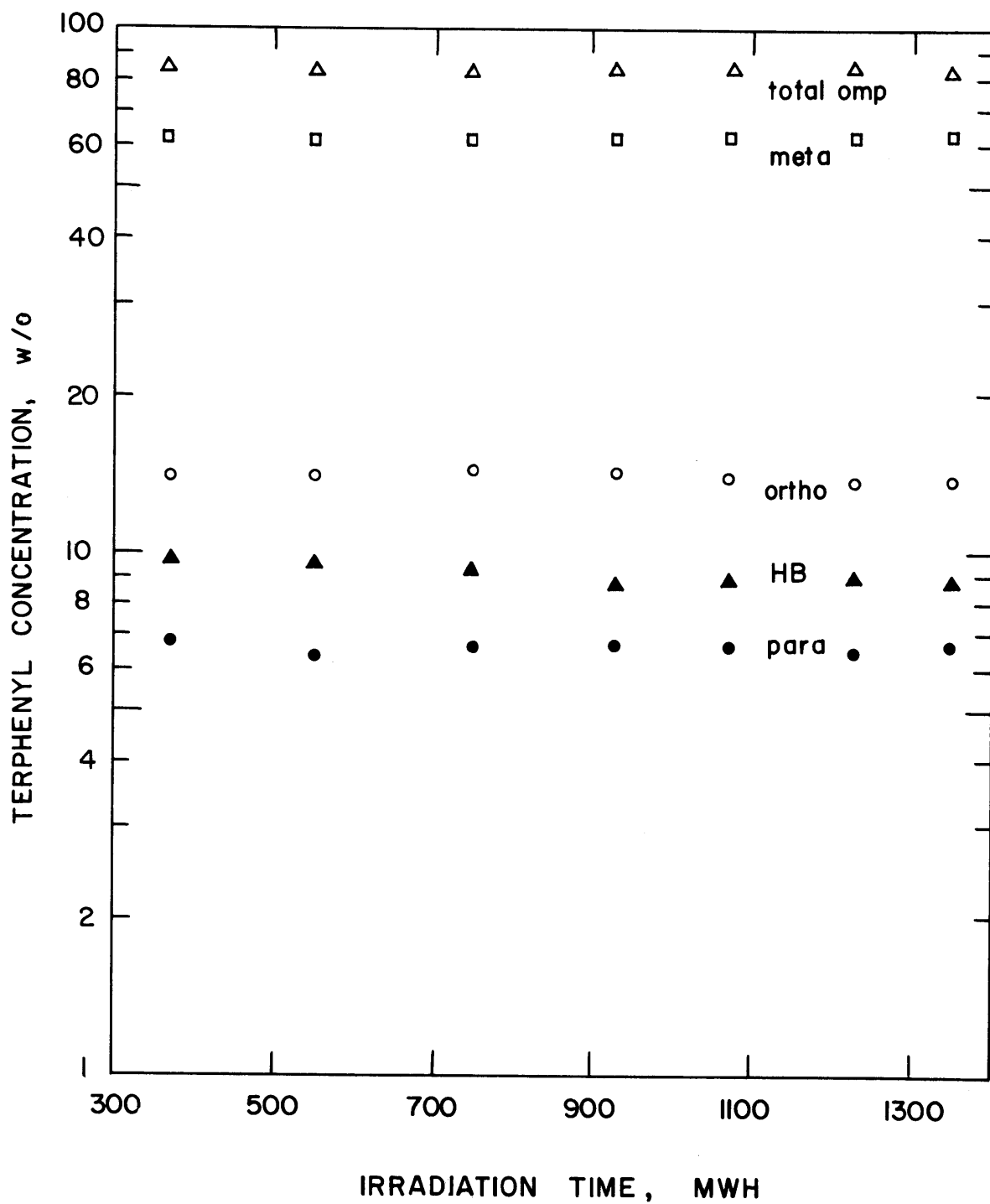
FIGURE A3.10   TERPHENYL AND HIGH BOILER CONCENTRATION
DURING RUN 26 AT 700°F (371 °C)

Table A3.14a

Summary of Irradiation of Santowax WR - Run 26

Sample No.	Sample Wt. (gram)	Accum. Run Time (MWH)	Terphenyl Concentration - w/o				Concentration Variance x10^8				HB w/o	σ^2(HB)x10^8
			O	M	P	OMP	σ^2(O)	σ^2(M)	σ^2(P)	σ^2(OMP)		
S-4	3240	366	14.2	61.5	6.6	82.3	22	202	13	297	9.7	155
S-5	3473	554	14.1	61.6	6.6	82.3	13	117	11	173	9.5	140
S-6	3734	745	14.1	61.8	6.6	82.4	7	68	6	100	9.3	80
S-7	3718	936	14.0	61.9	6.6	82.5	6	56	5	82	9.1	62
S-8	3034	1077	13.9	62.0	6.6	82.5	8	71	7	103	8.9	76
S-9	2802	1224	13.9	62.1	6.6	82.6	11	108	10	157	8.7	116
S-10	3114	1351	13.9	62.2	6.5	82.6	17	157	15	229	8.6	170
M-4	3769	316	16.4	70.7	7.2	94.2	7	392	10	409	0	
M-5	2736	456	16.6	70.2	7.1	93.9	5	58	16	79	0	
M-6	3501	557	15.6	68.7	7.2	91.5	60	663	5	729	0	
M-7	3496	749	15.7	69.7	7.1	92.6	10	133	5	149	0	
M-8	3776	822	15.6	68.6	7.1	91.3	6	89	12	107	0	
M-9	3783	1092	15.4	69.3	7.1	91.8	15	1	1	43	0	
M-10	3011	1231	15.2	68.1	6.9	90.2	33	162	10	205	0	
M-11	3037	1357	15.6	70.6	7.0	93.1	15	289	2	306	0	
L-3	16	436	14.1	61.2	6.4	81.8	10	68	6	126	9.7	155
L-4	10	582	14.1	61.2	6.5	81.7	7	49	4	91	9.5	140
L-5	21	691	14.0	61.2	6.5	81.7	6	40	3	73	9.3	80
L-6	19	832	13.9	61.2	6.5	81.6	5	34	3	62	9.3	80
L-7	21	1062	13.8	61.3	6.5	81.6	6	39	3	70	8.9	76
L-8	20	1180	13.8	61.3	6.5	81.6	7	48	4	86	8.7	116
L-9	21	1331	13.7	61.3	6.5	81.5	10	65	6	123	8.6	170
X-1	2360	836	15.8	69.5	7.1	92.3	60	660	5	729	0	

Note: (1) Concentrations and Variances of S and L Samples were calculated from least square analysis

(2) Makeup Tank Calibration = 210.9 ± 0.9 gms/in; Sample Tank Calibration = 211.4 ± 0.7 gms/in.

Table A3.14b

Degradation Rate Calculation

Run No. __26__

Santowax WR

Summary:

Date: From __11/16/67__ To __12/5/67__

Irradiation Temp. __700__ °F   Type of Distillation __HB__

Terphenyl Concentration __82.5__ w/o   HB Concentration __9.13__ w/o

Terphenyl Degraded __2117__ gms   LIB/HB __0.92__

Averaged Dose Rate, $\bar{r}$ __0.068__ Watts/gm

Density, ρ __0.832__ gms/cc   Length of Run __1053__ MWH

In Pile Dose Rate Factor, F_T^{SW} __85.3__ Watt-cc/MW-gm

Reactor Power __4.88__ MW   Fast Neutron Fraction, f_N __0.38__

G(-omp) __0.328__ $\sigma(G)$ __0.012__

Calculation of G:

	Total Coolant	$O\text{-}\emptyset_3$	$M\text{-}\emptyset_3$	$P\text{-}\emptyset_3$	omp	HB
1. Coolant Sample (L)						
(a) Avg. Conc.	1.000	0.139	0.613	0.065	0.817	0.091
(b) Grams Removed	128	18	78	8	104	12
2. Sample Tank (S)						
Tank Calib. (k_S) =	211.4gm/in					
(a) Avg. Conc.	1.000	0.140	0.619	0.066	0.825	0.091
(b) Grams Removed	23115	3237	14298	1522	19057	2109
3. Misc. Removals (X)						
(a) Avg. Conc.	1.000	0.157	0.695	0.071	0.923	0
(b) Grams Removed	2360	372	1640	167	2179	0
4. Makeup Sample (D)						
(a) Avg. Conc.						
(b) Grams Removed	0					

Degradation Rate Calculation, Cont'd.

	Total Coolant	$O\text{-}\phi_3$	$M\text{-}\phi_3$	$P\text{-}\phi_3$	omp	HB
5. Makeup Tank (M)						
Tank Calib. (k_M) = 210.9gm/in						
(a) Avg. Conc.	1.000	0.157	0.695	0.071	0.923	0
(b) Grams Returned	27109	4271	18835	1918	25024	0
6. Net Transferred						
(5.+4.-3.-2.-1.)	1507	644	2819	201	3684	-2121
7. Initial Conc.						
(a) Coolant	1.000	0.141	0.612	0.064	0.817	0.097
(b) Sample Tank	1.000	0.142	0.615	0.066	0.823	0.097
(c) Makeup Tank	1.000	0.161	0.714	0.073	0.948	0
8. Initial Mass						
(a) Coolant	4883	690	2993	315	3998	475
(b) Sample Tank	2853	404	1754	189	2347	277
(c) Makeup Tank	2061	332	1471	151	1954	0
9. Final Conc.						
(a) Coolant	1.000	0.137	0.613	0.065	0.815	0.086
(b) Sample Tank	1.000	0.138	0.622	0.066	0.826	0.086
(c) Makeup Tank	1.000	0.156	0.706	0.070	0.932	0
10. Final Mass						
(a) Coolant	4772	652	2924	312	3888	409
(b) Sample Tank	1017	141	633	67	841	87
(c) Makeup Tank	5515	859	3894	384	5137	0
11. Δ Correction						
(8.-10.)						
(a) Coolant	111	38	69	3	110	66
(b) Sample Tank	1836	263	1121	122	1506	190
(c) Makeup Tank	-3454	-527	-2423	-233	-3183	0
(d) Total Δ Corr.	-1507	-226	-1583	-108	-1567	256
12. Total Mass Degraded, W						
(6.+11.(d))	0	418	1586	113	2117	-1865
13. G(-omp), G(-i), G(HB)		0.065	0.245	0.018	0.328	0.289
14. $G^*(\text{-omp}) = G(\text{-omp})/C$,						
$G^*(\text{-i}) = G(\text{-i})/C_i$		0.463	0.396	0.266	0.397	----

Degradation Rate Calculation, Cont'd.

Statistics of G Calculation:

$(MWH)_1 = \underline{\hspace{1em} 308 \hspace{1em}}$, $(MWH)_2 = \underline{\hspace{1em} 1361 \hspace{1em}}$

$\sigma(F)/F = \underline{\hspace{1em} 0.03 \hspace{1em}}$

	$O-\emptyset_3$	$M-\emptyset_3$	$P-\emptyset_3$	omp	HB
15. Intercept, a_i	0.143	0.612	0.066	0.821	0.101
16. Slope, $b_i \times 10^5$	-0.330	0.763	-0.052	0.372	-1.157
17. $\sigma(a_i) \times 10^2$	0.071	0.217	0.067	0.263	0.189
18. $\sigma(b_i) \times 10^5$	0.074	0.225	0.069	0.273	0.193
19. $\sigma^2(C_{initial}) \times 10^8$					
(a) Coolant	10	68	6	126	155
(b) Sample Tank	22	202	19	297	155
(c) Makeup Tank	41	626	10	677	0
20. $\sigma^2(C_{final}) \times 10^8$					
(a) Coolant	10	65	6	123	170
(b) Sample Tank	17	157	15	229	170
(c) Makeup Tank	15	289	2	306	0
21. $\sigma^2(\Delta$ Correction)					
(a) Coolant	5	31	3	58	82
(b) Sample Tank	13	232	3	410	9
(c) Makeup Tank	22	455	4	741	0
(d) Total	40	718	10	1209	91
22. $\sigma^2(Net Transfer)$					
(a) Loop (D,L and X)	1	11	0	19	0
(b) Sample Tank	29	347	19	463	89
(c) Makeup Tank	12	150	8	240	0
(d) Total	42	508	27	722	89
23. $\sigma(W)/W$	0.022	0.022	0.054	0.021	0.007
24. $\sigma(G)/G$	0.037	0.037	0.062	0.037	0.030
25. $\sigma(G)$	0.002	0.009	0.001	0.012	0.009
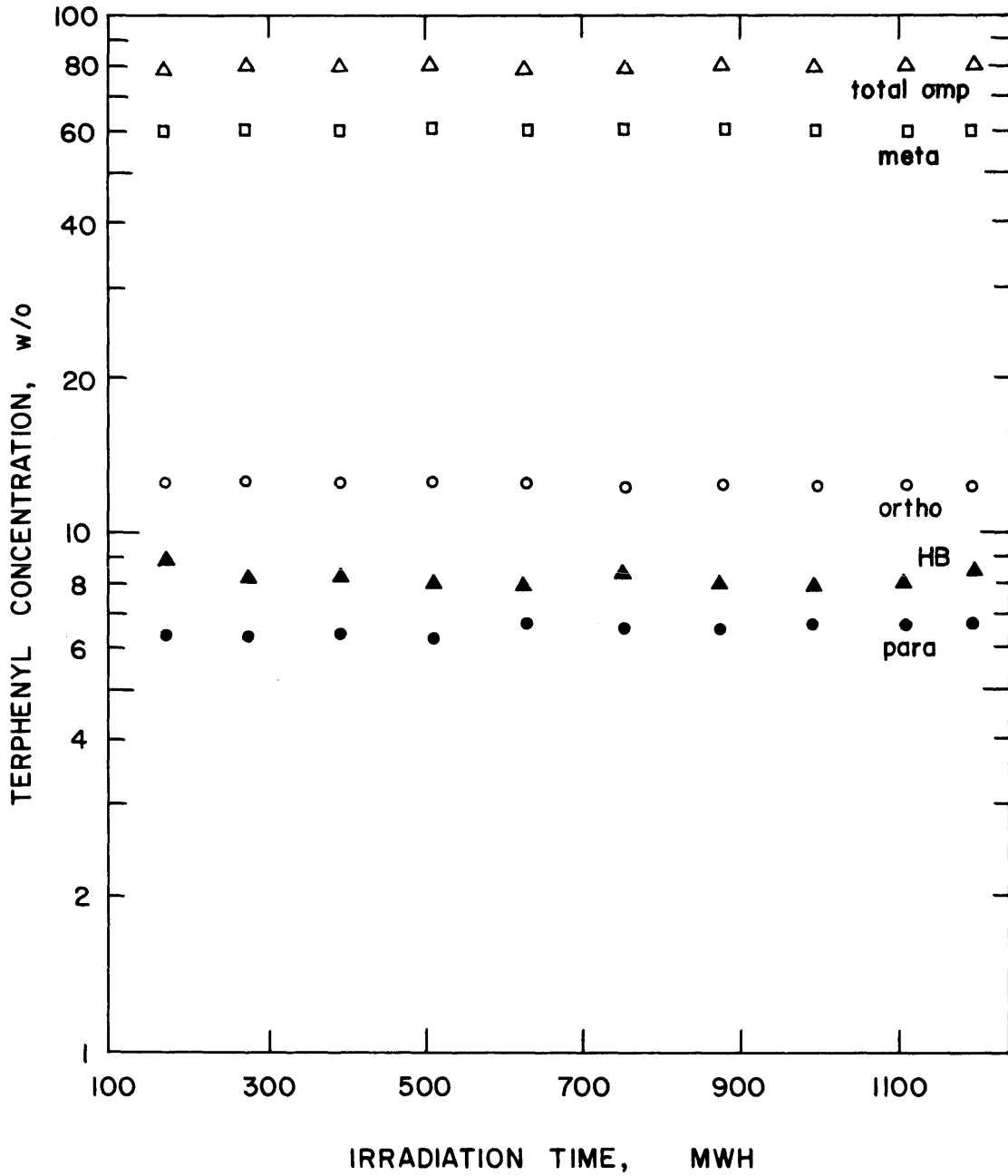
FIGURE A3.11   TERPHENYL AND HIGH BOILER CONCENTRATION
DURING RUN 27 AT 750°F (399°C)

Table A3.15a

Summary of Irradiation of Santowax WR - Run 27

Sample No.	Sample Wt. (gram)	Accum. Run Time (MWH)	Terphenyl Concentration - w/o				Concentration Variance x10^8				HB w/o	σ^2(HB)x10^8
			O	M	P	OMP	σ^2(O)	σ^2(M)	σ^2(P)	σ^2(OMP)		
S-4	3214	169	12.7	60.1	6.3	79.2	6	203	12	235	8.4	413
S-5	2353	268	12.7	60.2	6.4	79.2	5	152	9	176	8.3	312
S-6	2825	389	12.6	60.2	6.4	79.2	4	106	6	123	8.3	218
S-7	2793	501	12.5	60.3	6.4	79.3	3	78	4	90	8.2	157
S-8	2843	632	12.4	60.4	6.5	79.3	2	62	4	72	8.2	120
S-9	3000	754	12.4	60.4	6.6	79.3	2	65	4	74	8.1	118
S-10	3019	876	12.3	60.5	6.6	79.4	3	83	5	96	8.1	147
S-11	2503	994	12.2	60.5	6.6	79.4	3	118	7	135	8.0	205
S-12	2390	1107	12.1	60.6	6.7	79.4	5	165	10	190	7.9	288
S-13	1767	1197	12.1	60.6	6.7	79.4	7	212	13	240	7.9	373
M-5	3442	210	14.6	68.4	7.3	90.3	4	183	7	194	0	
M-6	3182	349	14.2	67.6	6.9	88.8	1	669	10	681	0	
M-7	2002	458	14.0	67.8	7.0	88.8	8	105	9	122	0	
M-8	3000	573	14.0	67.6	6.9	88.5	14	292	5	311	0	
M-9	2539	690	13.9	67.2	7.1	88.2	17	6	22	45	0	
M-10	2655	823	14.1	67.7	7.0	88.8	4	82	3	89	0	
M-11	3474	946	13.7	67.2	7.0	87.9	27	41	22	90	0	
M-12	3142	1049	13.5	67.4	7.2	88.2	11	184	3	198	0	
L-5	23	314	12.8	60.8	6.7	80.2	14	465	8	598	8.3	312
L-6	22	314	12.8	60.8	6.7	80.2	14	465	8	598	8.3	312
L-7	24	526	12.6	60.6	6.7	79.9	7	243	4	312	8.2	157
L-8	23	654	12.5	60.5	6.7	79.6	6	210	4	270	8.2	120
L-9	22	906	12.3	60.3	6.7	79.3	11	369	6	471	8.1	147
L-10	155	1141	12.2	60.1	6.7	78.9	23	781	13	997	7.9	373
D-1	157	1188	15.6	71.9	9.0	96.6	7	847	22	875	0	
X-1	311	683	12.4	60.4	6.5	79.3	6	120	9	230	8.2	310

Note: (1) Concentrations and Variances of S and L Samples were calculated from least square analysis

(2) Makeup Tank Calibration = 208.3 ± 0.8 gms/in; Sample Tank Calibration = 213.5 ± 0.4 gms/in

Table A3.15b

Degradation Rate Calculation

Run No. __27__

Santowax WR

Summary:

Date: From ____12/27/67____   To ____1/15/68____

Irradiation Temp. ___750___ ^{o}F   Type of Distillation ___HB___

Terphenyl Concentration _79.3_ w/o   HB Concentration ___8.2___ w/o

Terphenyl Degraded ___2541___ gms   LIB/HB _____1.52_____

Averaged Dose Rate, $\bar{r}$ ____0.065____ Watts/gm

Density, ρ ____0.808____ gms/cc   Length of Run ____1128____ MWH

In Pile Dose Rate Factor, F_T^{SW} ___83.5___ Watt-cc/MW-gm

Reactor Power ____4.87____ MW   Fast Neutron Fraction, f_N _0.38_

G(-omp) ____0.389____ $\sigma(G)$ ____0.013____

Calculation of G:

	Total Coolant	$O\text{-}\phi_3$	$M\text{-}\phi_3$	$P\text{-}\phi_3$	omp	HB
1. Coolant Sample (L)						
(a) Avg. Conc.	1.000	0.124	0.603	0.066	0.793	0.081
(b) Grams Removed	269	33	162	18	213	22
2. Sample Tank (S)						
Tank Calib. (k_S) =	213.5gm/in					
(a) Avg. Conc.	1.000	0.124	0.604	0.065	0.793	0.082
(b) Grams Removed	26707	3316	16124	1739	21179	2176
3. Misc. Removals (X)						
(a) Avg. Conc.	1.000	0.124	0.604	0.065	0.793	0.082
(b) Grams Removed	311	39	188	20	247	25
4. Makeup Sample (D)						
(a) Avg. Conc.	1.000	0.156	0.719	0.090	0.966	0
(b) Grams Removed	157	25	113	14	152	0

Degradation Rate Calculation, Cont'd.

	Total Coolant	O-$\emptyset_3$	M-$\emptyset_3$	P-$\emptyset_3$	omp	HB
5. Makeup Tank (M) Tank Calib. (k_M) = 208.3gm/in						
(a) Avg. Conc.	1.000	0.140	0.676	0.071	0.887	0
(b) Grams Returned	23436	3282	15849	1654	20785	0
6. Net Transferred (5.+4.-3.-2.-1.)	-3694	-81	-512	-109	-702	-2223
7. Initial Conc.						
(a) Coolant	1.000	0.127	0.601	0.063	0.792	0.084
(b) Sample Tank	1.000	0.127	0.602	0.063	0.793	0.084
(c) Makeup Tank	1.000	0.146	0.684	0.073	0.903	0
8. Initial Mass						
(a) Coolant	4614	587	2774	291	3652	386
(b) Sample Tank	2033	259	1222	128	1609	170
(c) Makeup Tank	4557	664	3117	332	4112	0
9. Final Conc.						
(a) Coolant	1.000	0.121	0.606	0.067	0.794	0.079
(b) Sample Tank	1.000	0.121	0.607	0.067	0.795	0.079
(c) Makeup Tank	1.000	0.135	0.674	0.072	0.882	0
10. Final Mass						
(a) Coolant	4817	582	2921	324	3827	381
(b) Sample Tank	818	99	496	55	650	65
(c) Makeup Tank	1874	254	1264	135	1653	----
11. Δ Correction (8.-10.)						
(a) Coolant	-204	5	-147	-33	-175	5
(b) Sample Tank	1215	160	726	73	959	105
(c) Makeup Tank	2683	410	1852	197	2459	0
(d) Total Δ Corr.	3694	575	2431	237	3243	110
12. Total Mass Degraded, W (6.+11.(d))	0	494	1919	128	2541	-2113
13. G(-omp), G(-1), G(HB)		0.076	0.294	0.020	0.389	0.324
14. G*(-omp) = G(-omp)/C, G*(-1) = G(-1)/C_1		0.608	0.487	0.302	0.491	----

Degradation Rate Calculation, Cont'd.

Statistics of G Calculation:

$(MWH)_1$ = _____ 70 _____, $(MWH)_2$ = _____ 1198 _____

$\sigma(F)/F$ = _____ 0.03 _____

|	$O\text{-}\emptyset_3$	$M\text{-}\emptyset_3$	$P\text{-}\emptyset_3$	omp	HB
15. Intercept, a_1	0.128	0.601	0.062	0.791	0.085
16. Slope, b_1 x 10^5	-0.616	0.497	0.417	0.291	-0.459
17. $\sigma(a_1)$ x 10^2	0.032	0.177	0.042	0.190	0.251
18. $\sigma(b_1)$ x 10^5	0.042	0.235	0.057	0.253	0.324
19. $\sigma^2(C_{initial})$ x 10^8					
(a) Coolant	7	203	12	235	413
(b) Sample Tank	7	203	12	235	413
(c) Makeup Tank	4	183	7	194	----
20. $\sigma^2(C_{final})$ x 10^8					
(a) Coolant	7	212	13	240	373
(b) Sample Tank	7	212	13	240	373
(c) Makeup Tank	11	184	3	198	----
21. $\sigma^2(\Delta$ Correction)					
(a) Coolant	4	93	6	106	175
(b) Sample Tank	6	154	2	263	9
(c) Makeup Tank	11	258	4	428	----
(d) Total	21	505	12	797	184
22. $\sigma^2(Net$ Transfer)					
(a) Loop (D,L and X)	5	12	2	20	2
(b) Sample Tank	12	230	8	322	166
(c) Makeup Tank	3	177	6	256	----
(d) Total	20	419	16	598	168
23. $\sigma(W)/W$	0.013	0.016	0.041	0.015	0.009
24. $\sigma(G)/G$	0.033	0.034	0.051	0.034	0.031
25. $\sigma(G)$	0.003	0.010	0.001	0.013	0.010
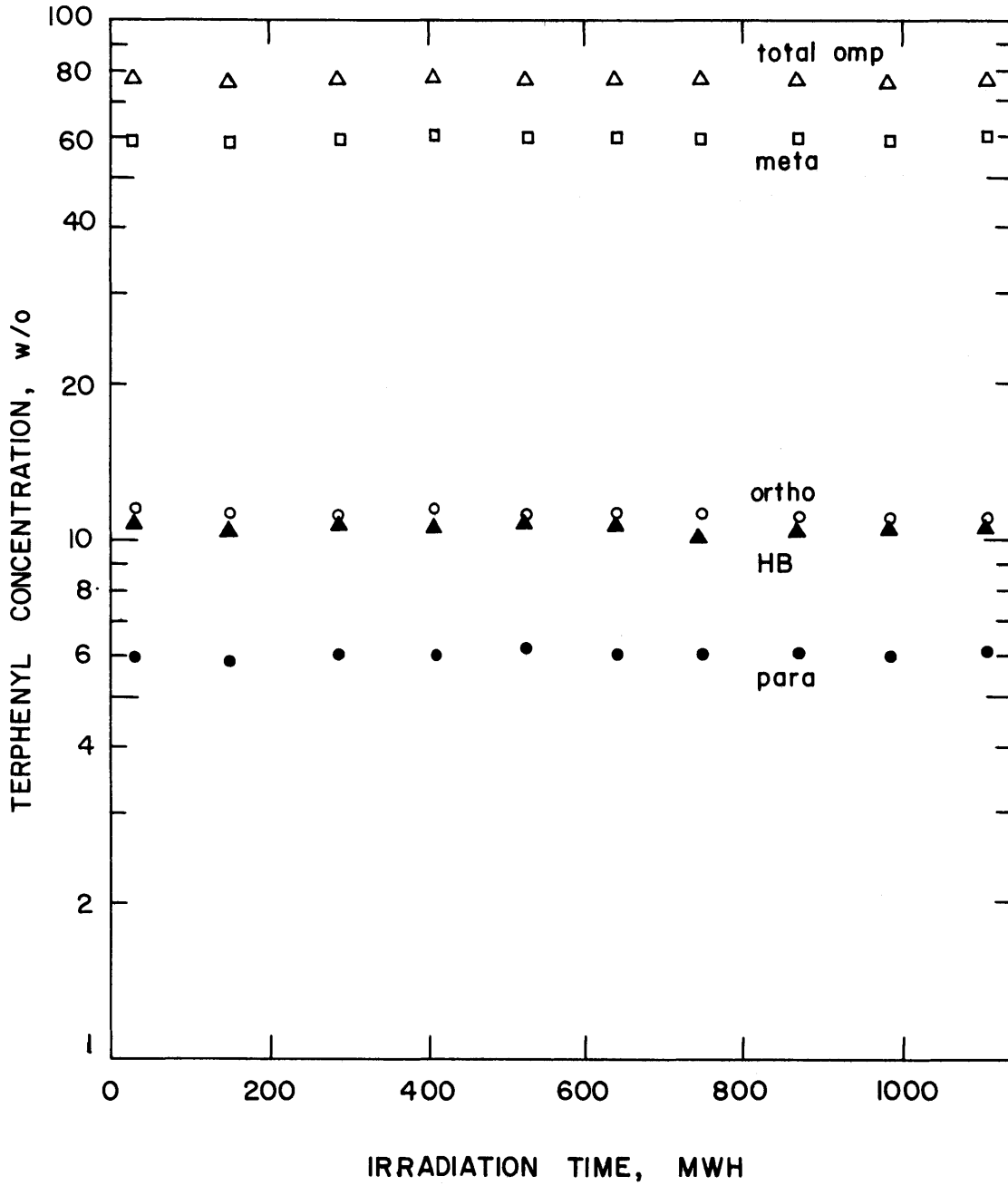
FIGURE A3.12   TERPHENYL AND HIGH BOILER CONCENTRATION
DURING RUN 28 AT 800°F (427°C)

Table A3.16a

Summary of Irradiation of Santowax WR - Run 28

Sample No.	Sample Wt. (gram)	Accum. Run Time (MWH)	Terphenyl Concentration - w/o				Concentration Variance x10^8				HB w/o	σ^2(HB)x10^8
			O	M	P	OMP	σ^2(O)	σ^2(M)	σ^2(P)	σ^2(OMP)		
S-10	3887	287	11.3	59.2	6.0	76.5	6	79	7	109	10.8	197
S-11	3714	404	11.2	59.2	6.0	76.4	4	58	5	81	10.7	144
S-12	3536	521	11.1	59.2	6.1	76.4	3	47	4	67	10.7	117
S-13	3436	640	11.1	59.2	6.1	76.4	3	46	4	68	10.7	116
S-14	3356	750	11.0	59.2	6.1	76.3	4	55	5	84	10.6	139
S-15	3452	868	11.0	59.2	6.1	76.3	5	74	7	115	10.6	190
S-16	3575	985	10.9	59.2	6.1	76.2	7	104	10	161	10.6	266
S-17	3487	1140	10.8	59.2	6.1	76.2	11	158	16	246	10.5	408
M-10	3587	326	13.3	68.5	6.5	88.2	19	40	25	84	0	
M-11	3573	420	13.1	68.2	6.7	87.9	5	793	51	849	0	
M-12	4215	541	13.2	67.5	6.7	87.5	5	54	4	63	0	
M-13	3488	658	12.9	67.8	6.6	87.3	1	47	14	62	0	
M-14	3123	769	13.0	68.9	6.7	88.6	8	78	27	113	0	
M-15	3481	892	12.9	67.7	6.8	87.4	40	43	5	88	0	
M-16	3764	1003	12.9	67.6	7.1	87.7	14	194	10	218	0	
M-17	3625	1128	12.7	68.1	7.0	87.8	11	49	25	85	0	
X-1	546	714	11.1	59.2	6.1	76.3	6	140	11	230	10.7	380

Note: (1) Concentrations and Variances of S Samples were calculated from least square analysis

(2) Makeup Tank Calibration = 212.6 ± 0.5 gms/in; Sample Tank Calibration = 211.4 ± 0.6 gms/in

Table A3.16b

Degradation Rate Calculation

Run No. __28__

Santowax WR

Summary:

Date: From ___2/6/68___ To ___2/16/68___

Irradiation Temp. ___800___ °F   Type of Distillation ___HB___

Terphenyl Concentration _76.3_ w/o   HB Concentration ___10.6___ w/o

Terphenyl Degraded ___3081___ gms   LIB/HB ___1.24___

Averaged Dose Rate, $\bar{r}$ ___0.065___ Watts/gm

Density, ρ ___0.788___ gms/cc   Length of Run ___876___ MWH

In Pile Dose Rate Factor, F_T^{SW} ___81.7___ Watt-cc/MW-gm

Reactor Power ___4.89___ MW   Fast Neutron Fraction, f_N _0.38_

G(-omp) ___0.636___ $\sigma(G)$ ___0.021___

Calculation of G:

	Total Coolant	$O-\emptyset_3$	$M-\emptyset_3$	$P-\emptyset_3$	omp	HB
1. Coolant Sample (L)						
(a) Avg. Conc.						
(b) Grams Removed	0					
2. Sample Tank (S)						
Tank Calib. (k_S) =	211.4 gm/in					
(a) Avg. Conc.	1.000	0.110	0.592	0.061	0.763	0.107
(b) Grams Removed	28443	3142	16837	1726	21704	3030
3. Misc. Removals (X)						
(a) Avg. Conc.	1.000	0.111	0.592	0.061	0.764	0.107
(b) Grams Removed	546	60	323	33	416	58
4. Makeup Sample (D)						
(a) Avg. Conc.						
(b) Grams Removed	0					

Degradation Rate Calculation, Cont'd.

	Total Coolant	$O\text{-}\phi_3$	$M\text{-}\phi_3$	$P\text{-}\phi_3$	omp	HB
5. Makeup Tank (M)						
Tank Calib. (k_M) = 212.6 gm/in						
(a) Avg. Conc. ^{M}	1.000	0.130	0.680	0.067	0.877	0
(b) Grams Returned	28856	3758	19622	1943	25323	0
6. Net Transferred						
(5.+4.-3.-2.-1.)	-133	556	2462	184	3202	-3088
7. Initial Conc.						
(a) Coolant	1.000	0.113	0.592	0.060	0.765	0.108
(b) Sample Tank	1.000	0.113	0.592	0.060	0.765	0.108
(c) Makeup Tank	1.000	0.134	0.682	0.064	0.880	----
8. Initial Mass						
(a) Coolant	4783	539	2831	288	3658	514
(b) Sample Tank	3803	429	2250	229	2908	409
(c) Makeup Tank	2469	330	1683	159	2172	----
9. Final Conc.						
(a) Coolant	1.000	0.108	0.592	0.061	0.761	0.105
(b) Sample Tank	1.000	0.108	0.592	0.061	0.761	0.105
(c) Makeup Tank	1.000	0.127	0.681	0.070	0.870	----
10. Final Mass						
(a) Coolant	4638	501	2746	284	3531	489
(b) Sample Tank	1610	174	953	99	1226	170
(c) Makeup Tank	4674	594	3183	325	4102	----
11. Δ Correction						
(8.-10.)						
(a) Coolant	145	38	85	4	127	25
(b) Sample Tank	2193	255	1297	130	1682	239
(c) Makeup Tank	-2205	-264	-1500	-166	-1930	----
(d) Total Δ Corr.	133	29	-118	-32	-121	264
12. Total Mass Degraded, W						
(6.+11.(d))	0	585	2344	152	3081	2824
13. G(-omp), G(-1), G(HB)		0.121	0.484	0.031	0.636	0.584
14. G*(-omp) = G(-omp)/C,						
G*(-1) = G(-1)/C_1		1.094	0.818	0.515	0.834	----

Degradation Rate Calculation, Cont'd.

Statistics of G Calculation:

$(MWH)_1 = $ _____271_____ , $(MWH)_2 = $ _____1147_____

$\sigma(F)/F = $ _____0.03_____

	$O\text{-}\emptyset_3$	$M\text{-}\emptyset_3$	$P\text{-}\emptyset_3$	omp	HB
15. Intercept, a_1	0.114	0.592	0.060	0.766	0.108
16. Slope, $b_1 \times 10^5$	-0.555	0.004	0.012	-0.376	-0.252
17. $\sigma(a_1) \times 10^2$	0.036	0.132	0.004	0.156	0.209
18. $\sigma(b_1) \times 10^5$	0.052	0.193	0.006	0.235	0.308
19. $\sigma^2(C_{initial}) \times 10^8$					
(a) Coolant	6	78	7	109	197
(b) Sample Tank	6	79	7	109	197
(c) Makeup Tank	5	464	16	485	----
20. $\sigma^2(C_{final}) \times 10^8$					
(a) Coolant	11	158	16	246	408
(b) Sample Tank	11	158	15	246	408
(c) Makeup Tank	11	49	24	85	----
21. $\sigma^2(\Delta \text{ Correction})$					
(a) Coolant	4	53	5	80	133
(b) Sample Tank	8	213	2	352	26
(c) Makeup Tank	12	292	6	477	----
(d) Total	24	558	13	909	159
22. $\sigma^2(\text{Net Transfer})$					
(a) Loop (D,L and X)	0	11	0	18	0
(b) Sample Tank	8	149	8	234	202
(c) Makeup Tank	17	261	22	356	----
(d) Total	25	421	30	608	202
23. $\sigma(W)/W$	0.012	0.013	0.044	0.013	0.007
24. $\sigma(G)/G$	0.032	0.033	0.053	0.033	0.031
25. $\sigma(G)$	0.004	0.016	0.002	0.021	0.018

APPENDIX A4

DEGRADATION RATE CALCULATIONS

FOR M.I.T. AUTOCLAVE PYROLYSIS EXPERIMENTS

Figures A4.1 through A4.6 show the change of the total
terphenyl concentration as a function of time for the M.I.T.
autoclave pyrolysis experiments. The various kinetics or-
der correlations used to represent these data are shown in
these plots. These correlations were obtained by least-
square analysis similar to the MNDEG computer program as
described in Appendix A3 assuming zero, first and second
order kinetics. Tables A4.1 through A4.6 tabulate the re-
sults of the degradation calculations for these runs.
The correlation coefficients for the total terphenyl degra-
dation rate by the various kinetics orders are also given.

The procedure and chronology of these pyrolysis experi-
ments are given in Chapter 2. A discussion of the results
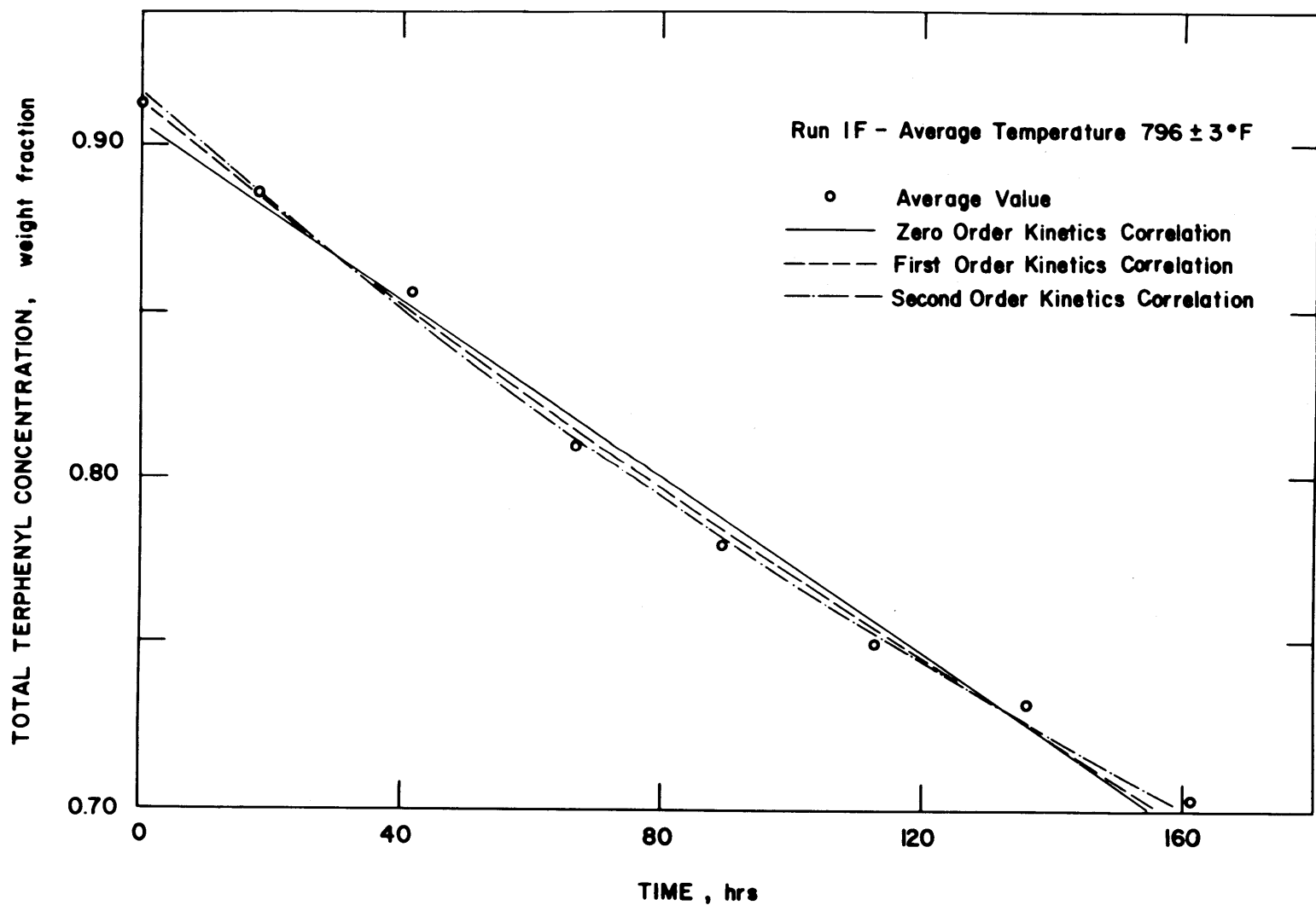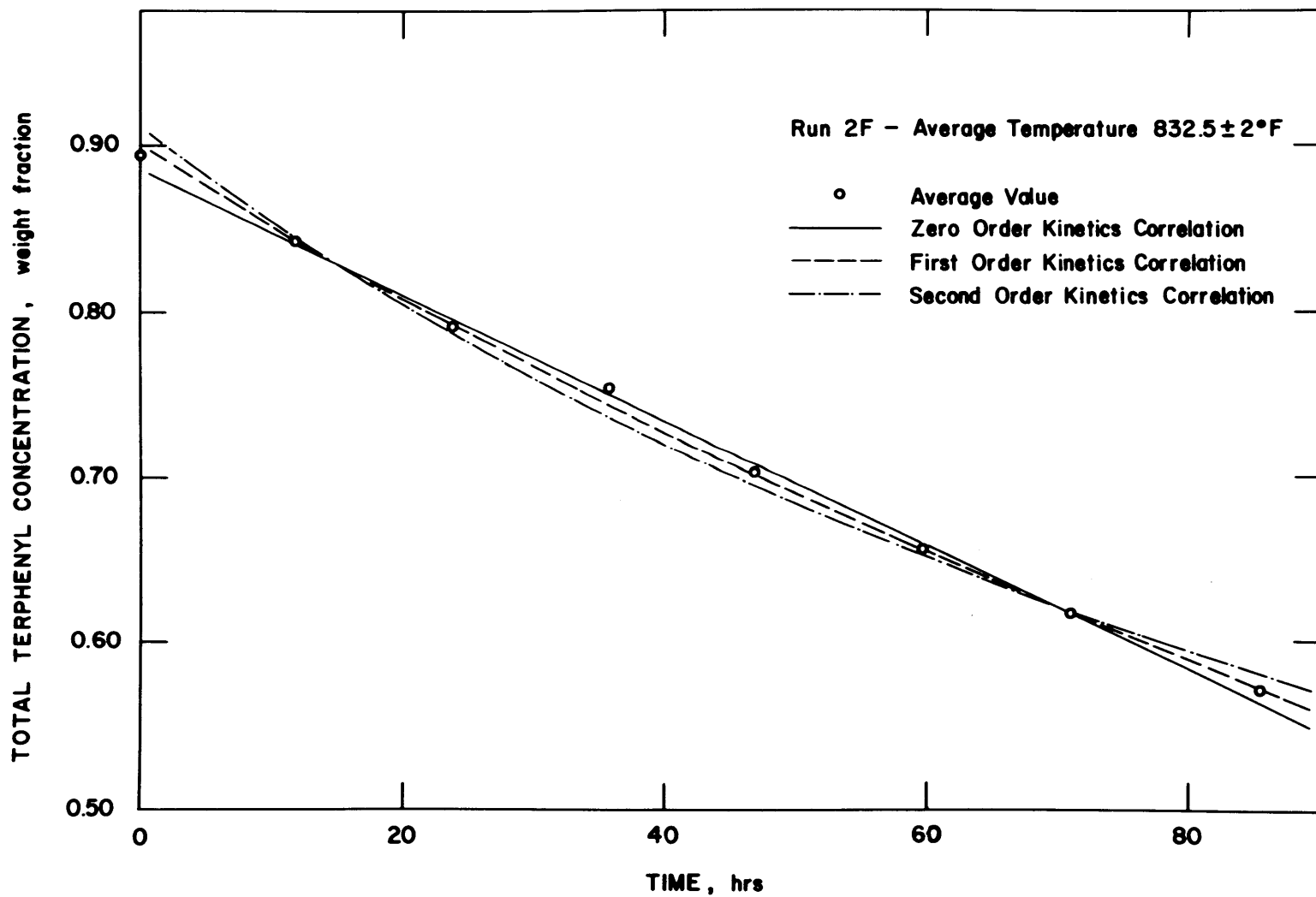of these experiments is presented in Chapter 5.

FIGURE A4.I   TOTAL TERPHENYL CONCENTRATION IN AUTOCLAVE DURING PYROLYSIS RUN IF OF UNIRRADIATED
SANTOWAX WR

Table A4.1

Summary of Results of Pyrolysis Run 1F

Unirradiated Santowax WR - 796.4 ± 3°F

Degradation Rate Constant, $K'(hr)^{-1}$[a]

| Terphenyl Isomer	K_0'(zero order)	K_1'(first order)	K_2'(second order)
ortho	$2.73 \pm 0.08 \times 10^{-4}$	$2.23 \pm 0.03 \times 10^{-3}$	$1.81 \pm 0.03 \times 10^{-2}$
meta	$1.01 \pm 0.03 \times 10^{-3}$	$1.61 \pm 0.04 \times 10^{-3}$	$2.54 \pm 0.05 \times 10^{-3}$
para	$4.54 \pm 0.42 \times 10^{-5}$	$9.08 \pm 0.78 \times 10^{-4}$	$1.80 \pm 0.15 \times 10^{-2}$
total omp	$1.33 \pm 0.06 \times 10^{-3}$	$1.67 \pm 0.05 \times 10^{-3}$	$2.09 \pm 0.05 \times 10^{-3}$
correlation coefficient (total omp)	0.9870	0.9939	0.9957

[a] error limits are 1σ

FIGURE A4.2   TOTAL TERPHENYL CONCENTRATION IN AUTOCLAVE DURING PYROLYSIS RUN 2F OF UNIRRADIATED SANTOWAX WR

Table A4.2

Summary of Results of Pyrolysis Run 2F

Unirradiated Santowax WR - 832.5 ± 2°F

Terphenyl Isomer	Degradation Rate Constant, $K'(hr)^{-1}$ [a]		
	K'_0 (zero order)	K'_1 (first order)	K'_2 (second order)
ortho	$7.61 \pm 0.14 \times 10^{-4}$	$7.22 \pm 0.08 \times 10^{-3}$	$6.73 \pm 0.24 \times 10^{-2}$
meta	$2.81 \pm 0.04 \times 10^{-3}$	$5.03 \pm 0.08 \times 10^{-3}$	$8.90 \pm 0.30 \times 10^{-3}$
para	$1.73 \pm 0.07 \times 10^{-4}$	$3.81 \pm 0.11 \times 10^{-3}$	$8.28 \pm 0.20 \times 10^{-2}$
total omp	$3.77 \pm 0.05 \times 10^{-3}$	$5.27 \pm 0.05 \times 10^{-3}$	$7.34 \pm 0.18 \times 10^{-3}$
correlation coefficient (total omp)	0.9988	0.9993	0.9965

[a] error limits are 1σ
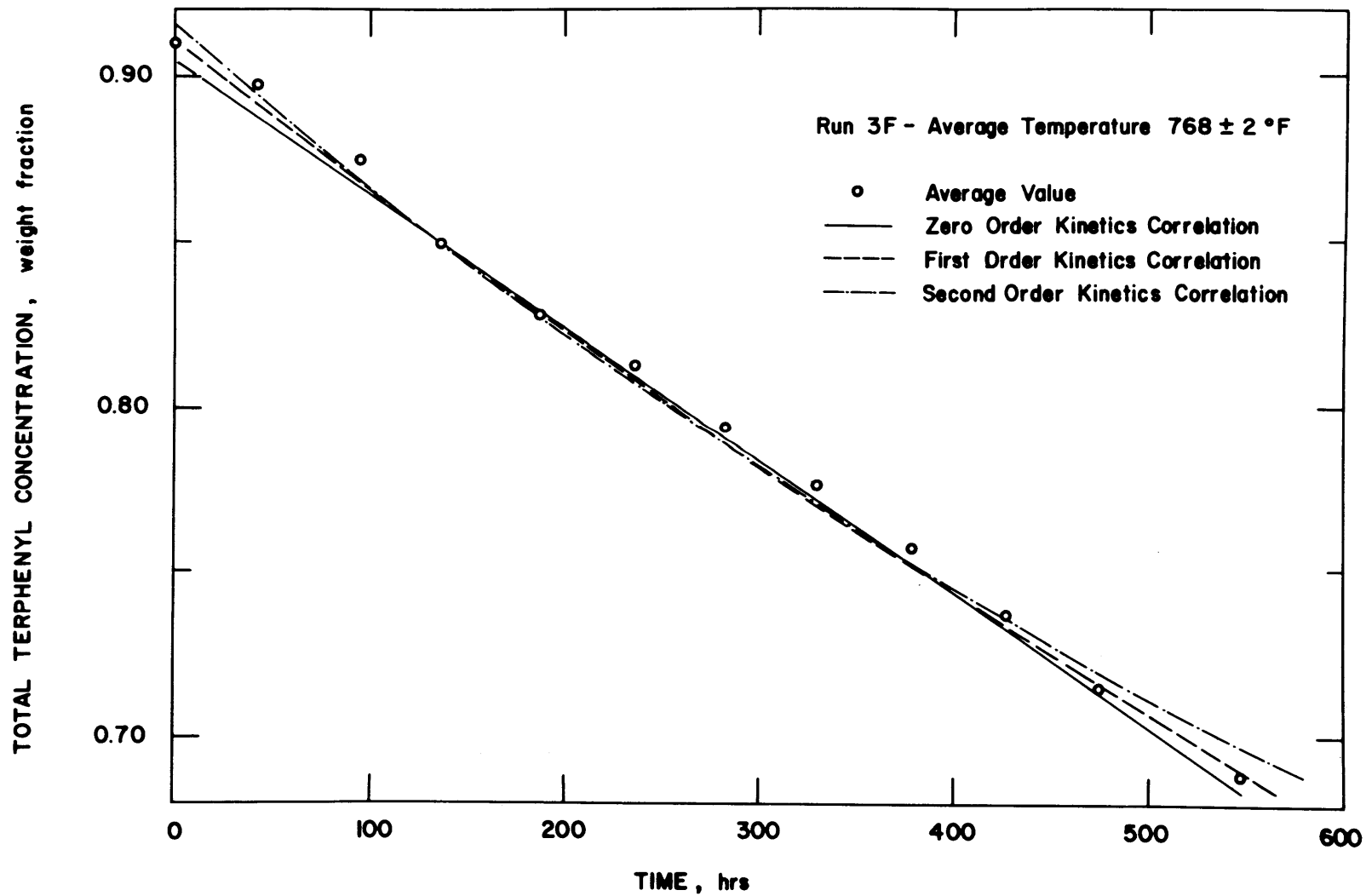
FIGURE A4.3   TOTAL TERPHENYL CONCENTRATION IN AUTOCLAVE DURING PYROLYSIS RUN 3F OF UNIRRADIATED SANTOWAX WR

Table A4.3

Summary of Results of Pyrolysis Run 3F

Unirradiated Santowax WR - 768.6 ± 3°F

Terphenyl Isomer	Degradation Rate Constant, $K'(hr)^{-1}$ [a]		
	K_0'(zero order)	K_1'(first order)	K_2'(second order)
ortho	$9.32 \pm 0.10 \times 10^{-5}$	$7.58 \pm 0.08 \times 10^{-4}$	$6.08 \pm 0.16 \times 10^{-3}$
meta	$3.04 \pm 0.05 \times 10^{-4}$	$4.83 \pm 0.07 \times 10^{-4}$	$7.58 \pm 0.18 \times 10^{-4}$
para	$8.92 \pm 1.67 \times 10^{-6}$	$1.72 \pm 0.32 \times 10^{-4}$	$3.32 \pm 0.61 \times 10^{-3}$
total omp	$4.01 \pm 0.08 \times 10^{-4}$	$5.07 \pm 0.06 \times 10^{-4}$	$6.28 \pm 0.14 \times 10^{-4}$
correlation coefficient (total omp)	0.9953	0.9983	0.9950

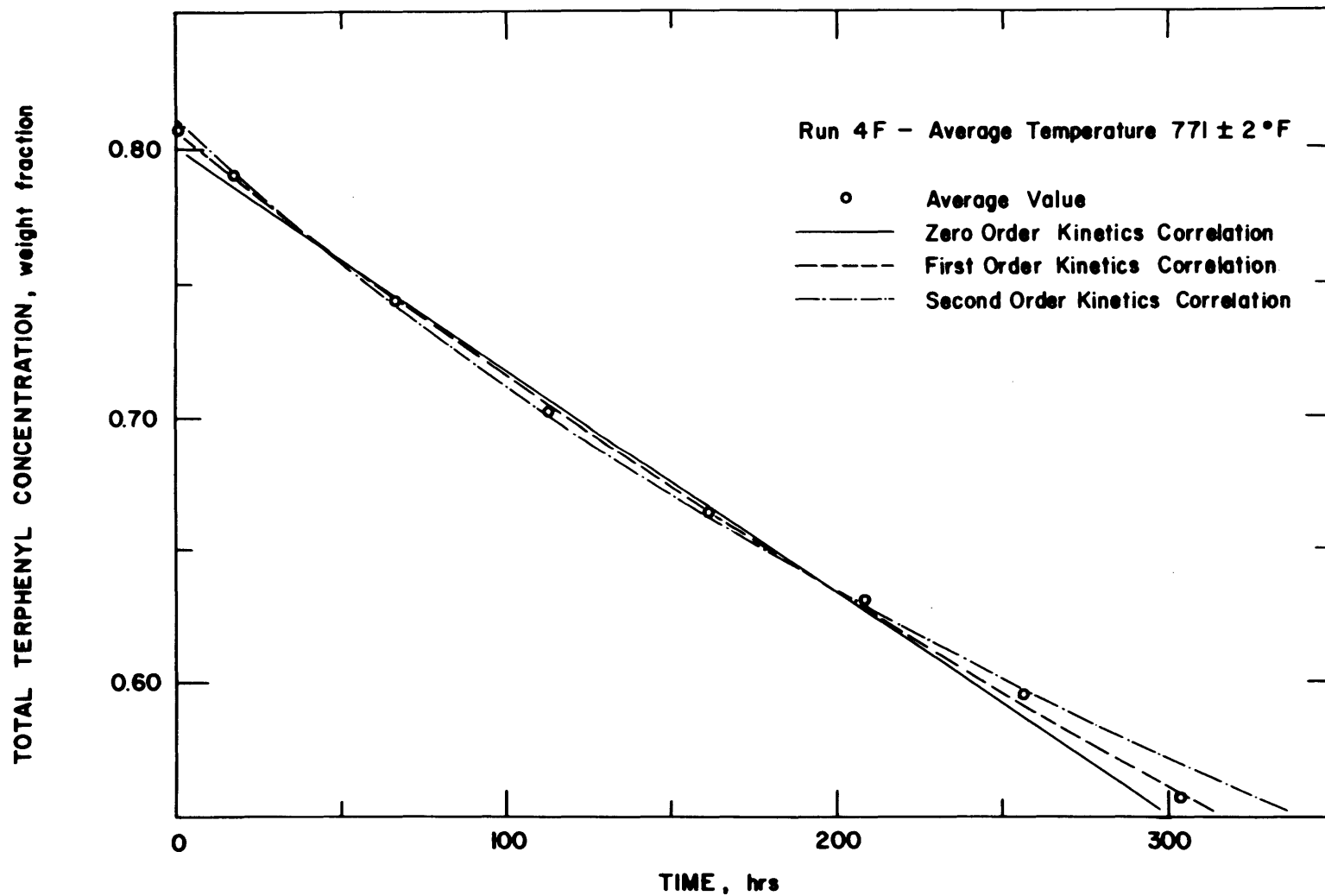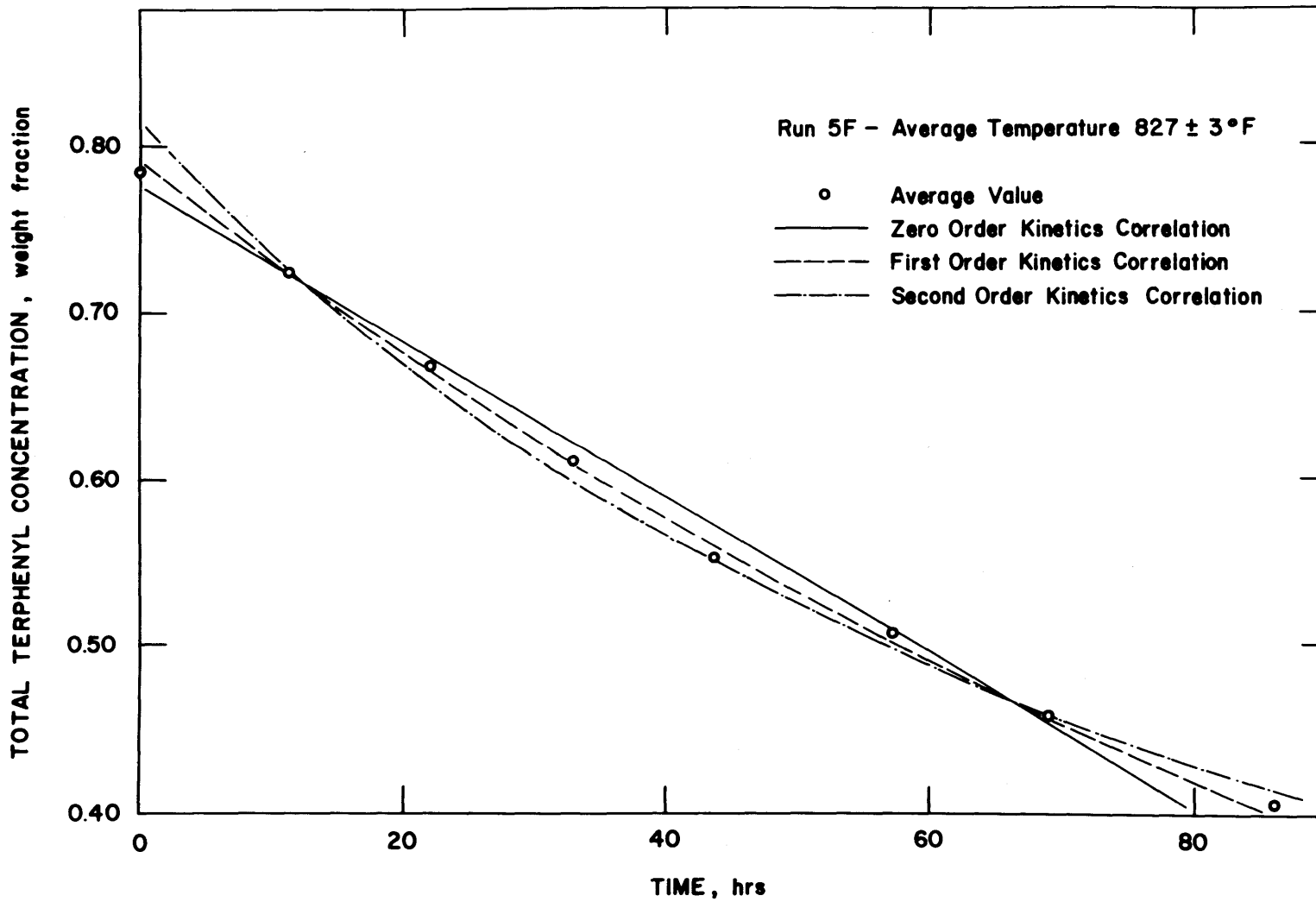[a] error limits are 1σ

FIGURE A4.4   TOTAL TERPHENYL CONCENTRATION IN AUTOCLAVE DURING PYROLYSIS RUN 4F OF IRRADIATED SANTOWAX WR

Table A4.4

Summary of Results of Pyrolysis Run 4F

Irradiated Santowax WR - 771.5 ± 2°F

Terphenyl Isomer	Degradation Rate Constant, $K'(hr)^{-1}$ [a]		
	K_0'(zero order)	K_1'(first order)	K_2'(second order)
ortho	$1.63 \pm 0.05 \times 10^{-4}$	$1.68 \pm 0.02 \times 10^{-3}$	$1.72 \pm 0.02 \times 10^{-2}$
meta	$5.91 \pm 0.12 \times 10^{-4}$	$1.11 \pm 0.01 \times 10^{-3}$	$2.05 \pm 0.05 \times 10^{-3}$
para	$7.03 \pm 0.44 \times 10^{-5}$	$1.19 \pm 0.06 \times 10^{-3}$	$2.00 \pm 0.10 \times 10^{-2}$
total omp	$8.32 \pm 0.25 \times 10^{-4}$	$1.20 \pm 0.02 \times 10^{-3}$	$1.17 \pm 0.03 \times 10^{-3}$
correlation coefficient (total omp)	0.9945	0.9991	0.9973

[a] error limits are 1σ

FIGURE A4.5   TOTAL TERPHENYL CONCENTRATION IN AUTOCLAVE DURING PYROLYSIS RUN 5F OF IRRADIATED
SANTOWAX WR

Table A4.5

Irradiated Santowax WR - 827.5 ± 3°F

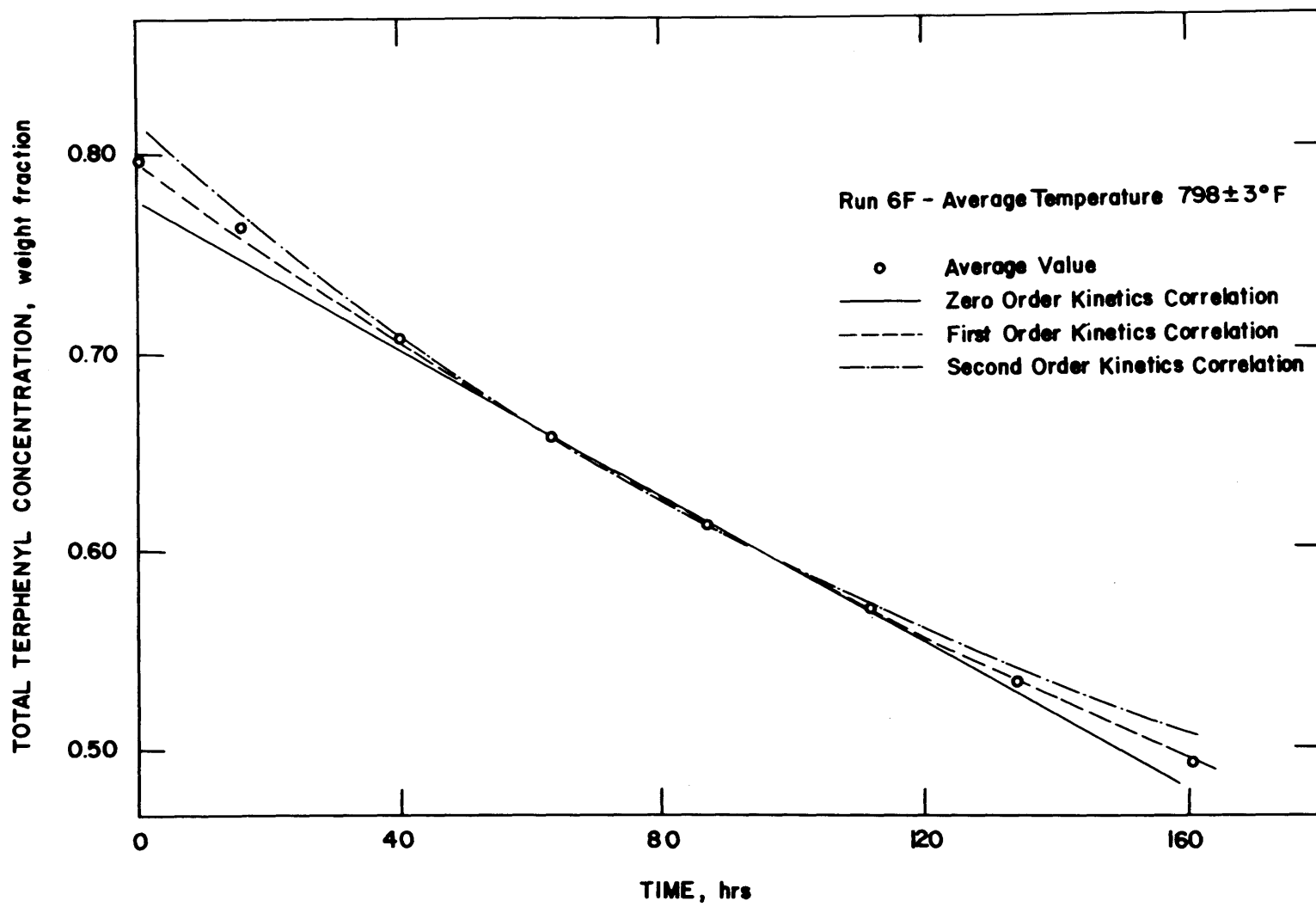| Terphenyl Isomer	Degradation Rate Constant, $K'(hr)^{-1}$ [a]		
	K'_0(zero order)	K'_1(first order)	K'_2(second order)
ortho	$8.72 \pm 0.30 \times 10^{-4}$	$1.07 \pm 0.01 \times 10^{-2}$	$1.29 \pm 0.05 \times 10^{-1}$
meta	$3.38 \pm 0.09 \times 10^{-3}$	$7.62 \pm 0.07 \times 10^{-3}$	$1.66 \pm 0.06 \times 10^{-2}$
para	$3.15 \pm 0.10 \times 10^{-4}$	$6.44 \pm 0.14 \times 10^{-3}$	$1.29 \pm 0.04 \times 10^{-1}$
total omp	$4.65 \pm 0.08 \times 10^{-3}$	$7.96 \pm 0.03 \times 10^{-3}$	$1.35 \pm 0.03 \times 10^{-2}$
correlation coefficient (total omp)	0.9982	0.9999	0.9954

[a] error limits are 1σ

FIGURE A4.6 TOTAL TERPHENYL CONCENTRATION IN AUTOCLAVE DURING PYROLYSIS RUN 6F OF IRRADIATED SANTOWAX WR

Table A4.6

Summary of Results of Pyrolysis Run 6F

Irradiated Santowax WR - 798.4 $\pm$ 3°F

Terphenyl Isomer	Degradation Rate Constant, $K'(hr)^{-1}$ [a]		
	K_0'(zero order)	K_1'(first order)	K_2'(second order)
ortho	$3.61 \pm 0.14 \times 10^{-4}$	$4.19 \pm 0.02 \times 10^{-3}$	$4.60 \pm 0.18 \times 10^{-2}$
meta	$1.34 \pm 0.03 \times 10^{-3}$	$2.85 \pm 0.01 \times 10^{-3}$	$5.87 \pm 0.17 \times 10^{-3}$
para	$1.27 \pm 0.06 \times 10^{-4}$	$2.38 \pm 0.08 \times 10^{-3}$	$4.39 \pm 0.14 \times 10^{-2}$
total omp	$1.85 \pm 0.06 \times 10^{-3}$	$2.99 \pm 0.02 \times 10^{-3}$	$4.66 \pm 0.12 \times 10^{-3}$
correlation coefficient (total omp)	0.9921	0.9996	0.9951

[a] error limits are 1σ

APPENDIX A5

OPERATIONAL PROCEDURES FOR THE CONTINUOUS
SAMPLING AND MAKEUP SYSTEMS

A5.1   Introduction

Detailed descriptions of the equipment and operational
procedures of the M.I.T. In-pile Loop Facility have been
given in earlier M.I.T. reports (A5.1, A5.2, A5.3, A5.4)
and in Chapter 2 of this report. A detailed description of
the continuous Sampling and Makeup systems (S & M I and
S & M II) have been given in Section 2.2.3 (Chapter 2)
of this report. The following sections present a brief
description for making transfers to charge the Makeup Tank
with reprocessed coolant (M-Type Transfer) and to drain the
degraded coolant from the Sampling Tank to be reprocessed
(S-Type Transfer).

As was pointed out in Chapter 2 of this report, nei-
ther S & M I nor S & M II operated satisfactorily. It was
necessary to correct for pump mismatch or failure by the
so-called F' and K' transfers. These were manual transfers
(without use of pumps) of organic coolant into and out of
the in-pile coolant loop via the Sampling and Makeup System
plumbing. Procedures for making these transfers are also
briefly described in the following sections.

Figures A5.1 and A5.2 show the schematic flow diagrams
of the S & M I and S & M II systems and their connections
to the in-pile circulating loop system.

A5.2   M-Type and S-Type Transfers

An M-type transfer was a transfer of processed coolant
from a Transfer Tank (TT) to the Makeup Tank (MT) and an
S-type transfer was a transfer of irradiated coolant from
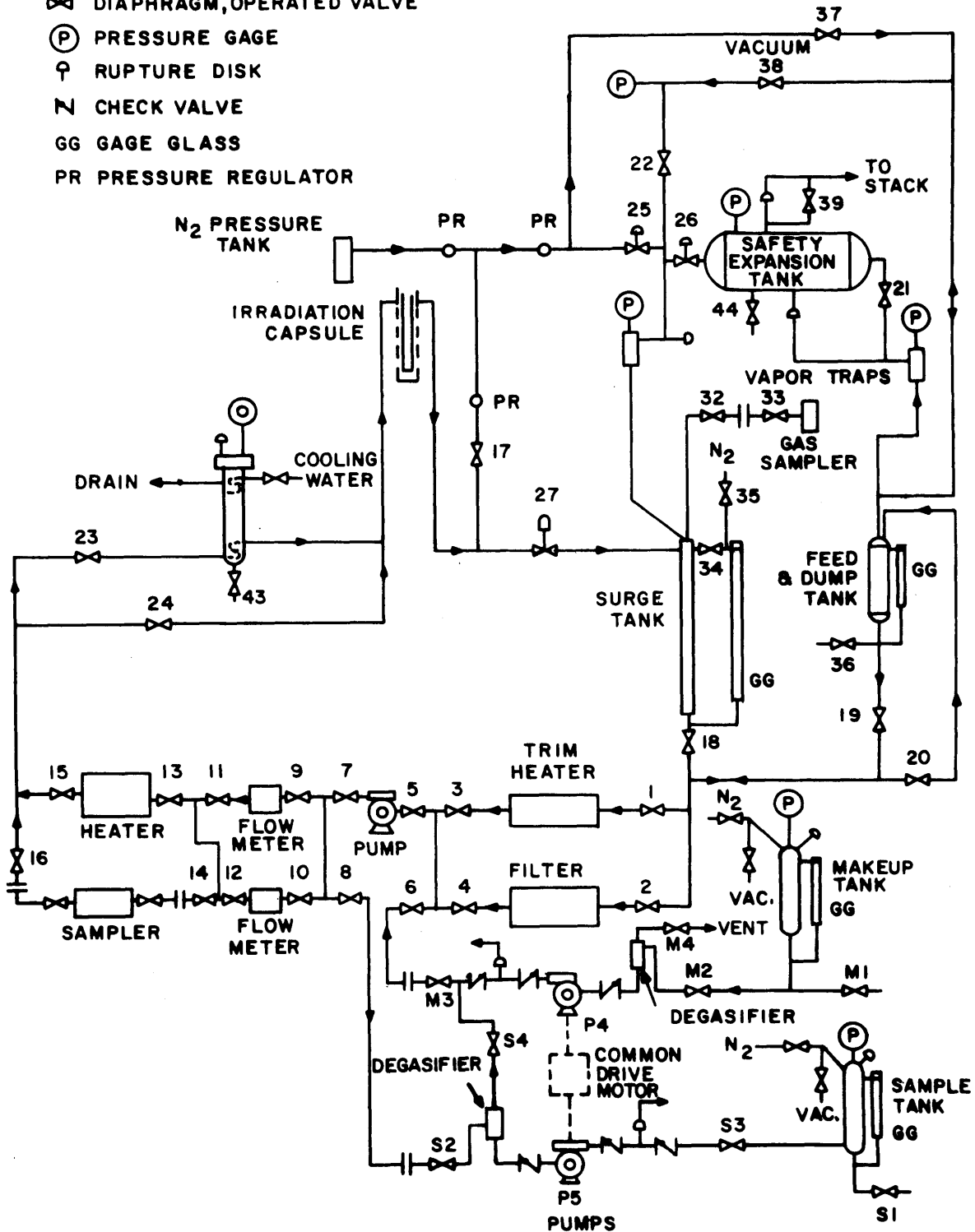the Sample Tank (SaT) to a Transfer Tank.

FIGURE A5.1   SCHEMATIC FLOW DIAGRAM OF MIT ORGANIC LOOP
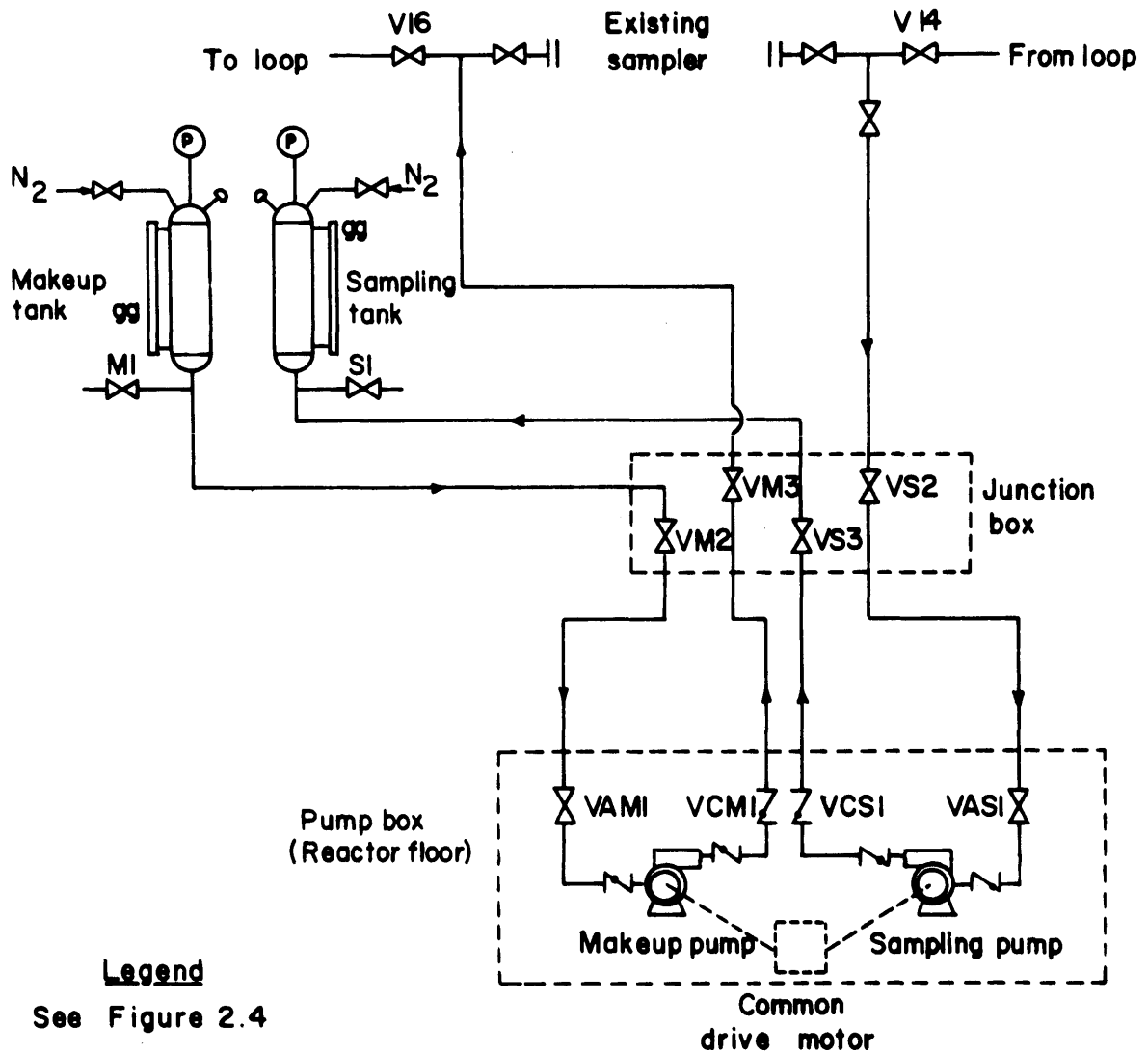WITH SAMPLING AND MAKEUP SYSTEM I

FIGURE A5.2 SCHEMATIC FLOW DIAGRAM OF SAMPLING AND
AND MAKEUP SYSTEM II, MIT ORGANIC COOLANT
LOOP

The Transfer Tanks were stainless steel cylinders with valves on both ends. In making transfers, a connecting line was installed between the lower end valve of the Transfer Tank and valve M1 of the Makeup Tank or valve S1 of the Sample Tank (see Figures A5.1 and A5.2).

In making an M-type transfer, the Transfer Tank was pressurized with nitrogen through the upper end valve to a pressure of about 100 psi above the pressure of the Makeup Tank. This pressure difference would thus force the coolant in the Transfer Tank to flow to the Makeup Tank through the connecting line.

In making an S-type transfer, the Transfer Tank was evacuated. The coolant in the Sample Tank thus flowed through the connecting line to the Transfer Tank.

The Transfer Tank and the connecting line were weighed before and after transfers to obtain the net amount of coolant transferred. The gage-glass on the Makeup and Sample Tanks were also recorded before and after transfers to obtain the tank calibration factors (grams per inch of gage-glass reading). Pressures in these tanks (MT and SaT) were restored to their initial readings (before transfer) after transfers. The normal pressure reading was 150 psi for the loop (Surge Tank), 100 psi for the Makeup Tank and 200 psi for the Sample Tank.

A5.3 F' and K' Type Manual Transfers

The F' and K' transfers as mentioned earlier were manual transfers (without use of pumps) of coolant into and out of the in-pile coolant loop via the Sampling and Makeup System plumbing.

In making F' transfers, the Makeup Tank pressure was increased through the nitrogen supply line to about 100 psi above the loop (Surge Tank) pressure. The valves between the Makeup Tank and the loop were then opened to start the flow. The flow was adjusted by valve 6 on S & M I and valve

16 on S & M II (see Figures A5.1 and A5.2).

In making K' transfers, the Sample Tank pressure was reduced by venting into the off-gas system to about 100 psi below the loop (surge Tank) pressure. The valves between the loop and the Sample Tank were opened to start the flow. The flow was adjusted by valve 8 on S & M I and valve 14 on S & M II (see Figures A5.1 and A5.2).

Pressures in the tanks (MT and SaT) were restored to initial values (before transfer) after transfers.

Records of gage-glass reading on the tanks (MT, Sat and Surge Tank) were kept so that amount of coolant transferred could be estimated.

APPENDIX A6

CALCULATION OF RADIOLYSIS AND RADIOPYROLYSIS
RATE CONSTANTS FROM DATA OF
M.I.T. AND OTHER LABORATORIES

A6.1   Radiolysis and Radiopyrolysis Rate Constants of Meta-
       rich Terphenyls

Mason and Timmins (A6.1) have made extensive survey of
irradiation of meta-rich terphenyls (e.g. Santowax WR, San-
towax OMP and OM-2) made by other laboratories at Euratom,
AECL Atomics International (AI), California Research and
AERE. They have summarized and compiled results of these
irradiations. These results were used to correlate the
effect of fast neutron fraction on radiolysis rate at 320°C
for the meta-rich terphenyls as reported in Section 4.3.2
(Chapter 4) of this report.

Mason and Timmins (A6.1) have also summarized results
of high temperature ($>700^\circ$F) irradiation of the meta-rich
terphenyls made by M.I.T., Euratom and California Research
up to June, 1966. Their values of first-order radiopyroly-
sis rate constants, $k_{P,omp,1}$, calculated according to Equa-
tion (5.2) for steady-state runs and Equation (5.10) for
transient runs of the earlier M.I.T. runs have been shown
in Chapter 5 of this report.

A6.2   Radiolysis Rate Constant from Irradiations of Pure
       Terphenyl Isomers

Mason and Timmins (A6.1) have reviewed and summarized
the results of irradiation of pure ortho and pure meta ter-
phenyls by AECL and AI. Their calculated values of $k_{R,omp,2}$
for these irradiations are plotted in Figures 5.11 and 5.12.

A6.3 Radiolysis Rate Constants of Ortho-rich Terphenyl – Santowax OM

In Chapter 4 the results of other laboratories are discussed. This section presents the methods used to normalize these results.

A6.3.1 Calculations of Radiolysis Rates from Transient Irradiations

Except for those steady-state irradiations at M.I.T. as presented in Chapters 4 and 5 of this report, all experiments with Santowax OM reported by other laboratories were made in transient operation. The radiolysis rate constants for transient experiments were calculated according to the following method; these rate constants were discussed in Chapter 4.

Where data on the terphenyl concentration versus dose were not available from the published results (A6.4) the rate constant was calculated from the reported initial G value by:

$$k_{R,omp,n} = \frac{G^O(-1)}{11.65} \tag{A6.1}$$

Where only one sample was irradiated at a given temperature (one dose data point), the constant was found by

$$k_{R,omp,1} = \frac{\ln C_1/C_2}{\tau} \tag{A6.2}$$

$$k_{R,omp,n} = \frac{1}{(n-1)\tau}\left[C_2^{1-n} - C_1^{1-n}\right] \tag{A6.3}$$
$$(n \neq 1)$$

where

C_1 is the initial terphenyl concentration, weight fraction

C_2 is the final terphenyl concentration, weight fraction

τ is the dose, watt-hr/gram

However, for temperatures above $700^{\circ}F$ where both radiolysis and radiopyrolysis effects were present, the first-order and second-order overall rate constants, $K_1(-i)$ and $K_2(-i)$, were found by

$$K_1(-omp) = \frac{\ln C_1/C_2}{\tau} \tag{A6.4}$$

and

$$K_2(-omp) = \frac{1}{\tau}\left[C_2^{-1} - C_1^{-1}\right] \tag{A6.5}$$

The $k_{R,omp,1.7}$ were then calculated, similar to Equation (5.10) by

$$k_{R,omp,1.7} = \frac{1}{\overline{C}_{omp}^{0.7}}K_1(-omp) - \frac{k_{P,omp,1}}{r\,\overline{C}_{omp}^{0.7}} \tag{A6.6}$$

where

$$\overline{C}_{omp} = K_1(-omp)/K_2(-omp) \tag{A6.7}$$

The values of $k_{P,omp,1}$ in Equation (A6.6) were calculated using Equation (5.15).

Where data on terphenyl concentration versus dose were given for constant temperature irradiations, a least-square analysis was made using Equation (A6.4) and (A6.5) to find $K_1(-omp)$ and $K_2(-omp)$ in the case of high temperatures. In the case of low temperature, $k_{R,omp,n}$ was found by using Equations (A6.2) or (A6.3) in the least-square analysis.

A6.3.2 Results of Electron Irradiation of Santowax OM

Mackintosh (A6.2) reported Van de Graaf irradiation of Santowax OM at $375^{\circ}C$ at dose rate of 73 watts/gram and doses ranging from 4.4 to 105.8 watt-hr/gram. Table A6.1 presents the irradiation data as reported and the calculated radiolysis rate constants at $320^{\circ}C$ and $375^{\circ}C$, $k_{R,omp,1.7}$ $(320^{\circ}C)$ and $k_{R,omp,1.7}(375^{\circ}C)$, using $\Delta E_R = 1$ kcal/mole.

The value of $k_{R,omp,1.7}(375^{\circ}C)$ calculated by least-square correlation of all the data points is $0.0202 \pm 0.0023(2\sigma)$ (watt-hr/gram)$^{-1}$

Table A6.1

Results of Electron Irradiation
of Santowax OM at 375°C by Mackintosh (A6.2)

Sample No.	Dose, wh/g	C_{omp} w/o	M. I. T. Correlation	
			$k_{R,omp,1.7}$ (375°C) (wh/g)$^{-1}$	$k_{R,omp,1.7}$ (320°C) (wh/g)$^{-1}$
	0	98.2		
58,62	4.4	81.7	0.0452	0.0421
61,66	6.6	81.5	0.0306	0.0285
48,49,69	8.9	74.7	0.0343	0.0319
60	13.2	71.1	0.0270	0.0251
54	17.6	55.9	0.0397	0.0369
63	26.4	62.4	0.0205	0.0191
56	35.2	46.7	0.0281	0.0261
67	44.0	42.9	0.0258	0.0240
64	52.8	46.8	0.0186	0.0173
57,59	64.2	36.0	0.0230	0.0214
65	88.0	33.7	0.0183	0.0170
71	96.8	27.2	0.0218	0.0203
70	105.8	24.2	0.0228	0.0212

The same report (A6.2) also presented electron irra-
diations of Santowax OM at temperatures ranging from 350°C
to 450°C at a fixed dose of 8.8 watt-hr/gm. However, only
the decomposition rate of total terphenyl plus biphenyl ($\emptyset_2$)
were reported. Table A6.2 presents the irradiation data
and the calculated $k_{R,omp+\emptyset_2,1.7}$ values.

Table A6.2

Results of Electron Irradiation of Santowax OM at Fixed Dose of 8.8 watt-hour/gram by Mackintosh (A6.2)

Temperature $^{\circ}C$	$C_{omp+\emptyset_2}$ w/o	M.I.T. Correlation of $k_{R,omp+\emptyset_2,1.7}$ $(wh/g)^{-1}$
350	80.4	0.0267
375	78.9	0.0293
390	75.6	0.0351
396	76.6	0.0333
405	77.1	0.0324
412	77.5	0.0317
420	73.2	0.0396
435	69.1	0.0479
450	65.8	0.0552

A6.3.3 Results of Mixed Irradiation of Santowax OM

Table A6.3 presents irradiation data reported by AECL (A6.3) using NRX X-Rod Facility at a dose rate of 0.33 ± 0.03 watts/gram and fast neutron fraction f_N = 0.3.

Tomlinson, et. al. (A6.4) reported sealed capsule irradiations of Santowax OM from $300^{\circ}-400^{\circ}C$ at doses ranging up to 14 watt-hour/gram and f_N = 0.51 and dose rate of approximately 0.1 watt/gram. Table A6.4 shows the irradiation data and M.I.T. correlations.

Table A6.3

Results of NRX X-Rod Irradiations of

Santowax OM at $f_N = 0.3$ (A6.3)

Sample No.	Temperature °C	Dose, wh/g	C_{omp} w/o	M.I.T. Correlation of $k_{R,omp,1.7}$ (a) $(wh/g)^{-1}$
X24	230	11.3	78.2	0.0222
X28	280	7.8	82.6	0.0238
X13	280-325	31.4	52.6	0.0253
X25	305	11.3	74.0	0.0280
X16	325	8.6	78.3	0.0289
X14	330	31.2	49.6	0.0284
X12	365-380	14.8	60.8	0.0389
X27	370	8.2	73.3	0.0400

(a) Assuming initial $C_{omp}(\tau = 0) = 98.2\%$

Table A6.4

Results of Reactor Irradiation of

Santowax OM at f_N = 0.51 by Tomlinson (A6.4)

Sample No.	Temperature °C	Dose, wh/g	Terphenyl Destroyed w/o	M.I.T. Correlation of $k_{R,omp,1.7}$ [a] $(wh/g)^{-1}$
1	298	2.70	13.6	0.0587
55	301	3.35	14.2	0.0497
13	301	11.2	39.9	0.0566
17	301	14.0	45.9	0.0570
21	321	4.37	16.8	0.0463
25	325	9.18	33.7	0.0537
29	351	4.42	22.2	0.0641
39	374	2.13	12.1	0.0650
45	379	4.30	14.9	0.0407
55	400	3.74	24.9	0.0775

[a] Initial C_{omp}(τ = 0) = 98.4%

APPENDIX A7

RESULTS OF HEAT TRANSFER CORRELATION

Heat transfer measurements on Santowax WR using Test Heater TH8 have been presented in Section 3.6.2 (Chapter 3) of this report. Detailed descriptions of the apparatus and the experimental data have been reported by Spierling (A7.1). This appendix presents the results of correlating the heat transfer data using both the Dittus-Boelter type of relation

$$Nu = aRe^b Pr^c \tag{A7.1}$$

and the Sieder-Tate type of relation

$$Nu = aRe^b Pr^c (\mu/\mu_w)^d \tag{A7.2}$$

The computer program MNHTR (A7.2) was used to evaluate the constants a, b, c and d in Equations (A7.1) and (A7.2) by allowing all these constants to vary or by fixing some of the constants in order to find the best values for the remaining.

Tables A7.1 and A7.2 show the results of such correlation using Equations (A7.1) and (A7.2) respectively. Two groups of data are shown for each type of correlation. Data Group I consists of all data points except those of Test Series 26 using the downstream section of TH8 and Data Group II consists of all data points except those of Test Series 26 using the upstream section of TH8. Data Group I covers a wider range of Reynolds Number and Prandtl number than Data Group II. The root-mean-square (RMS) deviations are also given in Tables A7.1 and A7.2 for each correlation.

Table A7.1

Correlation of Heat Transfer Measurement on Santowax WR
Using Test Heater TH8 by Dittus-Boelter Relation ($Nu = aRe^b Pr^c$)

Data Group I (630°F to 800°F; $3.0 \times 10^4 < Re < 13.1 \times 10^4$; $5.17 < Pr < 8.23$-Test Series 27, 28, 29 and upstream of 26)

(1)   Variation of all "Constants" (a, b and c)

$$Nu = 0.0136 \ Re^{0.862} Pr^{0.289}$$ RMS Deviation = 7.08%

(2)   c = 0.33

$$Nu = 0.0110 \ Re^{0.874} Pr^{0.33}$$ RMS Deviation = 6.34%

(3)   c = 0.33, b = 0.800

$$Nu = 0.0254 \ Re^{0.800} Pr^{0.33}$$ RMS Deviation = 6.70%

(4)   c = 0.40

$$Nu = 0.00755 \ Re^{0.896} Pr^{0.40}$$ RMS Deviation = 6.47%

(5)   c = 0.40, b = 0.800

$$Nu = 0.0223 \ Re^{0.800} Pr^{0.40}$$ RMS Deviation = 7.08%

Data Group II (700°F; $3x10^4 < Re < 9.7x10^4$; 6.0<Pr<7.4-Test Series 27, 28, 29 and downstream of 26)

(1) Variation of all "Constants" (a, b and c)

$$Nu = 0.0430 \ Re^{0.818}Pr^{-0.037}$$

RMS Deviation = 6.15%

(2) c = 0.33

$$Nu = 0.0150 \ Re^{0.851}Pr^{0.33}$$

RMS Deviation = 6.85%

(3) c = 0.33, b = 0.800

$$Nu = 0.0264 \ Re^{0.800}Pr^{0.33}$$

RMS Deviation = 6.89%

(4) c = 0.40

$$Nu = 0.0123 \ Re^{0.857}Pr^{0.40}$$

RMS Deviation = 7.15%

(5) c = 0.40, b = 0.800

$$Nu = 0.0232 \ Re^{0.800}Pr^{0.40}$$

RMS Deviation = 7.21%

Table A7.2

<u>Correlation of Heat Transfer Measurements on Santowax WR</u>

<u>Using Test Heater TH8 by Seider-Tate Relation</u> $Nu = aRe^b Pr^c (\mu/\mu_w)^d$

<u>Data Group I</u> (630°F to 800°F; $3.0 \times 10^4 < Re < 13.1 \times 10^4$; $5.17 < Pr < 8.23$- Test Series 27, 28, 29 and upstream of 26)

(1)   d = 0.14

$Nu = 0.00992 \ Re^{0.889} Pr^{0.28} (\mu/\mu_w)^{0.14}$ RMS Deviation = 6.63%

(2)   d = 0.14, c = 0.33

$Nu = 0.00753 \ Re^{0.905} Pr^{0.33} (\mu/\mu_w)^{0.14}$ RMS Deviation = 6.61%

(3)   d = 0.14, c = 0.33, b = 0.800

$Nu = 0.0245 \ Re^{0.800} Pr^{0.33} (\mu/\mu_w)^{0.14}$ RMS Deviation = 7.31%

Data Group II (700°F; $3 \times 10^4 < \text{Re} < 9.7 \times 10^4$; $6.0 < \text{Pr} < 7.4$-Test Series 27, 28, 29 and downstream of 26)

(1) $d = 0.14$

$$Nu = 0.0334 \ Re^{0.846} Pr^{-0.090} (\mu/\mu_w)^{0.14} \qquad \text{RMS Deviation} = 6.20\%$$

(2) $d = 0.14$, $c = 0.33$

$$Nu = 0.00999 \ Re^{0.884} Pr^{0.33} (\mu/\mu_w)^{0.14} \qquad \text{RMS Deviation} = 7.10\%$$

(3) $d = 0.14$, $c = 0.33$, $b = 0.800$

$$Nu = 0.0254 \ Re^{0.800} Pr^{0.33} (\mu/\mu_w)^{0.14} \qquad \text{RMS Deviation} = 7.31\%$$

APPENDIX A8

CHRONOLOGY OF ORGANIC LOOP OPERATIONS

A summary of operation of the M.I.T. In-pile Loop Facility has been presented in Table 2.3 (Chapter 2) of this report covering the period from July 1, 1966 to March 31, 1968.

This appendix describes in more details the chronology of loop operations, calorimetry and dosimetry with emphasis on irradiation runs made during this period.

Two Calorimetry Series (XXII and XXIII) and one Foil Dosimetry (No. 42C) were made in the Fuel Position 1 before the In-pile Section No. 4 was installed on October 29, 1966. The results of these measurements are shown in Appendix Al.

The loop was charged with fresh (unirradiated) Santowax OM and Run 19 was started on November 1, 1966. Since the new processing system (S & M I) employing pump feeding of makeup coolant and pump bleeding of loop coolant (see Section 2.2) was still in the process of being installed, capsule system similar to that described in earlier M.I.T. reports (A8.1, A8.2) were used for this run. The coolant was degraded from an initial terphenyl concentration of about 97% to about 63%. Considerable time was spent in testing the new processing system and in trying to adjust the sampling rates in order to obtain a steady-state terphenyl concentration of around 60%. Beginning December 9, 1966, the steady-state Run 19A was established. It lasted through December 30, 1966 and totaled 1257 accumulated MWH of reactor operation at 5 MW nominal power and 572°F irradiation temperature with a steady-state average terphenyl concentration of 63%. During Run 19A, Foil Dosimetry No. 43C was made on December 15, 1966 through the aluminum monitoring tube of the in-pile section.

The new processing system was completely installed and tested by the end of 1966. Therefore Run 20 was started at an irradiation temperature of 572°F on January 3, 1967 using the new processing system. The concentration of the loop coolant was raised from 63% to approximately 90% by diluting with fresh (unirradiated) Santowax OM. The initial transient brought the coolant concentration from 90% down to 87% and steady-state Run 20A began on Jan. 10, 1967. During Run 20A the processing pumps were found to be pumping at irregular rates less than the preset values. The run was terminated two weeks later on January 24, 1967 totaling 964 MWH, at an average terphenyl concentration of 86% and an irradiation temberature of 572°F.

Run 20B was started immediately after Run 20A while the pumps were being examined and tested. The processing rate was found to have improved with longer pump strokes. Steady-state portion of Run 20B began on January 30, 1967 and ended on February 17, 1967 totaling 1454 MWH at an average terphenyl concentration of 80% and an irradiation temperature of 572°F.

The nominal operating power of the M.I.T. reactor was lowered to 2 MW on February 27, 1967 due to a leak in one of its two heat exchangers. In order to take advantage of this lower power level (and therefore lower dose rate of irradiation) to study the dose rate effect on degradation, Run 21 was scheduled at an irradiation temperature of 750°F. Initial loop dilution was made on March 9, 1967 with fresh terphenyl to bring the loop terphenyl concentration to about 80%. Steady-state condition began on March 13, 1967. On March 28, 1967, the rupture disk on the makeup side of the processing system located between valve M3 and pump P4 (see Figure 2.4) was ruptured. Coupled with failure of the check valve between valve M3 and the disk, both the loop and the Makeup Tank were drained through the ruptured disk into the Safety Expansion Tank. Run 21 was therefore terminated with an accumulated irradiation of 423 MWH at an

average terphenyl concentration of 78% and an irradiation
temperature of 750°F.

Foil Dosimetry No. 44C was made on April 3, 1967 through
the aluminum monitoring tube of the in-pile section at Fuel
Position 1 with reactor operating at 2 MW nominal power.

Run 22 was started on April 3, 1967. Steady-state
operation was reached on April 5, 1967. On April 11, 1967,
the same rupture disc that ruptured on March 28, 1967 failed
again. This time the check valve prevented any dump of the
loop coolant through the ruptured disc. However, approxi-
mately 760 grams of processed organic material from the
Makeup Tank was lost to the Safety Expansion Tank through
the ruptured disc. The rupture disc was made of Inconel
rated at 710 psi (70°F). The loop was operated at about
150 psi and the Makeup Tank at 90 psi. There was no evi-
dence of overpressure on the loop system from instrumenta-
tion. The most likely cause of rupture might be due to the
high temperature (about 500°F) at the disc. Subsequently
the trace heating around the disc was removed. On April
18, 1967, a heat transfer run was made using the Test Heater
TH7. The experimental heat transfer coefficient was found
to have reduced by approximately a factor of 1.5 with the
test heater wall temperature approaching 900°F (See Chapter
3). It was decided to terminate Run 22 which was runing
at 800°F and 79% average terphenyl concentration. The
total irradiation time amounted only to 290 MWH.

Run 23 was started on April 25 1967 at an irradiation
temperature of 700°F with reduced Test Heater power. Mean-
while, heat transfer runs were continued to determine if
any additional fouling was being formed. Some difficulties
with the chromatographic equipment were experienced toward
the end of Run 22. The analytical results for terphenyl
concentrations were not reproducible. A backlog of samples
were therefore accumulated after the equipment was repaired.
Run 23 reached steady-state on May 17 as a result of this
delay, and was terminated on June 4, 1967 when the reactor

power was raised back to 5 MW. The accumulated MWH for the steady-state period of Run 23 was 382 MWH at an average terphenyl concentration of 81%.

Run 23A followed immediately after Run 23 and continued at steady-state condition at 700°F. The run was terminated on June 18, 1967 with an accumulation of 580 MWH at an average terphenyl concentration of 82%. During this run, heat transfer measurements were made regularly and no increase in fouling was measured (see Chapter 3)

Run 24 began on June 18, 1967 immediately after Run 23A at 750°F. The run reached steady-state on June 20, 1967 and was completed on July 7, 1967 with an accumulation of 1068 MWH at an average terphenyl concentration of 80%. Continuous heat transfer measurements indicated no significant change in heat transfer coefficient at the Test Heater. Foil Dosimetry No. 45C was made on June 21, 1967 at Fuel Position 13, and Calorimetry Series XXIV was also made at the same Fuel Position.

Run 25 began on July 12, 1967 at an irradiation temperature of 800°F. Initial dilution of the loop coolant with processed terphenyl brought the loop coolant concentration to about 78%. Steady-state condition was reached on July 17, 1967 and the run was completed on July 28, 1967 with an accumulation of 908 MWH at an average terphenyl concentration of 76%. Heat transfer measurements made during this period again showed no significant change in heat transfer coefficient at the Test Heater.

Run 19 through Run 25 completed the irradiation series on Santowax OM. On July 28, 1967, In-pile Section No. 4 was removed from Fuel Position 1, and Foil Dosimetry No. 47 and Calorimetry Series XXV were made. A new fuel element (FE5MR32) was installed at Fuel Position 1 on August 30, 1967. Foil Dosimetry No. 48 and Calorimetry Series XXVI were made through the stainless steel thimble in the new fuel element. On October 8, 1967, In-pile Section No. 5 was installed at Fuel Position 1.

During the period from the removal of In-pile Section No. 4 and the installation of In-pile Section No. 5, two major events also took place. First, Test Heater TH7 was removed and replaced by Test Heater TH8. (See Chapter 3). Secondly, due to the fact that the processing system had not been functioning quite satisfactory since its installation in the hydraulic console, a set of new pumps were installed on the reactor room floor about 12 feet below the hydraulic console. Modification and testing of the new pumping system (S & M II) was completed on November 6, 1967. Meanwhile, Foil Dosimetry No. 49C was made at Fuel Position 1 through the aluminum monitoring tube.

Run 26A began on November 6, 1967 with the loop charged with fresh Santowax WR at an irradiation temperature of 700^OF. Steady state (Run 26) was reached on November 16, 1967. On November 30, 1967, a massive leak between the makeup pump and the loop occurred due to a loose fitting. Approximately 2000 grams of processed terphenyl was lost through the leak during the two weeks period. The leak was fixed and the run was continued. On December 8, 1967, the sampling side of the processing system failed to pump. Visual check found extensive leak of coolant through the teflon packings around the plunger of the sampling pump. Run 26 was terminated then with an accumulation of 1053 MWH at an average terphenyl concentration of 83%.

Run 27 began on December 18, 1967 at an irradiation temperature of 750^OF. While the sampling pump of the processing system was being repaired, both the sampling pump and the makeup pump were by-passed. The processing of the loop coolant was carried out manually every two to three hours throughout the run by means of F' & K' operation (See Section 2.2 and Appendix A5). Run 27 was completed on January 15, 1967 with an accumulation of 1128 MWH at an average terphenyl concentration of 79%. Foil Dosimetry No. 50C was make on January 5, 1967 through the aluminum moni-

toring tube at Fuel Position 1.

Run 28 began on January 22, 1968 at an irradiation temperature of 800°F with manual processing same as Run 27. The run reached steady state on February 6, 1968 and was completed on February 16, 1968 with an accumulation of 876 MWH at an average terphenyl concentration of 76%.

Foil Dosimetry No. 51C and Calorimetry Series XXVII were made before the In-pile Section No. 5 was removed from Fuel Position 1 on February 24, 1968. Foil Dosimetry No. 52C and Calorimetry Series XXVIII, XXIX and XXX were made after the removal inside the stainless steel thimble at Fuel Position 1.

APPENDIX A9

NOMENCLATURE

A = constant.

A = inside surface area of test heater wall; ft^2.

A_i = atomic or molecular weight of species i.

a = constant.

a_i = constant.

B = weight per cent Bottoms; w/o.

b = constant.

b_i = constant.

C, C_i, C_{omp} = concentration of component i in a mixture, wt % or weight fraction. Subscript i refers most frequently to ortho, meta, para or total terphenyl.

C_i^f, C_{omp}^f = concentration of component i or concentration of total terphenyl in the feed; weight fraction.

$C_{i,j}$ = concentration of component i in sample j; weight fraction or w/o

$\overline{C}_{omp}$ = total terphenyl concentration near the mid-point of a transient determined as that concentration where both first- and second-order kinetics correlations give the same value for the total degradation rate, $-dC_{omp}/d\tau$; weight fraction.

C_p = specific heat of material; cal/(gm)($^{\circ}$C).

C_b = background tritium activity in coolant; μc/gram.

c = constant.

DP = degradation products. That fraction of the irradiated coolant which are not terphenyls.

D_j = mass of coolant in the jth makeup capsule; grams.

d = constant.

E = neutron energy; ev or Mev.

E_c = cadmium cutoff energy; ev.

E_{eff} = effective threshold energy of a threshold detector; Mev.

ΔE = activation energy; kcal/mole.

e = constant.

F, F_T = total in-pile dose rate factor; (watt)(hr)(cm^3)/(MWH)(gm).

F_N = in-pile dose rate factor due to fast neutron interactions; (watt)(hr)(cm^3)/(MWH)(gm).

F_γ = in-pile dose rate factor due to gamma-ray interactions; (watt)(hr)(cm^3)/(MWH)(gm).

f_N = fraction of absorbed dose due to fast neutron interactions.

f_γ = fraction of absorbed dose due to gamma-ray interactions.

$G_R(-i)$ = radiolytic decomposition yield of component i in the coolant, expressed as molecules of component i degraded per 100 ev absorbed in the total coolant, where i refers to ortho terphenyl (o-$\emptyset_3$), meta terphenyl (m-$\emptyset_3$), para terphenyl (p-$\emptyset_3$), or total terphenyl (omp).

$G(\rightarrow HB)$ = radiolytic production yield of HB in the coolant, expressed as equivalent molecules of omp degraded to form HB/100 ev absorbed in the total coolant.

$G(\rightarrow LIB)$ = radiolytic production yield of LIB in the coolant, expressed as equivalent molecules of omp degraded to form LIB/100 ev absorbed in the total coolant.

$G'(-i)$ = total experimental G value, molecules of component i degraded/100 ev absorbed in the total coolant.

$G^*(-i)$ = $G(-i)/C_i$.

$G_N(-i)$ = decomposition yield of component i in the coolant for fast neutron interactions.

$G_\gamma(-i)$ = decomposition yield of component i in the coolant for gamma-ray interactions.

$G_\gamma^o(-i)$ = initial decomposition yield of component i in the coolant for gamma-ray interactions (i.e., at 100% terphenyl concentration).

g_i = average fraction of neutron energy lost per collision with nuclide i, equal to $2A_i/(A_i + 1)^2$. Subscript i refers to hydrogen (H), carbon (C), beryllium (Be) or aluminum (Al).

H_M = mass of coolant heldup below zero inch Makeup Tank to the circulating loop; grams.

H_S = mass of coolant heldup below zero inch Sampling Tank to the circulating loop; grams.

HB   = high boilers. Those fractions of irradiated coolant having higher boiling points than that of para-terphenyl.

h   = film coefficient of convective heat transfer; $Btu/(hr)(ft^2)(^\circ F)$.

h_S = scale coefficient of heat transfer; $Btu/(hr)(ft^2)(^\circ F)$.

I_i = energy transfer integral for nuclide i, watts/atom. Subscript i refers to hydrogen (H), carbon (C), beryllium (Be) or aluminum (Al).

J_M = Makeup Tank gage-glass level; inches

J_S = Sampling Tank gage-glass level; inches

K = constant.

$K_n(-1), K_{i,n}$ = overall rate constant for disappearance of component i in a transient run determined by n^{th} order kinetics; gms/watt-hr.

k_R^O = constant.

k = thermal conductivity of the irradiated coolant; cal/(cm)(sec)(^{O}C).

k_M = average Makeup Tank level calibration; grams/inch.

k_S = average Sampling Tank level calibration; grams/inch.

$k_{R,omp,n}$ = n^{th} order radiolysis reaction rate constant for total terphenyl (omp) in the coolant; gm/(watt)(hr).

$k_{R,i,a+b}$ = radiolysis reaction rate constant for component i (terphenyl isomer) for kinetics order a for component i and kinetics order a + b for total terphenyl; gms/watt-hr.

$k_{P,omp,m}$ = m^{th} order thermal decomposition reaction rate constant for total terphenyl (omp) in the coolant; hr^{-1}.

$k_{P,i,c+d}$ = thermal decomposition reaction rate constant for component i (terphenyl isomer) for kinetics order c for component i and kinetics order c + d for total terphenyl; hr^{-1}.

L = length of test heater; inches.

L_j = mass of coolant in the jth sampling capsule; grams.

L_L = distance of the bottom of the in-pile capsule from the reactor core center; inches.

L_T = distance of the top of the in-pile assembly from the reactor core center; inches.

LIB = low and intermediate boilers. Those fractions of the irradiated coolant having boiling

points equal to or less than those of the terphenyls (w/o DP - w/o HB = w/o LIB).

M = mass of coolant; grams.

M_j = mass of coolant in the jth batch of Makeup Tank; grams.

M_C = circulating mass of coolant in the loop; grams.

M_N = coolant mass contained in Zone N of the coolant loop; lbs.

MT = Makeup Tank of S & M System

MW_N = number average molecular weight; grams/gram-mole.

MWH = period of reactor operation; megawatt-hours.

m = kinetics order of pyrolysis or radiopyrolysis.

N = number of data points in degradation calculations or designated zone of the coolant loop.

N_i = number of atoms per gram of nuclide i.

Nu = Nusselt number = hD/k.

n = kinetics order of radiolysis.

OMP,omp = ortho, meta, and para terphenyl.

P, P_o = reactor power level; MW.

Pr = Prandtl number; $C_p \mu / k$.

p = constant.

Q/A = heat flux; Btu/ft^2-hr

Q = number of batches of coolant transferred during a steady-state run.

Q_{tot} = total rate of heat produced at test heater wall; watts or Btu/hr.

Q_{in} = net rate of heat input to coolant of a test heater; watts or Btu/hr.

Q_{loss} = rate of heat loss through the test heater insulation; watts.

q = constant.

R = universal gas constant; kcal/(gram-mole)(^{O}K)

Re = Reynolds number, $DV\rho/\mu$.

R_T^j = total dose rate in material j, watts/gm. Superscript j refers to Santowax OMP (SW), polyethylene (PE), polystyrene (PS), carbon (C), beryllium (Be) or aluminum (Al).

R_N^j = fast neutron dose rate in material j; watts/gm.

R_γ^j = gamma ray dose rate in material j; watts/gm.

R_{th}^j = thermal neutron dose rate in material j; watts/gm.

R_{Cd} = cadmium ratio.

$\bar{r}$ = average dose rate; watts/gm = $d\tau/dt$.

S = conversion factor; 1.6 x 10^{-43}(cm^2)(watt)(sec)/(barn)(ev).

SaT = Sampling Tank of S & M System.

ST = Surge Tank of S & M System.

S_j = mass of coolant in the jth batch of Sampling Tank; grams.

SW = Santowax.

T = temperature; ^{O}F and ^{O}R, or ^{O}C and ^{O}K.

T_o = reference point temperature; ^{O}F, ^{O}R, ^{O}K.

T_B = bulk temperature of coolant in test heater; ^{O}F.

TT = Transfer Tank of S & M System.

$T_{w,i}$ = average inside wall surface temperature; ^{O}F.

t = time.

t	$=$	Student's t.
U	$=$	measured heat transfer coefficient; Btu/(hr) $(ft^2)(^oF)$, from inside test heater wall to bulk coolant.
V	$=$	velocity; ft/sec.
W_{omp}	$=$	total degradation rate for terphenyl; lbs/hr or gms/hr.
W_R	$=$	radiolysis degradation rate for terphenyl; lbs/hr or gms/hr.
W_P	$=$	radiopyrolysis degradation rate for terphenyl; lbs/hr or gms/hr.
W_i	$=$	total mass of terphenyl or terphenyl isomer degraded, or HB produced; grams or lbs.
w_i	$=$	organic coolant feed rate to the system; grams/ hr or lbs/hr.
w/o	$=$	weight per cent.
X	$=$	volume per unit length of in-pile capsule; cc/inch.
X_j	$=$	mass of coolant of the jth sample of miscellaneous coolant removal from the loop; grams.
$\overline{Y}$	$=$	weighted mean of Y_j values.
Y_j	$=$	j^{th} data point for independent variable.
y	$=$	Surge Tank gage-glass level; inches.
Z	$=$	number of VPC chromatographic analysis or number of tritium analysis.
γ	$=$	gamma radiation.
δ	$=$	net change of coolant mass in the loop; grams.
Δ	$=$	correction factor for G value calculations in steady-state-HB periods (net accumulation term); grams.
β	$=$	beta radiation.

μ_o = constant; centipoise, cp.

μ = bulk liquid coolant viscosity; cp.

μ_w = coolant viscosity measured at the inside test heater wall temperature; cp.

ρ = density; gm/cc.

$\sum$ = summation sign.

σ, σ^2 = standard deviation and variance, respectively.

σ = neutron cross section; barns.

σ_s = elastic scattering neutron cross section; barns.

$\overline{\sigma_{eff}}$ = effective threshold neutron cross section; barns.

σ_{res} = resonance component of neutron cross section; barns.

$\sigma_{1/v}$ = 1/v component of neutron cross section; barns.

σ_{2200} = 2200 meter/sec neutron absorption cross section; barns.

τ = specific dose absorbed by irradiated coolant; watt-hr/gm coolant.

$\emptyset(E)$ = neutron flux per unit energy; $n/(cm^2)(sec)(ev)$.

$\emptyset(\geq E)$ = integrated fast neutron flux above energy E; $n/(cm^2)(sec)$.

$\emptyset_o$ = epithermal neutron flux constant; $n/(cm^2)(sec)$.

$\emptyset_{2200}$ = 2200 meter/sec neutron flux, $n/(cm^2)(sec)$.

$\sim$ = approximately.

APPENDIX A10

M.I.T. REPORT DISTRIBUTION LIST

U. S. Atomic Energy Commission
Headquarters
Division of Reactor Development and Technology
Washington, D. C. 20545

1   Attn: Chief, HWR Branch

1   Attn: Chief, Desalting Branch

1   Attn: Assistant Director, Reactor Engineering

1   Attn: Assistant Director, Reactor Technology

U. S. Atomic Energy Commission
RDT Site Office
P. O. Box 591
Canoga Park, California, 91305

1   Attn: Senior Site Representative,
     Atomics International

U. S. Atomic Energy Commission
RDT Site Office
P. O. Box 500
Windsor, Connecticut 06095

1   Attn: Site Representative,
     Combustion Engineer, Inc.

3   USAEC Scientific Representative
   Chalk River Liaison Office
   c/o Atomic Energy of Canada Limited
   Chalk River, Ontario, Canada

1   USAEC Technical Representative
   Toronto Branch, Chalk River Office
   c/o Atomic Energy of Canada Limited
   Sheridan Park, Ontario, Canada

E.I. du Pont de Nemours and Company
Savannah River Laboratory
Aiken, South Carolina 29802

1   Attn: Supervisor, Technical Information
     Service Research Manager - Experimental
     Physics.

3   U. S. Atomic Energy Commission
New York Operations Office
376 Hudson Street
New York, New York 10014

2   U. S. Atomic Energy Commission
Division of Technical Information Extension
Post Office Box 62
Oak Ridge, Tennessee

APPENDIX All

REFERENCES

(1.1)   Bolt, R. O. and Carroll, J. G., "Radiation Effects
        on Organic Materials", Academic Press, New York,
        1963.

(1.2)   Morgan, D. T. and Mason, E. A., "The Irradiation
        of Santowax OMP in the M.I.T. In-pile Loop", M.I.T.,
        Cambridge, Massachusetts, (MITNE-22), IDO-11,105,
        1962.

(1.3)   Sawyer, C. D. and Mason, E. A., "The Effect of Reac-
        tor Irradiation on Santowax OMP at 610°F and 750°F,"
        M.I.T., Cambridge, Massachusetts, (MITNE-39), IDO-
        11,107, September, 1963.

(1.4)   Timmins, T. H., Mason, E. A. and Morgan, D. T.,
        "Effect of Reactor Irradiation on Santowax WR: Irra-
        diations from 425°F to 800°F at 40% Fast Neutron
        Fraction," M.I.T., Cambridge, Massachusetts, (MITNE-
        68), MIT-334-34, February, 1966.

(1.5)   Mason, E. A., Timmins, T. H., Morgan, D. T., Bley,
        W. N., "Effect of Reactor Irradiation on Santowax WR:
        (1) Radiolysis Reaction Order and Fast Neutron
        Effect, (2) Radiopyrolysis," M.I.T., Cambridge,
        Massachusetts, (MITNE-78), MIT-334-70, October, 1966.

(1.6)   Tomlinson, M., Bailey, M. G. and Tymko, R. R.,
        "The Radiation Decomposition Characteristics and
        Physical Properties of Three Low-Melting Organic
        Coolants for Reactors," Whiteshell Nuclear Research
        Establishment, Pinawa, Manitoba, Canada, AECL-1915,1964.

(1.7)   Mackintosh, W. D. and Miller, O. A., "The Pyrolysis
        of the Potential Power Reactor Coolant, Santowax
        O-M," AECL, Chalk River, Ontario, Canada, AECL-2218,
        June,1965.

(1.8) Mackintosh, W. D., "The Electron Irradiation of the
       Potential Organic Coolant for Power Reactors, San-
       towax OM," Paper Presented at the Third Conference
       on Nuclear Reactor Chemistry, Gatlinburg, Tennessee,
       TID-7641, October, 1962.

(1.9) Houllier, A., "Interpretation des Resultats Experi-
       mentaux de Radiolyse au 31 Aout 1963 Obtenus Avec
       les Boucles a Liquide Organique No. 2 et No. 3 -
       Influence de la Pyrolyse sur la Vitesse de Decom-
       position du Terphenyle OM-2," Communication Euratom
       No. 589, Lyon, France, November, 1963.

(1.10) Juppe, G., Alvarenga, A., Hannaert, H., "The Pyroly-
       tic Decomposition of Terphenyls," Euratom, EUR 1647.
       e, 1964.

(1.11) Mandel, H., "Heavy Water Organic Cooled Reactor,
       Physical Properties of Some Polyphenyl Coolants,"
       AI-CE-15, April 15, 1966.

(1.12) Hatcher, S. R. and Tomlinson, M., "Composition and
       Physical Properties of Organic Coolants," Whiteshell
       Nuclear Research Establishment, Pinawa, Manitoba,
       Canada, AECL-2644, May, 1966.

(1.13) McAdams, W. H., "Heat Transmission," 3rd Edition,
       McGraw-Hill, New York, 1954.

(1.14) Tomlinson, M., Boyd, A. W. and Hatcher, S. R.,
       "The Irradiation and Thermal Decomposition of Ter-
       phenyls and Hydroterphenyls, (A Summary of Canadian
       Experince)," AECL-2641, Whiteshell Nuclear Esta-
       blishment, Pinawa, Manitoba, Canada, May, 1966.

(1.15) Progress Reports, April 1 - June 30, 1961, PR-CM-
       26 (Section 7), Atomic Energy of Canada Limited,
       Chalk River, Ontario, Cnanda.

(1.16) Gercke, R. M. J. and Trilling, C. A., "A Survey of
       the Decomposition Rates of Organic Reactor Coolants,"
       NAA-SR-3835, Atomics International, Canoga Park, Cali-
       fornia, June, 1959.

(1.17) Tomlinson, M. and et al., "Reactor Organic Coolant:
       1. Characteristics of Irradiated Hydrogenated Ter-
       phenyls," Nuclear Science and Engineering, 26, pp
       547-558 (1966).

(1.18) "Heavy Water Organic Cooled Reactor, 1000 MWe Nuclear Power Plant Preliminary Conceptual Design," AI-CE-Memo 6, Volumes I and II, Combustion Engineering Inc. and Atomics International, October 1, 1965.

(2.1) Morgan, D. T. and Mason, E. A., "Organic Moderator-Coolant In-pile Irradiation Loop for the M.I.T. Nuclear Reactor, Part II, Equipment Design, Procedures and Results of Irradiation to October 5, 1961," (MITNE-22), IDO-11,105, May, 1962.

(2.2) Sawyer, C. D. and Mason, E. A., "The Effects of Reactor Irradiation on Santowax OMP at 610°F and 750°F," M.I.T., Cambridge, Massachusetts, (MITNE-39), IDO-11,107, September, 1963.

(2.3) Timmins, T. H., Mason, E. A. and Morgan, D. T., "Effect of Reactor Irradiation on Santowax WR: Irradiation from 425°F to 800°F at 40% Fast Neutron Fraction," M.I.T., Cambridge, Massachusetts, (MITNE-68), MIT-334-34, February 1966.

(2.4) Mason, E. A., Timmins, T. H., Morgan, D. T. and Bley, W. N., "Effect of Reactor Irradiation on Santowax WR: (1) Radiolysis Reaction Order and Fast Neutron Effect, (2) Radiopyrolysis," M.I.T., Cambridge, Massachusetts, (MITNE-78), MIT-334-70, October, 1966.

(3.1) Morgan, D. T. and Mason, E. A., "Organic Moderator-Coolant In-Pile Irradiation Loop for the M.I.T. Nuclear Reactor, Part II, Equipment Design, Procedures and Results of Irradiation to October 5, 1961," M.I.T., Cambridge, Massachusetts, (MITNE-22), IDO-11,105, May, 1962.

(3.2) Mason, E. A., Timmins, T. H., Morgan, D. T. and Bley, W. N., "Effect of Reactor Irradiation on on Santowax WR: (1) Radiolysis Reaction Order and Fast Neutron Effect, (2) Radiopyrolysis," M.I.T., Cambridge, Massachusetts, (MITNE-78), MIT-334-70, October, 1966.

(3.3) Sawyer, C. D. and Mason, E. A., "The Effect of Reactor Irradiation on Santowax OMP at 610°F and 750°F," M.I.T., Cambridge, Massachusetts, (MITNE-39), IDO-11,107, September, 1963.

(3.4)   Timmins, T. H., Mason, E. A. and Morgan, D. T.,
        "Effect of Reactor Irradiation on Santowax WR:
        Irradiation from 425°F to 800°F at 40% Fast Neu-
        tron Fraction," M.I.T., Cambridge, Massachusetts,
        (MITNE-68), MIT-334-34, February, 1966.

(3.5)   Mandel, H., "Heavy Water Organic Cooled Reactor,
        Physical Properties of Some Polyphenyl Coolants,"
        AI-CE-15, April 15, 1966.

(3.6)   Elberg, S and Fritz, G., "Physical Properties of
        Organic Nuclear Reactor Coolants," ORGEL Program,
        EUR-400.e (1963)

(3.7)   Hatcher, S. R. and Tomlinson, M., "Composition and
        Physical Properties of Organic Coolants," White-
        shell Nuclear Research Establishment, Pinawa, Mani-
        toba, AECL-2644, May, 1966.

(3.8)   Bley, W. N. and Mason, E. A., "The Nature of the
        High Boiler Degradation Products from Irradiated
        Santowax OMP," (MITNE-55), MIT-334-11, Department
        of Nuclear Engineering, M.I.T., Cambridge, Massa-
        chusetts, February 1, 1965.

(3.9)   Swan, A. H. and Mason, E. A., "Friction Factor and
        Heat Transfer Correlation for Irradiated Organic
        Coolants," M.I.T., Cambridge, Massachusetts, MIT-
        334-23, September, 1965.

(3.10) Gercke, R. H. J. and Asanovich, G., "Thermo-
        physical Properties of Irradiated Polyphenyl
        Coolants: Part I, Density and Viscosity," NAA-
        SR-4484, 1960.

(3.11) Hatcher, S. R., Finlay, B. A. and Smee, J. L.,
        "Heat Transfer, Impurities and Fouling in Organic
        Coolants," Whiteshell Nuclear Research Establish-
        ment, Pinawa, Manitoba, Canada, AECL-2642, May, 1966.

(3.12) McAdams, W. H., "Heat Transmission" 3rd Ed., McGraw-
        Hill, New York, 1954.

(3.13) Spierling, H., "Heat Transfer Characteristics of
        Santowax WR in Forced Convection and Pool Boiling,"
        Master Thesis, Department of Nuclear Engineering,
        M.I.T., Cambridge, Massachusetts, June, 1968.

(3.14)   Bessouat, R., et al., "Etudes Thermiques sur les Caloporteurs Organiques," Paper Presented at 7th N Nuclear Congress, Rome, June 1962.

(3.15)   Stone, J. P., et al., "Heat Transfer Studies on Some Stable Organic Fluids In a Forced Convection Loop," Journal of Chemical and Engineering Data, I, 519-529, October, 1962.

(4.1)   Mason, E. A., Timmins, T. H., Morgan, D. T., Bley, W. N., "Effect of Reactor Irradiation on Santowax WR: (1) Radiolytic Reaction Order and Fast Neutron Effect, (2) Radiopyrolysis," M.I.T., Cambridge, Massachusetts, (MITNE-78), MIT-334-70, October, 1966.

(4.2)   Timmins, T. H., Mason, E. A., Morgan, D. T., "Effect of Reactor Irradiation on Santowax WR: Irradiation from 425°F to 800°F at 40% Fast Neutron Fraction," M.I.T., Cambridge, Massachusetts, (MITNE-68), MIT-334-34, February, 1966.

(4.3)   Mackintosh, W. D., "The Electron Irradiation of the Potential Organic Coolant for Power Reactors, Santowax OM," Paper Presented at The Third Conference on Nuclear Reactor Chemistry, TID-7641, Gatlinberg, Tennessee, October, 1962.

(4.4)   Terrien, J. F., Mason, E. A., "Relative Roles of Pyrolysis and Radiopyrolysis In The Degradation of Terphenyls," M.I.T., Cambridge, Massachusetts, MITNE-48, June, 1964.

(4.5)   A.E.C.L. Progress Report, April 1 - June 30, 1961, PR-CM-26 (Section 7), Atomic Energy of Canada Limited, Chalk River, Ontario.

(4.6)   Tomlinson M., Bailey, M. G. and Tymko, R. R., "The Radiation-Decomposition Characteristics and Physical Properties of Three Low-Melting Organic Coolants For Reactors," Whiteshell Nuclear Research Establishment, Pinawa, Manitoba, Canada, AECL-1915, April, 1964.

(4.7)   Gercke, R. M. J. and Trilling C. A., "A Survey of the Decomposition Rates of Organic Reactor Coolants," NAA-SR-3835, Atomics International, Canoga Park, California, June, 1959.

(4.8)   Tomlinson, M., and et al., "Reactor Organic Coolant: 1. Characteristics of Irradiated Hydrogenated Terphenyls," Nuclear Science and Engineering, 26, 547-558 (1966).

(5.1)   Tomlinson, M., Boyd, A. W. and Hatcher, S. R. "The Radiation and Thermal Decomposition of Terphenyls and Hydroterphenyls, (A Summary of Canadian Experince)," AECL-2641, Whiteshell Nuclear Establishment, Pinawa, Manitoba, May, 1966.

(5.2)   Timmins, T. H., Mason, E. A., Morgan, D. T., "Effect
        of Reactor Irradiation on Santowax WR: Irradiation
        from 425°F to 800°F at 40% Fast Neutron Fraction,"
        M.I.T., Cambridge, Massachusetts,(MITNE-68), MIT-334-
        34, February, 1966.

(5.3)   Mason, E. A., Timmins, T. H., Morgan, D. T., Bley,
        W. N., "Effect of Reactor Irradiation on Santowax WR:
        (1) Radiolysis Reaction Order and Fast Neutron Effect,
        (2) Radiopyrolysis," M.I.T., Cambridge, Massachusetts,
        MITNE-78, MIT-334-70, October, 1966.

(5.4)   Mackintosh, W. D., "The Electron Irradiation of the
        Potential Organic Coolant for Power Reactors, Santo-
        wax OM" Paper Presented at The Third Conference on
        Nuclear Reactor Chemistry, Gatlinburg, Tennessee,
        TID-7641, October, 1962.

(5.5)   Progress Reports, April 1 - June 30, 1961, PR-CM-26
        (Section 7), Atomic Energy of Canada Limited, Chalk
        River, Ontario, Canada.

(5.6)   Tomlinson, M., Bailey, M. G. and Tymko, R. R., "The
        Radiation-Decomposition Characteristics and Physical
        Properties of Three Low-Melting Organic Coolants For
        Reactors," Whiteshell Nuclear Research Establishment,
        Pinawa, Manitoba, Canada, AECL-1915, April, 1964.

(5.7)   Mackintosh W. D. and Miller O. A., "The Pyrolysis
        of the Potential Power Reactor Coolant, Santowax
        O-M," Chalk River, Ontario, Canada, AECL-2218, June,
        1965.

(5.8)   Houllier, A., "Interpretation des Resultats Experi-
        mentaux de Radiolyse au 31 Aout 1963 Obtenus Avec
        les Boucles a Liquide Organique No. 2 et No. 3 -
        Influence de la Pyrolyse Sur La Vitesse de Decompo-
        sition du Terphenyle OM-2" Communication Euratom
        No. 589, Category 1.2, Lyon, France, November, 1963.

(5.9)   "Heavy Water Organic Cooled Reactor, 1000 MWe Nuclear
        Power Plant Preliminary Conceptual Design," AI-CE-
        Memo 6, Volumes I and II, Combustion Engineering Inc.
        and Atomics International, October 1, 1965.

(5.10) Terrien, J. F., Mason, E. A., "Relative Roles of
        Pyrolysis and Radiolysis In The Degradation of Ter-
        phenyl," M.I.T., Cambridge, Massachusetts, MITNE-48,
        June, 1964.

(5.11) Boyd, A. W. and Connor, H. W. J., "The Radiolysis of
        Ortho-and Meta-Terphenyl I: With a Mixture of Fast
        Neutrons and Gamma rays at Dose Rates of 0.1 and
        0.3 w/g," AECL CRC-1219, Atomic Energy of Canada
        Limited, May, 1965.

(5.12) Boyd, A. W. and Connor, H. W. J., "The Radiolysis
        of Ortho-and Meta-Terphenyl II: With Gamma Rays
        at Dose Rates of 0.15-0.2 w/g," AECL-2589, Atomic
        Energy of Canada Limited, 1966.

(5.13) Boyd, A. W. and Connor, H. W. J., "The Radiolysis
        of Ortho-and Meta-Terphenyl III: With A Mixture of
        Fast Neutrons and Gamma Rays at a Dose Rate of 1
        w/g," AECL Report in preparation.

(5.14) "Effect of High Temperature on Radiolytic and Pyroly-
        tic Damage of Polyphenyls," Excerpts from NAA-SR-
        8888, Annual Technical Progress Report, AEC Unclassi-
        fied Program FY63, Atomics International, Canoga
        Park, California.

(5.15) Scarborough, J. M., "Radiolytic and Pyrolytic Decom-
        position of Ortho Terphenyl at High Temperature,"
        NAA-SR-8277, June 1, 1964.

(5.16) Tomlinson, M., et al., "The Radiation-Decomposition
        Characteristics and Physical Properties of Three
        Low-Melting Organic Coolants For Reactors," White-
        shell Nuclear Research Establishment, Pinawa, Manitoba,
        AECL-1915, April, 1964.

(5.17) "Heavy Water Organic Cooled Reactor," Quarterly Tech-
        nical Progress Report, Inception Through June, 1965,
        AI-CE-3, Combustion Engineering, Inc. and Atomics
        International, August 15, 1965.

(5.18) Personal Communication from R. S. Harding, Combustion
        Engineering, Inc. to W. N. Bley, M.I.T. March, 1966.

(5.19) Juppe, G., et al., "The Pyrolytic Decomposition of
        Terphenyls," EUR 1647.e, 1964.

(5.20) Rigamonti, J., "Comparison of Pyrolysis of Unirra-
        diated and Irradiated Santowax WR," Master Thesis
        under Preparation, Department of Nuclear Engineer-
        ing, M.I.T., Cambridge, Massachusetts.

(A1.1) Morgan D. T., Mason, E. A., "Organic Moderator -
        Coolant In-Pile Irradiation Loop for the M.I.T.
        Nuclear Reactor, Part II, Equipment Design, Proce-
        dures and Results of Irradiation to October 5, 1961,"
        MITNE-22, IDO-11,105, May, 1962.

(A1.2) Sawyer, C. D., Mason E. A., "The Effects of Reactor
        Irradiation on Santowax OMP at 610°F and 750°F,"
        M.I.T., Cambridge, Massachusetts, MITNE-39, IDO-11,
        107, September, 1963.

(A1.3) Sefchovich-Itzcovich, E., "Neutron Dose Rates in the
        M.I.T. Reactor," S. M. Thesis in Nuclear Engineering
        M.I.T., Cambridge, Massachusetts, January, 1962.

(A1.4) Timmins, T. H., Mason, E. A., Morgan, D. T., "Effect of Reactor Irradiation on Santowax OM: Irradiation from 425°F to 800°F at 40% Fast Neutron Fraction," M.I.T., Cambridge, Massachusetts, MITNE-68, MIT-334-34, February, 1966.

(A1.5) Mason, E. A., Timmins, T. H., Morgan, D. T., Bley, W. N., "Effect of Reactor Irradiation on Santowax WR: (1) Radiolysis Reaction Order and Fast Neutron Effect, (2) Radiopyrolysis," M.I.T., Cambridge, Massachusetts, MITNE-78, MIT-334-70, October, 1966.

(A1.6) Trice, J. B., et al., "A Series of Thermal, Epithermal and Fast Neutron Flux Measurements in the MTR," ORNL-CF-55-10-140, Oak Ridge National Laboratory, Oak Ridge, Tennessee, October, 1955.

(A1.7) Watt, B. E., "Energy Spectrum of Neutrons from Thermal Fission of U^{235}," Physics Review, 87, p. 1037, 1957.

(A1.8) Mason, E. A. and Bley, W. N., "Measurement of Neutron and Gamma Dose Rates in a Nuclear Reactor," M.I.T., Cambridge, Massachusetts, MIT-334-95, Report under Preparation.

(A2.1) Morgan, D. T. and Mason, E. A., "Organic Moderator-Coolant In-Pile Irradiation Loop for the M.I.T. Nuclear Reactor, Part II, Equipment Design, Procedures and Results of Irradiation to October, 1961," MITNE-22, IDO-11,105, Man 1962.

(A2.2) Mason, E. A., Timmins, T. H., Morgan, D. T., Bley, W. N., "Effect of Reactor Irradiation on Santowax WR: (1) Radiolytic Reaction Order and Fast Neutron Effect, (2) Radiopyrolysis," M.I.T., Cambridge, Massachusetts, MITNE-78, MIT-334-70, October, 1966.

(A2.3) Terrien, J., Mason, E. A., "Relative Roles of Pyrolysis and Radiolysis In The Degradation of Terphenyls," M.I.T., Cambridge, Massachusetts, MITNE-48, SRO-87, June, 1964.

(A3.1) Mason, E. A., Timmins, T. H., Morgan, D. T., Bley, W. N., "Effect of Reactor Irradiation on Santowax WR: (1) Radiolytic Reaction Order and Fast Neutron Effect, (2) Radiopyrolysis," M.I.T., Cambridge, Massachusetts, MITNE-78, MIT-334-70, October, 1966.

(A3.2) Sawyer, C. D., Mason, E. A., "The Effects of Reactor Irradiation on Santowax OMP at 610°F and 750°F," M.I.T., Cambridge, Massachusetts, MITNE-39, IDO-11,107, September, 1963.

(A3.3) Young, H. D., "Statistical Treatment of Experimental Data," McGraw-Hill, 1962.

(A3.4)   Selby, S. M. and et al., "Handbook of Mathematical
         Tables," Chemical Rubber Publishing Company, Cleve-
         land, Ohio, 1962.

(A5.1)   Morgan, D. T., Mason, E. A., "Organic Moderator-
         Coolant In-Pile Irradiation Loop for the M.I.T.
         Nuclear Reactor, Part II, Equipment Design, Proce-
         dures and Results of Irradiation to October 5, 1961,"
         MITNE-22, IDO-11,105, May, 1962.

(A5.2)   Sawyer, C. D., Mason, E. A., "The Effect of Reactor
         Irradiation on Santowax OMP at 610°F and 750°F,"
         M.I.T., Cambridge, Massachusetts, MITNE-39, IDO-
         11,107, September, 1963.

(A5.3)   Timmins, T. H., Mason, E. A., Morgan, D. T., "Effect
         of Reactor Irradiation on Santowax WR: Irradiation
         from 425°F to 800°F at 40% Fast Neutron Fraction,"
         M.I.T., Cambridge, Massachusetts, MIT-334-34, Febru-
         ary, 1966.

(A5.4)   Mason, E. A., Timmins, T. H., Morgan, D. T., Bley, W.
         N., "Effect of Reactor Irradiation on Santowax WR:
         (1) Radiolysis Reaction Order and Fast Neutron Effect,
         (2) Radiopyrolysis," M.I.T., Cambridge, Massachusetts,
         MITNE-78, MIT-334-70, October, 1966.

(A6.1)   Mason, E. A., Timmins, T. H., et al., "Effect of Reac-
         tor Irradiation on Santowax WR: (1) Radiolysis Reac-
         tion Order and Fast Neutron Effect, (2) Radiopyroly-
         sis," (MITNE-78), MIT-334-70, Massachusetts Institute
         of Technology, Cambridge, Mass., October, 1966.

(A6.2)   Mackintosh, W. D., "The Electron Irradiation of the
         Potential Organic Coolant for Power Reactors, Santo-
         wax OM," Paper Presented at the Third Conference on
         Nuclear Reactor Chemistry, Gatlinburg, Tenn., TID-
         7641, October, 1962.

(A6.3)   AECL Progress Reports, April 1 - June 30, 1961, PR-
         CM-26 (Section 7), Atomic Energy of Canada Limited,
         Chalk River, Ontario, Canada.

(A6.4)   Tomlinson, M., et al., "The Radiation-Decomposition
         Characteristics and Physical Properties of Three
         Low-Melting Organic Coolants for Reactors," White-
         shell Nuclear Research Establishment, Pinawa, Mani-
         toba, Canada, AECL-1915, April, 1964.

(A7.1)   Spierling, H., "Heat Transfer Characteristics of
         Santowax WR in Forced Convection and Pool Boiling,"
         Master Thesis, Department of Nuclear Engineering,
         M.I.T., Cambridge, Massachusetts, June, 1968.

(A7.2)   Sawyer, C. D., Mason, E. A., "The effect pf Reactor
         Irradiation on Santowax OMP at 610°F and 750°F,"
         M.I.T., Cambridge, Massachusetts, MITNE-39, IDO-
         11,107, September, 1963.

(A8.1)   Morgan, D. T. and Mason, E. A., "Organic Moderator-
         Coolant In-Pile Irradiation Loop for the M.I.T.
         Nuclear Reactor, Part II, Equipment Design, Proce-
         dures and Results of Irradiation to October 5, 1961,"
         MITNE-22, IDO-11,105, May, 1962.

(A8.2)   Sawyer, C. D. and Mason, E. A., "The Effects of Reac-
         tor Irradiation on Santowax OMP at 610°F and 750°F,"
         M.I.T., Cambridge, Massachusetts, MITNE-39, IDO-
         11,107, September, 1963.